論文 / 著書情報
Article / Book Information

題目(和文)	
Title(English)	Study of Quartz Crystal Microbalance behavior with viscous sensing film and its interpretation using Mason equivalent circuit
著者(和文)	NASONGKHLA SAWIT
Author(English)	Sawit Na Songkhla
出典(和文)	学位:博士(学術), 学位授与機関:東京工業大学, 報告番号:甲第12011号, 授与年月日:2021年3月26日, 学位の種別:課程博士, 審査員:中本 高道,山口 雅浩,中村 健太郎,長谷川 晶一,吉村 奈津江
Citation(English)	Degree:Doctor (Academic), Conferring organization: Tokyo Institute of Technology, Report number:甲第12011号, Conferred date:2021/3/26, Degree Type:Course doctor, Examiner:,,,,
学位種別(和文)	博士論文
Type(English)	Doctoral Thesis

Study of Quartz Crystal Microbalance behavior with viscous sensing film and its interpretation using Mason equivalent circuit

by
Sawit Na songkhla

A thesis submitted to
The Department of Information and Communications Engineering
in partial fulfillment of the requirements
for the degree of
Doctor of Philosophy
in the subject of Engineering

Tokyo Institute of Technology
February, 2021

Abstract

Since the behavior of Quartz Crystal Microbalance with viscous loading has not been thoroughly studied, the positive shift of resonant frequency, which is different from normal behavior, we encounter in the experiment cannot be explained. Thus, the repeatable experiment setup with the controlled environment was developed. To tackle the low Q factor due to viscous loading, the vector network analyzer was used to measure the QCM conductance, and then, the curve fitting technique together with Savitzky-Golay filter was used to improve its signal-to-noise ratio. Next, the microdispenser was used to simulate vapor exposures over the QCM. The measured frequency and resistance including positive frequency shift can be qualitatively explained using mason equivalent circuit model with viscous acoustic load.

Contents

Chapter 1

Introduction

1.1 Background

1.1.1 Mass loading and viscous loading effect in acoustic wave device

QCM (quartz crystal microbalance) sensor works based on piezoelectric effect. The deposited mass acts as an extension of its thickness increases the travelling distance of shear wave, resulting in decrease of resonant frequency. This effect is called mass loading effect, explored by Sauerbrey in 1959 [1]. The simple illustration of mass loading effect is shown in figure 1.1. This effect is valid for rigid, firmly attached film. Nonetheless, it is also viable for thin film depositions. For viscous loading, the most simplified case is a bulk liquid loading. An investigation of QCM in bulk liquid medium conducted in 1985 by Kanazawa [2], consider a semi infinite amount of liquid. The generated shear wave is vanishing as its travel into liquid, i.e., the distance the shear wave amplitude attenuates to 1/e into liquid is called penetration depth. This effect also causes QCM resonant frequency to decrease. However, it also increases QCM resistance. Figure 1.2 shows the viscous loading effect.

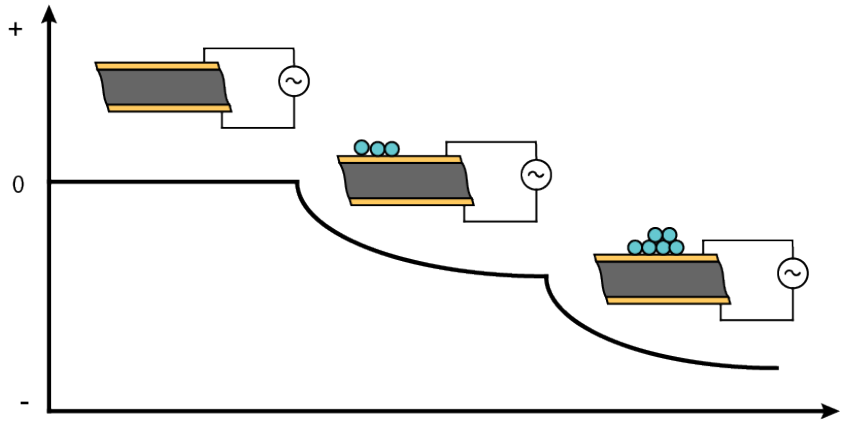

Figure 1.1: Mass loading effect.

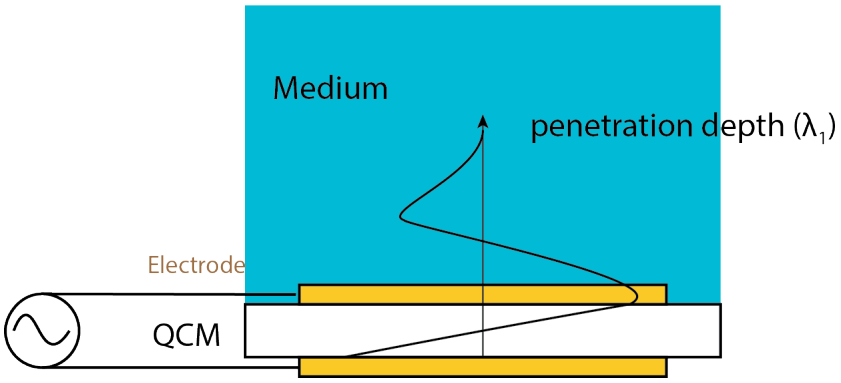

Figure 1.2: Viscous loading loading effect.

1.1.2 Unusual frequency shift in QCM

QCM has high sensitivity (approximately 1 ng per Hz) and high quality factor, QCM has a relatively high signal-to-noise ratio (SNR) compared to its counterpart acoustic sensors. QCM itself does not have any specificity, it has to be coated with sensing film to achieve certain specificity. The typical response of QCM is the frequency decrease when the mass is deposited on QCM or bulk liquid loading as discussed in the previous section.

Surprisingly, sometimes the frequency change becomes positive especially in the sensing application, which needs viscous sensing film for the QCM to have specificity measurand. In biosensor application this behavior appears quite frequently.

In 1986, the study about biosensor, IgG and IgA, were immobilized directly to QCM silver electrode [3]. After loading the buffer solution with antigens, QCM frequency rises when exposed to IgG. The author explains this result by stating that the attachment still not reaching the equilibrium with respect to viscosity, and after 60 min the reaction reached equilibrium. The QCM response is as shown in figure 1.3

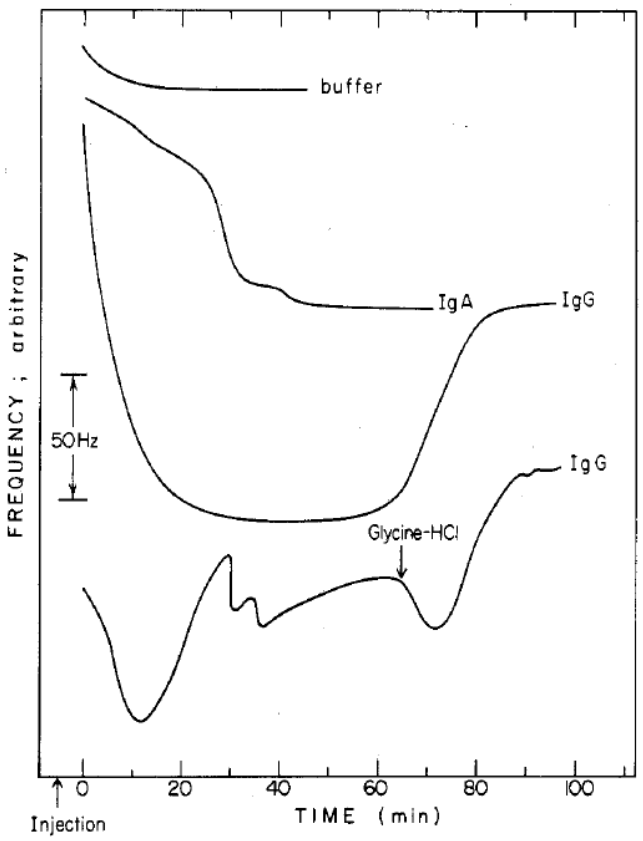

Figure 1.3: Frequency-time responses for crystal/electrode surface antigen after loading with IgG, IgA, and buffer solutions (10 pg of IgG/IgA per 10 /uL of solution.) Glycine HCI is flowed continuously above the crystal surface of IgG experiment starting at 65 min after solution loading. Reprinted with permission from [3]. Copyright (1986) American Chemical Society.

The research about molecular imprinting, to fabricate artificial antibodies, also found positive frequency change when detecting tobacco mosaic virus (TMV) [4]. At a lower TMC concentration of 10 $\mu g/ml$, the positive frequency change occurred when the polyurethanes film is not imprinted as is shown in figure 1.4 . The author concluded that the virus would not attach firmly and slip from the surface caused the positive frequency change. The author also explained that at the higher concentration of 100 $\mu g/ml$ the viruses form a bigger aggregate that strongly adhere to the surface, resulted in typical negative frequency change.

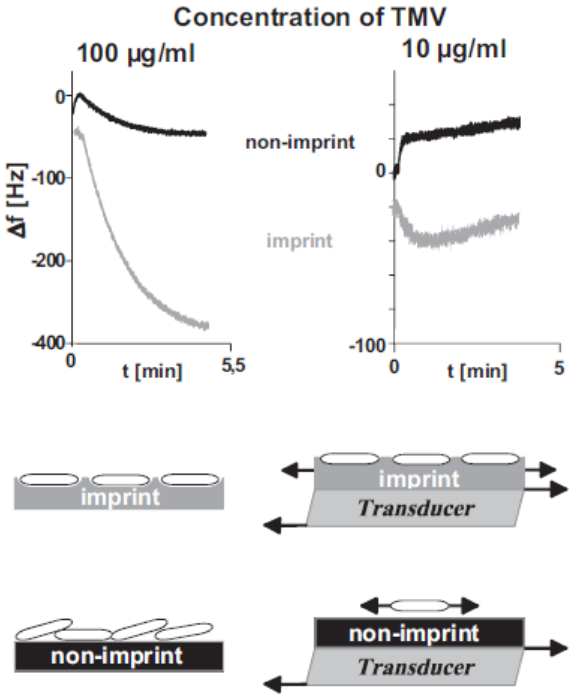

Figure 1.4: Sauerbrey and non-Sauerbrey behavior on nonimprinted surfaces at low TMV concentrations; the imprinted layers always show a Sauerbrey response. Reproduced from [4] with permission from John Wiley and Sons and Copyright Clearance Center.

Another example of antibody-antigen detection, the report by Latif [5] in 2013, Anti-sesame antibodies as a coating of a 10 MHz QCM, a negative frequency shift was observed for sesame protein, whereas, almond protein showed positive frequency change (figure 1.5). This was explained by the weak bond of the mismatch allergen from almond protein. From the biosensor point of view, it seems the weak bond of the analyte is the main cause of positive frequency change.

Another interesting observation of positive frequency shift comes from the field of the humidity sensor. On research using TiO_2 as a humidity sensor[6], the result when the material absorbs the water the QCM frequency increases.

In the application of the QCM, several sensors with different coatings were adopted. The individual sensor response usually has not been readily reported. However, we observed positive frequency from some of our previous experiments also from several researches that are represented here. The positive frequency change occurred and we want to investigate.

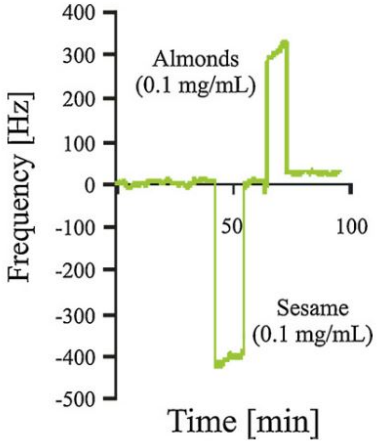

Figure 1.5: Anti-sesame antibodies as coating of a 10 MHz QCM, a negative frequency shift is observed for sesame protein, whereas almond protein shows anti-Sauerbrey effect. Reprinted from [5] with permission from Elsevier.

1.2 Chemical sensor based on acoustic wave

Chemical sensors are used to sense analyte molecules to produce a detectable signal which is generally an electrical signal. Its fundamental structure is shown in figure 1.6.

The analyte(target) among many molecules interacts with the sensitive coating material. Most of the sensors based on acoustic waves work under the piezoelectric effect. The piezoelectric material can generate an electric charge in response to applied mechanical stress.

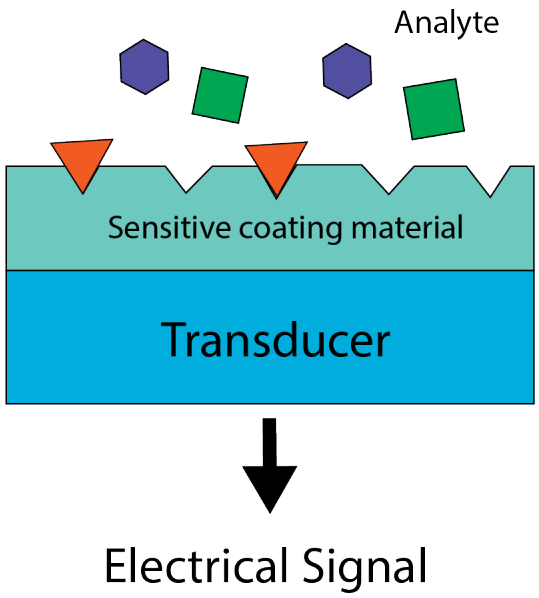

Figure 1.6: Generalize structure of chemical sensor.

1.2.1 Surface Acoustic Wave sensor (SAW sensor)

SAW device is made of the piezoelectric substrate and electrodes. The electrode is developed with a comb-shaped interdigital transducer (IDT) pattern is formed on the electrode surface. The electrodes are generally made of metal such as gold, copper, or alloy. When an AC voltage is applied to the electrode, an acoustic wave is generated and travels along the crystal surface perpendicular to the IDT. The acoustic wave is confined mostly to the substrate within only several wavelengths. This concept was first explained by Rayleigh in 1885 [7]. SAW filter can be configured as a one-port or two-port resonator as is shown in figure 1.7. one-port SAW has an IDT electrode at the center and two reflectors at both sides. An acoustic wave radiates from the center IDT and is reflected by the reflectors, which generate the standing wave. Therefore, this configuration has a high Q factor, suitable for an oscillator. The two-port SAW device generally is used as a narrow band filter. There is 2 set of IDTs on the opposite side of the crystal. It is also called the delay line, with the area where sensing film is usually coated. Since this is a two-port configuration, one is the transmitter IDT or can be called an input electrode. On the other hand, the other receiver IDTs can be called an output electrode. Since the acoustic wave travels mostly along the surface. Any perturbation to this wave alters the acoustic wave properties(Amplitude, phase, frequency, etc). The acoustic wave arriving at the receiver IDT port is converted to an electrical signal.

The operating frequency of SAW is determined by the spacing between the IDT electrode. Several more parameters can be optimized by varying the dimension of IDT. The frequency change due to coating and deposited mass can be expressed as

$$\Delta f = (k_1 + k_2) f_0^2 t_f \rho \tag{1.1}$$

where $k_1 + k_2$ are material constants of substrate, t_f is film thickness, ρ is film density and f_0 is resonant frequency.

SAW sensors operate at between a few hundred MHz, though Gigahertz range SAW also have been fabricated [8] and the noise level of bare SAW device was kept within 8 Hz at 1 GHz operating frequency. The materials such as AIN and ZnO are also under investigation [9]. Although the developments are not for gas sensing, the higher frequency is attractive for sensing applications because of its higher sensitivity.

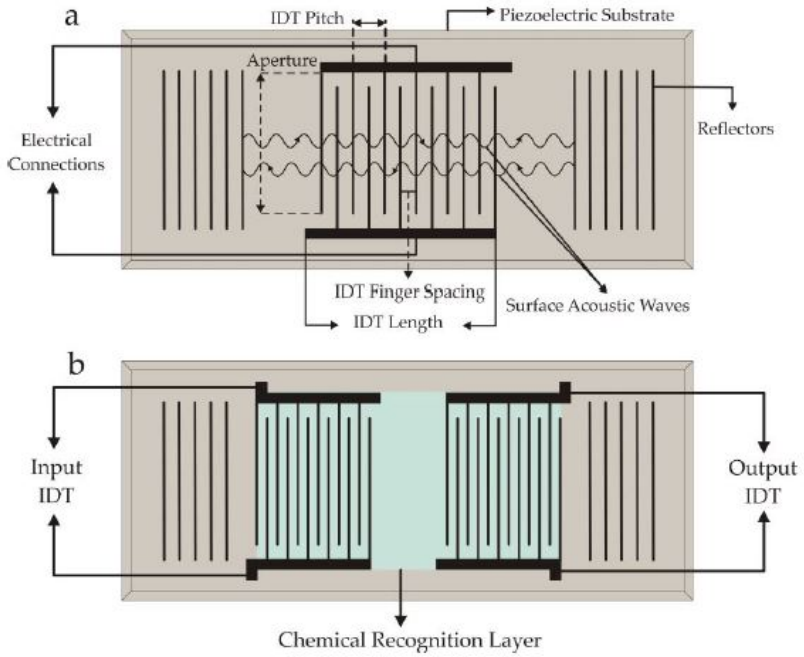

Figure 1.7: (a) one-port SAW resonator configuration (b) two-port SAW filter configuration. Reprinted from [10] under an open access Creative Common.

SAW device first uses as a gas sensor was in 1979 by Wohltjen [11] using ST-cut, X propagating quartz and $LiNbO_3$ substrates and it showed response proportional to $\sqrt{molecular\,weight}$. The concept of the sensitive coating was carried out by Jay W. Grate and the team using an array of SAW sensors with 4 polymer coatings together with thermally desorbed preconcentrator tube (PCTs) to measure organo phosphorous gas [12]. Recent work in SAW gas sensor focused on coating and its application, such as Fullerene C60-cryptand was coated on SAW for detecting various organic compounds [13]. The sensor set-up is shown in figure 1.8.

Also, the concept of electronic noses which utilizes an array of sensors with broad selectivitiy, the algorithm, and the selections of materials was proposed. Fernández using 8 sensors with 7 different coating polymers, principal component analysis (PCA), probabilistic neural networks (PNN), and partial least squares (PLS) were used to classify 3 gases (Methyl Ethyl ketone, octane, and toluene) [14]. The experimental setup of array SAW sensors is shown in figure 1.9(a) and the PCA result in figure 1.9(b) shows the separation among gases. One specific aim of this electronic nose is sensor selections. When an algorithm was applied to select the optimum number of the sensor for a specific task [15]. For milk and fish spoilage and freshness detection, the fuzzy c-means clustering was used [16].

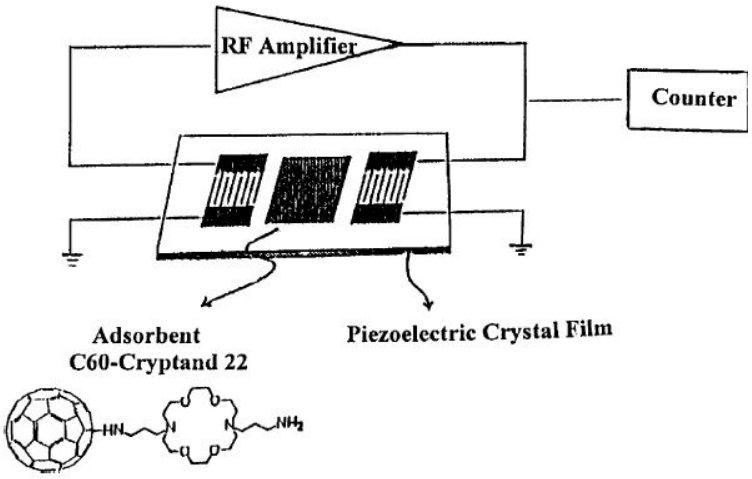

Figure 1.8: Fullerene C60-cryptand 22 coated 250MHz surface acoustic (SAW) sensor. Reprinted from [13], with permission from Elsevier.

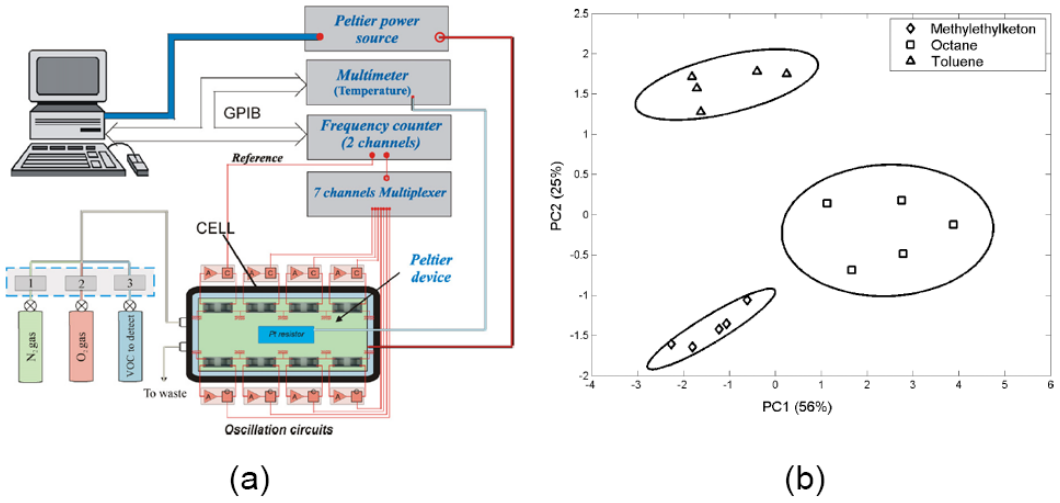

Figure 1.9: (a) Experimental set-up of the whole SAW sensor system. (b) PCA plot of response to the three different gases measured at 50 ppm. Reprinted from [14], with permission from Elsevier.

1.2.2 flexural plate wave sensor (FPW)

The mathematical development of Lamb wave was dated back to 1881 by Horace Lamb which explores the acoustic wave in plate support 2 infinite sets of Lamb wave [17]. The flexural plate wave (FPW) or Lamb wave was first fabricated by Wenzel and white in 1988 [18]. The structure is similar to SAWs sensor with IDT electrodes. However, the substrate thickness is much thinner and has to be thinner than Lamb wavelength for the device to exhibit flexural characteristics. The Lamb waves give rise to a series of plate modes, one of which has a frequency that is much lower than those of the other possible modes. Typically, the piezoelectric layer is sputtered onto a silicon plate. Decreasing the ZnO layer increases its mass sensitivity and also decreasing the oscillator frequency. The sensitivity of FPW sensor is approximately one order of magnitude higher than SAW one, this encourages the use of FPW at a lower frequency which simplifies the driving electronic component and has a lower noise level [19].

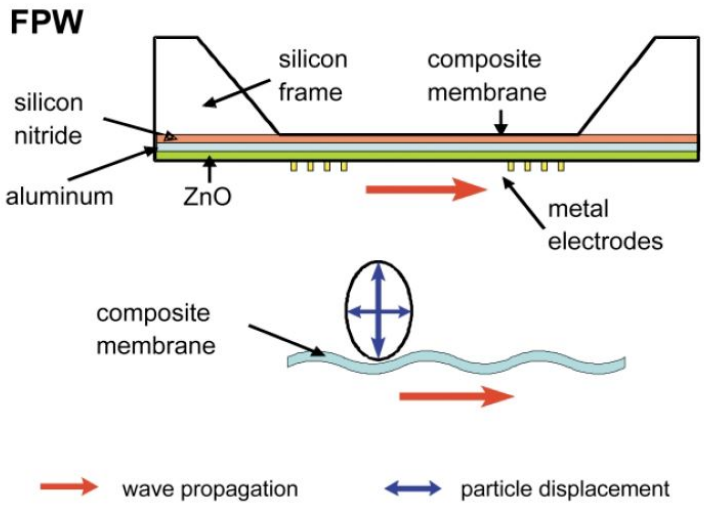

Figure 1.10: Schematic of flexural plate wave device(FPW). Reprinted from [20] by permission from Royal Society of Chemistry.

Since the Lamb wave travels through a flexural plate, the sensing material can be deposited on the opposite side of the electrode, avoiding exposure of the circuitry side to an analyte [20]. A sensor array of 6 FPWs with polymer coating had been used to detect 8 VOC gases and recognize the vapor using EDPCR/Monte Carlo analysis [21]. The structure of the sensor is shown in figure 1.11.

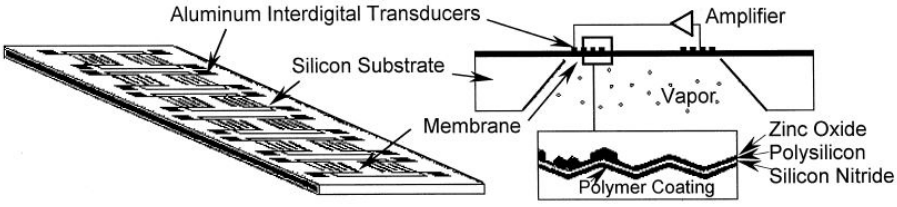

Figure 1.11: Integrated FPW six-sensor array and structure of individual sensor.Reprinted from [21], with permission from Elsevier.

With the MEMS technology the on-chip microchemical array was fabricated,

consisted of 8 micro-chemical analysis arrays (μCANARY), and detected various human proteins and intact bacteria, FPW device was also used in the liquid phase [22]. Basic sensor diagram and photo of an array FPW sensors are shown in figure 1.12.

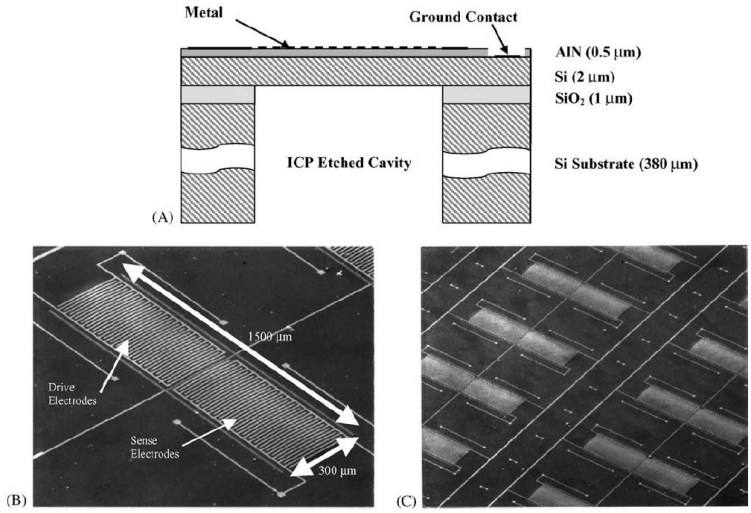

Figure 1.12: Cross-section diagram of the FPW resonating membrane structure, (B) SEM photo of a sensor element from the top surface of the wafer showing detail of metal electrode structure, and (C) SEM photo of several integrated FPW membranes within a section of an integrated sensor array. Reprinted from [22], with permission from Elsevier.

The application as biosensors using FPW is also quite prevalent. The detection of Tetrahydrocannabinol in Human Urine was tested and reported the detection limit as 1.5 ng/mL [23]. The portable point-of care unit to detect chemokine from Respiratory Syncytial Virus (RSV) was made, the mass sensitivity of 70 Hz/(pg/mms) was archived [24].

1.2.3 Bulk Acoustic Wave sensor (BAW)

Bulk acoustic wave is the acoustic wave propagate into the thickness of the piezoelectric substrate. The advantages of BAW is its high Q factor and simple structure.

FBAR

The first to be discussed here is the thin-film bulk acoustic resonator (FBAR or TFBAR) first produced in 1981 by Lakin [25]. FBAR can operate in thickness-shear mode (TSM) like QCM or operate in longitudinal mode. However, for application-saccompanied with highly viscous damping, the longitudinal mode cannot achieve sufficient Q-factor for the operation. The structure of FBAR is thin-film clamped between two electrodes similar to QCM. However, the thin film thickness is ranging from several micrometers down to one-tenth of a micrometer. The material for FBAR can be Zinc Oxide (ZnO) or Aluminium Nitride (AlN) or ternary compounds such as lead zirconate titanate (PZT) or barium strontium titanate (BST). Due to a thin film structure, the resonance frequency can be several hundred MHz to several

GHz. There are two structures of FBAR based on fabrication technology **free-standing** and **solidly mounted** (SMR) resonators (figure 1.13 and figure 1.14, respectively). FBAR is fabricated by depositing piezoelectric substrate. To minimize energy loss the FBAR need to be released from the substrate, the free-standing structure uses micro machining to form an air cavity below the piezoelectric layer. On the contrary, an acoustic mirror structure was fabricated between the resonator and substrate. The acoustic mirror (Bragg reflector) structure was used. By alternating the material with high and low acoustic impedance a reflector can be formed. To achieve maximum acoustic reflectivity the thickness of the material is optimized.

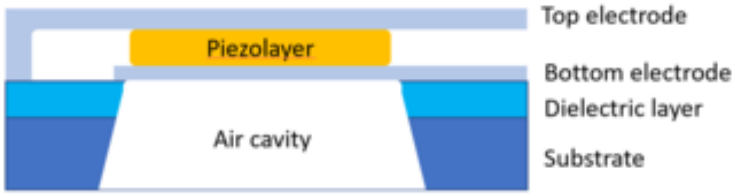

Figure 1.13: A schematic of FBAR: free-standing. Reproduced from Wikipedia under the Creative Commons Attribution-Share Alike 4.0 International License.

Figure 1.14: A schematic of FBAR: solidly mounted (SMR). Reproduced from Wikipedia under the Creative Commons Attribution-Share Alike 4.0 International License

Recently, TSM FBAR has been developed for various application in liquid phase, the high frequency of FBAR exhibit higher sensitivity than QCM but also with the higher noise level. The fabrication of FBAR was developed with composite AlN/SiO_2. It was designed to operate in the second harmonic and was tested its frequency change in water. The fabricated FBAR was temperature-compensated and tested in temperature ranging from 20 to 95 °C [26]. The cross section of fabricated FBAR is shown in figure 1.15. The study of FBAR operates in shear mode and longitudinal mode was conducted. It has been confirmed that longitudinal mode in liquid is not feasible due to high deterioration of Q factor [27].

Advantage of FBAR is that the technology to fabricate to thin-film semiconductor technology can also be applied to FBAR fabrication. FBAR can be made into a thin sensor array on silicon wafer. The array of 64 FBARs for mass detection has been fabricated[28]. Figure 1.16a shows the cross section of FBAR and figure 1.16b shows the photo of FBAR sensor array.

Biosensing and gas sensing application also feasible with coated FBARs. Basic application such as biosensor using Biotin Label DNA and target protein Streptavidin was investigated[29]. Author also investigated the uses as a humidity sensor when coated with polyimide film[29]. By combining gas chromatography column

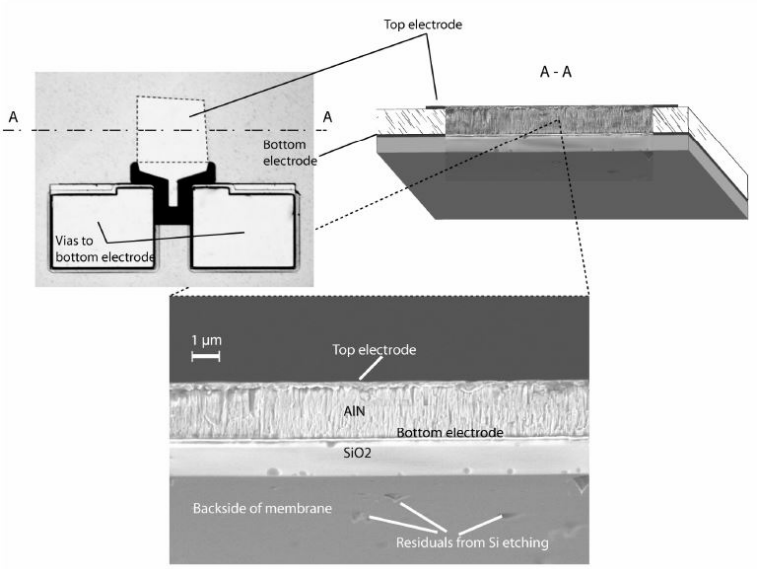

Figure 1.15: (Upper left) Top view of the fabricated resonator, the marked area defines the active area 300x300 µm^2. (Lower) SEM cross section image of a composite membrane. Reprinted from [26] with permission from IEEE.

with various polymer coated FBAR sensors, the FBAR sensor can identify n-pentane and acetone and compared with flame ionization detector (FID) [30]. The illustration of the sensing system is shown in figure 1.17.

The main drawback of FBAR is that it has a higher noise level compared to QCM. Recent research on FBAR is to improve its oscillator circuit using software called Advanced Design System (ADS) simulation [31]. The system phase noise was improved when the optimum capacitors in the Clapp oscillator were selected. The design of FBAR has many parameters, and the electrode thickness is also one of the parameters that can be optimized to improve sensitivity, Mirea studies the combination of bottom and top electrode thickness and found the best combination of each thicknesses experimentally [32]. Figure 1.18 shows the illustration of FBAR.

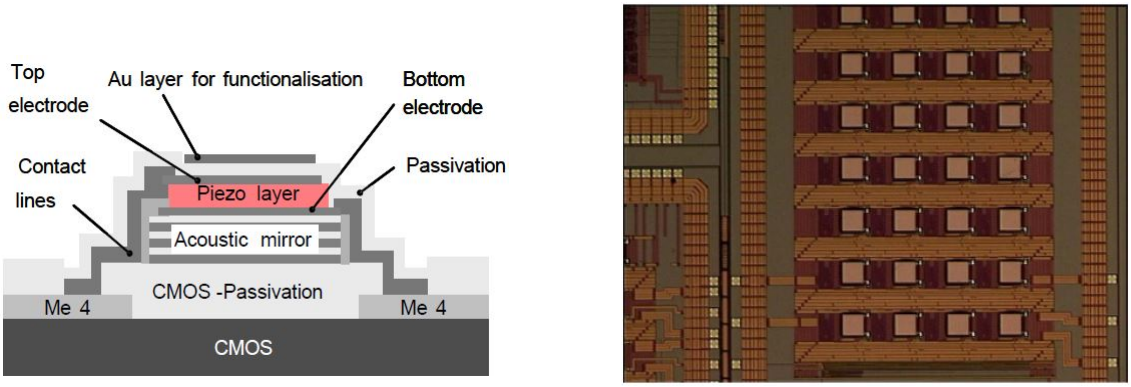

(a) (b)

Figure 1.16: Schematic and photo of FBAR array(a)Schematic cross section of a monolithically integrated FBAR. (b)Section of a monolithically integrated FBAR sensor array on CMOS wafer. Reprinted from [28], with permission from Elsevier.

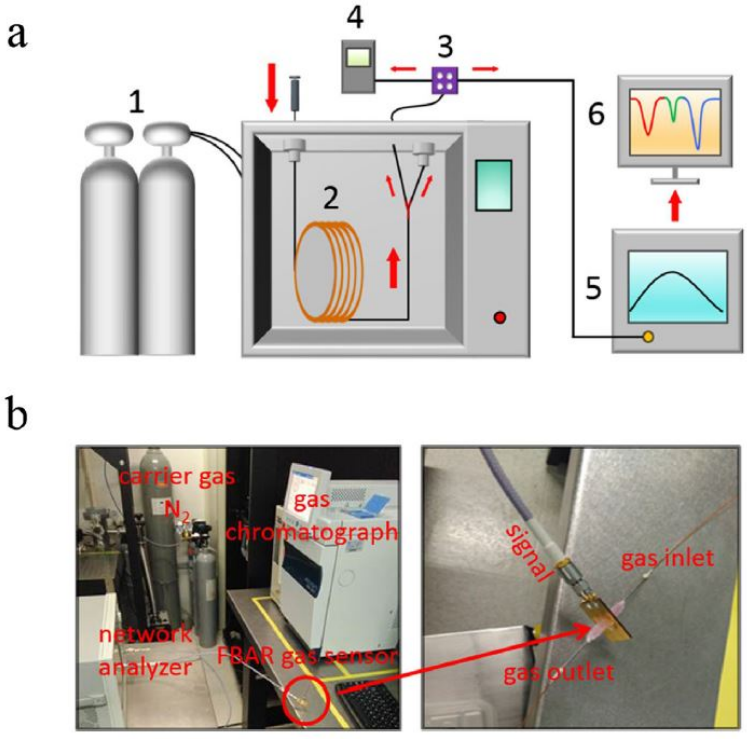

Figure 1.17: Illustration showing the prototype GC-FBAR chromatography sensing system. (a) it illustration (1) Nitrogen (99.99%); (2) gas chromatograph; (3) FBAR array device; (4) photo-ionization detector; (5) vector network analyzer; (6) personal computer. (b) The photo showing experimental setup. Reprinted from [30], with permission from Elsevier.

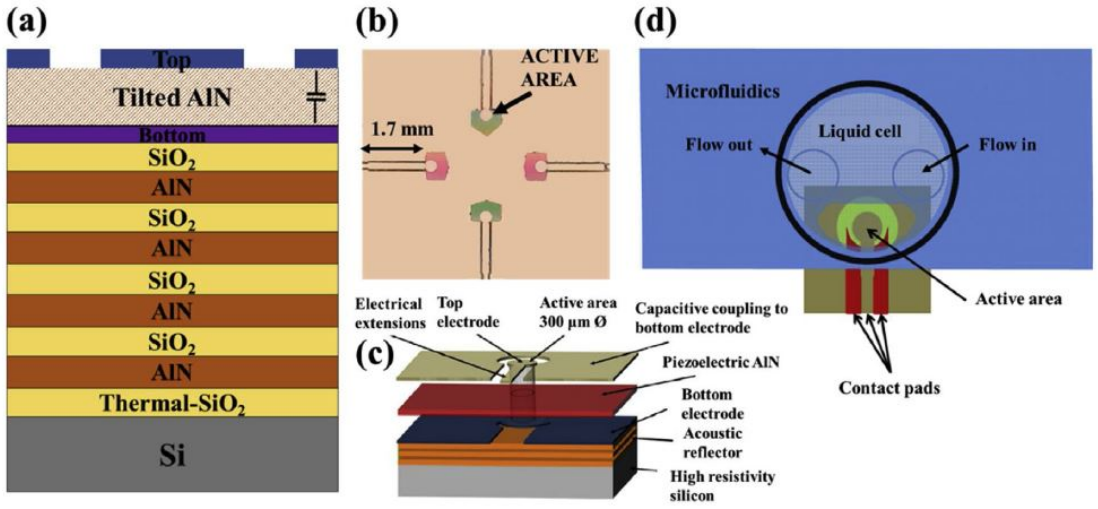

Figure 1.18: Illustration of FBAR cross section and its structure (a) Transversal sketch of the SMR structure, (b) plain optical image of an actual chip containing four SMRs, (c) sketch showing the structure of the SMR including the etched bottom electrode below the electrical extensions, and (d) schematic of the microfluidic cell mounted on the active area of the device. Reprinted from [32], with permission from Elsevier.

QCM

Quartz Crystal Microbalance (QCM) is one of the most prominent gravimetric sensors in terms of publications. The structure of QCM is a crystal plate coupled with an electrode similar to FBAR but thicker. The AT-CUT crystal is mainly used is for zero temperature coefficient at 25 °C with the inflection points make it usable throughout -40 °C to 125°C. QCM operates in Thickness Shear Mode (TSM) which makes it possible to use even in a highly damping environment since the energy dissipates less than the longitudinal mode. The diagram of QCM is shown in figure 1.19. The first proposal of using QCM with sensitive coating was dated back to 1964 [33]. In this research, various hydrocarbon gases sample together with GC coating materials. More coatings material were tested including gas-liquid chromatography (GLC) stationary phases [34]. Polypyrrole as a conducting polymer is a good porous material and was deposited on QCM. Its frequency change was observed during cyclic voltammetry cycle [35].

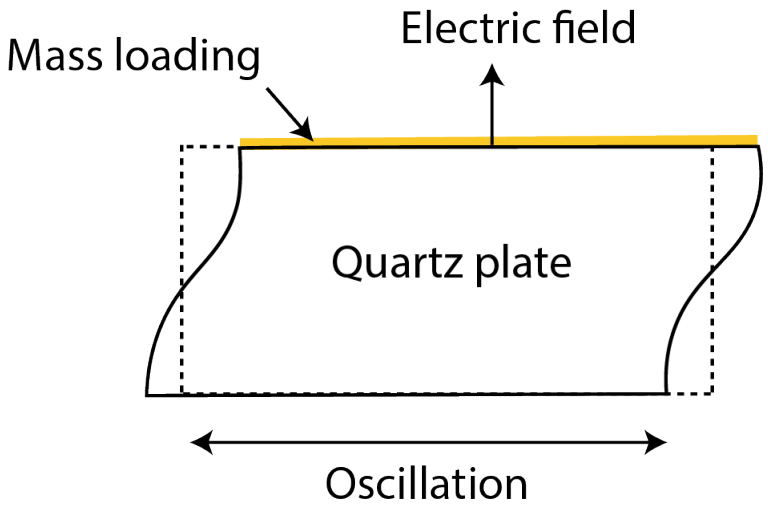

Figure 1.19: Diagram of Quartz Crystal Microbalance.

Self-assembly layer was also used [36][37]. For the study of imprinted polymer to detect pollen allergen, the QCM was measured using both oscillator circuit and VNWA [38]. The negative frequency change was observed when the imprinted coated polymer was exposed to a small amount of pollen, while the non-imprinted layer showed positive frequency change.This may be due to the pollen on the non-imprinted layer surface can move freely on the surface. This caused the non-Sauerbrey Bisphenol Abehaviour(positive frequency shift). The QCM response is shown in 1.20. Matsumoto developed the chemical sensor to detect Bisphenol A (BPA) in water, the design based on hydro gel and conducting polymer. The imprinted polymer significantly improved the response from 30.8 ng cm^{-2} to 205.8 ng cm^{-2} [39].The QCM response is shown in 1.21.

QCMs are also frequently used as a biosensor. Even as dated back in 1986, Thompson coated QCM with polyacrylamide gel bound with anti-human IgG [3]. The frequency change caused by reaction between human IgG and IgA with anti-human IgG were recorded. The detection of 3 strains of *E.coli* with the label-free method was reported [40]. The AFM scan of *E. Coli* is shown in figure 1.22 and the QCM response is shown in figure 1.23. The QCM response shows The frequency

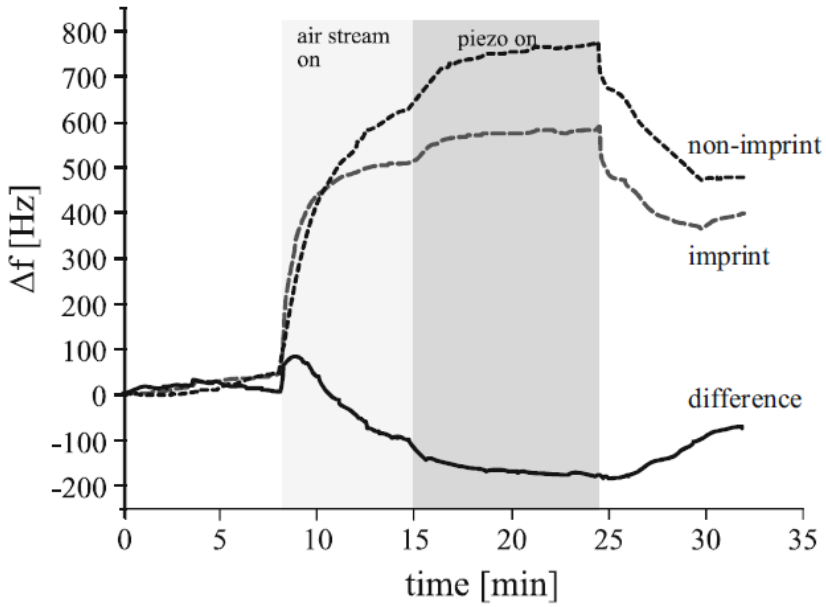

Figure 1.20: Sensor characteristic of a QCM coated with nettle pollen MIP and a non-imprint, respectively. Reprinted from [38] by permission from Springer Nature.

measure of QCM operating in an oscillator circuit compared with measurements from VNWA.

The Electronic nose applications of QCM are very common. An array of QCMs with various coating was used to classify perfume, The use of neural network compared with PCA method had been conducted [41]. Electronic noses have many applications in the medical field. The non-invasive for detecting blood glucose and HbA1c was investigated. QCMs were coated with various phthalocyanine compounds. Acetone vapor is a marker for blood glucose. The data were implemented to radial basis function neural network (RBFNN) [42]. The use of olfactory receptor(OR) in the QCM sensor was also reported. $Anti - His_6$ Aptamer was immobilized covalently onto the gold electrode QCM. The aptamer capture His_6-tagged ODR10. The detection limit was 1.5 ppm(v/v). The selectivity of ODR10 was also investigated, diacetyl has the highest response. Molecularly imprinted polymers (MIPs) were also used in electronic nose technology. The polyacryric acid(PAA) had been used as host polymer and hexanal, heptanal, and nonanal as pattern molecules. QCMs coated with those MIPs were used as a sensor after gas chromatography column to characterize human body odors [43].

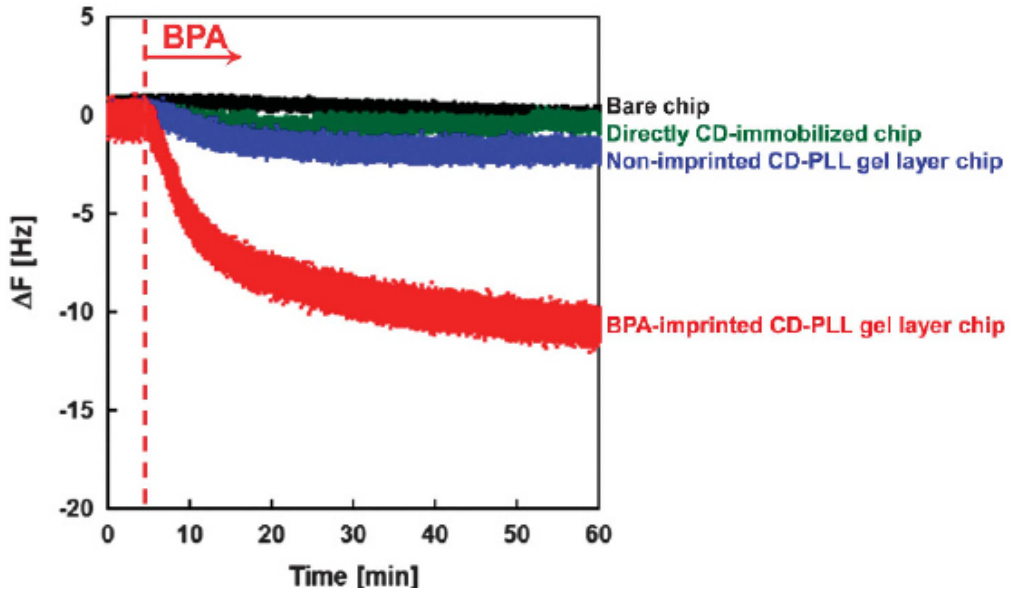

Figure 1.21: QCM responses of a BPA-imprinted CD-PLL gel layer chip, a non-imprinted CD-PLL gel layer chip, a directly CD-immobilized chip and a bare chip after the injection of an aqueous 400 µM BPA solution. Reprinted from [39] by permission from Springer Nature.

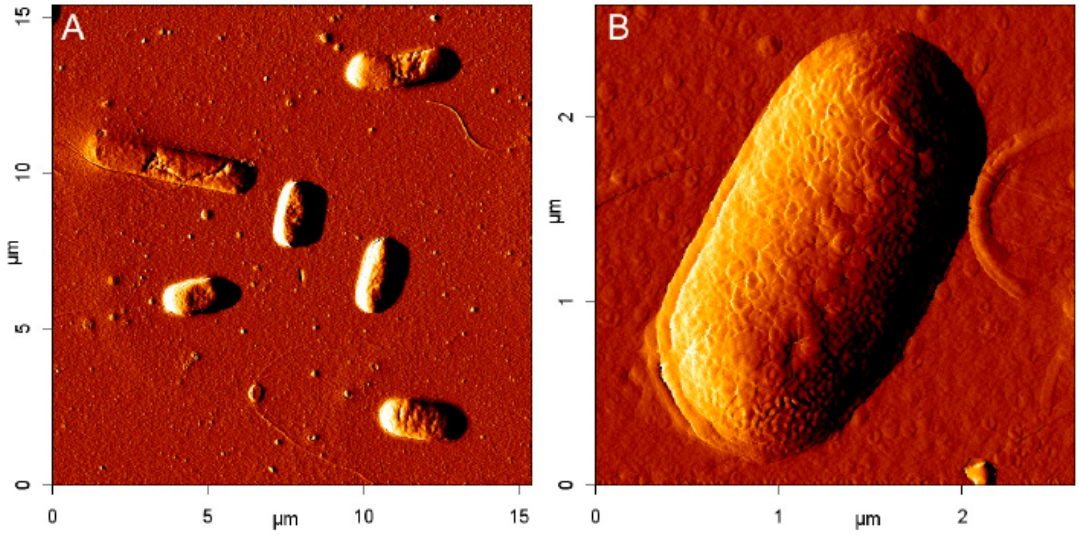

Figure 1.22: AFM scan of E. coli K-12 specifically bound on the cover slip modified by APTES and antibody Serotec 4329-4906. The "Error" signal is shown. (A) Overview and (B) detail of a single cell. Reprinted from [40] under the Creative Commons CC BY 4.0 license.

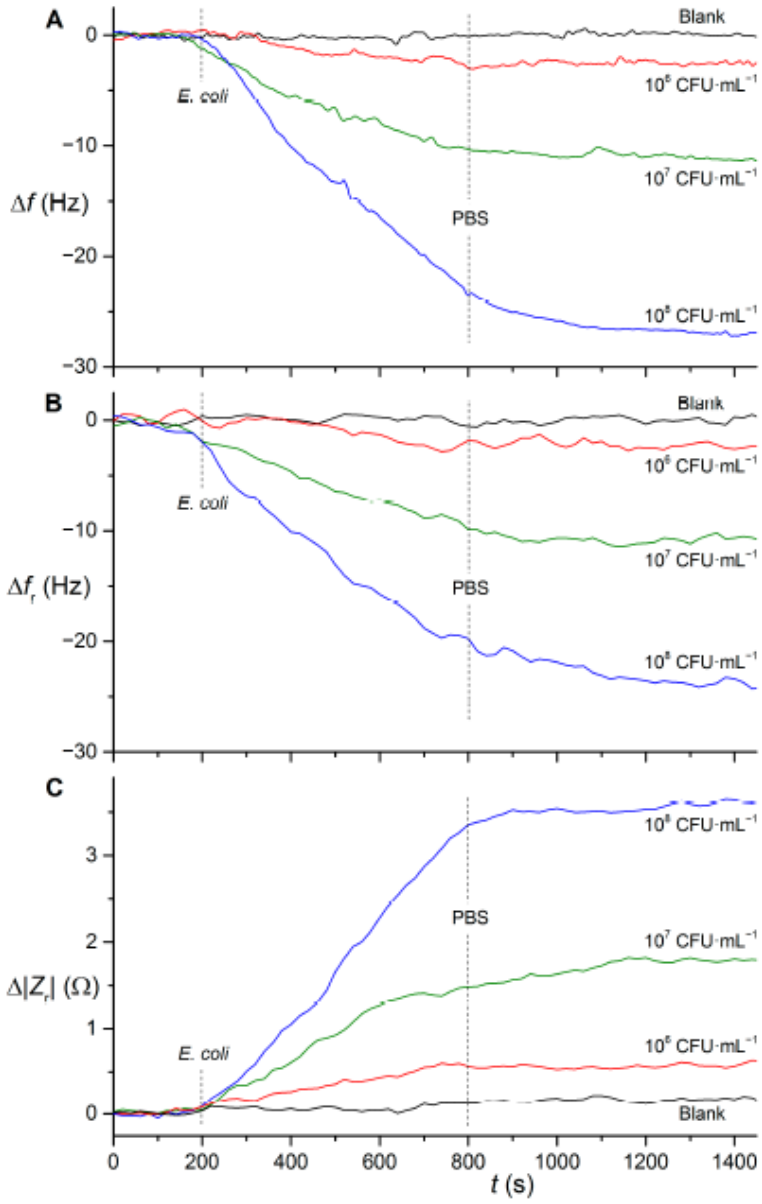

Figure 1.23: 4. Binding interactions between E. coli DH5α and antibody Abcam ab25823 immobilized directly using glutaraldehyde. (A) Frequency measured in active mode using the QCM Analyzer (B) Frequency measured in passive mode using Agilent 4294A (C) Amplitude of impedance at the resonant frequency measured in passive mode. Reprinted from [40] under the Creative Commons CC BY 4.0 license.

1.2.4 Summary

In this section, we summarize the study of the acoustic wave sensor in various applications. QCM has been applied to many application including medical, gas sensing, biosensing, and electronic nose. Recently, FBAR is becoming more attractive since MEMS technology becomes easier to obtain, with working principle similar to QCM and working at a higher frequency. However, QCM still dominates the overall applications and usage, mainly due to it readily commercially available, high Q factor, and its simple structures. The recent study of acoustic sensors are as shown in table 1.1.

Table 1.1: Summary of the recent chemical sensor based on acoustic wave

Sensor type	**Application**	**Piezoelectric material**	**Coating material**	**Analyte**	**Phase**	**Ref.**
FPW	Allergy detection	ZnO	SAM IgE antibody, Cystamine/ Glutaraldehyde	IgE antigen	Liquid	[44]
QCM	lung cancer signalling VOCs in breath	AT-cut Quartz	RuTPP, RhTPP, MnTPP, CoTPP, SnTPP, CoNO2TPP, CoOCH3TPP, MnOMC	alkanes and methylated alkanes	Gas	[45]
SAW	Spoilage detection of milk and fish	N/A	26 potentials polymer such as: PIB, PECH ,OV-202 , etc.	34 spoilage marker gases such as: Acetic acid, Acetaldehyde, etc.	Gas	[16]
FPW	Narcotic test in human urine	ZnO	cystamine SAM, glutaraldehyde, THC antibody, THC antigen	tetrahydrocannabinol (THC)	Liquid	[23]
QCM	Classification of multiple chinese liquors	AT-cut Quartz	PVC, Polyamide, Polyethylene, AgCl, CuCl2, Polytef, Azithromycin	10 chinese liquors	Gas	[46]
SAW	Water quality monitoring	36° YX-LiTaO3	diisononyl cyclohexane-1,2-dicarboxylate-polystyrene	Benzene	Liquid	[47]
FBAR	Gas chromatographic analysis	AlN	Polycaprolactone (PCL), polyisobutene (PIB)	n-pentane (C5),n-hexane (C6), n-heptane (C7), acetone	Gas	[30]
FPW	Respiratory Syncytial Virus (RSV) detection	LNO/PZT	N/A	Chemokine	Liquid	[24]
FBAR	VOCs gas discrimation	ZnO	poly (3,4-ethylenedioxythiophene):poly(styrene sulfonate) (PEDOT:PSS)	ethanol, methanol, pentanol, acetone and tetrahydrofuran	Gas	[48]
SAW	hydrogen gas sensor	LiNbO3	Pd/Cu nanowires	hydrogen	Gas	[49]
QCM	VOCs gas discrimation	AT-cut Quartz	Room Temperature Ionic Liquids (RTIL)	hexanol, butyl acetate, 2-hexanone, and hexanoic acid	Gas	[50]

1.3 Behavior of QCM under viscous environment

1.3.1 liquid phase

Working in a liquid phase is rather challenging due to the high damping by nature of the liquid. However, the response seems to be rather more stable when working in this environment. Vector Network Analyzer (VNWA) is the first choice for measuring the impedance. Nonetheless, there are several studies on using the oscillator circuit even for a highly viscous environment. However, most of the systems for the liquid phase are for biosensing application and much less for gas sensing. Using QCM in liquid phases are more difficult since liquid typically adds a high amount of loading. longitudinal mode almost not working in liquid phase due to high energy loss compared to thickness shear mode. Kanazawa's first develop the equation of QCM behavior when in contact with bulk liquid. Kanazawa's equation is based on the experimental result and expressed as an empirical equation. However, further, development using stress equations also confirm its response. The limitation of Kanazawa's equation is the simplification to bulk liquid. The thin viscous film cannot be predicted accurately by the Kanazawa's equation.

For the application of QCM as a sensor in the liquid phase, it was dated back in 1986, by Tompson, to test for the interaction of antigen IgG with antihuman IgG in liquid [3]. Since the usage of QCM is unavoidable and becomes a main arsenal for the biosensing, also including gas sensing application. Resonant frequency change alone is not enough to interpret the behavior of QCM. To gain more information about QCM the impedance measurement is needed. There was an experiment of QCM immersed in various concentrations of water-ethanol [51]. The QCM was conducted with a single side and both side QCM in the measurement cells. There are a lot of correlation plots of parameters. The relation plot between $\sqrt{\rho\eta}$ and Δf showed a linear relationship, with some deviation when using two-sided cells. On the other hand, the relation between $\sqrt{\rho\eta}$ and ΔR shows good linearity in all cases. This result suggests the validity of using both resistance and resonant frequency for viscous loading measurement.

Recent studies over the usage of QCM in a viscous environment including the design of oscillator, dedicated circuit or using VNWA. There is a design of an active bridge oscillator for using in viscous liquid up to 15 cP, confirmed by glycerol solutions [52]. As a biosensor in figure 1.24, Latif using an imprinting technique to make a sensitive layer for yeast cell detection [5]. In his experiment using duplex yeast cells for imprinting, the experiment showed the negative frequency change when exposing to a duplex yeast cell, but showed positive frequency when exposing to a single yeast cell. The author explained the positive frequency change causes this anti-Sauerbrey behavior as the single yeast cells are not tightly bound to the recognition layer.

Our team also extensively investigated QCM sensing under liquid and found it feasible with observable response[Nakamoto2015]. Figure1.25 shows the experimental setup of QCM immersed in water with an SAW device as a preconcentrator. The advantage was this system had not been influenced from air humidity.

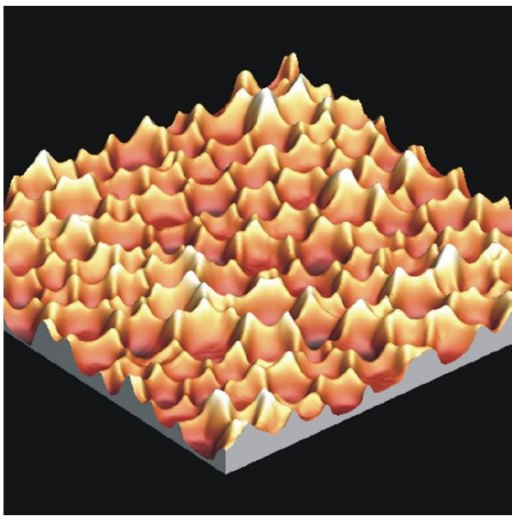

(a) AFM image of yeast-imprinted polyurethane layer

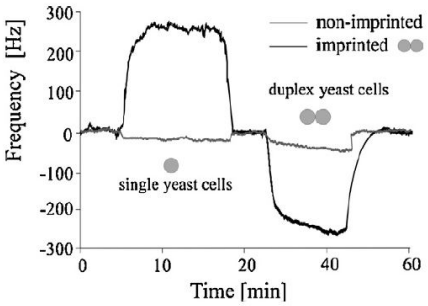

(b) 10 MHz QCM sensor responses while exposing to single and duplex yeast cell

Figure 1.24: The image of yeast imprinting polyurethanelayer and the QCM response. Reprinted from [5], with permission from Elsevier.

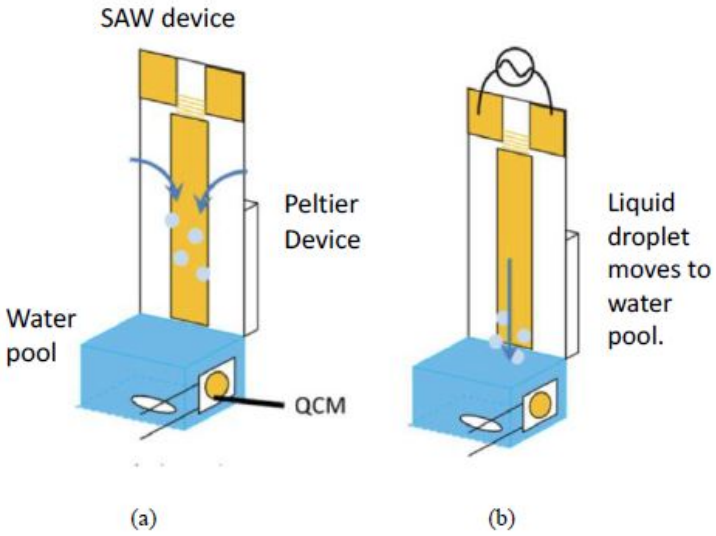

Figure 1.25: Proposed preconcentrator system. (a) odorant molecules are accumulated at the substrate surface and (b) liquid droplet is carried due to acoustic streaming effect. 2015 IEEE. Reprinted, with permission, from [53].

1.3.2 vapor phase

The major applications of QCM in vapor phase are gas sensing, humidity sensing and electronic nose. Volatile organic compounds (VOC) are organic chemicals that have a high vapor pressure at room temperature. VOC is responsible for the odor, scents, perfume, and also pollutants. In 1964, King developed the first QCM gas sensor with materials sensitive to detect various VOC [33]. The simple drop coating was used, and the experimental result shows the detection limit of xylene at 1 ppm. Some VOCs are dangerous to human health, while also frequently used in many industries. 2 polymers were investigated to use in Detecting VOC in manufacturing factory, poly(4-vinylbenzyl chloride) (PVBC) and poly(4-vinylbenzyl chloride-co-methyl methacrylate) (P(VBCco-MMA)) both polymers showed potential application in the monitoring and controlling the concentration of p-xylene vapor [54].

The breakthrough in electronic nose technology is the use of olfactory receptor cells(OR) and the neurophysiological of olfaction. Both of these can lead to an elaborated system for odor. The study of His6 tagged OR-10 immobilized to QCM with the Anti-His6 aptamer, the bond between aptamer and OR improved its frequency change response [55]. Its specificity to diacetyl was also evaluated, the measurement system diagram and QCM response is shown in figure 1.26. The usage of OR is fascinating but still very limited due to short lifetime of the cell and the complicated procedure in preparation.

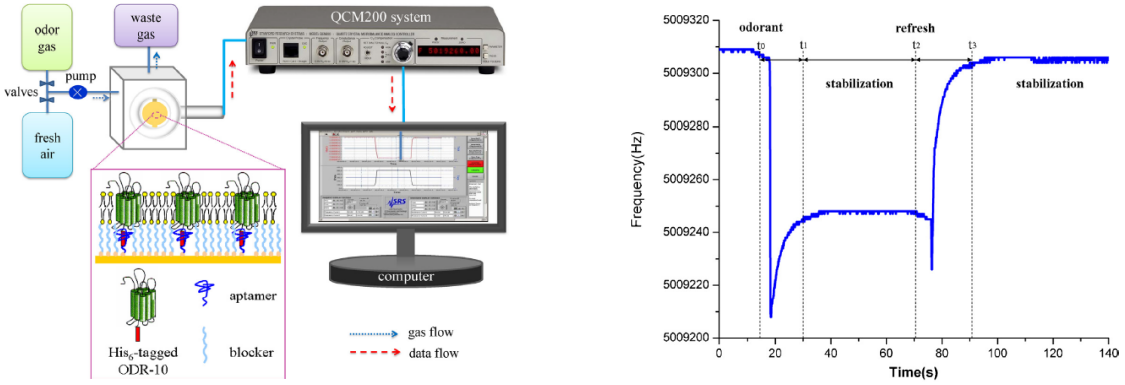

(a) (b)

Figure 1.26: Schematic and photo of QCM array (a)Piezoelectric olfactory receptor biosensor and measurement system. The inset figure illustrated the aptamer-assisted ODR-10 immobilization mechanism. (b)One typical odorant response cycle curve of the ODR-10 based QCM biosensor. Reprinted from [55], with permission from Elsevier.

The application of e-nose in the food sector is prominent, and QCM is one of the chosen sensors for this application. There was a study to identify the different type of Chinese liquors using an array of QCM with SVM classifier [46].

The application in food is not only classification but also the spoilage detection including meat product [56], where the freshness of beef fillet was monitored by QCMs based electronic nose compared with microbiological of total viable counts. The samples were classified into 3 quality class (fresh, semi-fresh, and spoiled). Overall classification accuracies of prediction above 89% for all 3 quality classes.

The discrimination analysis plot of beef fillet at different storing temperatures are shown in figure 1.27.

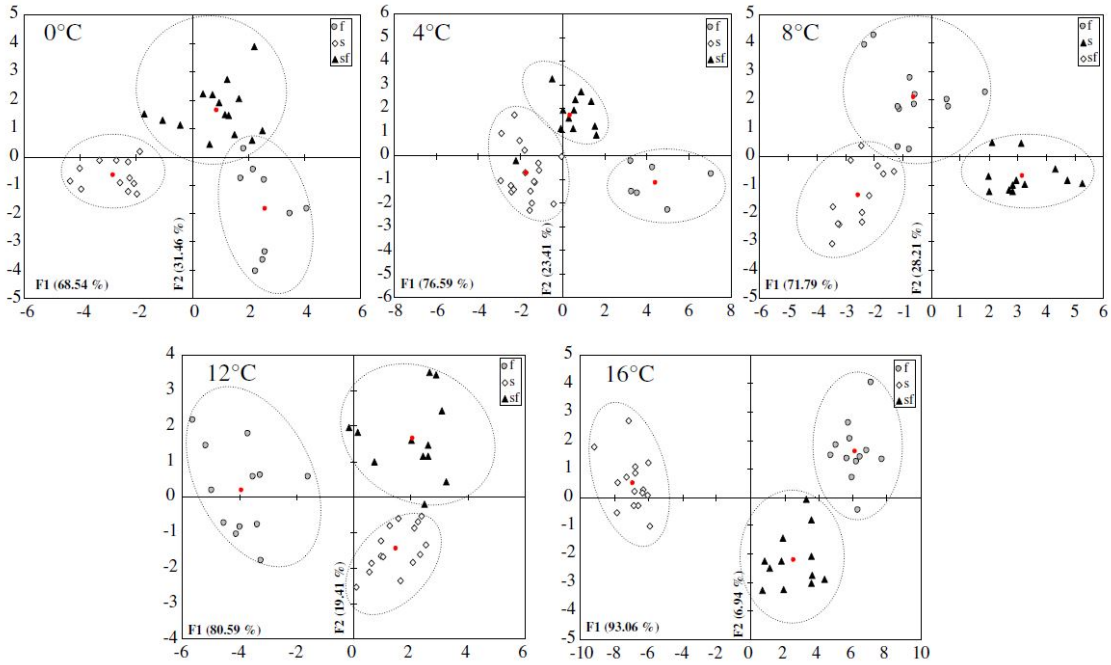

Figure 1.27: Discriminant analysis similarity map for the different sensory quality groups (fresh, semi-fresh, spoiled) of beef fillets stored at various temperatures as determined by the first two discriminant functions. (The red dots indicate the centroids of the clusters). Reprinted from [56], with permission from Elsevier.

E-nose can also detect ripeness or even the infection of fruit products. The ripeness of an apple typically measured by Streif index which measures the firmness of the apple. The QCM electronic nose system was used and calibrated the maturity according to Streif index. [57].

QCM based electronic nose also has it place in medical applications. Typically exhale breath analysis. The study of exhale gas to detect Blood Glucose and HbA1c level using a radial basis function neural network (RBFNN).The accuracies were 83.03% and 74.76% for HbA1c parameter predictions and glucose parameter predictions, respectively. The detection of lung Cancer utilizing electronic nose also had been studied. Air samples were collected in the lungs by endoscopic probe (figure 1.28a). Partial Least Squares Discriminant Analysis (PLS-DA) has been used. The electronic nose could discriminate between cancer and non cancer patients with more than 90% correct classification (figure 1.28b) [45].

Recent research on Room-temperature Ionic Liquid as a sensing material was an attempt by our group [50], this material has good stability and promising when using together with a conventional sensor.

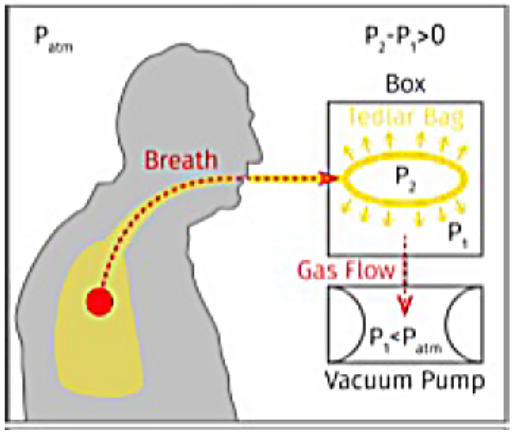

(a) Breath gas sampling procedure

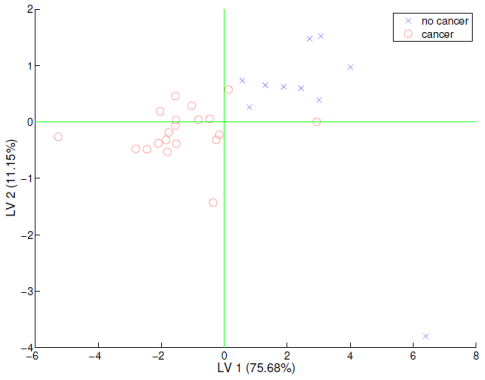

(b) Electronic nose data: scores plot of the PLS-DA

Figure 1.28: An Investigation about the origin of the lung cancer signalling VOCs in breath. 2014 IEEE. Reprinted, with permission, from [45].

1.4 QCM measurement methods

QCM structure is of crystal oscillator using in microcomputer was developed by Cady in 1921. With this similar structure, QCM can also be operated as an oscillator and measure the mass loading effect by indirectly estimate from oscillation frequency instead of the resonant frequency. However, as the damping becomes larger the lower Q factor cannot maintain stable oscillation. There are several methods to overcome this problem with a dedicated designed circuit or opt for the vector network analyzer.

1.4.1 Dedicated circuits

Dedicated circuits including oscillator circuits were the first approach to QCM sensing application. The most basic circuit which incorporating QCM is pierce oscillator (figure 1.29). The circuit consists of a digital inverter, feedback resister, and 2 capacitors. This design is used throughout microcomputer technology due to its simple design and good stability of clock generating application.

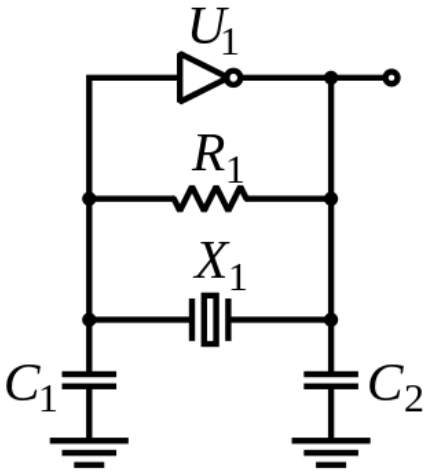

Figure 1.29: Pierce oscillator circuit diagram. Reproduced from Wikipedia under the Creative Commons Attribution-Share Alike 3.0 Unported License.

However, as the application of QCM has expanded to various sensing, the coating to improve QCM sensitivity is unavoidable and unfortunately, those coatings are viscous. This loading making the traditional oscillator circuit unstable many dedicated circuits need to be designed to solve this problem. Also the dissipation or loss in the QCM also a valuable parameter which can not be obtained from oscillator circuit alone but need an additional circuit.

The automatic gain control circuit together with frequency sweeping making it possible to extract both resonant frequency and Q factor as is shown in figure 1.30 [58]. However, the circuit consists of a lot of complicated electrical parts, and the accuracy in determining the resonant frequency still difficult due to difficulty in tracking the peak conductance.

Another proposal to detect both resonant frequency and loss in the QCM [59]. Using the oscillator circuit together with a relay switch to separate QCM from the oscillator circuitas is shown in figure 1.31. The result is the oscillation signal will

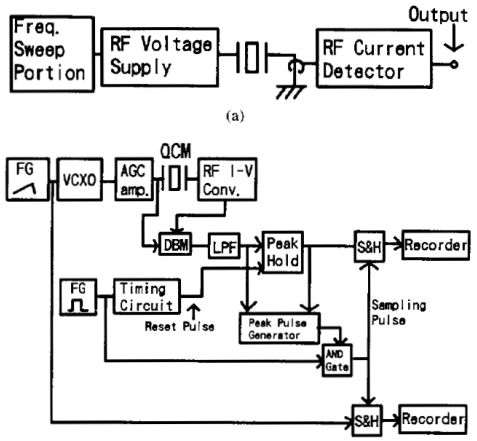

Figure 1.30: Circuit diagram of the system which measure both Q factor and resonant frequency. 1994 IEEE. Reprinted, with permission, from [58].

decay over time inversely proportional to the dissipation factor. The performance of this system was tested by a droplet of aqueous glycerol solution.

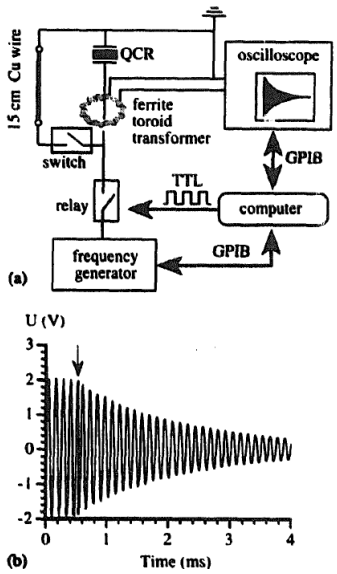

Figure 1.31: Circuit block diagram (a) schematic diagram. (h) Circuit diagram in detail. Reprinted from [60], with permission from Elsevier.

Not only at a fundamental frequency, but QCM can also be operated at a higher harmonic frequency which can be useful as some viscous loading because QCM behave differently at harmonic frequency [61]. Ferrari proposed an oscillator circuit that can excite and tracks two harmonic (figure 1.32) [62]. The automatic gain control is also included for measuring resistance values. More information can be extracted from a single quartz crystal resonator.

To simplify the QCM measurement system and reduce the cost, a recent approach in making the QCM measurement circuit using direct digital synthesizer (DDS) to generate several reference frequencies [63]. The frequency change will be measured using heterodyne demodulation from the oscillating signal. This simplifies the reference frequency generation. However, the dissipation is not measured in this

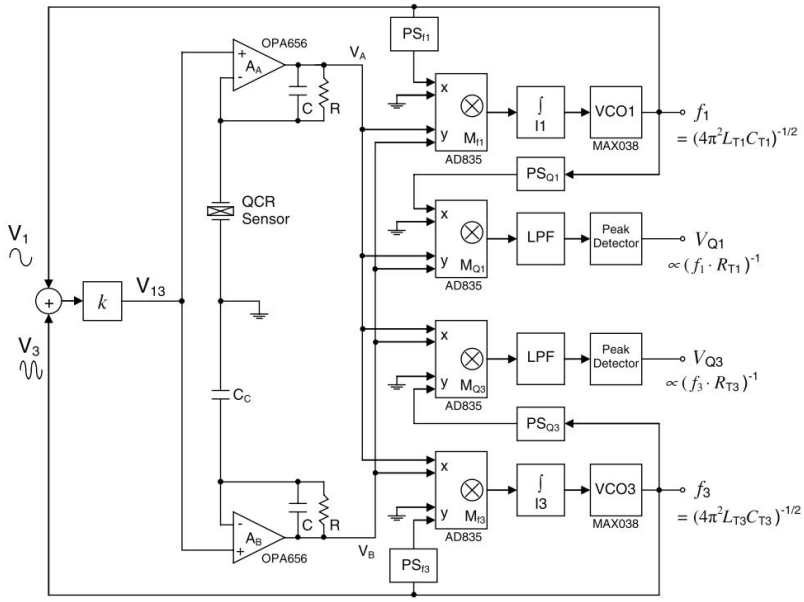

Figure 1.32: Block diagram of the dual-harmonic oscillator. Reprinted from [62] by permission from IOP Publishing, Ltd.

research.

The oscillator circuit is still applicable in a liquid environment. By carefully designing the circuit topology of the proposed active bridge oscillator, the stability of the oscillator immersed in water is drastically improved.

1.4.2 Vector Network analyzer

One of the biggest advantages of VNWA is that the resonant frequency of QCM can be directly extracted from the measurement. The frequency of the oscillation cannot always agree witht the resonant frequency change, the oscillation frequency is smaller when the loss increasing [64].This effect can be illustrated in figure 1.33.Although the loss due to viscous loading cannot be avoided, we can overcome this problem by using VNWA .

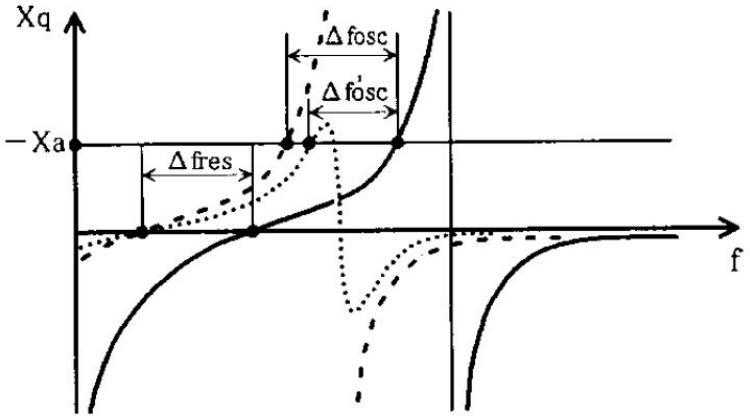

Figure 1.33: Dependendy of reluctance upon frequency, Solid line: No coating and no sorption, Thick dashed line: Only mass loading without loss increase, Thin dash ling: Mass Loading with additional loss. oscillation frequency deviates from actual resonant frequency change when loss increases. 1996 IEEE. Reprinted, with permission, from [64].

.

The Vector network analyzer is used to characterize two-port networks such as amplifiers and filters. The vector network analyzer utilizes the concept of measuring the transmitted and reflected waves as a signal passes through a device under test(DUT). The Vector Network Analyzer measures both the reflected signal from the input side, as well as the passes through the signal to the output side of the DUT. VNWA measurement in terms of S parameter. S parameter represents ratio of transmitted or reflected voltage to the incident voltage. S11 parameter is commonly used for QCM measurement. It indicates the ratio of reflected signal from port1 ($\frac{b_1}{a_1}$), where a_1 incident voltage at port 1 and b_1 is reflect voltage at port 1. The basic diagram of the vector network analyzer is as shown in figure 1.34.

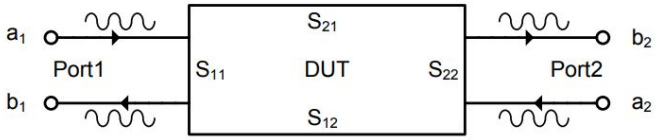

Figure 1.34: Basic concept of a vector network analyze.

To compensate for interface mismatch of the network analyzer and QCM, a PI network was proposed for QCM load matching [65]. However, the exact QCM parameter may not necessary for sensor application.

Figure 1.35: Small-sized vector network analyser

Typically, VNWAs are considerably large laboratory equipment and not suitable for portable applications. However, the full-size VNWA was used for pollen sensing [38]. The gas sensing applications also reported the use of VNWA to analyze the QCM response of NH_3 gas when the ZnO nanorod was synthesized on QCM. However, the dissipation factor was not utilized in data analysis [66]. To determine the improvement in sensitivity after modifying the QCM surface with Parylene-C, From figure 1.36 the authors chose a peak-to-peak value of measured impedance to indicate the signal to noise ratio [67]. Peak-to-peak value was evaluated similar to Q factor and found that after film deposition the peak-to-peak value was slightly improved. . The commercially available small-sizes QCM measurements with dissipation were investigated and compared the measurement result with bench-top VNWA, the results showed the difference of frequency measurement of 0.2%. This encouraged the use of small-sized VNWA. [68].

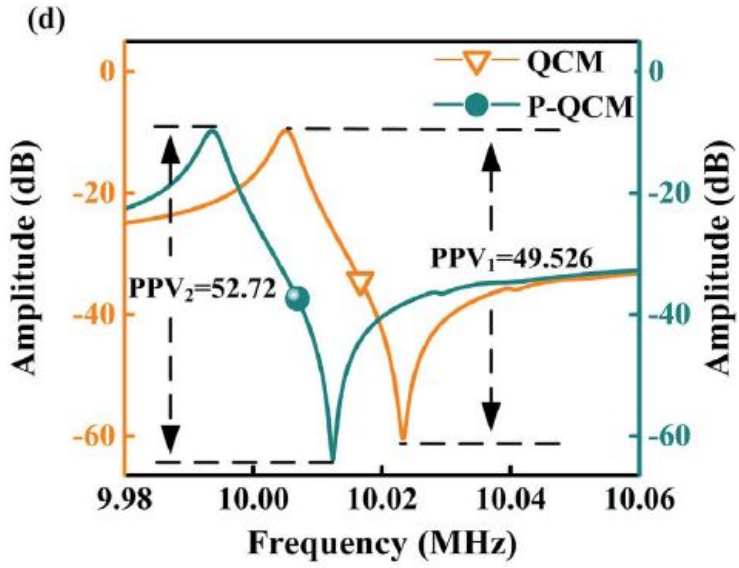

Figure 1.36: Evaluation of peak-to-peak value between typical QCM and Parylene-C coated QCM in air. Reprinted from [67], with permission from Elsevier.

.

However, recently the small-size NWAs are commercially available, an example is figure 1.35, making on-site measurement with an array of QCM sensors feasible. Our recent work using this small-sized network investigates the QCM sensor with RTIL coating materials for odorant sensing [50].

1.4.3 Summary

The developed QCM measurement methods typically including frequency and Q factor measuring. The oscillator circuit and frequency sweep technique were the prominent methods for resonant frequency measurement. While the method to measure Q factor has more variations. VNWA also becoming popular in recent years since there are several manufacturers that develop the small-sized VNWA.

Table 1.2: Summary of the recent QCM measurement methods

Title	**Principles**	**Advantages**	**Disadvantages**	**Ref.**
Development of Circuit for Measuring Both Q Variation and Resonant Frequency Shift of Quartz Crystal Microbalance.	Frequency sweep and Automatic gain control amplifier.	Complete design, test results comparable with Impedance analyzer.	Complicate circuit design. Difficulty in peak detection at low Q factor.	[58]
Frequency and dissipation-factor responses to localized liquid deposits on Frequency and dissipation-factor responses to localized liquid deposits on a QCM electrode.	Oscillator circuit , measurement of decay signal to calculate dissipation factor.	Relatively simple circuit, Dissipation factor can be calculated easily from time constant.	At high dissipation factor the time constant becomes shorter and harder to measure.	[59]
An oscillator circuit for dual-harmonic tracking of frequency and resistance in quartz resonator sensors.	Dual harmonic oscillator and Automatic gain control amplifier.	Fundamental and 3rd Harmonic operate simultaneously.	Need compensating capacitor to cancel out C_0, Circuit design a little bit complicated.	[62]
A DDS-based multi-harmonic frequency meter for QCM sensor applications.	Oscillator. Using Direct Digital Synthesizer (DDS) to synthesize reference frequency and measured frequency change using heterodyne.	Fully embedded measurement system. Operate at 3 harmonic frequencies.	Measure only frequency change, does not measure Q factor.	[63]
Stability enhanced, repeatability improved Parylene-C passivated on QCM sensor for aPTT measurement.	bench-top VNWA: Peak to peak value of s parameter was used to evaluate hydrophobicity.	Interesting choice of parameter to evaluate the result.	Did not utilize other parameter such as resonant frequency and dissipation factor.	[67]
Verification of Quartz Crystal Microbalance Array Using Vector Network Analyzer and small-sized VNWA.	Portable VNWA.	Comparison between portable VNWA and bench-top VNWA.	The measurement time and measurement method were not discussed here.	[68]
Simple and ultrafast resonance frequency and dissipation shift measurements using a fixed frequency drive.	Fixed frequency drive and network analyzer.	Operate at a single frequency ensures very fast measurement time of 112 us.	Limited information on circuit design.	[69]

1.5 Modeling of QCM behavior

QCM modeling are being continuously developed. The sensitivity film coating and the complexity of bonding to these layer making the detection behavior more complicated and its model is being developed. In this section we will discuss the proposed models from various researchers which are not used as a reference in our modelling. The related models will be discussed in the next chapter.

There was a proposal of "missing mass" concept which modified the mass term in sauerbrey equations making the equation also applicable to viscous film loading [70]. The effect of 'missing mass', predicts the reduction in liquid phase measurements of surface mass M_s comparing with the 'true' mass M of the film:

$$M_s = M\{1 - \frac{\eta_2\rho_2\omega}{\rho_1}\frac{G''}{G'^2 + G''^2}\}, M = \rho_1 h_1 \tag{1.2}$$

Some researcher propose the sensitivity of QCM sensor in terms of phase shift [71]. This equation showed the phase shift depends on the ratio of coating mass over the summation of unperturbed resonator and the liquid.

$$\phi \cong -\Delta m_c/(m_q + m_L), \Delta m_q = \eta_q\pi/2v_q, m_L = \rho_L\delta_L/2 \tag{1.3}$$

To differentiate the QCM response between mass loading and viscous loading is the challenge of using QCM sensor in liquid environment [72]. Since the usage of VNWA become more prevalent, the measure QCM conductance showed that the frequency at half maximum point does not shifted as shown in fig. 1.37.

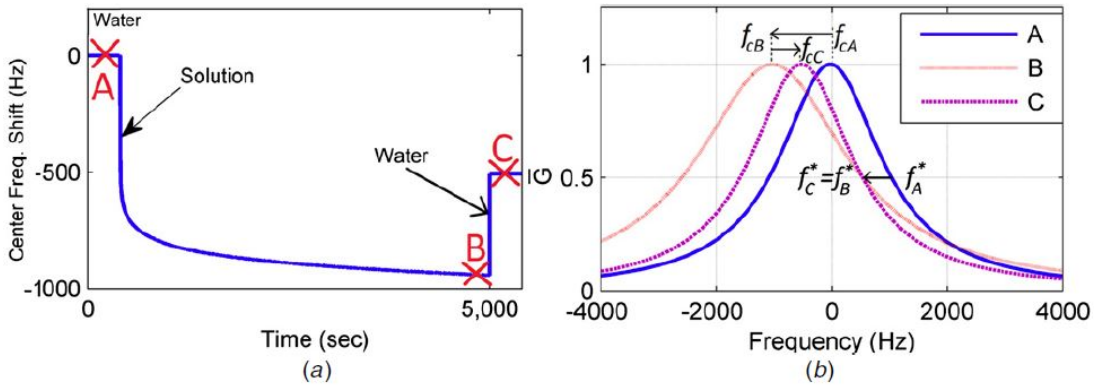

Figure 1.37: a) The center frequency shift of the crystal is depicted for mass adsorption in a viscous and dense fluid. Water is assumed to be the buffer solution. (b) Normalized conductance at different time points along the time trace of a measurement is simulated. Reprinted from [72] by permission from IOP Publishing, Ltd.

Separation between viscosity and density of liquid is also one of the most challenging problem for using QCM in liquid environment. Typically the frequency change is porportional to $\sqrt{\rho_L\eta_L}$, where ρ_L is the liquid density, η_L is the liquid viscosity. One study on this problem propose that the frequency shift not only contributed by $\sqrt{\rho_L\eta_L}$ but also the overall liquid volume and density as expressed in equation

$$\Delta f = K_{pf}\Delta P f_0 + K_{Tf}\Delta T f_0 \tag{1.4}$$

where K_{Pf} is the pressure-frequency sensitivity coefficient, K_{Tf} is the stress-frequency sensitivity coefficient, ΔP is the pressure variation, ΔT is the stress variation. The stress change caused by the liquid properties is:

$$\Delta T = C_{Lf}\sqrt{\rho_L \eta_L} \tag{1.5}$$

The pressure change induced by the added liquid on upper surface of QCM sensor can be given as:

$$\Delta T = C_{pf}\sqrt{\rho_L \eta_L} \tag{1.6}$$

where $C_P f$ is the pressure frequency coefficient, V_L is the liquid volume loaded onto the sensor surface. using These two equation they can resolve viscosity and density when at least 2 various liquid volumes were measured [73].

Since the QCM becomes more prominent in biosensing application, recent research of QCM model which focused on the living cells attachment was developed [74]. This model focused on spherical particle attachment in liquid environment. The result was the modification of equivalent circuit as is shown in figure 1.38.

There is also a developed model trying to explain posivitve frequency with a different concept. The authors proposed a QCM as as two weights connected with two springs(figure 1.39a). The simulation showed that under certain conditions QCM may response in positive frequency as is shown in figure 1.39b.

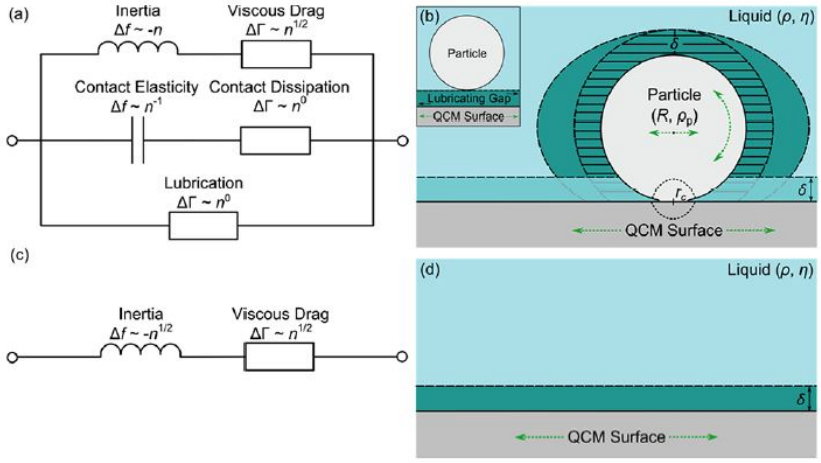

Figure 1.38: Proposed circuit for the load impedance showing the overtone dependence of inertial, elastic, and dissipative loads and corresponding physical picture for a particle adhering to the crystal (a, b) and a free crystal (c, d) oscillating in water. Darker shading designates regions in fluid affected by crystal and particle oscillations. Arrows designate the translational and rotational motion of the particle. Reprinted with permission from [74]. Copyright 2018 American Chemical Society.

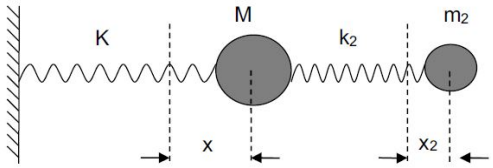

(a) Scheme and designations.

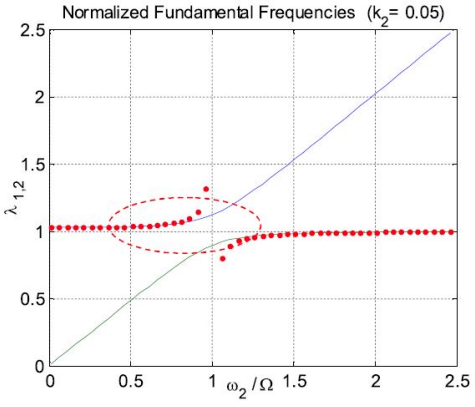

(b) Exact (lines) and approximate (points) roots of Eq. (4) for k2= 0.05.

Figure 1.39: QCM model as a system of two elastically bound weights. Reprinted from [75], with permission from Elsevier.

1.5.1 Summary

The development of QCM model was constantly under the interesting of many researchers. Some models are tailored to explain some mechanical interactions. Some model are more general and did not consider non uniform interaction

Table 1.3: Summary of the recent Modeling of QCM behavior

Title	**Principles**	**Advantages**	**Disadvantages**	**Ref.**
'Missing mass' effect in biosensor's QCM applications.	The modification to the concept of loading mass to have some correction factor for viscous loading.	Compatible with conventional sauerbrey equation.	Simulation result, investigate only a single layer model.	[70]
A different point of view on the sensitivity of quartz crystal microbalance sensors	The resonance phase shift indicate ratio of deposit mass over crystal and liquid mass	providing both simulation result and experimental result, the equations are simple and straight forward	The used of phase shift need dedicated circuit or NWA	[71]
Decoupling mass adsorption from fluid viscosity and density in quartz crystal microbalance measurements using normalized conductance modeling.	frequency half maximum value of QCM conductance does not change under liquid loading.	providing both simulation result and experimental result. The method is straight forward snd useful.	Need NWA, The equation did not suggest any new QCM behavior.	[72]
Separate density and viscosity measurements of unknown liquid using quartz crystal microbalance.	Propose to method to decoupling viscosity and density.	Rather sample method in separating viscosity from density by varying deposition volume.	The frequency due to volume change has small effect and difficult to practice.	[73]
Modeling QCM-D Response to Deposition and Attachment of Microparticles and Living Cells.	Modify QCM equivalent to accommodate the assumption of shperical particle attach to QCM in liquid environment.	providing both simulation result and experimental result.	The model cover only frequency change and not expand to dissipation. The model is not generalize.	[74]
QCM model as a system of two elastically bound weights.	Propose the QCM model as and elastic load with spring and two weights.	Different point of view. Maybe useful if there are experimental result to support.	Simulation result only. Does not suggest QCM interaction.	[75]

1.6 Purpose of research

QCM belongs to a gravimetric sensor which means it senses the deposited mass change. Gravimetric sensor is non specific to analyte, its selectivity owing to the coating with sensing material. This drawback can be compensated by its high mass sensitivity (1 ng/Hz for 9 MHz QCM), even the small change of mass of film properties can be detected. The structure of QCM is simple. it consists of quartz crystals sandwiched by electrodes. This made QCM relatively easy to manufacture and reduce its cost. Lastly, QCM has the highest Q factor among piezoelectric sensors and also can operate in thickness shear mode (TSM). These factors make it feasible to use QCM in viscous environments and also operable in both gas and liquid phases. This make QCM has a vast variety of applications including odorant sensor.

The parameters measured from a QCM are resonant frequency and resistance. Resonant frequency occurs due to the piezoelectric property of QCM, and its mechanical resonant frequency can be also converted to electrical components. Resonant frequency of QCM can be expressed as a series of inductors and capacitors. Resistor determines the sharpness of the resonant frequency response. The conventional method to extract resonant frequency is to use QCM in an oscillator circuit. The frequency counter was used to measure oscillator frequency which can be approximated as resonant frequency. The advantage of this method is the simplicity of circuit and also the accuracy of oscillation frequency. However, this is only possible if the Q factor remains high, if not the QCM may not be able to maintain its oscillation. Furthermore, this method cannot measure resistance. Additional circuits need to be implemented to measure this parameter.

Our measurement method proposes the use of VNWA to measure QCM parameters. Using VNWA ease the complication in designing dedicated circuit for measurement both resonant frequency and resistance. The conventional method for determining resonant frequency for VNWA is the motional admittance method by finding the resonant frequency at peak conductance curve. The shortcoming of VNWA is its sweeping frequency step depends on the number of datapoints, higher number of datapoints and decreased frequency step size. However, higher number of datapoints resulted in longer measurement time and the quantization error still exists. We propose a curve fitting method in real time to extract both resonant frequency and resistance value from the fitted model. Also the application of Savitzky-Golay filter to further smoothen the data without distortion. We expect our proposed measurement method should at least reduce the noise from derivatives in the motional admittance method. With the application of Savitzky-Golay filter our measurement should be able to operate even within a highly viscous environment.

The conventional models of QCM behavior are Sauerbrey equation and Kanazawa equation. Sauerbrey equation explains the “mass loading” behavior. Mass loading causes the QCM resonant frequency to decrease proportion to the amount of mass deposited on QCM. However, its limitation is the mass has to be firmly attached and rigid. Kanazawa approached the QCM from liquid application. The QCM frequency change is influenced by viscosity and density of the liquid. The limitation of both models is that it did not consider the viscous film which was not infinite thickness as in the case of the Kanazawa equation. Our proposed model is based

upon a mechanical stress equation and Mason equivalent circuit which represent one dimension model of QCM. This model was previously derived with rigid film and bulk liquid boundary condition and was found to be of Sauerbrey and Kanazawa equations, respectively. We want to further expand this equation to viscous film condition and expect to be able to explain the behavior of various viscosity films and predict unusual frequency behavior that we would like to reproduce.

Unusual frequency behavior of QCM when under exposure needs to be stated. Several researchers reported unusual positive frequency shifts even though the QCM sensor sorption was confirmed, usually a brief explanation of this behavior was given but not approached mathematically. Some researchers proposed models that predict the positive frequency change may occur under some conditions. However, the controlled sensor deposition combined with mathematical explanation has never been made. We want to reproduce various QCM responses including this unusual positive frequency change using a microdispenser to deposit water over various coating material, and also explain the response using our developed model. The merit of this research is that we expect our model to be generally applicable to various film conditions.

Thus, the purpose of the study is to reveal unusual behavior of QCM both theoretically and experimentally using noise reduction technique of a vector network analyzer.

1.7 Thesis structure

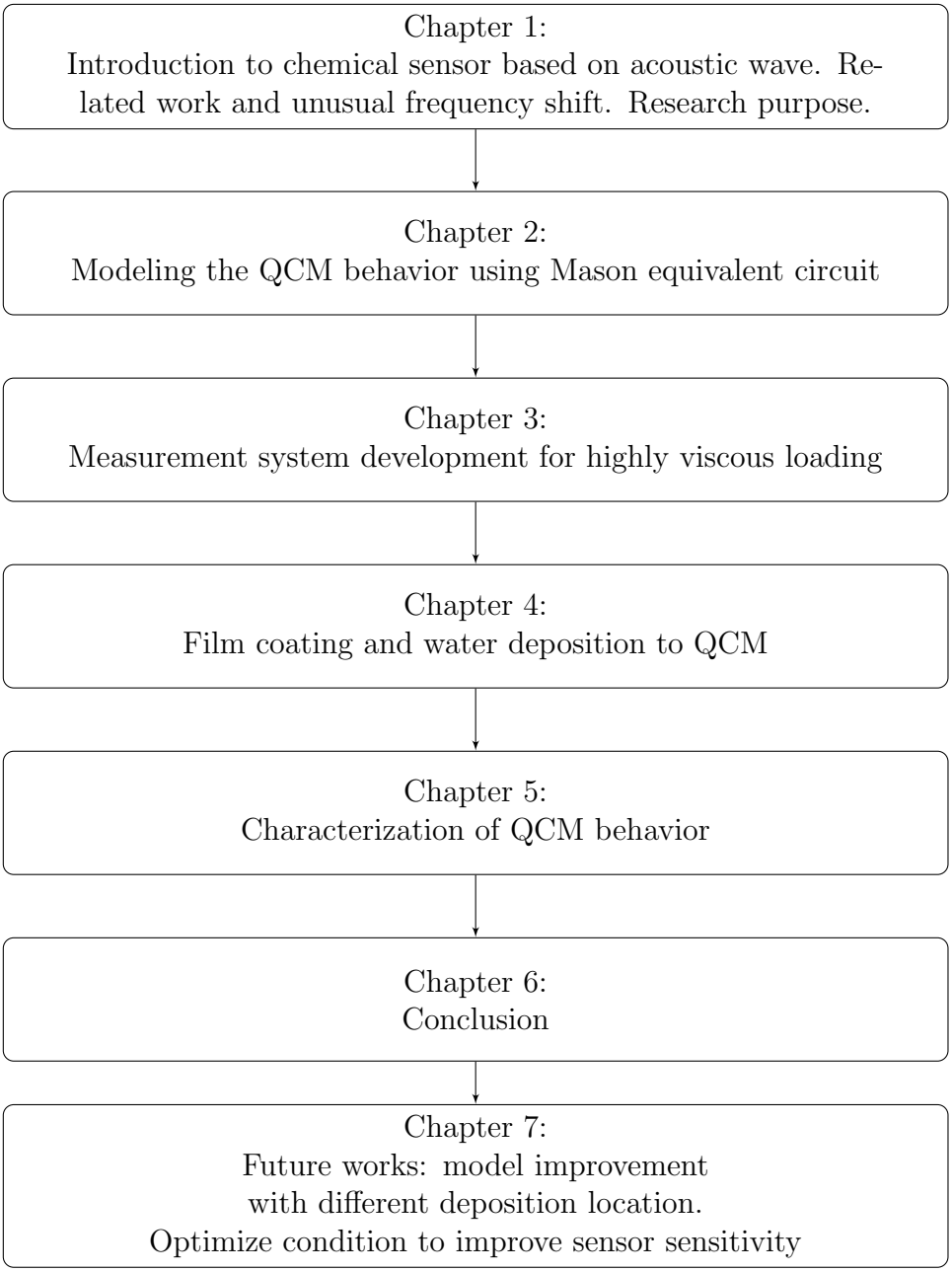

Figure 1.40: Structure of thesis

Chapter 2

Modeling of QCM

2.1 Principle of QCM

2.1.1 The piezoelectric effect

Piezoelectric effect occurs when certain materials become electrically polarized when they are strained. That is, when the material is deformed, the atoms in the crystal are displaced. The displacement produces electrical dipoles in the material. Some material, the summation of these dipoles generate an average macroscopic moment. This effect is called *direct piezoelectric effect* and occurs with the crystalline materials with no inversion symmetry.The direct piezoelectric effect is also reversible and this effect is called *converse piezoelectric effect*. The material becomes strained when under an applied electric field. The converse piezoelectric effect is the working principle of QCM.

Piezoelectricity is applied for many useful applications. such as microphone, micropump, piezoelectric inkjet printing, precision motor, clock generator and microbalances sensor.

2.1.2 Physical structure

The QCM structure consists of a certain cut of piezoelectric material coupled between conductive electrodes. When an electrical field is applied, the internal strain occurs in the quartz plate. If the frequency of the applied electric field is close to the resonant frequency of the crystal plate, the crystal stably vibrates (high Q factor). The simple structure of QCM is shown in figure 2.1.

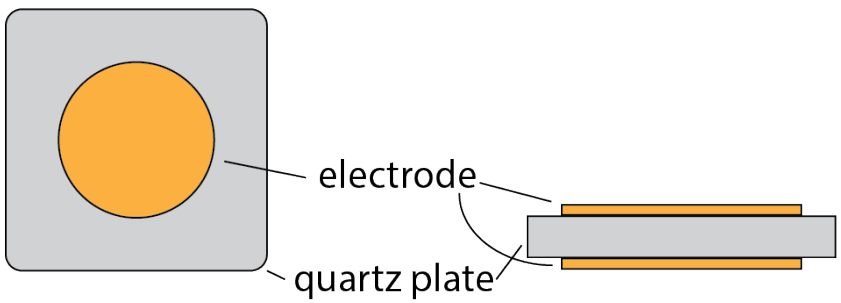

Figure 2.1: Basics structure of QCM

The specific characteristics depend on the mode of vibration and the angle at which the quartz is cut (relative to its crystallographic axes). The advantage of quartz crystal is that the frequency dependence on temperature is very low. AT-CUT crystal is the most common commercially available crystal cut, at an angle of 35°15‘ to the crystal z axis. The cut provides with frequency-temperature curve with inflection point at 25°C for thickness shear mode. The fundamental frequency of this crystal cut is between 1 and 30 MHz. QCM can also operate in overtone mode. One of the biggest advantages of QCM is its high Q factor, which can be as high as 10^6. This makes it possible to operate as an oscillator in sensing application.

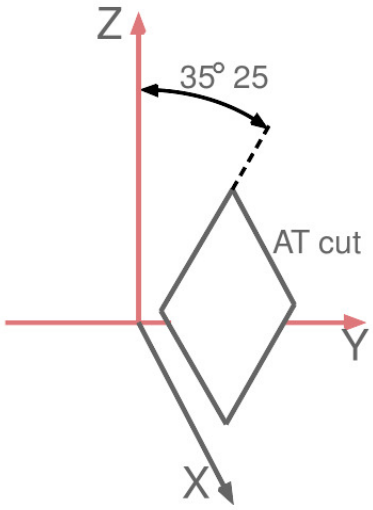

Figure 2.2: AT-CUT orientation of quartz.

2.1.3 QCM behavior in gas

QCM behavior in the gas phase means that the majority of the environment surrounding QCM is gas, which can be ambient atmosphere or the carrier gas through the gas flow system. The most simple behavior of QCM is the frequency change due to mass deposited or attached uniformly on the QCM surface.

The QCM frequency change with deposited mass was experimentally explained by Sauerbrey in 1959. The equation was made with the assumption of deposited mass as an extension of QCM thickness.This simplification made the relationship between frequency and mass become independent from electrode geometry. The Sauerbrey equation is defined as

$$\Delta f = -\frac{2f_0^2}{A\sqrt{\rho_q \mu_q}}\Delta m. \tag{2.1}$$

Where:
f_0 - Resonant frequency of the fundamental mode (Hz)
Δf - Frequency change (Hz)
Δm - Mass change (g)
A - Electrode area (cm^2)

ρ_q - Density of quartz (g/cm^3)
μ_q - Shear modulus of quartz for AT-cut crystal (g cm^{-1} s^{-2})

However, for Sauerbrey's equation to be applicable there are 3 conditions that need to be met: the deposited mass must be rigid, the deposited mass must be distributed evenly and the frequency change has to be less than 5% of $\Delta f/f$. The frequency change due to mass deposition is called " Mass loading" effect. Typically, Mass loading effect does not affect the Q factor of the QCM. The benefit is the frequency characteristic remains sharp, and the resonant frequency can be easily determined.

Sauerbrey's equation is good for measuring small amount of deposition and can be used to monitor coating film thickness since at the small film thickness the effect of loss due to viscosity is less significant than the amount of deposited mass which is the film thickness itself.

This equation is not valid for viscous loading including viscous film, bulk liquid, multi layer film or complicated structure such as porous polymer and biomaterials, etc. Some correction term to the deposited mass can be made to keep the equation valid for various types of material. However, Sauerbrey's equation only predicts negative frequency change. As discussed in chapter 1 , positive frequency change can be occured in many sensing applications. Further development in mathematical models to overcome the limitations of Sauerbrey's equation is needed.

2.1.4 QCM behavior in liquid

QCM behavior when immersed in liquid was developed in 1985 by Kanazawa, His calculation was based on shear velocity of liquid in contact with the quartz plate. His equation is defined as

$$\Delta f = -f_0^{3/2}(\frac{\eta_l \rho_l}{\pi \rho_q \mu_q})^{1/2}. \tag{2.2}$$

where:
f_0 - Resonant frequency of the fundamental mode (Hz)
η_l - liquid viscosity (cP)
ρ_l - liquid density (g/cm^3)
ρ_q - Density of quartz (g/cm^3)
μ_q - Shear modulus of quartz for AT-cut crystal (g cm^{-1} s^{-2})

This equation is based on vanishing shear waves into liquid, the distance the wave can travel into liquid is called penetration depth (figure 2.3). The definition of penetration depth is defined in equation 2.3. The shear wave amplitude attenuates to $1/e$ at the point λ away from the quartz plate.

$$\lambda = \frac{1}{2}\left(\sqrt{\frac{\rho_L \omega}{2\eta}}\right)^{-1} \tag{2.3}$$

The concept of penetration depth should define the maximum thickness of the liquid layer over the QCM that still influences the frequency shift. With this concept a certain thickness of viscous film can be estimated as bulk liquid and applicable

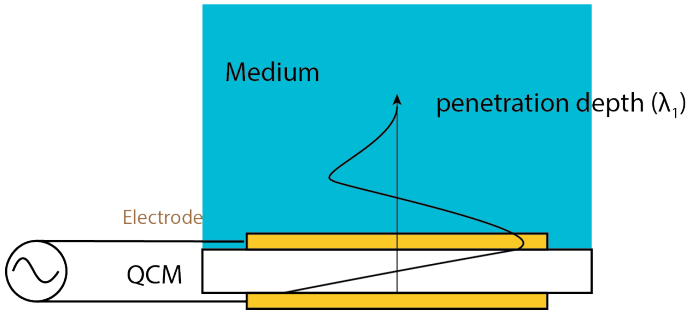

Figure 2.3: Penetration of QCM immersed in liquid medium.

to Kanazawa equation. The detection of frequency change is caused by viscosity or density change of the liquid layer.

However, many researchers found that the QCM responses are much more complicated. Sometimes the QCM frequency shifts even if the perturbation is beyond the penetration depth. The more unusual case was a positive frequency shift when exposed to measurand.

Kanazawa's equation is too simplified and did not consider coating layer thickness, which is one of the important parameters for sensor response. Also, similar to Sauerbrey's equation, the positive frequency change cannot be explained by Kanazawa's equation.

2.2 Mason equivalent circuit

In this section, we proposed the mason equivalent, derived from piezoelectric stress equation, This is one dimensional model and the notation is shown in figure 2.4.

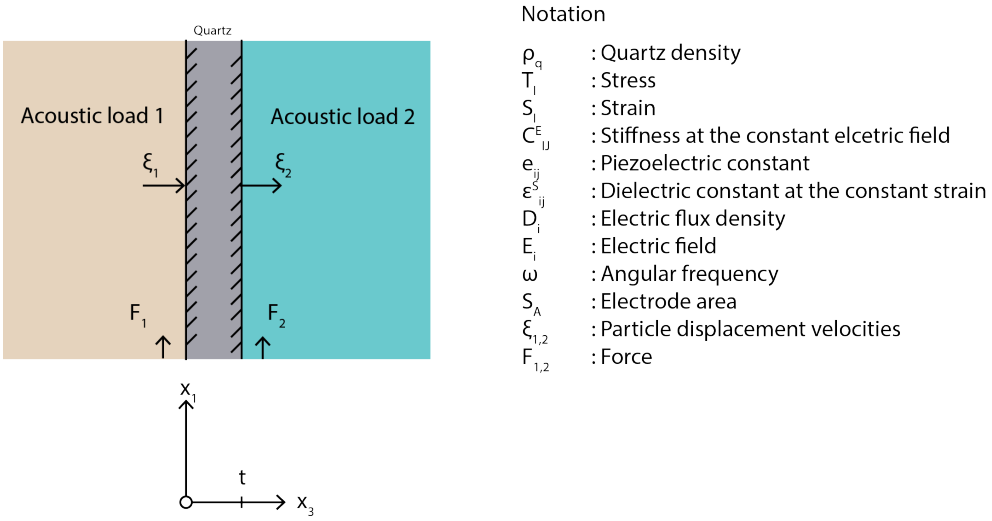

Figure 2.4: QCM model coordinate system and notations.

The AT-cut QCM operates in thickness shear mode(TSM). The piezoelectric

effect only couples in the direction x_1 in the figure 2.4. So, the piezoelectric equation is expressed as

$$\left.\begin{aligned} T_5 &= C_{55}^E S_5 - e_{35} E_3 \\ D_3 &= e_{33}^S E_3 + e_{35} S_5 \end{aligned}\right\} \tag{2.4}$$

Because of no net charge in quartz,

$$\frac{\partial D_3}{\partial x_3} = 0\,. \tag{2.5}$$

Equations 2.4 and 2.5, yield

$$\begin{aligned} \rho_q \frac{\partial^2 u_1}{\partial t^2} = \frac{\partial T_5}{\partial x_3} &= \frac{\partial}{\partial x_3}\left[C_{55}^E S_5 - e_{35}(D_3 - e_{35} S_5)/\varepsilon_{33}^S\right] \\ &= \left(C_{55}^E + \frac{e_{35}^2}{\varepsilon_{33}^S}\right)\frac{\partial^2 u_1}{\partial x_3^2}. \end{aligned} \tag{2.6}$$

From equation 2.6 the wave velocity is

$$v_q = \sqrt{C'_{55}/\rho_q}\,, \tag{2.7}$$

where

$$C'_{55} = C_{55}^E + e_{35}^2/\varepsilon_{33}^S\,. \tag{2.8}$$

The QCM surface forces F_1 and F_2, displacement current I and the voltage between two electrodes are derived from

$$F_{1,2} = S_A T_5|_{x_3=0,t}, I = (j\omega D_3) S_A \text{ and } V = -\int_0^t E_3\, dx_3\,, \tag{2.9}$$

where S_A is an electrode area. These expressions can be converted into Mason equivalent circuits, as is shown in figure 2.5. The mason equivalent circuit consists of two acoustic ports, representing acoustic characteristics of QCM surfaces, and one electrical port, representing electrical characteristics. Z_0 is the acoustic impedance (density*velocity) multiplied by the surface area. Φ is the transformer ratio. Z_1 and Z_2 are pure reactive components.

The mason circuit simplification and the various effects of acoustic loads will be described in the next section.

$$Z_1 = jZ_0 \tan(\omega l/2v_q), \quad Z_0 = \rho_q v_q S_A$$

$$Z_2 = -jZ_0 / \sin(\omega l/v_q), \quad \Phi = e_{35} \cdot S_A / t$$

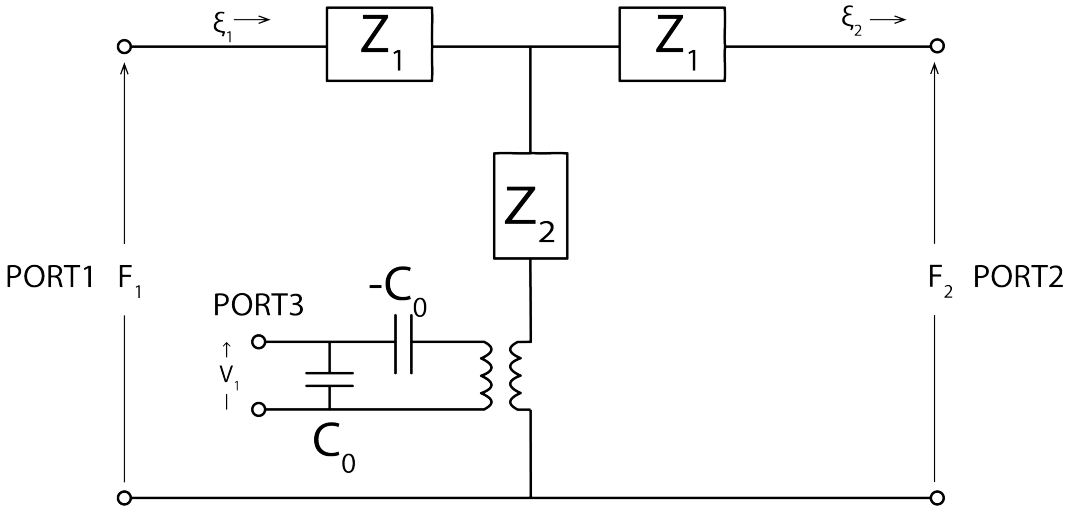

Figure 2.5: Mason equivalent circuit.

2.3 Butterworth-Van Dyke circuit

Mason equivalent circuit can be further simplified. The simplification gives us an easier interpretation of QCM response. Assuming port 1 is a shorted circuit, indicating its stress-free surface. Port 2 is the QCM surface which is exposed to various kinds of acoustic loading. We will consider the conditions of loading in the later section. Since we shorted the port 1, the circuit collapsed into figure 2.6.

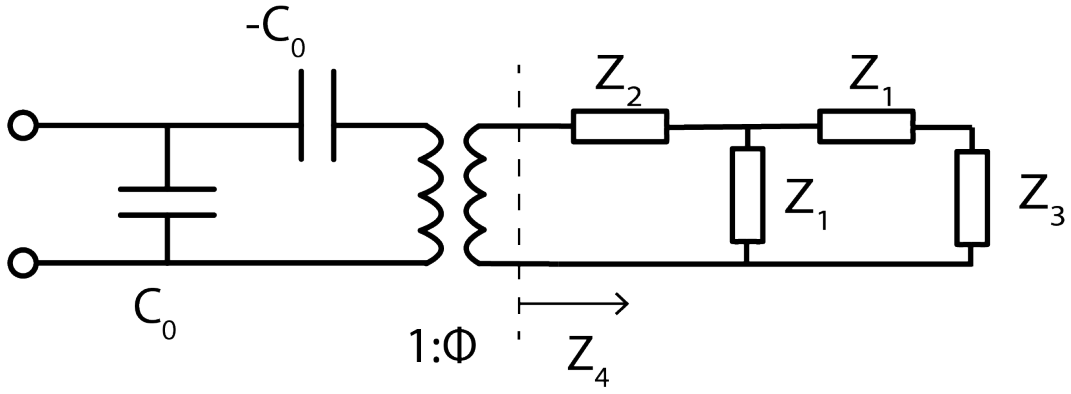

Figure 2.6: Transformation of Mason equivalent circuit. Excerpt from [76].

Z_3 is the acoustic load of port 2. Z_4 is the impedance seen from the dash line to right side. It is given by

$$Z_4 = Z_2 + \frac{Z_1(Z_1 + Z_3)}{2Z_1 + Z_3}. \tag{2.10}$$

Z_1 and Z_2 were defined in terms of Z_0, equation 2.10 is changed to

$$Z_4 = Z_5 + \frac{1}{1/Z_6 + 1/Z_7} \tag{2.11}$$

where:

$$Z_5 = (-j/2)Z_0 \cot \frac{\omega t}{2v_q}\,, \tag{2.12}$$

$$Z_6 = \frac{Z_3}{4} \tag{2.13}$$

and

$$Z_7 = j\frac{Z_0}{2} \tan \frac{\omega t}{2v_q}\,. \tag{2.14}$$

Utilizing Mittag-Leffer's theorem, tangent function can be expanded as

$$\frac{\tan a}{a} = \sum_{n\ odd}^{\infty} \frac{P_n}{1 - (a/a_n)^2}, \tag{2.15}$$

where

$$P_n = \frac{1}{n^2}\frac{8}{\pi^2}\ ,\ a_n = n\pi/2\,. \tag{2.16}$$

When the fundamental mode is considered, only the case n equals to one is considered. If the overtone mode is included, the higher number of n needs to be taken into consideration. Using equations 2.15 and 2.16, these simplify equations 2.12 and 2.14 to

$$Z_5 = \frac{jZ_0t}{8v_q}\omega - j\frac{\pi^2 Z_0 v_q}{8t}\frac{1}{\omega} \tag{2.17}$$

and

$$Z_7 = \frac{1}{\frac{1}{j\omega 2Z_0t/\pi^2 v_q} + j\frac{t}{2Z_0v_q}\omega}, \tag{2.18}$$

where only the fundamental mode is considered. Therefore, the equivalent circuit in figure 2.6 is simplified into figure 2.7(a). At near resonant frequency the parallel L and C in figure 2.7(a) can be ignored. This parallel tank needs to be taken into consideration if the frequency shift is considerably large.

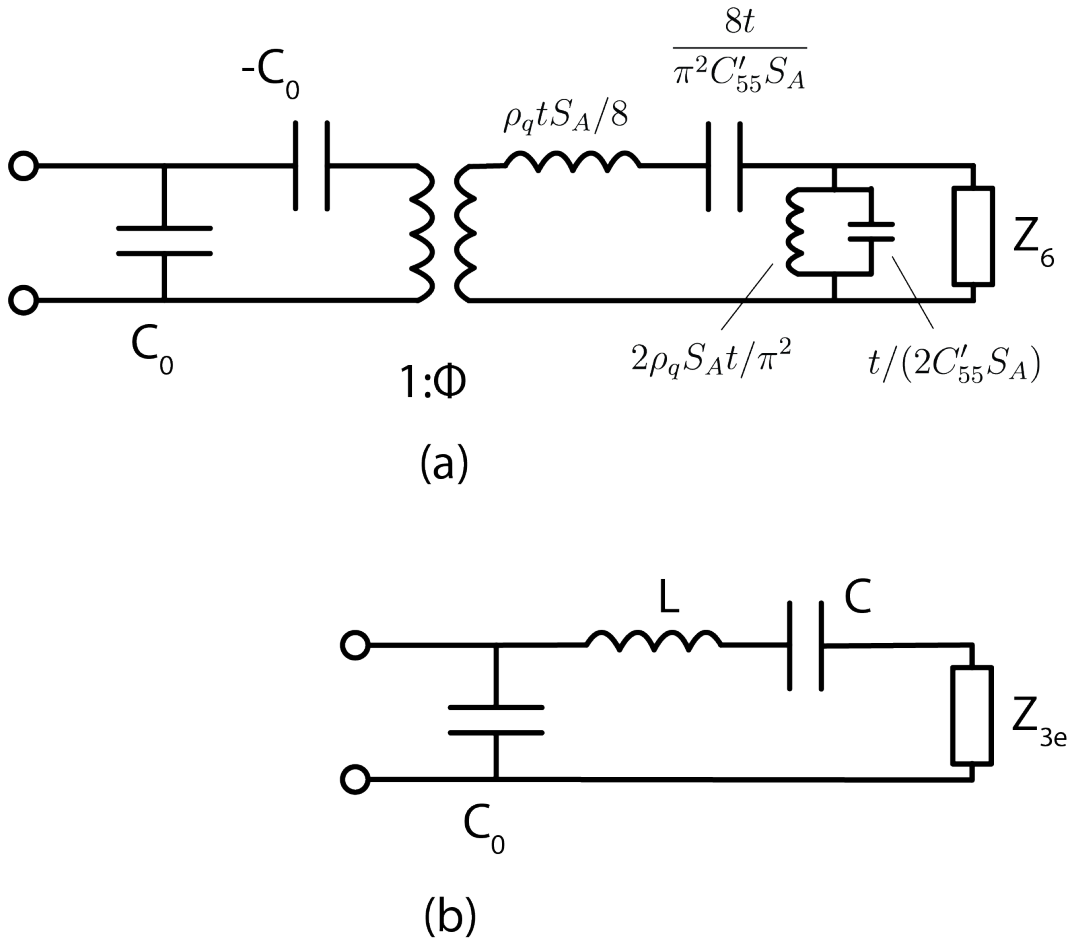

Figure 2.7: Simplified Mason equivalent circuit. (a) The simplify circuit that retains the transformer, (b) the final equivalent circuit (Butterworth-Van Dyke circuit).

Transformer part of the equivalent circuit in figure 2.7(a) can be further simplified to equivalent circuit in 2.7(b). This circuit topology is called Butterworth-Van Dyke circuit. The component L,C and Z_{3e} are given by

$$L = \frac{\rho_q t^3}{8e_{35}^2 S_A}, \tag{2.19}$$

$$C = \frac{-C_0 C'}{-C_0 + C'}, \tag{2.20}$$

where

$$C_0 = \varepsilon_3^S 3\varepsilon_0 S_A / t, \tag{2.21}$$

$$C' = \frac{8 S_A e_3^2 5}{\pi^2 C_5' 5t} \tag{2.22}$$

and

$$Z_{3e} = \frac{S_A Z_3}{4\phi^2} = \frac{t^2 Z_3}{4e_{35}^2 S_A}\,. \tag{2.23}$$

2.3.1 Electrical Admittance

In this section, we will discuss Butterworth-Van Dyke (BVD) circuit which is the final product of simplification of Mason equivalent circuits. The BVD circuit (figure 2.8) consists of resonant components R_1, L_1 and C_1 in parallel with C_0. Typically, when the acoustic loading occurs, the additional resistance and reactance is added to the resonant part. While the C_0 is an intrinsic capacitance due to an electrode coupled with piezoelectric material which also has dielectric constant value.

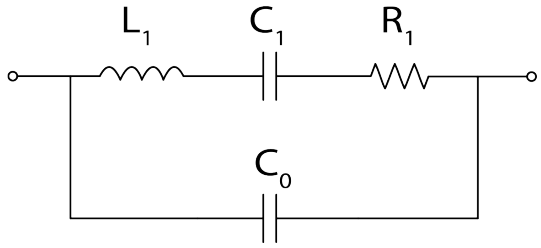

Figure 2.8: Butterworth-Van Dyke model

The Butterworth-Van Dyke (BVD) circuit can simply explain QCM behavior around resonant frequency. The admittance plot of BVD circuit is shown in figure 2.9. The direction of frequency sweep is indicated by arrows.

The admittance plot is a relatively round circle with the Y-offset equal to ωC_0 this is considered constant around resonant frequency value. The series resonance frequency is the right most point of the admittance plot, which is the maximum conductance value. The distance from y-axis to this point is the reciprocal of the resistance R_1 in the BVD equivalent circuit.

The admittance of BVD circuit is expressed as

$$Y = \frac{1}{R_1 + j\omega L_1 - \frac{1}{j\omega C_1}} + j\omega C_0\,. \tag{2.24}$$

Considering only real part of admittance (conductance), the equation can be rearranged as

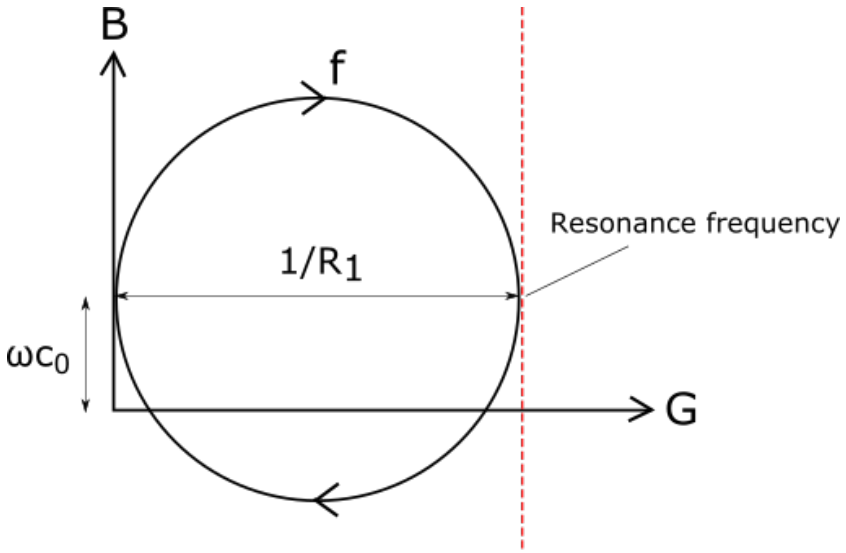

Figure 2.9: Admittance plot of QCM

$$G = \frac{R_1}{R_1^2 + \left(2\pi f L_1 - \frac{1}{2\pi f C_1}\right)^2}. \tag{2.25}$$

This equation 2.25 includes only circuit components from the resonant part without involving C_0. This is useful for extracting resonant frequency and resistance value using only conductance.

2.3.2 Resonant frequency and Resistance

The resonant frequency and resistance are the commonly measured parameters from QCM. Resonant frequency is the most prevalently used. Mainly, due to the conventional equation being developed based on frequency change. This makes sense because the previous usage of QCM is to act as a resonant port for oscillator application.

The QCM resonant frequency is determined by its crystal properties and mechanical dimension of QCM such as crystal plate thickness and electrode area. Sauerbrey's equation indicates negative frequency shift, this can be interpreted to be that there is additional reactance to the resonant branch of BVD circuit.

Resistance determines the sharpness of frequency response which influences Signal-to-noise ratio or quality factor. QCM with low quality factor cannot be used in an oscillator because the stable positive feedback of oscillating frequency cannot be maintained. In terms of resonant frequency measurement, the dependency of conductance upon frequency becomes dull and the detection of the peak response also becomes difficult.

Q factor is alternatively defined as the ratio of a resonator's centre frequency to its bandwidth, for more general definition Q factor is the ratio of angular frequency times maximum energy stored to power loss. These two definitions are identical. Higher Q indicates a lower rate of energy loss and the oscillations die out more slowly. A pendulum suspended from a high-quality bearing, oscillating in air, has a high Q, while a pendulum immersed in oil has a low one. Resonators with high quality factors have low damping, and thus they ring or vibrate longer.

2.4 Boundary conditions for various film attachment

In this section, various acoustic loads model and its boundary conditions are introduced. Then, we solved the acoustic impedance for each proposed model.

2.4.1 Rigid film

Consider the thin solid film is uniformly attached on a quartz plate, as illustrated in figure 2.10.

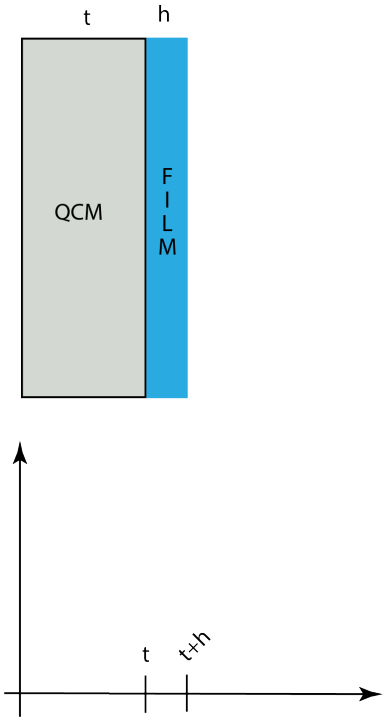

Figure 2.10: Model of mass loading (rigid film)

Whose film thickness is h; shear wave velocity, v_{A1}; and density, ρ_A. The particle displacement equations of u_1 and the shear stress T_5 in the deposited layer are expressed as

$$u_1 = Ae^{-j(\omega/v_{A1})x_3} + Be^{j(\omega/v_{A1})x_3} \tag{2.26}$$

and

$$T_5 = \mu S_5 = \mu \frac{\partial u_1}{\partial x_3} = j\frac{\omega}{v_{A1}}\mu \left(-Ae^{-j(\omega/v_{A1})x_3} + Be^{j(\omega/v_{A1})x_3}\right) \tag{2.27}$$

where A and B are constant,μ is film shear modulus. Consider the film surface at $X_3 = t + h$, the stress is free ($T_5 = 0$). The ratio of A to B can be derived to

$$\frac{A}{B} = e^{j(2\omega/v_{A1})(t+h)} \tag{2.28}$$

Using equations 2.26, 2.27 and 2.28, the acoustic impedance can be solved to

$$Z_{3M} = -\frac{T_5}{j\omega u_1}\bigg|_{x_3=t} = \frac{\mu}{v_{A1}}\frac{1-e^{j(2\omega/v_{A1})}}{1+e^{j(2\omega/v_{A1})}} = jZ_{A1}\tan\frac{\omega h}{v_{A1}}, \tag{2.29}$$

where $Z_{A1} = \rho_{A1}v_{A1}$.

Tangent function can be approximated to the argument value itself when the argument value is much less than 1. When $\omega h/v_{A1} << 1$, $\tan(\omega h/v_{A1}) \approx \omega h/v_{A1}$ and equation 2.29 reduces to

$$Z_{3M} = j\rho_{A1}v_{A1}\frac{\omega h}{v_{A1}} = j\omega dM/S_A, \tag{2.30}$$

Where dM is the deposited mass. From equations 2.23 and 2.29 it is found that the impedance Z_3 is purely inductive. The mass loading contributes to inductance increase, dL describe as below.

$$dL = \frac{t^2}{4e_{35}^2 S_A}\frac{dM}{S_A} \tag{2.31}$$

The resonant frequency is defined as

$$f_r = 1/(2\pi\sqrt{LC}). \tag{2.32}$$

When there is mass loading, the resonant frequency shift to $f_r + df$, which is expressed by

$$f_r + df = \frac{1}{2\pi\sqrt{(L+dL)C}} \approx \frac{1}{2\pi\sqrt{LC}}(1 - dL/2L), \tag{2.33}$$

assuming that $dL << L$. The frequency shift is

$$df = -\frac{1}{2\pi\sqrt{LC}}\frac{dL}{2L}, \tag{2.34}$$

Combining equations 2.20, 2.22, 2.32, and 2.35, df becomes

$$dL = -f_r\frac{dM}{\rho_q t S_A} = -f_r\frac{dM}{M}, \tag{2.35}$$

where M is the mass of the quartz plate. This equation 2.35 is the same as Sauerbrey's equation, proven that the df is the function of film mass only. This remains true if the frequency shift is not too large.

2.4.2 Bulk liquid

In case of liquid loading, its model is shown in figure 2.11. Liquid loading influences both resonant frequency and Q factor of the QCM. The equation of motion incase of liquid is expressed as

$$\rho_L \frac{\partial^2 u_1}{\partial t^2} = \frac{\partial T_5}{\partial x_3} \tag{2.36}$$

and

$$T_5 = j\omega\eta S_5, \tag{2.37}$$

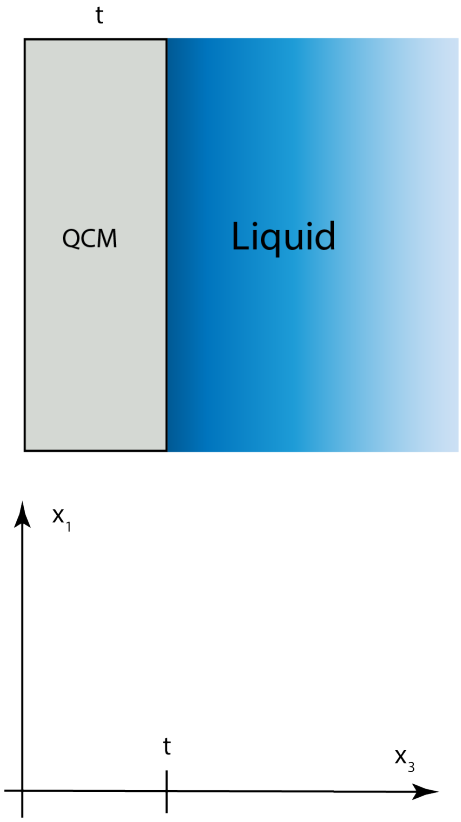

Figure 2.11: Model of liquid loading

where ρ_L is liquid density and η is viscosity. By substituting equation 2.37 into equation 2.36, the wave velocity is

$$v_w = \sqrt{\frac{j\omega\eta}{\rho_L}}. \tag{2.38}$$

The equation 2.37 indicates that the wave is evanescent, we can eliminate the positive exponential terms for the liquid loading case. This yield,

$$u_1 = Ue^{-j(\omega/v_w)x_3} \tag{2.39}$$

where U is constant.

Utilizing equations 2.37 and 2.39, the acoustic impedance of liquid is given by

$$Z_{3L} = -\frac{T_5}{j\omega}\bigg|_{x_3=t} = \sqrt{j\omega\eta\rho_L} = \sqrt{\frac{\omega\eta\rho_L}{2}} + j\sqrt{\frac{\omega\eta\rho_L}{2}}, \tag{2.40}$$

Substitute Z_{3L} into equation 2.23, the electrical impedance is

$$Z_{3e} = \frac{t^2}{4e_{35}^2 S_A}\sqrt{j\omega\eta\rho_L} = \frac{t^2}{4e_{35}^2 S_A}\left(\sqrt{\frac{\omega\eta\rho_L}{2}} + j\sqrt{\frac{\omega\eta\rho_L}{2}}\right). \tag{2.41}$$

This equation indicates that liquid loading causes both resistance change and frequency change.

2.4.3 Viscous film

In case of, viscous film. This condition is expanding the rigid film condition to cover viscous film. The boundary condition is by replacing shear wave velocity term with shear wave velocity in liquid. This concept ignores the imaginary part of complex viscosity. however it simplifies the equation and still proven to be useful in predicting viscous film response.

The model is similar to figure 2.10. The only different condition is the liquid shear wave velocity was used. let us substitute equation 2.38 into equation 2.29, it becomes

$$Z_{3e} = \frac{t^2}{4e_{35}^2 S_A} j\sqrt{j\rho_L\eta_L\omega}\tan(\omega h\sqrt{\frac{\rho_L}{j\omega\eta_L}}) \tag{2.42}$$

The simulation using this equation with the parameters of water as film material is shown in figure 2.12.

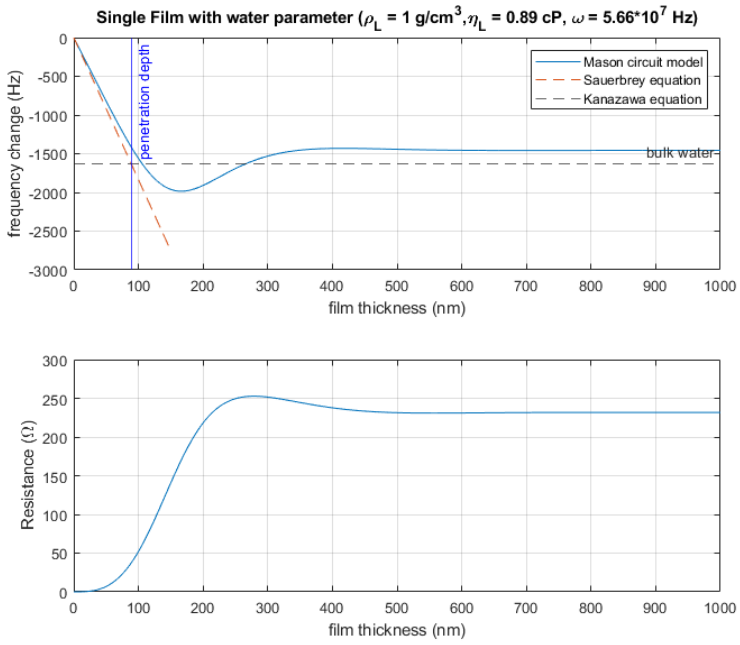

Figure 2.12: QCM response simulation using Mason equivalent circuit, using parameters of water

The simulation using water parameters of 9 MHz QCM and water, $\rho_L = 1$ g/cm^3, $\eta_L = 0.09$ cP, $\omega = 5.66\text{x}10^7$ Hz, t=200 um, $S_A = 0.196$ cm^2, e_{35} = -0.095, L = 12.65 mH, C = 2.47x10^{-14} F. The simulation showed that the frequency change at small loading is agreeable with Sauerbrey's equation and at infinity the frequency change converges to that of Kanazawa's equation. The film thickness higher than penetration depth exhibits an interesting transition. Consider frequency change of the figure. The negative frequency continues to decrease as the film thickness increases until around 170 nm. Then, the direction of frequency shift goes inversed toward increasing and then saturates. Resistance change follows a similar trend but the resistance increases first and until around 260 nm slightly decreases and then saturates. Interestingly, the turning points of frequency shift and resistance are different film thickness. This property becomes important in explaining why positive frequency change occurs while the resistance still increases.

Figure 2.13 shows the simulation while varying the viscosity from 1 cP to 10 cP. The plot shows that as the viscosity increases the film thickness which is related to minimum frequency point also increases. The overall negative frequency change also increases.

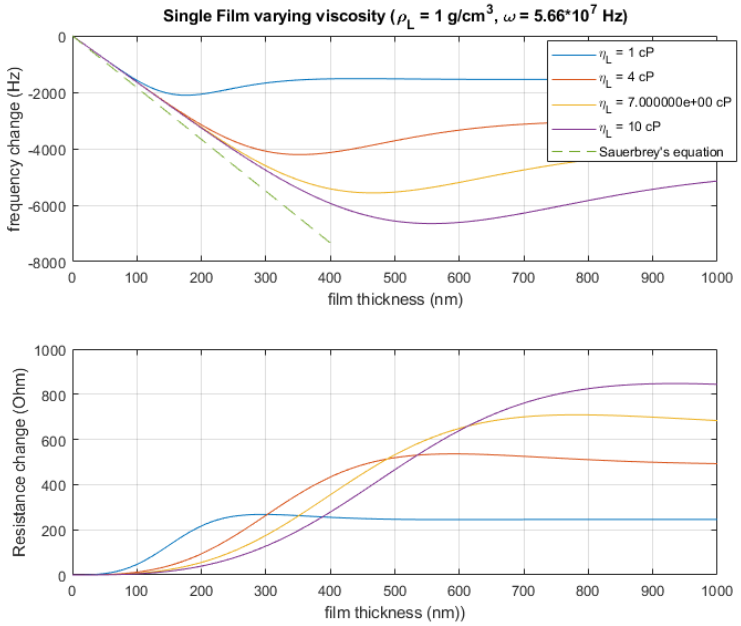

Figure 2.13: QCM response simulation using Mason equivalent circuit varying viscosity

Equation 2.42 will be our main tool for investigating various QCM responses since it is a more generalized equation that can also explain rigid film and liquid loading.

2.4.4 Two-layer film

In this section, we propose the extension of film layer to double layers. The model is shown in figure 2.14.

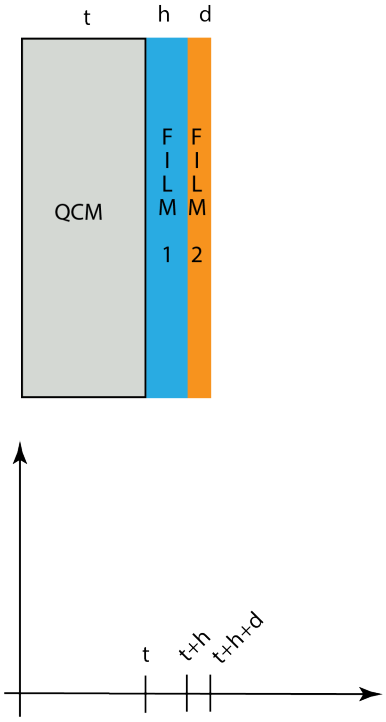

Figure 2.14: Model of double viscous film

Consider the outermost surface: $x_3 = t + h + d$
The particle displacement is: $U_2 = A_2 e^{\frac{-j\omega x_3}{v_{A2}}} + B_2 e^{\frac{j\omega x_3}{v_{A2}}}$, where v_{A2} is shear velocity of film 2. Shear stress of film 2 is expressed as

$$(T_5)_{film2} = \mu_2 S_5 = \mu_2 \frac{\partial u_2}{\partial x_3} = j\frac{\mu_2 \omega}{v_{A2}} \left[-A_2 e^{\frac{-j\omega x_3}{v_{A2}}} + B_2 e^{\frac{j\omega x_3}{v_{A2}}} \right] \tag{2.43}$$

Stress is free at the out most surface ($T_5 = 0$), the ratio of A_2 and B_2 is given by,

$$\frac{A_2}{B_2} = e^{\frac{2j\omega(t+h+d)}{v_{A2}}} \tag{2.44}$$

Consider the contact point of film 1 and film 2 ($x_3 = t + h$), the particle displacement of film 1 is $U_1 = A_1 e^{\frac{-j\omega x_3}{v_{A1}}} + B_1 e^{\frac{j\omega x_3}{v_{A1}}}$.
The stress equations of film 1 and film 2 are expressed as

$$(T_5)_{film1} = \mu_1 \frac{\partial U_1}{\partial x_3} = \mu_1 \frac{j\omega}{v_{A1}} \left[A_1 e^{\frac{-j\omega x_3}{v_{A1}}} + B_1 e^{\frac{j\omega x_3}{v_{A1}}} \right]. \tag{2.45}$$

$$(T_5)_{film2} = \mu_2 (\frac{j\omega}{v_{A2}}) \left[A_2 e^{\frac{-j\omega x_3}{v_{A2}}} + B_2 e^{\frac{j\omega x_3}{v_{A2}}} \right]. \tag{2.46}$$

Utilizing equations 2.45 and 2.46 and the continuity of T_5 at $x_3 = t+h$, the ratio of $\frac{A_1}{B_1}$ can be expressed as,

$$\frac{A_1}{B_1} = \frac{\left[(v_{A1} - v_{A2}) + (v_{A1} + v_{A2})e^{\frac{2j\omega d}{v_{A2}}}\right]}{\left[(v_{A1} + v_{A2}) + (v_{A1} - v_{A2})e^{\frac{2j\omega d}{v_{A2}}}\right]} e^{\frac{2j\omega(t+h)}{v_{A1}}} \tag{2.47}$$

Utilizing equations 2.45, 2.46 and 2.47, the acoustic impedance at $x_3 = t$ is

$$Z_{3L2} = \frac{-T_5}{j\omega u_1}\bigg|_{x_3=t} = \frac{\left[\frac{-A_1}{B_1}e^{\frac{-2j\omega t}{v_{A1}}} + 1\right]}{\left[\frac{A_1}{B_1}e^{\frac{-2j\omega t}{v_{A1}}} + 1\right]} \tag{2.48}$$

Substitute Z_{3L2} by equation 2.47, the acoustic impedance is

$$Z_{3L2} = \frac{\mu_1}{v_{A1}} \left\{ \frac{(v_{A1} + v_{A2})\left(1 - e^{2j\omega[\frac{d}{v_{A2}} + \frac{h}{v_{A1}}]}\right) + (v_{A1} - v_{A2})\left(e^{\frac{2j\omega d}{v_{A2}}} - e^{\frac{2j\omega h}{v_{A1}}}\right)}{(v_{A1} + v_{A2})\left(1 + e^{2j\omega[\frac{d}{v_{A2}} + \frac{h}{v_{A1}}]}\right) + (v_{A1} - v_{A2})\left(e^{\frac{2j\omega d}{v_{A2}}} + e^{\frac{2j\omega h}{v_{A1}}}\right)} \right\} \tag{2.49}$$

We checked the validity of the equation2.49 by letting $v_{A1} = v_{A2}$

$$Z_{3L2} = \frac{\mu_1}{v_{A1}} \left[\frac{1 - e^{2j\omega(\frac{d+h}{v_1})}}{1 + e^{2j\omega(\frac{d+h}{v_1})}}\right] = jZ_{A1}\tan(\frac{\omega(d+h)}{v_{A1}}) \tag{2.50}$$

The final equation is consistent with equation 2.42. So, this equation 2.49 should be feasible to predict the response of QCM with 2 layers of film deposition. The important parameter is wave velocity. In case of liquid this value can be calculated from density and viscosity. Let us think about the combination of water film and glycerol film.

We assume that glycerol/water inteface is maintain although glycerol is actually dissolved into water, the simulation of 2 layers model was conducted with the parameter of water and glycerol as listed in table 2.1.

Table 2.1: simulation parameters

Parameters	**Viscosity(cP)**	**Density(g/ml)**	**Notes**
Base layer (glycerol)	5	1.261	Viscosity of 5 cP was our assumption
Top layer (water)	0.89.	1.0	

Figure 2.15a has a top layer thickness as a parameter. At infinite base layer film thickness the frequency reaches saturation of the bulk glycerol. However, the top layer seems to induce the initial frequency change and flatten the positive frequency change as the base layer grows. This is not reflected practical application since the base layer typically remains static, unlike the top layer which the deposition can continue. The graph is re-plotted as is shown in figure 2.15. Base layer thickness now is a parameter. The lateral axis shows the film thickness of top layer. Positive frequency change due to water deposition can be observed when the base layer is less than 700 nm, as the purple and orange line shows positive frequency change.

The dotted blue line shows frequency change of the Sauerbrey's equation. The sensitivity of both glycerol only and water only are higher than the calculation. But the curves seem to become flatter when both layers are presented.

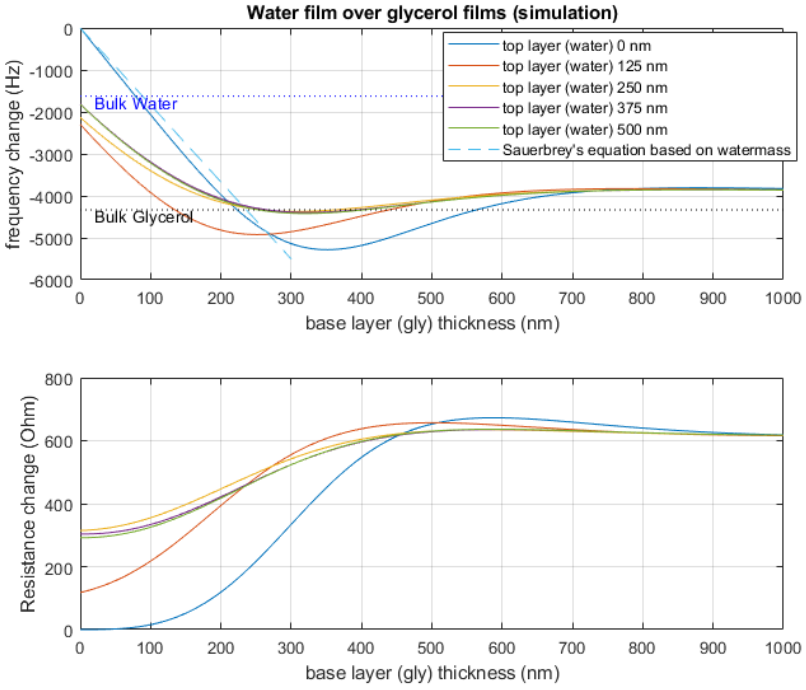

(a)

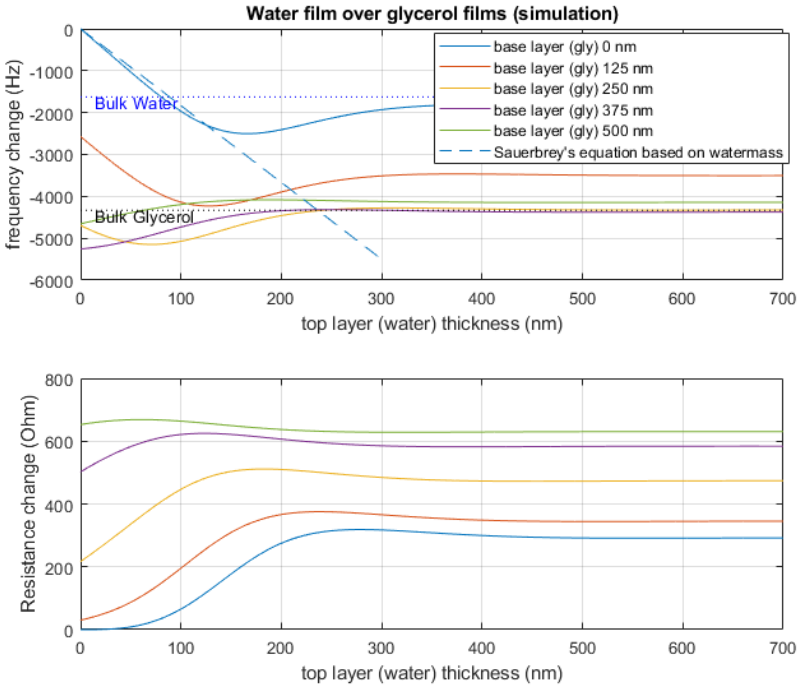

(b)

Figure 2.15: QCM response simulation using Mason equivalent circuit of two-layer film. (a) curve as a parameter of top layer film thickness. (b) curve as a parameter of base layer film thickness

2.5 Summary

Since QCM working based on piezoelectric effect, it is appropriate to explain the QCM behavior using resonant frequency. The conventional Sauerbrey's and Kanazawa's equations both were developed based on resonant frequency. Sauerbrey described the QCM resonant frequency change as "Mass loading", the frequency of QCM change is linear proportional to amount of mass deposited on QCM with the assumption of uniformly attached and rigid mass. Kanazawa explains the QCM behavior under liquid loading, where the frequency changes is proportional to square root of liquid viscosity and density. The Q factor or loss was not explored by the conventional equations. But it is an important information to further improve an understanding on QCM behavior.

We proposed the QCM model based on Mason equivalent circuit, which represent one dimensional model of QCM. The model has 3 ports. 2 ports are dedicated to QCM surface, one is for electrical behavior. Various boundary conditions can be applied to the model to represent different loading. We explored rigid film and bulk liquid conditions and confirm that the equations are consistent with Sauerbrey's and Kanazawa's, respectively. We further expand the boundary equation with viscous film and the simulation result showed a good approximation for thin layer when compared to Sauerbrey's equation and Kanazawa's equation at infinite film thickness (bulk liquid). The simulation also showed the positive frequency change occurred at certain film thickness. This may lead the possibility of using this model to predict the QCM unusual behavior. Lastly, we touch briefly on two-layer model and found that the base film thickness can influences frequency change when the second layer of film is deposited. It can even shift the QCM behavior to positive frequency change when the second layer film is deposited.

Chapter 3

Measurement system development for highly viscous loading and its evaluation

3.1 Introduction

In this thesis, the QCM measurement system is fabricated based on VNWA. The advantages of VNWA are 1) resonant frequency can be directly obtained, the resonant frequency is the intrinsic characteristic of QCM, whereas the oscillation frequency is influenced by the oscillator circuit 2) the measurement always possible as long as the sweeping frequency range can capture conductance peak 3) resistance value can be obtained together with frequency change without additional measurement method.

Normally, VNWA is a bench top laboratory equipment, designed for measuring RF characteristic. Recently, small sized VNWAs are commercially available. To use VNWA in sensing applications becomes more feasible.

We fabricated our measurement and evaluated its performance using viscous liquid. The advantage of using liquid over viscous coating is the ease of preparation and temperature control of liquid is easier using a water circulator. Curve fitting technique and Savitzky-Golay filter were implemented and evaluated compared to conventional methods. Also the parameters of VNWA and Savitzky-Golay filter were also optimized to obtain the lowest noise level.

3.2 experimental setup for highly viscous loading

3.2.1 Vector Network Analyzer

Instead of using frequency counter together with an oscillator circuit to measure oscillation frequency, vector Network Network analyzer was used.

VNWA measured in terms of network scatter parameter (S-parameters).S-parameter can describe the behavior of linear electrical network when feeding with various single frequency electrical signals. The S-parameter definition is in terms of incident and reflected power. Two-port S parameter is shown in figure 3.1.

This is the most commonly used scenario and serves as the building block for

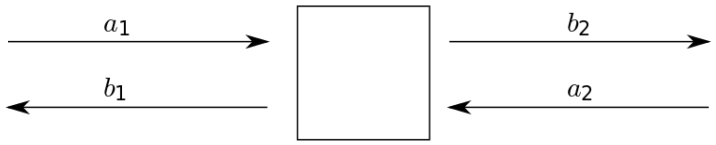

Figure 3.1: two-port network

more complicated network. The S-parameter matrix is given by $\begin{bmatrix} b_1 \\ b_2 \end{bmatrix} = \begin{bmatrix} S_{11} & S_{12} \\ S_{21} & S_{22} \end{bmatrix} \begin{bmatrix} a_1 \\ a_2 \end{bmatrix}$. If we define the incident wave as $a_1 = V_1^+$ and $a_2 = V_2^+$ with the reflected wave as $b_1 = V_1$ and $b_2 = V_2$, yield $S_{11} = \frac{b_1}{a_1} = \frac{V_1}{V_1^+}$ and $S_{21} = \frac{b_2}{a_1} = \frac{V_2}{V_1^+}$ Similary, $S_{12} = \frac{b_1}{a_2} = \frac{V_1}{V_2^+}$ and $S_{22} = \frac{b_2}{a_2} = \frac{V_2}{V_2^+}$

For our measurement the configuration for measurement is as shown in figure 3.2. This configuration is measured in reflection mode and the S_{11} is measured.

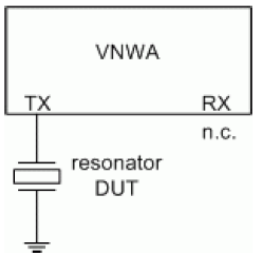

Figure 3.2: Diagram of crystal measure in reflection (S_{11})

Another configuration is transmission mode (figure 3.3) the measured parameter is S_{21} parameter. The only advantage of transmission mode measurement is the ease of calibration since only a single calibration is needed, while for reflection measurement, 3 calibrations are needed (short, open, load). Nonetheless, the QCM measurement with reflection mode was adopted for our experiment. This is due to the ease of setup by using only one connector. VNWA needs calibration for each frequency sweeping range, this is due to the frequency behavior at the port can vary drastically for each frequency, this is due to intrinsic passive components at the VNWA port. The calibration process for VNWA in reflection mode requires 3 steps. 1) calibrate for short circuit connection, this requires short circuit terminator 2) calibrate for open circuit, this require nothing 3) calibrate for load, this requires load 50 Ω terminator.

The S parameter needs to be converted to impedance or admittance for easier data analysis. Built-in GUI software attached to the equipment used in our thesis also has a function to convert S-parameter various plotting. The use of numerical computing environments such as Matlab or using the SciPy library in python language also have built-in functions to convert this S-parameter to impedance. In reflection mode where only S_{11} exists, equation 3.1 shows the relationship between S_{11} parameter and impedance (Z_{11}). Typically $Z_0 = 50\ \Omega$.

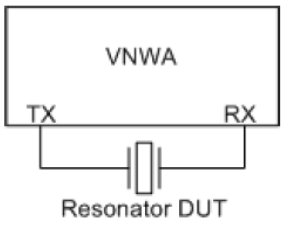

Figure 3.3: Diagram of crystal measure in transmission (S_{21})

$$Z_{11} = \frac{1 + S_{11}}{1 - S_{11}} Z_0 \tag{3.1}$$

The VNWA using in our experiment is a small network analyzer (DG8AQ VNWA, SDR-Kits) using a SMA connector and wiring through a coaxial cable.The network analyzer was connected to a PC via a USB connection. The measurement software was developed on the Matlab (Mathworks) platform.

3.2.2 Glycerol solution

Glycerol solution is used to calibrate and validate our measurement system. glycerol was chosen because of its high viscosity. Its viscosity exceeding 1000 cP at room temperature makes it extremely versatile for preparing a wide range of viscosity. Glycerol is colorless, odorless, water soluble and non-toxic.

Glycerol is alcohol with three hydroxyl groups, the structure of its molecule is shown in figure 3.4.

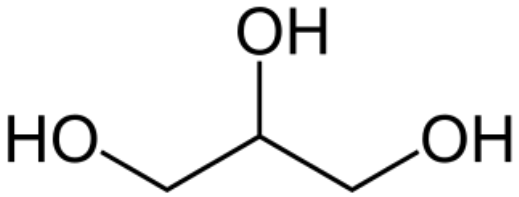

Figure 3.4: Chemical structure of glycerol

3.2.3 QCM

9 MHz AT-Cut QCMs with gold electrodes were used throughout all of our experiments. The quartz plate thickness is 181 um with an electrode diameter of 5.05 mm. The quartz plate is square with a length of 7.85 mm The drawing with dimensions is shown in figure 3.5.

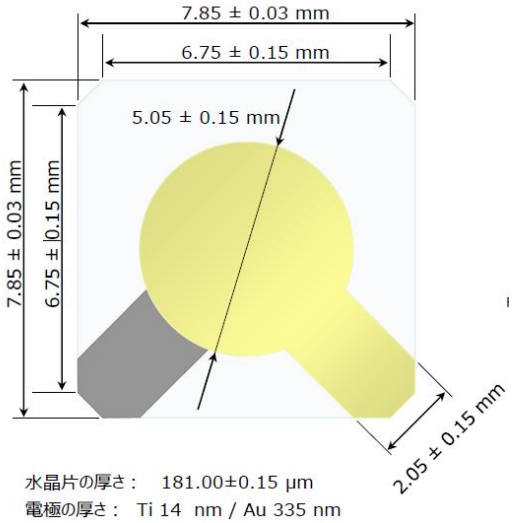

Figure 3.5: Chemical structure of glycerol

3.2.4 QCM measurement cell

QCM measurement cell was used to exclude one side of the electrode from the liquid. The only single side of the electrode is in contact with liquid. Its purpose is to isolate electrical coupling from one electrode to another electrode via liquid when the QCM is immersed into the liquid. The parasitics components make our QCM more complicated and becomes undesirable. Especially, it influences the accuracy when the dielectric constant of liquid such as water is very high. The structure of a measurement cell (QA-CL3, Seiko EG&G) is as shown in figure 3.6. Measurement cell material is Teflon (PTFE), which is well known for its chemical inertness. Anyhow, our testing does not require its extreme property. The dimension of the measurement cell is 25.5 (W) x 20 (D) x 12 (H) mm.

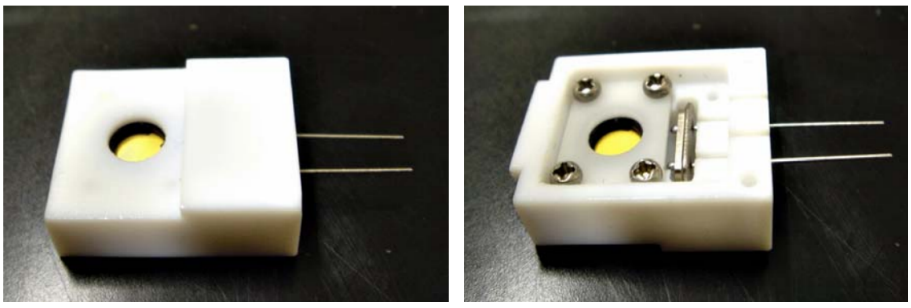

Figure 3.6: QCM measurement cell

3.2.5 Temperature controlled water circulator

Temperature is one of the parameters that also affect viscosity of the solution, figure 3.7 shows the viscosity of aqueous glycerol solution at different concentration and temperature.

For example at high concentration as 50% w/w if the temperature increases from 20 °C to 30 °C the viscosity decreases from 6 cP to 4.21 cP. If we calculated in terms of frequency change of 9 MHz QCM. The frequency change is as high as 700 Hz/ 10 °C, or 70 Hz/°C

Table 17. Viscosity of Aqueous Glycerol Solutions
Centipoises

Glyc. % Wt.	Temperature (°C)										
	0	10	20	30	40	50	60	70	80	90	100
0*	1.792	1.308	1.005	0.8007	0.6560	0.5494	0.4688	0.4061	0.3565	0.3165	0.2838
10	2.44	1.74	1.31	1.03	0.826	0.680	0.575	0.500	—	—	—
20	3.44	2.41	1.76	1.35	1.07	0.879	0.731	0.635	—	—	—
30	5.14	3.49	2.50	1.87	1.46	1.16	0.956	0.816	0.690	—	—
40	8.25	5.37	3.72	2.72	2.07	1.62	1.30	1.09	0.918	0.763	0.668
50	14.6	9.01	6.00	4.21	3.10	2.37	1.86	1.53	1.25	1.05	0.910
60	29.9	17.4	10.8	7.19	5.08	3.76	2.85	2.29	1.84	1.52	1.28
65	45.7	25.3	15.2	9.85	6.80	4.89	3.66	2.91	2.28	1.86	1.55
67	55.5	29.9	17.7	11.3	7.73	5.50	4.09	3.23	2.50	2.03	1.68
70	76	38.8	22.5	14.1	9.40	6.61	4.86	3.78	2.90	2.34	1.93
75	132	65.2	35.5	21.2	13.6	9.25	6.61	5.01	3.80	3.00	2.43
80	255	116	60.1	33.9	20.8	13.6	9.42	6.94	5.13	4.03	3.18
85	540	223	109	58	33.5	21.2	14.2	10.0	7.28	5.52	4.24
90	1310	498	219	109	60.0	35.5	22.5	15.5	11.0	7.93	6.00
91	1590	592	259	127	68.1	39.8	25.1	17.1	11.9	8.62	6.40
92	1950	729	310	147	78.3	44.8	28.0	19.0	13.1	9.46	6.82
93	2400	860	367	172	89	51.5	31.6	21.2	14.4	10.3	7.54
94	2930	1040	437	202	105	58.4	35.4	23.6	15.8	11.2	8.19
95	3690	1270	523	237	121	67.0	39.9	26.4	17.5	12.4	9.08
96	4600	1580	624	281	142	77.8	45.4	29.7	19.6	13.6	10.1
97	5770	1950	765	340	166	88.9	51.9	33.6	21.9	15.1	10.9
98	7370	2460	939	409	196	104	59.8	38.5	24.8	17.0	12.2
99	9420	3090	1150	500	235	122	69.1	43.6	27.8	19.0	13.3
100	12070	3900	1410	612	284	142	81.3	50.6	31.9	21.3	14.8

* Viscosity of water taken from "Properties of Ordinary Water-Substance," N. E. Dorsey, p. 184. New York (1940)

Figure 3.7: Viscosity & Temperature of Glycerol solution. Excerpt from [77]

.

3.3 Methods to obtain resonant frequency

3.3.1 Motional admitance

The most conventional method in determining resonant frequency is motional admittance method. Figure 3.8 shows the admittance plot around resonant frequency. The motional admittance method is the method to find the right most point of the admittance plot. If we focus on only conductance (x-axis), we can plot the relation between sweeping frequency and conductance as is shown in figure 3.9. The peak of this bell shape indicates the series resonant frequency. Typically, the peak of any curve can be determined by obtaining critical points using first order derivative. However, the derivative method is typically not robust against noise and becomes more difficult to find an exact point as the conductance curve gets flatten. Noise in motional admittance comes from the derivative method which require subtraction, another source of noise is the quantization error from frequency sweep step. Next section is our proposed method for finding the resonant frequency.

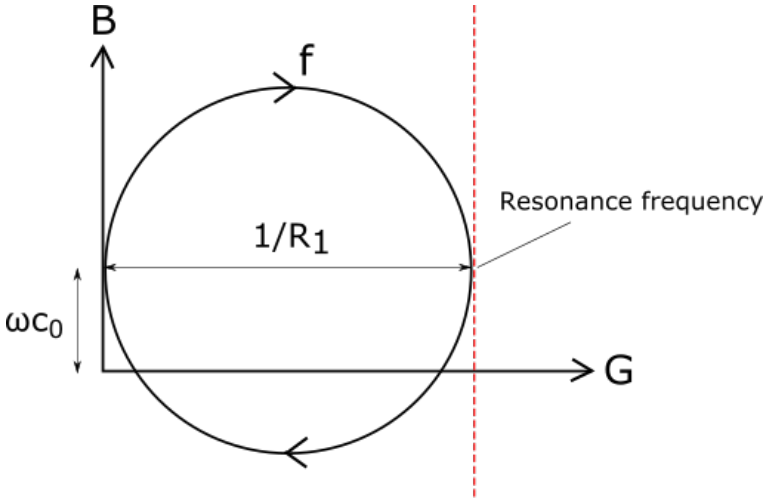

Figure 3.8: Admittance plot of QCM around resonant frequency.

3.3.2 Conductance curve fitting

Instead of relying on three points of data to find the peak of the curve. The curve fitting method is proposed in this section. As we represent the QCM characteristic around resonant frequency with BVD equivalent circuit, we can exploit this circuit by trying to fit the actual(measured) conductance data to the calculated conductance form equivalent circuit. The R_1, L_1, C_1 values that minimize the error between measurement data and from BVD circuits are selected. The detailed explanation is as follows. First, apply equation 3.2 to the measurement data. a_i is the difference between the model and the measurement data at the frequency f_i. Next, apply equation 3.3, b is the square sum of components of in the equation 3.2 is obtained. Last, we use *fminsearch* Matlab function to minimize the function b. This function optimizes the values of R_1, L_1 and C_1.

$$a_i = \frac{R_1}{R_1^2 + (2\pi f_i L_1 - \frac{1}{2\pi f_i C_1})^2} - Measured\ impedance. \tag{3.2}$$

$$b = \sum_{i=1}^{n} a_i^2 \tag{3.3}$$

Figure 3.9 shows the conductance curve fit compared with motional admittance method. the curve was fitted to 1000 datapoints using the parameters obtained from the equivalent circuit. The number of datapoints of 1000 was optimized for the best SNR which is discussed in the next section. We can obtain R_1, L_1, and C_1 from the curve fitting. Then, the resonance frequency is calculated using $f_r = \frac{1}{2\pi\sqrt{L_1 C_1}}$. The blue circle is the measured resonant frequency using motional admittance method.

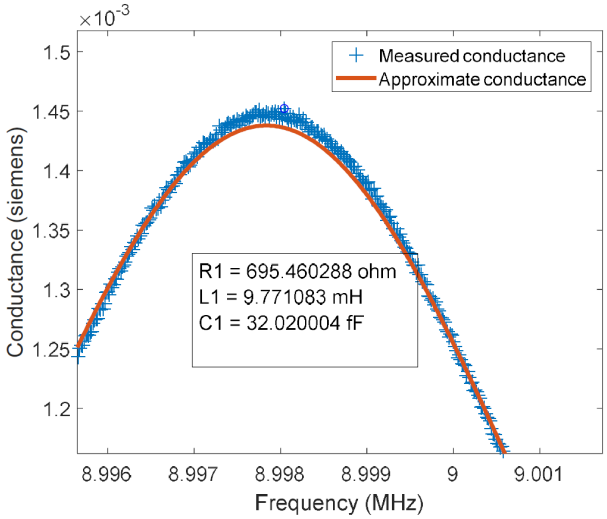

Figure 3.9: Curve fitting using the equivalent circuit. The QCM was immersed in 50% glycerol solution.

Frequency fluctuation was greatly reduced to a few Hz even under highly viscous loading as shown in figure 3.10 compared with maximum conductance frequency obtained from motional admittance method. However, a fluctuation of less than 1 Hz is preferable. Our proposed curve fitting technique greatly improved Signal to Noise Ration (SNR). Measurement data from motional admittance method is also shown in the same figure as 2 distinct stripes, this may due to some parasitic components that caused the conductance between these 2 frequencies to become dominant. The measurement time for each datapoints in figure 3.10 was 1.43 s.

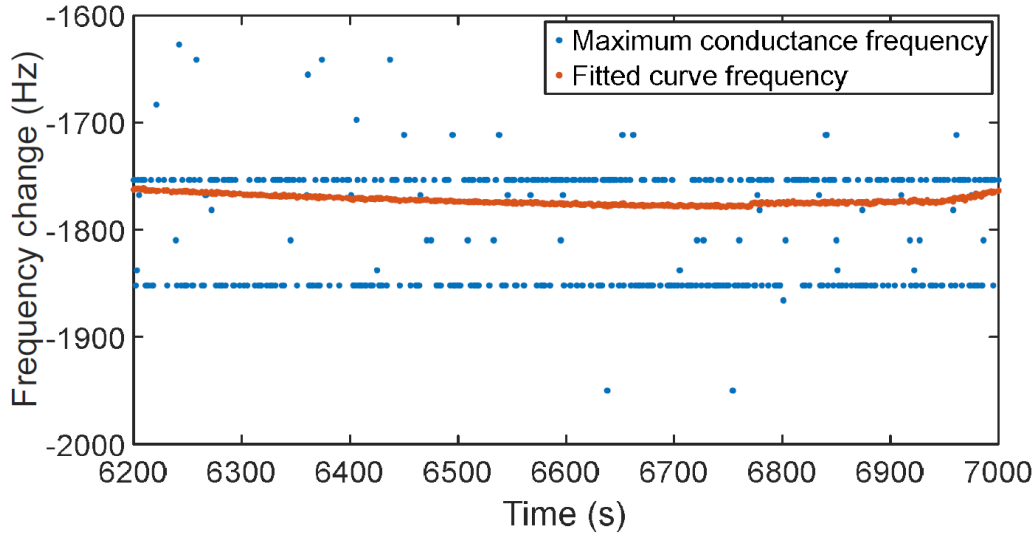

Figure 3.10: Comparison of data obtained by curve fitting and raw maximum conductance measurement. A 9 MHz AT-cut QCM was immersed in a 40% glycerol solution.

3.4 Noise reduction technique

3.4.1 Savitzky-Golay filter

Even if we had already improved the SNR by using a curve fitting method, the further improvement can be done by applying a digital filter. Savitzky-Golay filter can smoothen the data while retaining the signal features. A low-order polynomial is fitted to the surrounding datapoint within a predetermined window, the linear least square is used to fit the data and the center point of the polynomial is an output from the filter. The procedure of this filter is shown in figure 3.11.

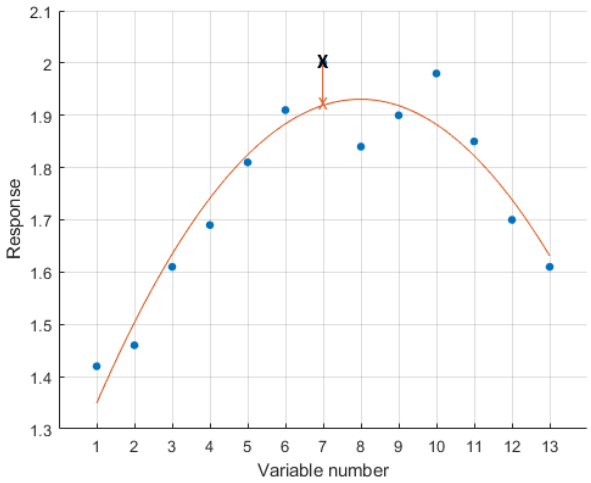

Figure 3.11: Principle of Savitzky-Golay filter. 1) Choose data point 2) Expand the window of data 3) Fitting data within the window using a polynomial 4) The center position of the window is the filter output. This figure shows a polynomial fit with a window size of 13 points. The smoothed value of data point 7 is indicated as X.

The parameters of Savitzky-Golay filter are polynomial order and window size; the optimization of these parameters will be discussed in the later section. The benchmarks of the noise reduction technique are shown in Table 3.1. The use of the curve fitting technique together with the Savitzky–Golay filter exhibited markedly improved results compared with conventional techniques such as smoothing and averaging. The transition time was obtained from the simulation result as is shown in figure 3.12.

Table 3.1: simulation and experimental parameters

Parameters	**VNWA raw data (conductance peak detection)**	**Moving average (window size: 25)**	**Curve fitting + Savitzky-Golay filter (polynomial order: 2, window size: 25)**	Note
Time resolution (s)	single sweep time of VNWA	Smoothing: a single sweep time of VNWA	single sweep time of VNWA	
Stability (standard deviation)	135 Hz	9.7 Hz	0.04 Hz	Experimental: 50% glycerol solution/ sampling data 30 s
Transition time (10% to 90%)	N/A	21 s	11 s	Simultion: Unit step with white noise, SNR = 10

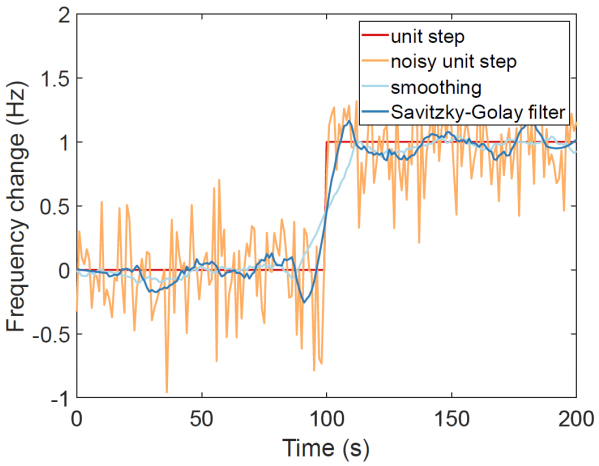

Figure 3.12: Simulation of unit step function with Gaussian noise and smoothing filter (moving average filter, window size: 25) compared with Savitzky-Golay filter (2nd order, window size: 25).

3.5 Optimizing data acquisition from Vector Network Analyzer

To use VNWA in measurement, several parameters must be optimized. Our curve fitting method utilized all data. The time per datapoints, the number of datapoints, and the frequency sweeping range, all these can affect the performance of our technique.

Time per datapoint should be the first parameter to be determined since it directly contributes to the total sampling time. The sweeping frequency was 16 kHz (sweep from 8.990 MHz to 9.006 MHz). The number of datapoints were 100, 300,

1000, and 3000, and the time used per datapoint were 0.16 ms, 0.34 ms, 1.33 ms, and 3.33 ms, respectively.

Figure 3.13 shows the relationship between the number of datapoints and the standard deviation as a parameter of time per datapoint, where the standard deviation was calculated using measurement data within 100 s prior to the end of the experiment at 900 s. The standard deviation saturated at 1000 datapoints every time. However, the lowest standard deviation was achieved when the number of datapoints and measurement time per datapoints were the greatest.

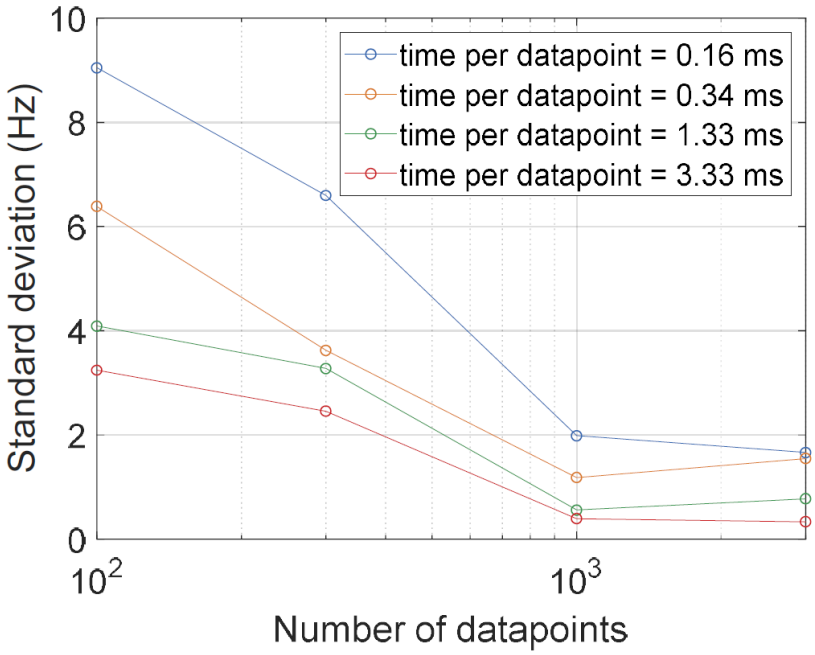

Figure 3.13: The standard deviation compared with number of datapoints when sweeping frequency range is 2 times of bandwidth (Sweep from 8.990 MHz to 9.006 MHz). The standard deviations were calculated from QCM immersed in 50% (w/w) aquaous glycerol solution.

Figure 3.14 shows the relationship between the total sampling time and the number of datapoints as a parameter of time per datapoint. The upper limit of 2 seconds is suitable for application of the system in real time. The total sampling time consists of the time for VNWA measurement and the time for calculation. The time for VNWA measurement is the measurement time per datapoint multiplied by the number of datapoints, and the time for software calculation was approximately 0.1 s for each measurement. Figures 3.13 and 3.14 show that the standard deviation was lowest under the constraint of a total sampling time less than 2 s when the number of datapoints was 1000 and the time per datapoint was 1.33 ms. This time per data points of 1.33 ms is a good selection for time per datapoint.

Table 3.2 is the selections of sweep frequency based on bandwidth of the conductance curve. We define the bandwidth of the conductance curve as the frequency range with conductance above 70.7% (-3 dB) of the maximum one. Bandwidth value of QCM immersed in 50% glycerol was used, the conductance plot with bandwidth marker is shown in figure 3.15.

Figure 3.16 shows the relationship between the standard deviation and the datapoint frequency interval as a parameter of sweeping frequency range. The plot

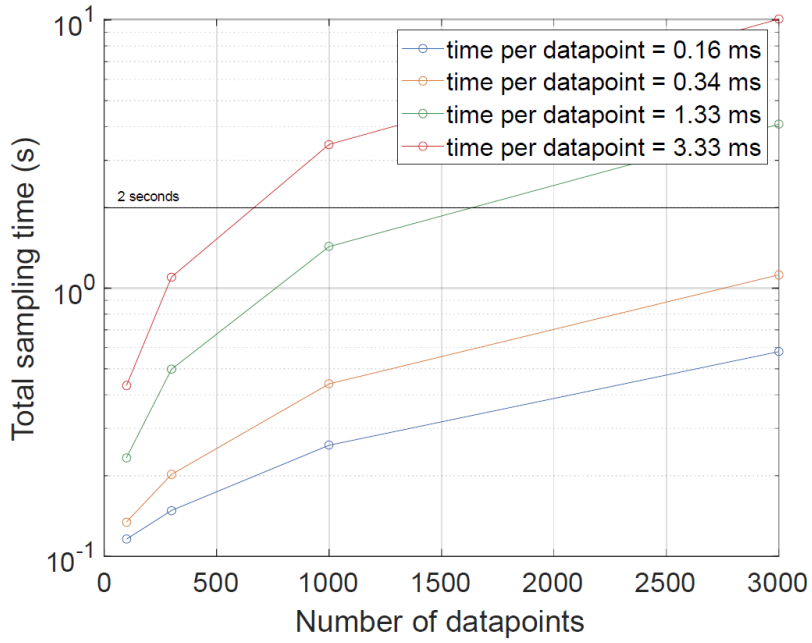

Figure 3.14: The total sampling time compared with the number of datapoints.

Table 3.2: simulation parameters

Bandwidth	**Sweep frequency range**	**Start frequency**	**Stop frequency**
0.5 BW	4 kHz	8.996 MHz	9.000 MHz
1 BW	8 kHz	8.994 MHz	9.002 MHz
2 BW	16 kHz	8.990 MHz	9.006 MHz
3 BW	24 kHz	8.986 MHz	9.010 MHz

also shows the measurement time above each data. Since the standard deviation should be as small as possible, there are several choices within the group of standard deviation points around 2 Hz inside the red circle. The sweeping frequency range of 16 kHz (2 BW) with the measurement time of 1.43 s was selected due to it having the fastest sampling without sacrificing the standard deviation too much.

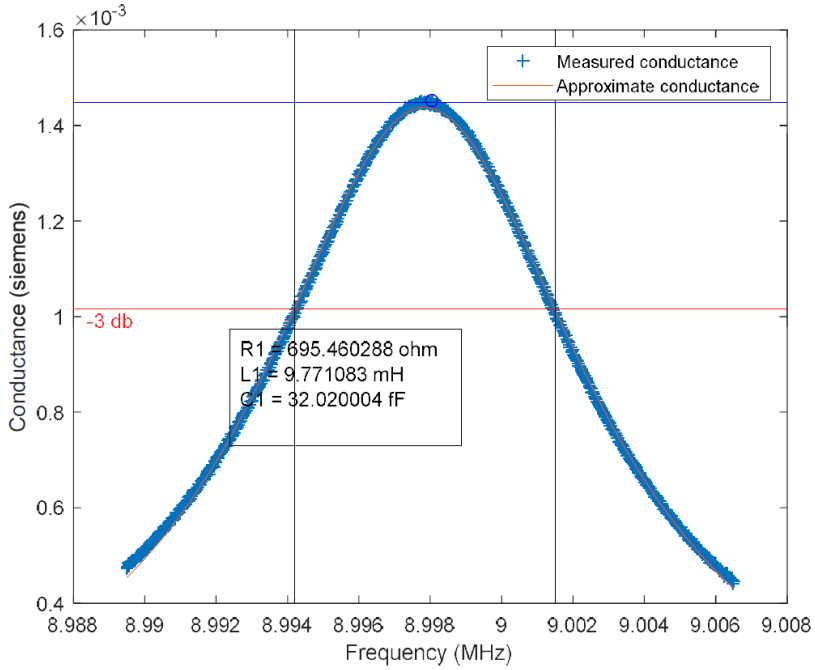

Figure 3.15: Conductance plot of QCM immersed in 50% glycerol. The frequency with the maximum conductance is located approximately at 8.998 MHz.

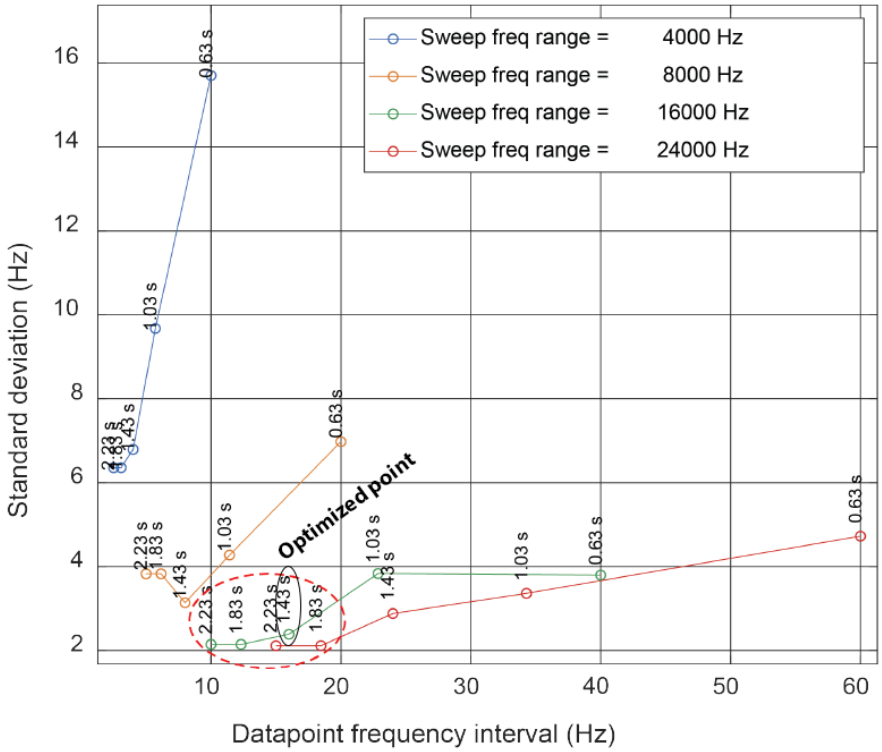

Figure 3.16: The relationship between frequency interval and standard deviation as a parameter of sweep frequency range.

3.6 Noise level and detection limit of the measurement system

We investigated thoroughly to determine the detection limit of our measurement system. Also in this section the savitzky golay parameters were optimized using QCM immersed in varying high concentrations of glycerol solutions. The effect of small stepwise changes in glycerol concentration around 50% (w/w) was studied to evaluate the feasibility of the Savitzky–Golay filter. The Q value of QCM with 50% glycerol concentration was 790, whereas that of the QCM without loading was 6200.

The experiments were conducted using a micropipette to add pure glycerol to the solution until concentrations of 50 %,50.005%, 50.01%, and 50.015% were obtained. Since the experiment was conducted with a small step of concentration change, small variation in temperature causing the viscosity change. The water circulator(CTE82A, Yamato-Komatsu) was used to maintain a constant temperature. Figure 3.17 shows the experimental setup.

Figure 3.18 shows raw data obtained in the experiment and the data after processing using the Savitzky–Golay filter. second-order polynomial with a window size of 25 or 101 was used. This confirmed that the fluctuation was reduced when the Savitzky–Golay filter was used.

The effect of the filter window size was further investigated. Data from 820 s to 850 s, from 1120 s to 1150 s, from 1420 s to 1450 s, and from 1720 s to 1750 s were used to calculate the standard deviation at glycerol concentration of 50%, 50.005%, 50.01% and 50.015% (w/w), respectively.

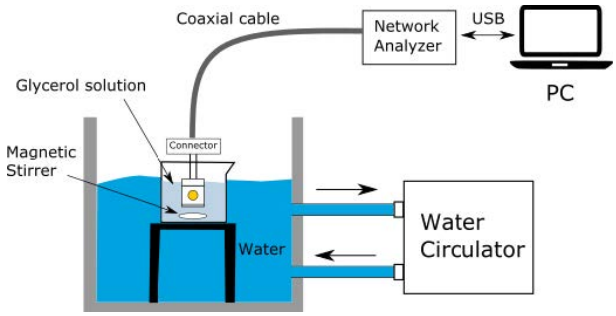

Figure 3.17: Experimental setup for measurement using glycerol solution.

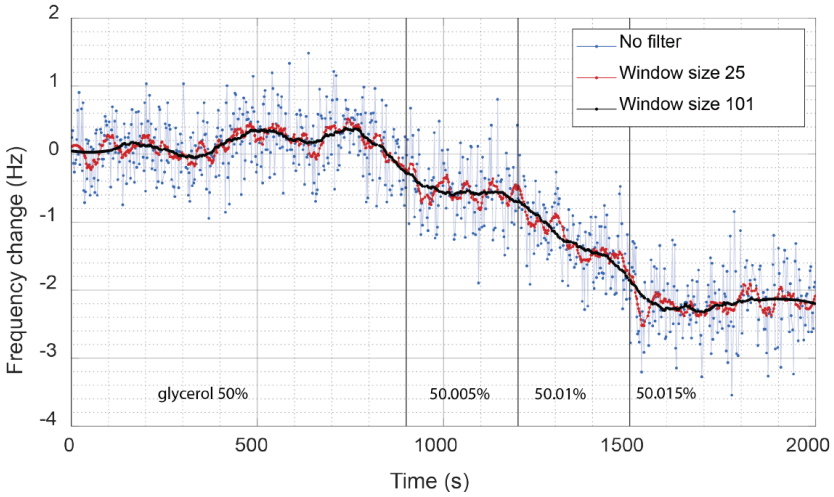

Figure 3.18: The frequency shift without a filter and with a filter for polynomial order 2 and window size 51 and 101 (Glycerol as solute was added at 900 s for 50.005%(w/w), 1200 s for 50.01%(w/w) and 1500 s for 50.015%(w/w), respectively.

Figure 3.19 shows the relationship between the window size and standard deviation. With no filter (window size = 0) the standard for 25 data, deviation ranged from 0.37 Hz to 0.65 Hz. When the window size was greater than 50, the standard deviation ranged from 0.01 Hz to 0.06 Hz and no significant improvement was observed for a larger window size. The effect of the polynomial order should also be considered. Only low-order polynomials were used since the high-order polynomial may have led to overfitting.

Next, the effect of the polynomial order from the first order to the third order was investigated. The average of the standard deviation for the four concentrations(50%, 50.005% 50.01%, and 50.015%) for various polynomial orders is shown in figure 3.20. The standard deviation of the first order polynomial drops more rapidly with increasing window size than those of the second and third orders polynomial. However, for windows size larger than 50 there is no improvement in standard deviation. For this reason, the windows size of less than 50 is preferred.

Generally, a smaller window size is preferable since an abrupt signal change can be retained. For the first order polynomial the standard deviation decreases drastically up to a window size of 25 and is smaller than those for the second and third order polynomials. However, the second and third order polynomials are better at retaining rapid signal changes. If rapid signal changes are a concern the second or third polynomial should be selected.

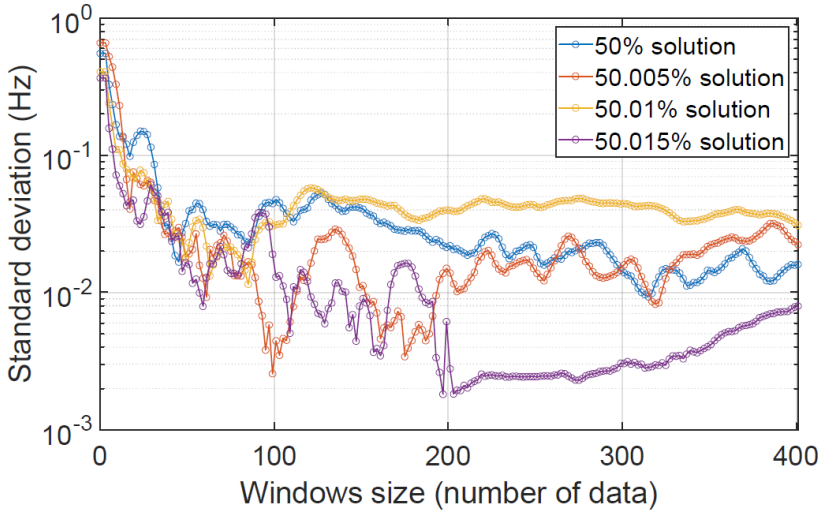

Figure 3.19: Relationship between window size of Savitzky-Golay filter and standard deviation as a parameter of glycerol concentration, polynomial order: 2.

An independent t-test (matlab command *ttest2*) was performed to statistically examine whether the glycerol concentration change at each step was detected as is shown in table 3.3. The independent t-test was chosen because we want to comparing the means for two different samples. which in this case is the resonant frequency of each glycerol concentrations.

Ten data were sampled 100 s prior to each concentration change. The results obtained with and without the Savitzky–Golay filter are compared. The t-test shows that a concentration difference of 0.005% was not always significant at the 5% level when no filter was applied to the raw data. However, the null hypothesis was rejected for the first-order polynomial with window size larger than 3. For the second- order polynomial with window size larger than 5, the test also rejected the null hypothesis and it was concluded that the differences in concentration between 50% and 50.005%, 50.005% and 50.01%, and 50.01% and 50.015% are significant at the 5% confidence level. This means that the smallest possible window size of each corresponding polynomial order is adequate to detect each concentration change.

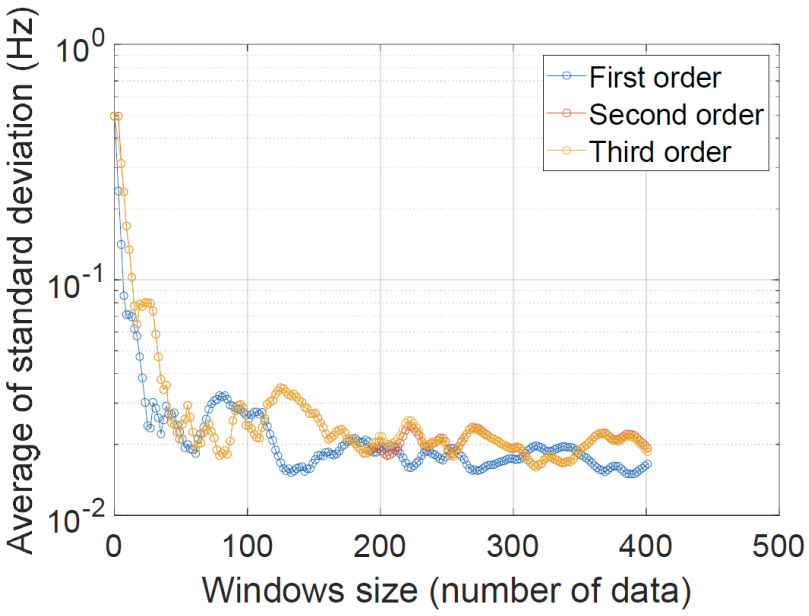

Figure 3.20: Average of standard deviation for each polynomial order.

Table 3.3: INDEPENDENT T-TEST FOR EACH CONCENTRATION OF GLYCEROL SOLUTION (SIGNIFICANCE LEVEL: 5%)

Glycerol concentrations (%w/w)	50%/50.005%	50.005%/50.01%	50.01%/50.015%
No filter			
Null hypothesis(0 = accept/ 1 = reject)	0	1	1
p-value	0.1732	9.29e-4	2.67e-4
Number of data used in t-test	10	10	10
Polynomial order 1			
Null hypothesis(0 = accept/ 1 = reject)	1	1	1
p-value	0.0046	3.02e-6	9.71e-4
Savitzky–Golay filter window size	3	3	3
Number of data used in t-test	10	10	10
Null hypothesis(0 = accept/ 1 = reject)	1	1	1
p-value	5.31e-6	8.78e-10	5.03e-14
Savitzky–Golay filter window size	5	5	5
Number of data used in t-test	10	10	10
Polynomial order 2			
Null hypothesis(0 = accept/ 1 = reject)	0	1	1
p-value	0.1732	9.24e-4	2.67e-4
Savitzky–Golay filter window size	3	3	3
Number of data used in t-test	10	10	10
Null hypothesis(0 = accept/ 1 = reject)	1	1	1
p-value	0.0305	5.23e-6	2.04e-8
Savitzky–Golay filter window size	5	5	5
Number of data used in t-test	10	10	10
Null hypothesis(0 = accept/ 1 = reject)	1	1	1
p-value	0.0044	3.54e-6	3.14e-11
Savitzky–Golay filter window size	7	7	7
Number of data used in t-test	10	10	10

3.7 Summary

In this chapter we fabricated a QCM measured system based on VNWA. The system was evaluated with highly viscous loading using glycerol solution. The ease of adjusting the liquid viscosity only adding solute was the reason we tested our system based on liquid. Several parameters of VNWA need to be optimized. The time per data points, the number of datapoints, and the frequency sweeping range are the parameters which affect the performance of our measurement, especially the curve fitting technique since all data were used. The best conditions out of these parameters are sweeping frequency range of 16 kHz (2 BW), the sampling time of 1.33 ms and number of data points of 1000 data. The standard deviation from these conditions is less than 2 Hz. This value was obtained from QCM immersed in 50% w/w glycerol solution.

To improve the SNR of the measurement that usually suffers from high viscous loading, the curve fitting technique was proposed. Our preliminary experiment showed that this technique greatly reduced the measured frequency fluctuation, the fluctuation only remained a few Hz compared to more than 100 Hz when the motional admittance was used. Savitzky-Golay filter was also used together with curve fitting technique to further improve SNR. Savitzky-Golay filter was selected due to its property in keeping signal feature even rapid signal change occur. This was proved using small stepwise changes in glycerol concentration around 50% (w/w). The independent t-test showed that For the second- order polynomial with window size larger than 5, the test also rejected the null hypothesis and it was concluded that the differences in concentration between 50% and 50.005%, 50.005% and 50.01%, and 50.01% and 50.015% are significant at the 5% level. The selection of this concentration change is determined by the detection limit of our measurement system.

Chapter 4

Film coating and water deposition to QCM

4.1 Introduction

In this chapter we further extended our system to test with QCM that coated with various kinds of film. Also together with a microdispenser, we can make depositions over sensing film with liquid. First, The experiment to confirm deposition amounts from micro dispenser. Next, The experiment for deposition directly to bare QCM also conducts to confirm mass loading and viscous loading. Last, the experiments to deposit water over various films. With all these experiments we aim to understand the viscous film response to vapor exposure and expected to see both negative and positive frequency shifts. Moreover, we aim to interpret the data using our Mason equivalent circuit model in the next chapter.

4.2 Experimental setup for vapor deposition over film coated QCM

The simple diagram of the test setup is in figure 4.1. The micro dispenser was added to our system and the QCMs were coated with various films. It was controlled manually by a function generator. The measurement equipment was the VNWA setup we developed previously. The additional microdispensor and QCM holder are to be explained in the next subsections.

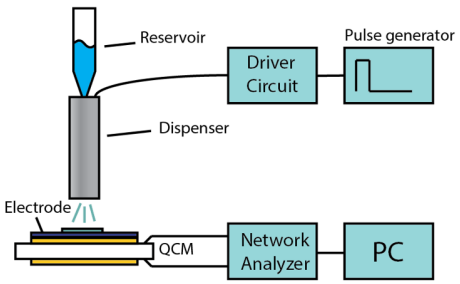

Figure 4.1: Diagram of our experiment setup

4.2.1 Microdispensor

The next experiment setup would be an investigation on how odorants have an effect on QCM response with various coatings. The micro dispenser is necessary to control the precise amount of odorant exposure. The structure of the micro dispenser is a solenoid valve with a nozzle that allows the liquid to spray out. The drawing of the dispenser (The lee company, INKA2438510H) used in this thesis is in figure 4.2. And the mechanical and electrical specification is as shown in figure 4.3. The material "FFKM" is perfluoroelastomeric compounds, they are commonly used to make O-rings and gaskets that are used in applications that involve contact with hydrocarbons or highly corrosive fluids.

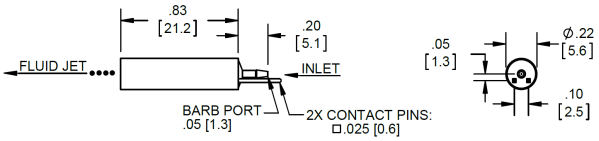

Figure 4.2: Drawing of micro dispenser used in this thesis

PART NUMBER	STYLE	ORIFICE DIAMETER	SEAL MATERIAL	LOHMS	MIN. SPIKE DURATION (ms)	PRESSURE (psig)
INKA2438510H	VJ	0.003" (0.076 mm)	FFKM	110,000	0.5	30

- Weight: 1.8 grams
- Internal Volume: LT Style: 30 µL
  VJ Style: 55 µL
- Pulse Voltage: 24 vdc
- Hold Voltage: 7.5 vdc (maximum), 5.0 vdc (recommended)
- Wetted materials (in addition to seal): Stainless Steel, PEEK, PPS, Sapphire, Epoxy

Figure 4.3: Specification of solenoid valve used in this thesis

The driver circuit for the dispenser is shown in figure 4.4a and the driving pulse profile 4.4b. The driving circuit is the simple open collector darlington transistor (ULN2803), controlled by a function generator. The driving pulse profile at the output is 24 Vpp and the pulse width of 2 ms. Longer pulse width influence volume of liquid slightly, but most cases the pulse width was set to 5 ms.

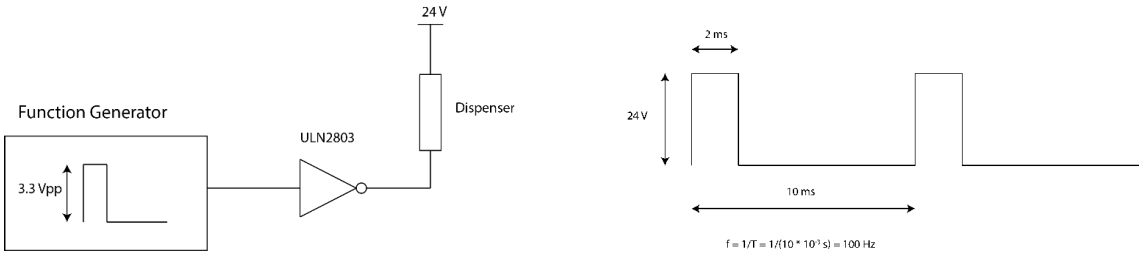

Figure 4.4: Driving circuit diagram and pulse profile for micro dispenser. (a) Driver circuit. (b) Pulse profile.

The repeatability and the amount of liquid per deposition need to be confirmed. The simple method of using weight balance to measure the weight increase of laboratory paper wipers after depositing water. The plot data of number of pulses and

adsorb weight is shown in figure 4.5. The calibration line in the plot does not pass through origin this due to a slight measurement error. However, the slope of the calibration line was used to estimate the dispenser deposition volume. The slope of this plot indicates water volume is 3 nL per pulse.

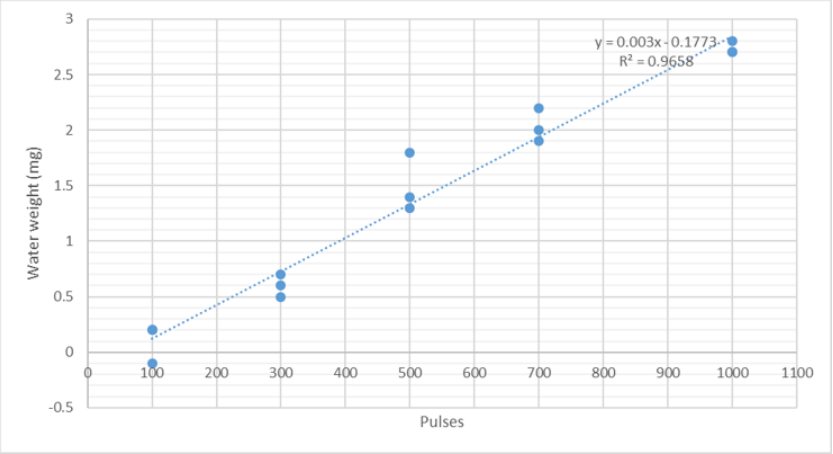

Figure 4.5: Increase in weight due to water deposition as a function of pluses.

Further experiment was also conducted with PEG20M dissolved in chloroform and Glycerol dissolved in acetone. The concentration of the solutions is 0.01 g/mL. The similar plot between the number of deposition pulse and deposited mass weight were obtained as is shown in 4.6. Please note that the deposited mass weight is the amount of weight after the solvent has evaporated. The slope of this plot indicates PEG20M is deposited 5 nL/pulse. Further experiment with glycerol dissolved in acetone showed sensitivity of 6 nL/pulse. The viscosity of solvent may regulate droplet volume, lower viscosity may flow easier resulting in larger amounts of liquid. The viscosity of liquids are in order of $\eta_{water}1cP > \eta_{chloroform}0.536cP > \eta_{acetone}0.316cP$.

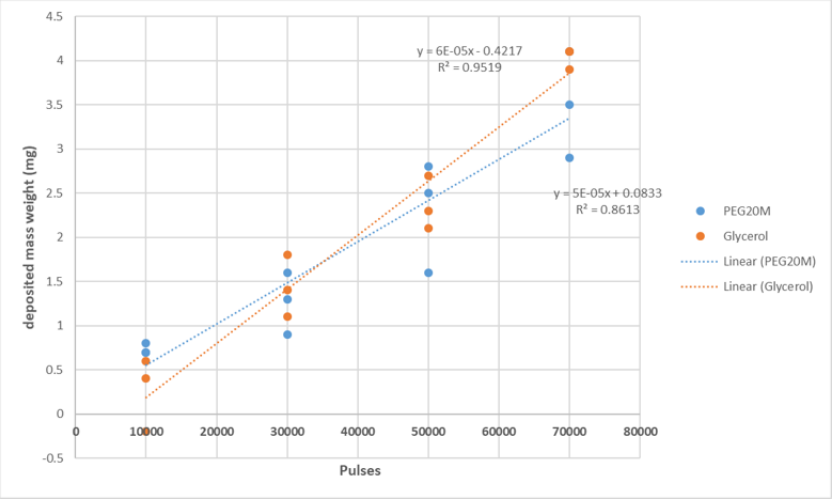

Figure 4.6: Number of deposition pulses compared with water weight gained.

4.2.2 QCM holder

The position of the micro dispensing tip related to the QCM surface is needed to be precisely fixed for a consistent measurement. The liquid spray from the dispenser in a cone shaped pattern. The distance from nozzle to the QCM plate determined the diameter of the circular shape. From our previous research, the distance of 3 mm from nozzle to QCM plate, the spray pattern had a diameter of 1 mm [78]. Our design of QCM holder is shown in figure 4.7.

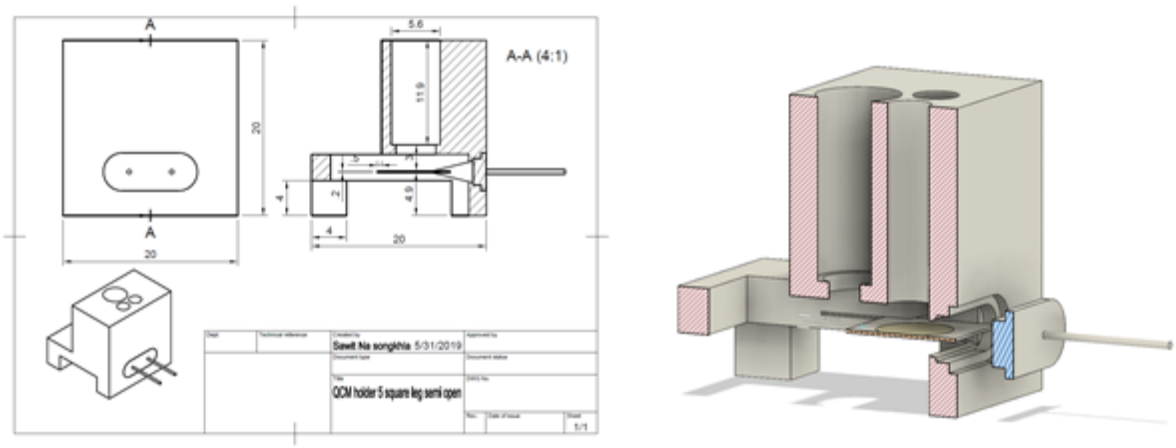

Figure 4.7: Drawing and 3D model of QCM holder.

The dispenser was fabricated by a 3D printer. With this design the dispenser nozzle was set to the center of QCM electrode, with this setup it is possible to approximate the deposition film thickness. Figure 4.8 shows the simple diagram for film thickness estimation. For example knowing the density of PEG20M is 1.33 g/mL [79], and refer to the previous dispenser volume test: 1 deposition = 50ng. The estimated film thickness per deposition is 47.87 nm. Of course this estimation does not account for the spreading of liquid at the higher amount of depositions, and the uniformity of the film shape.

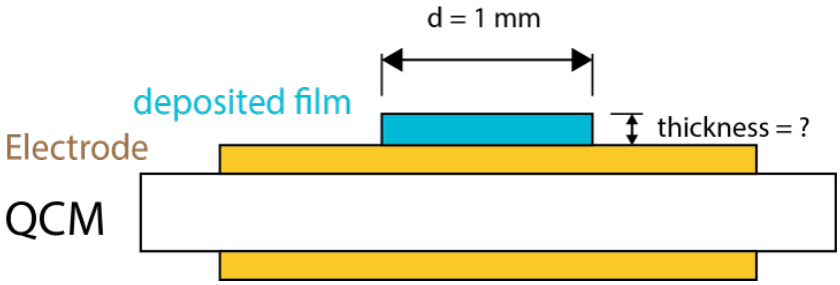

Figure 4.8: Drawing and 3D model of QCM holder.

4.3 Study of film coating with dip coating method

4.3.1 Film materials

Film material was chosen with different viscosity in mind. also it should be safe and easy to handle. 3 materials were chosen as a coating material: Glycerol,

PEG20M, and PEG2000. These 3 materials can be dissolved in volatile organic compounds. Glycerol is dissolved well in acetone, and PEGs are dissolved well in chloroform.

Glycerol is highly viscous and its viscosity can exceed 1000 cP at 20° C [Handbook of chemistry and physic]. However, at high frequency vibration of QCM, the data of the dynamic viscosity has not been reported. PEG2000 may have viscosity around 50 cP while PEG20M can be considered as rigid material.

4.3.2 Pull-up speed

The coating method we used in this thesis is dip coating. The principle is basically dip the substrate needs to be coated into the coating solution and pull it up slowly. The material deposits itself on the substrate while it is pulled up. Then, the solvent evaporated from the liquid forming a thin coating layer. The dip coater machine (VLAST45-06-0100, THK Co., Ltd., Tokyo, Japan) is shown in the figure 4.9. The pull-down and pull-up speed can be set separately from 1 μm/s to 99 mm/s .

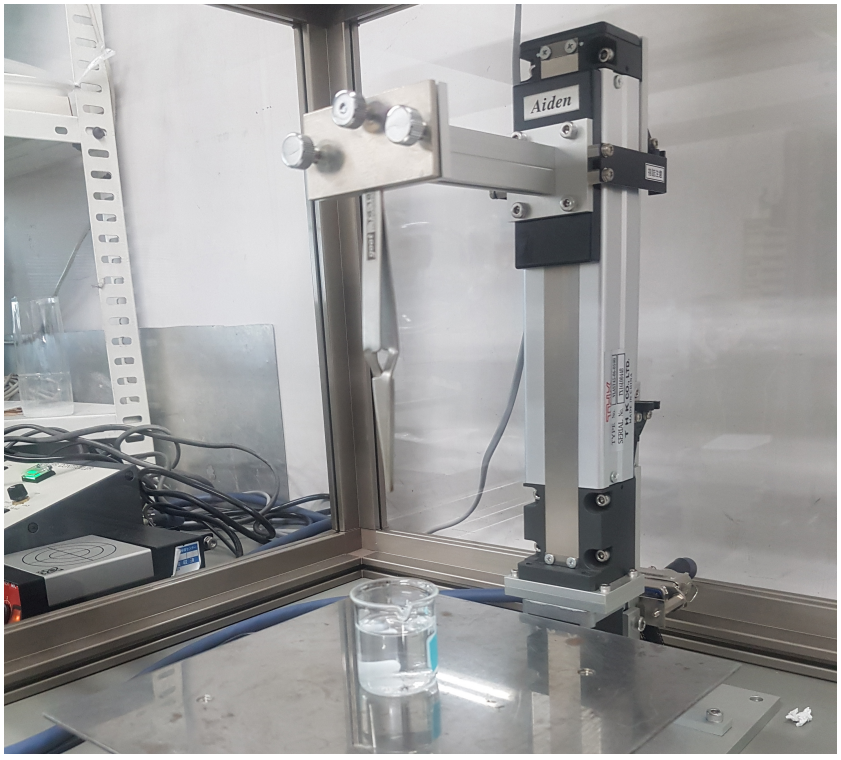

Figure 4.9: Dip coating machine used in this thesis.

The withdrawal speed or so called pull-up speed determined the film thickness and coating condition. The investigation needs to be made for the proper coating condition. Glycerol film coating solution was prepared by dissolving glycerol in acetone to the concentration of 0.01 g/cm^3. Figure 4.10 shows the relationship between pull-up speed and QCM frequency change after coating. The plot shows that as the pull up speed increases the resonant frequency decreases until it reaches some saturation at around 100 Hz frequency. The pull down speed is not strictly set but typically set at 1 mm/s.

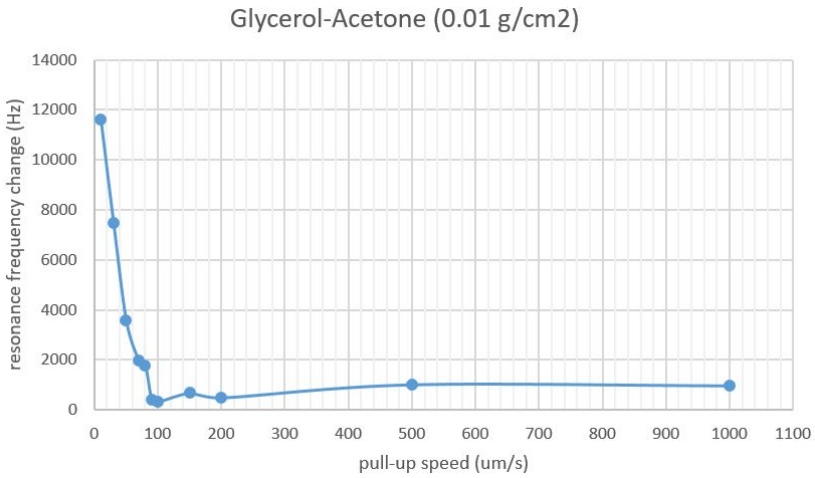

Figure 4.10: Frequency and resistance change of various pull-up speed: glycerol solution 0.01 g/cm^3

Nonetheless, fast pull-up speed letting the uniformity of the coating layer getting worse. Figure 4.11 shows the QCM at 3 different pull-up speeds: 10 ,80 and 500 um/s. If the pull-up speed was too slow the surface condition was also not good as shown in case of speed of 10 um/s, the coated surface shows a stripe like pattern. While at the fast speed of 500 um/s, there seem to be many domains that formed on the surface, creating an uneven surface. From our experiment only at moderate speed around 20 to 100 μm/s that have an acceptable uniform film coating. At too high speed such as 500 μm/s the QCM was not all covered by the coating material. This may cause by at the end of coating process, the coating solution separated from the substrate too abruptly due to liquid surface tension. This causes the non uniform coating.

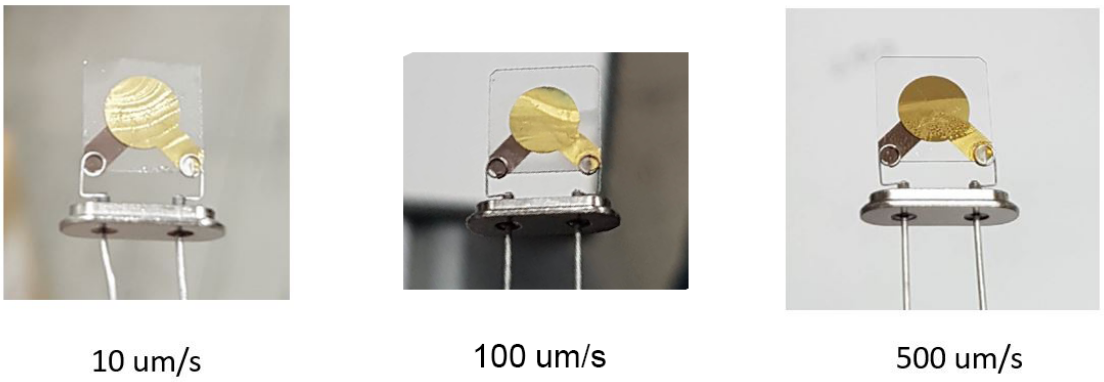

Figure 4.11: Picture of QCM with 3 different pull-up speeds: 10 ,100 and 500 um/s

We found that the surface condition was only depended upon pull-up speed. Even if we dilute the solution the film coating still remains good within the same condition. This concluded that the pull-up speed should have been predetermined and changed the solution concentration to obtain the desired film thickness.

4.4 Bare QCM response

Bare QCM deposition was also being investigated even if it is not the ultimate target for this thesis. The deposition has an advantage of the controllable amount of deposition. This makes our investigation regarding Sauerbrey's equation. And also further investigation on water deposition over coated film which represent QCM sensor response.

4.4.1 Water deposition

Experiments of water deposition were conducted briefly, since at small depositions, water evaporates rapidly. Since no existing film to capture the water and prevent it from evaporation. The experiment of 1 pulse water deposition at every 300 s (Except at 900 s, interval period is 600 s) is shown in figure 4.12. Dispenser pulse frequency was 1 Hz. The experiment showed that the evaporation occured so quickly that the frequency almost remained unchanged. Please note that the frequency change is magnified.

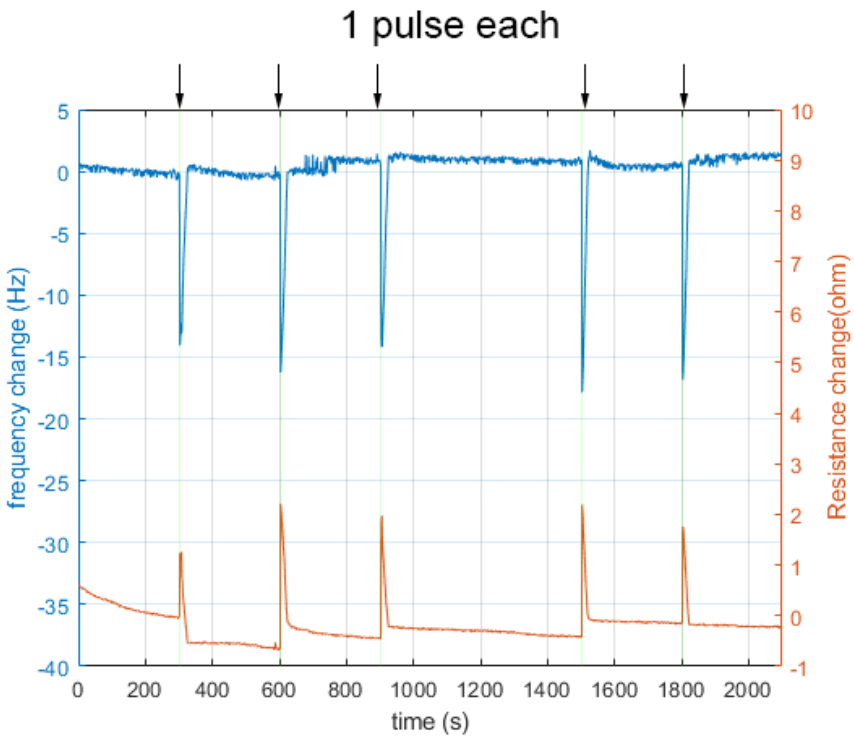

Figure 4.12: Frequency and resistance change of water deposition over bare QCM, 1 pulse every 300 s

The experiment at higher number of deposition pulses was also conducted (figure 4.13. For 10 pulses every 300 s, the result also showed that the evaporation cause the frequency change immediately, this may due to the liquid is spreading thinly and the frequency recovery due to evaporation can be observed.

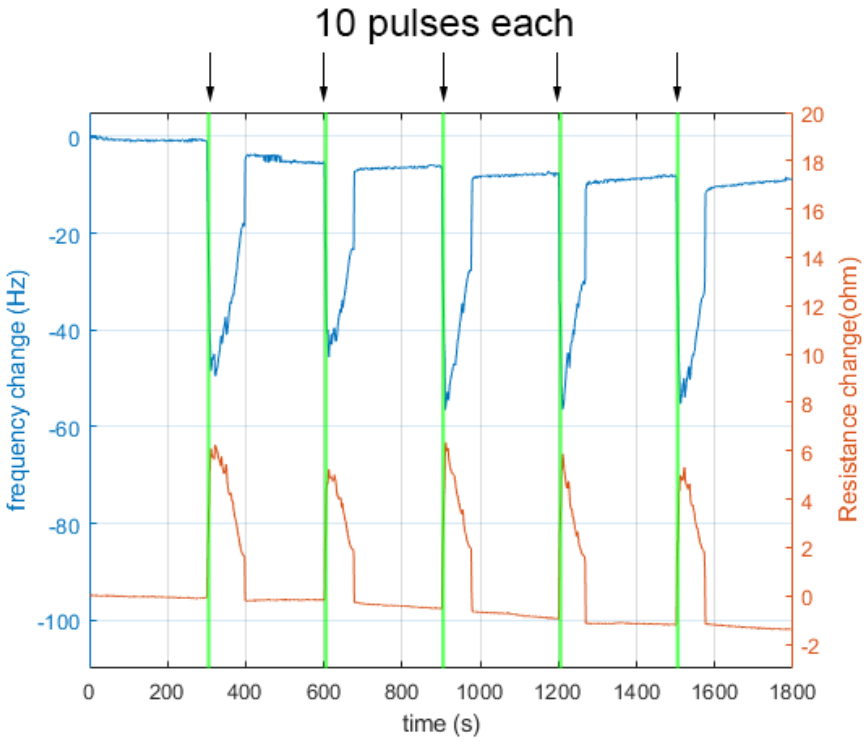

Figure 4.13: Frequency and resistance change of water deposition over bare QCM, 10 pulses every 300 s

Figure 4.14 shows the experiment conducted with 1000 deposition pulses. The dispenser frequency was increased to 100 Hz, with the pulse width of 1 ms. This showed the saturation of frequency change after depositions. Then it gradually returned to its initial frequency. The excess amount of water larger than viscous penetration depth caused the saturation in frequency change. The frequency change was not as large as bulk liquid, since the water did not cover all the QCM surface.

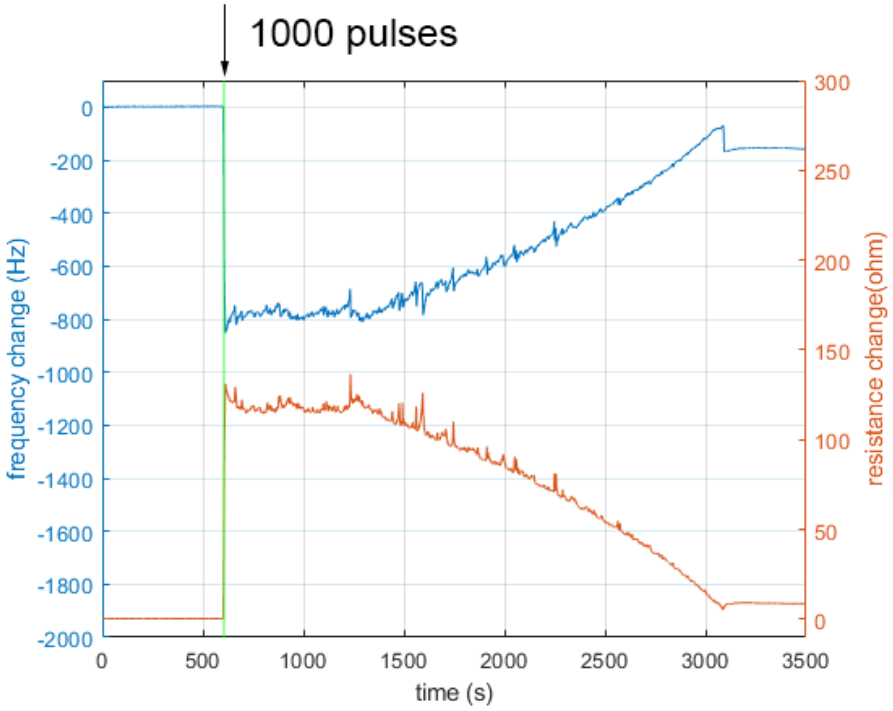

Figure 4.14: Frequency and resistance change of water deposition over bare QCM, 1000 pulses at 100 Hz.

4.4.2 PEG20M deposition

PEG20M was a good selection to represent pure mass loading. PEG20M was dissolved in chloroform until with the solution concentration of 0.01 g/ml. The experiment was conducted in a number 10 pulses 3 times followed by 1 pulse 4 times. Good signal stability and linearity as expected from the mass loading experiment was obtained from the experiment. Figure 4.15 shows the frequency and resistance plot. The results showed a stable frequency change without drifting, and also the resistance value almost did not change. This confirms that PEG20M is almost ideal rigid film material.

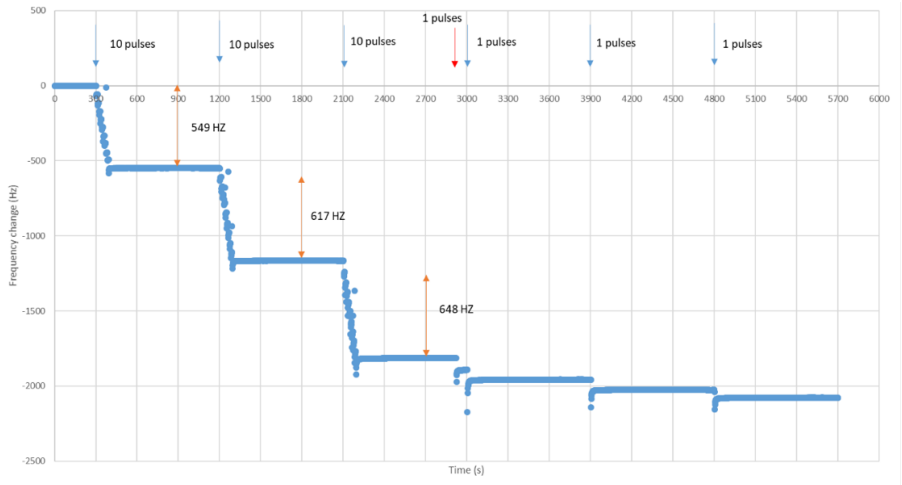

(a)

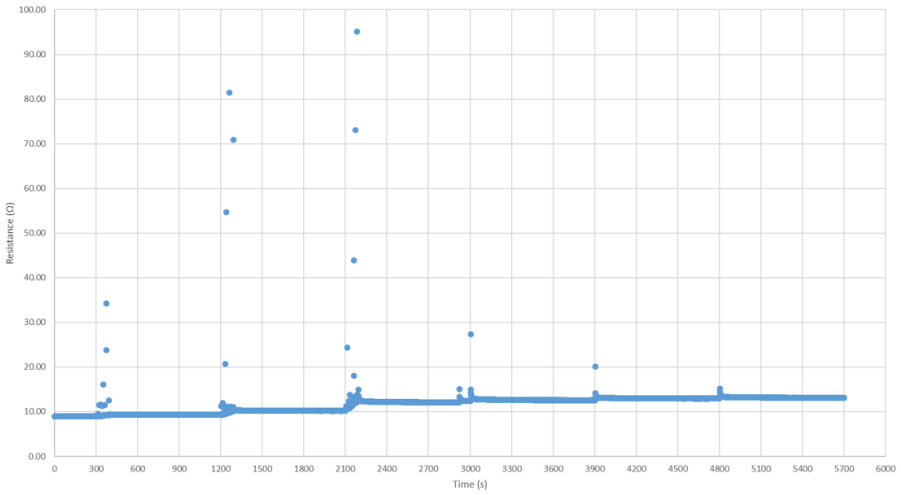

(b)

Figure 4.15: QCM frequency change and resistance change after depositions to PEG20M. (a)frequency change. (b)resistance change.

The relationship between the number of depositions and frequency change is shown in figure 4.16. The plot shows good linearity, the mass sensitivity was also comparable with theory (Sauerbrey's equation). For 9 MHz QCM with electrode diameter of 5 mm, the mass sensitivity calculated from Sauerbrey's equation is -0.93 Hz/ng, while sensitivity calculated from figure 4.16 is -1.28 Hz/ng. This experimental result relatively agreed with the theoretical value.

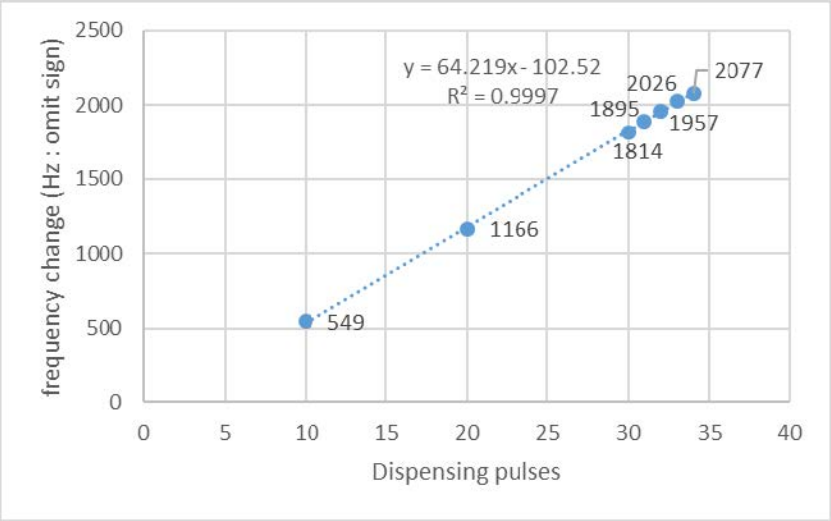

Figure 4.16: Relationship between the number of pulse and frequency change (ignore negative sign).

4.4.3 Glycerol deposition

In this section, the depositions of glycerol will be explored. Glycerol is a highly viscous liquid. We dissolved glycerol in acetone with a target concentration of 0.01 g/ml. We performed the deposition 1 pulse every 300s and stop at the 5^{th} pulse. The experiment was repeated 3 times. We have compared the result with the same experiment setting with PEG20M (solution 0.01 g/ml). Figure 4.17 is the experiment result of PEG20M and figure 4.18 is the experiment result of glycerol. Figure 4.19a shows the relationship between deposition pulses and frequency change of both PEG20M and Glycerol. Similarly, figure 4.19b shows the resistance change of PEG20M and Glycerol. The results show that the frequency change of PEG20M was slightly higher than the calculation from the Sauerbrey's equation (orange line), while the glycerol deposition, the frequency change was less than PEG20M. On the other hand, PEG20M almost has no resistance change when deposited, while in case of glycerol the positive resistance change was observed. This experiment result suggests that for a viscous medium, resistance change is also an important information to determine film property.

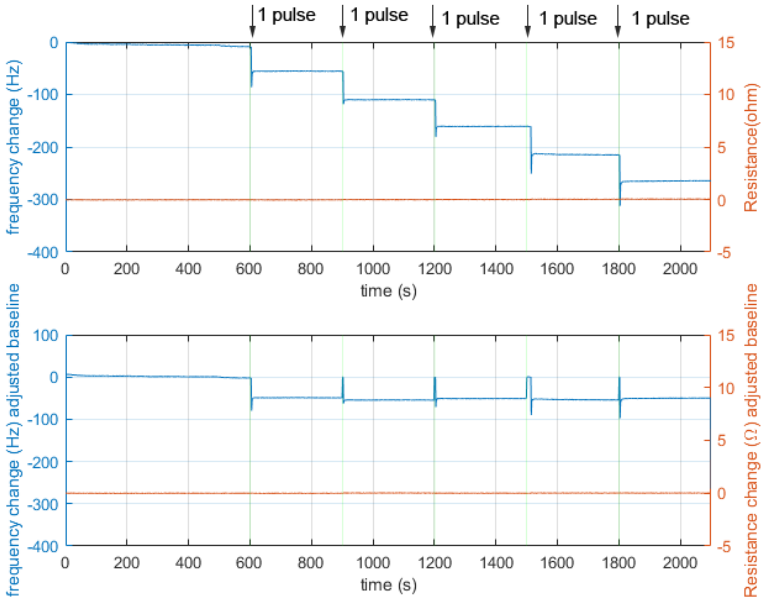

Figure 4.17: Frequency and resistance change of PEG20M solution deposited over bare QCM.

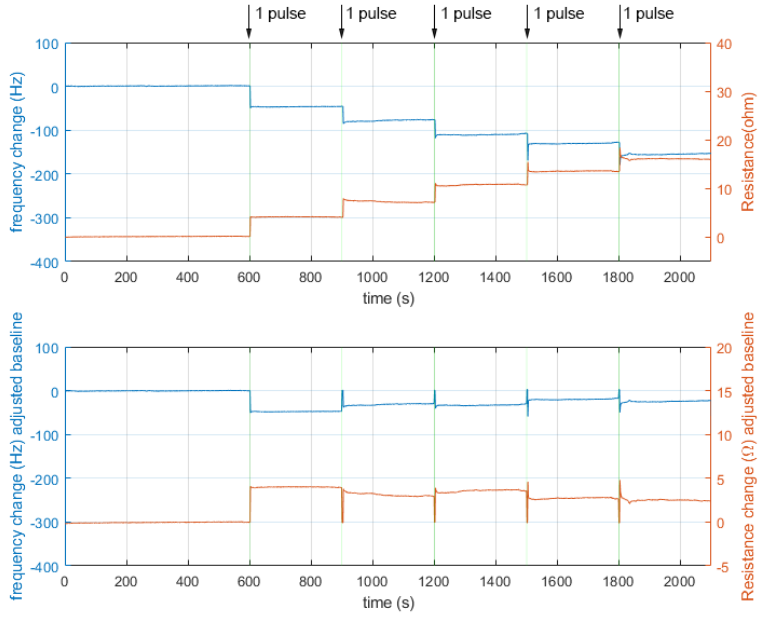

Figure 4.18: Frequency and resistance change of glycerol solution deposited over bare QCM.

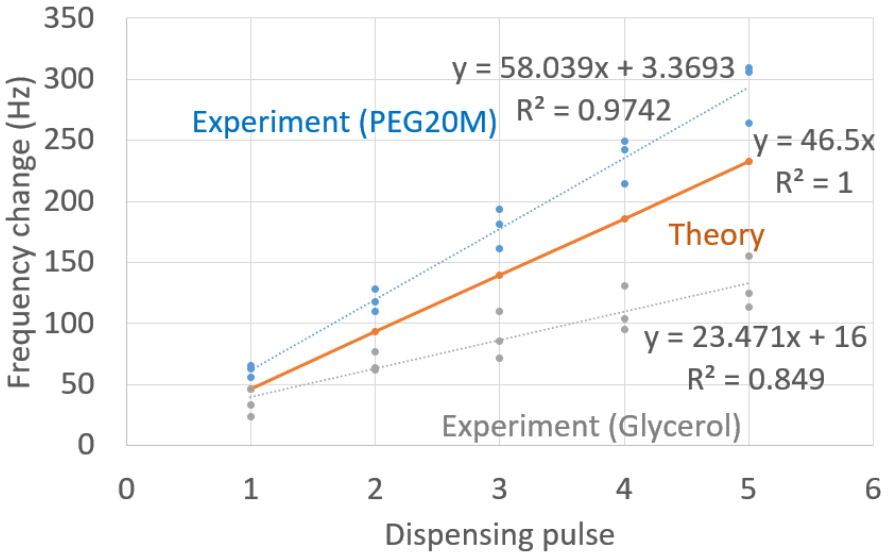

(a)

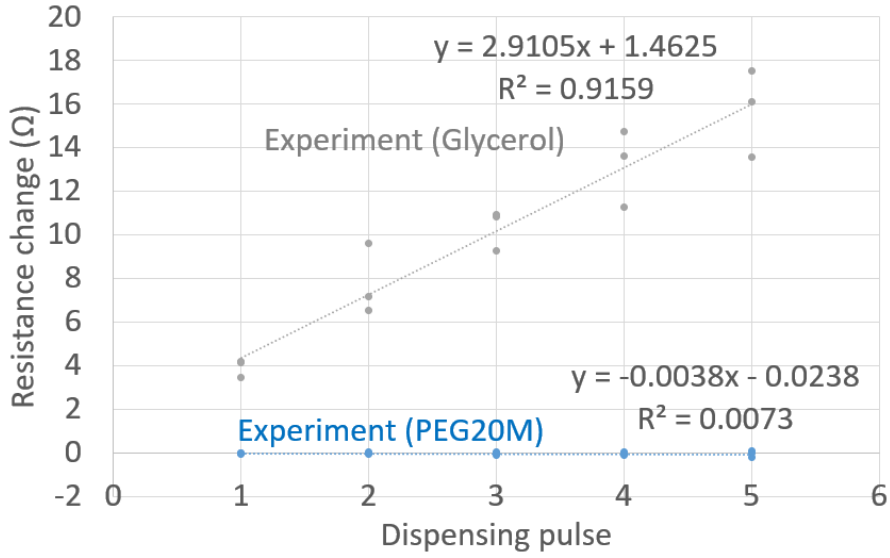

(b)

Figure 4.19: QCM frequency change and resistance change after depositions to PEG20M and Glycerol. (a) frequency change. (b) resistance change.

The experiment of glycerol deposition continues with the goal of reaching saturation frequency. This is to estimate viscosity of bulk loading. The experiment was conducted with 300 pulses of depositions for each exposure step. Figure 4.20 shows frequency and resistance change after glycerol depositions, the frequency change approached saturation at -12,000 Hz and resistance change of 1300 Ohm. The saturation may occurred after the overall glycerol layer is thicker than the penetration depth and together with the spreading of glycerol may cover all electrode area stops further response.

In the later section, there are discussions about the optimization to the Mason equivalent circuit model.

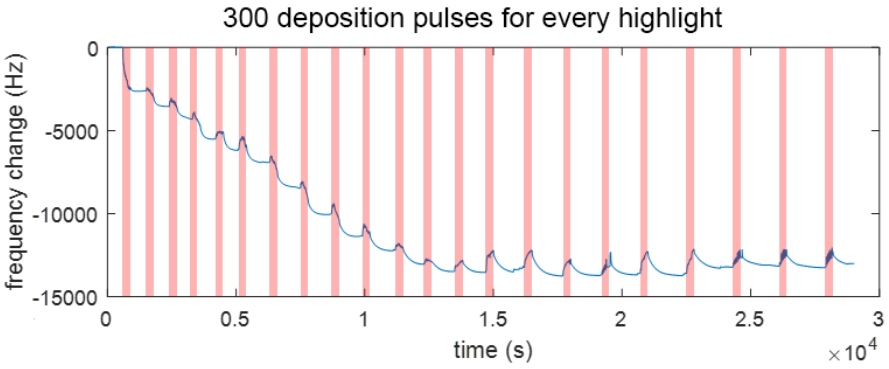

(a)

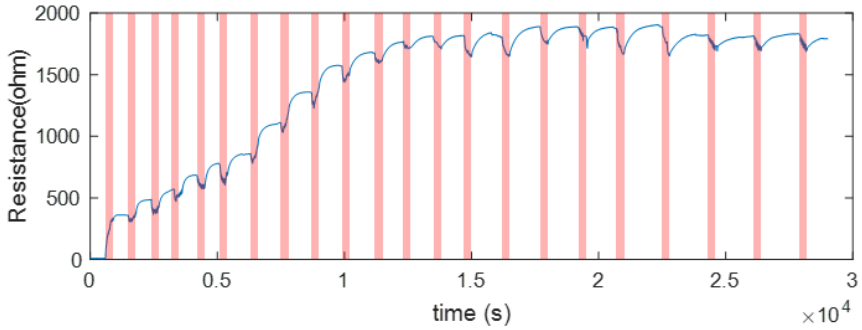

(b)

Figure 4.20: QCM frequency and resistance change after depositions to glycerol. (a) frequency change. (b) resistance.

4.5 Coated QCM response to water deposition

The observation of the behavior due to coated film is the main focus of our research. The unusual positive frequency occurs when sensing film is exposed to the vapor. Several films were selected with various viscosity the cover various film conditions. In these experiments film coating conditions are also as important as the depositions itself. The following experiments were conducted with glycerol and PEGs film coated by dip coating method.

4.5.1 Glycerol film

We did quite extensive experiments of water depositions over glycerol film. Results of different film thicknesses also affect our experiment results not only in terms of responses, but also the direction of frequency and resistance change. The first experiment (QCM1), water deposition was in order of 1 pulse, 3 pulses,10 pulses, 30 pulses, 100 pulses, and 300 pluses, progressively as is shown in figure 4.21. The depositions were repeated 3 times for each number of pulses. QCM2 experiment is shown in figure 4.22. The difference of QCM2 experiment from QCM1 was the depositions start from 1 up to 100 pluses while QCM2 start from 3 pluses. The depositions were also repeated 3 times for each number of pulses.

Table 4.1 shows the QCM frequency and resistance change before and after coating. The QCM1 experiment showed positive frequency but negative resistance change. This may be due to the water dissolving glycerol film, decreasing its viscosity and reducing overall viscous loading.

During the experiment of QCM2, this time the film thickness was significantly thicker observed from frequency change in table 4.1. There were positive frequency changes during water deposition, but quickly decayed after. This behavior was unusual and cannot be described by bulk viscous loading alone. However, the frequency change is relatively small and quickly decayed after water deposition. The interpretation of QCM2 result is still unclear.

Table 4.1: Film coating conditions.

Film materials	f_{pre} **(Hz)**	f_{post} **(Hz)**	Δf **(Hz)**	R_{pre} **(Hz)**	R_{post} **(Hz)**	ΔR **(Hz)**
QCM1 (Thin film)	8,998,939	8,995,035	-3,904	10	500	490
QCM2 (Thick film)	9,003,262	8,993,705	-9,557	14	824	810

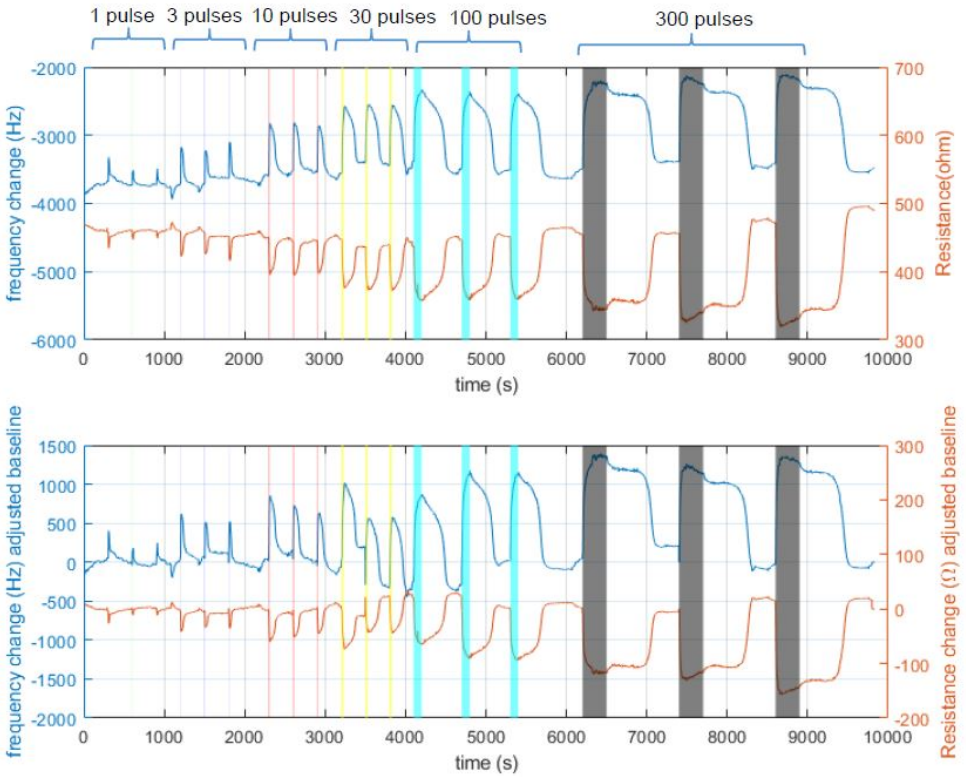

Figure 4.21: Raw QCM data on deposition of water over glycerol films: (Top) frequency change and resistance value. (Bottom) frequency change and resistance value after adjust baseline before every deposition. .

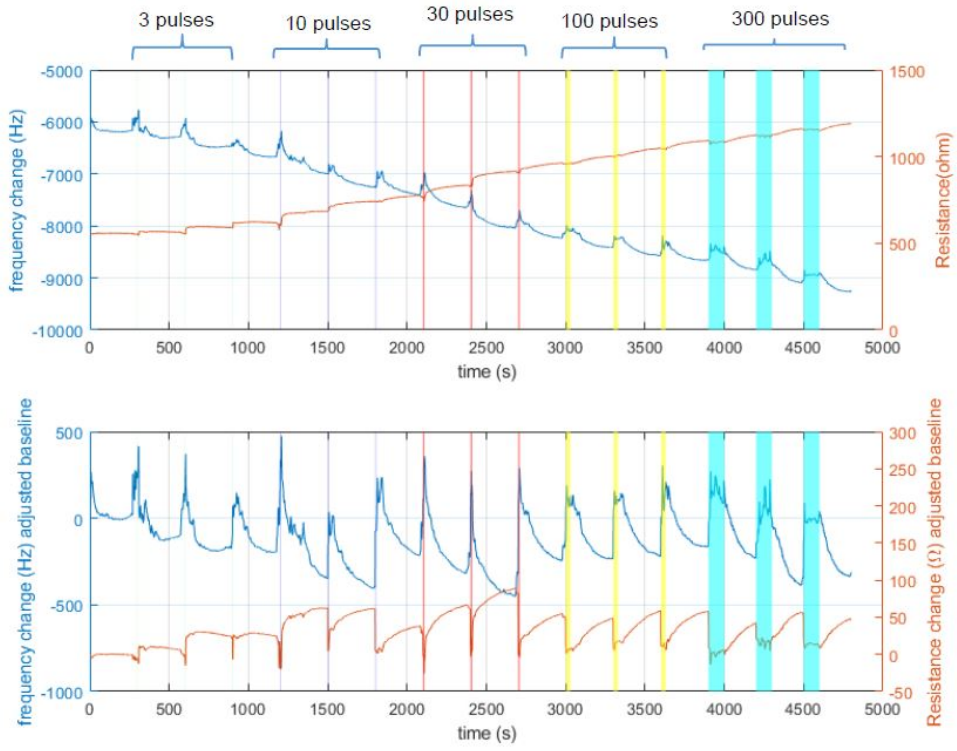

Figure 4.22: Raw QCM data on deposition of water over glycerol films: (Top) frequency change and resistance value. (Bottom) frequency change and resistance value after adjust baseline before every deposition. .

4.5.2 PEG films

PEG20M and PEG2000 are the film materials selected for film material. PEG20M represents rigid film material as confirmed by the previous experiment. PEG2000 has a viscosity in between rigid and highly viscous of glycerol. The table 4.2 shows the QCM frequency and resistance change before and after coating. Both experiments have the exposures in the order of 100 pulses, 300 pulses, and 1000 pulses. The depositions were repeated three times for each number of pulses.

Table 4.2: Film coating conditions.

Film materials	f_{pre} **(Hz)**	f_{post} **(Hz)**	Δf **(Hz)**	R_{pre} **(Hz)**	R_{post} **(Hz)**	ΔR **(Hz)**
PEG20M	9,001,721	8,999,474	-2,246	15.92	18.28	2.36
PEG2000	9,001,739	8,999,439	-2300	10.98	172.22	161.2

Figure 4.23 shows PEG20M had a negative frequency shift and a positive resistance change. This negative frequency and positive resistance shift response can be interpreted as viscous loading. However, PEG2000 (figure 4.24) had a positive frequency and also a positive resistance change. This unusual response cannot be interpreted directly by a combination of Sauerbrey's equation and Kanazawa's equation. Our proposed Mason equivalent circuit had a region with both a positive and negative frequency and resistance change. The interpretation of the QCM result will be discussed in the next section.

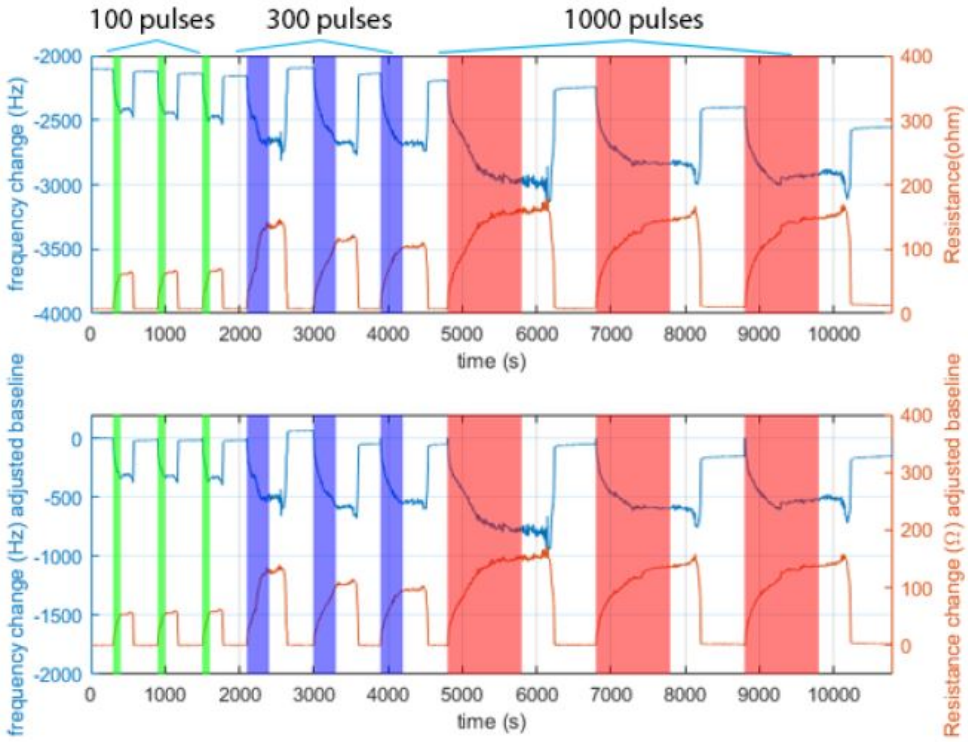

Figure 4.23: Raw frequency change and resistance value of QCM data on the deposition of water over PEG20M film. Top figure shows the raw data; the bottom figure shows the data after adjusting the baseline before each deposition.

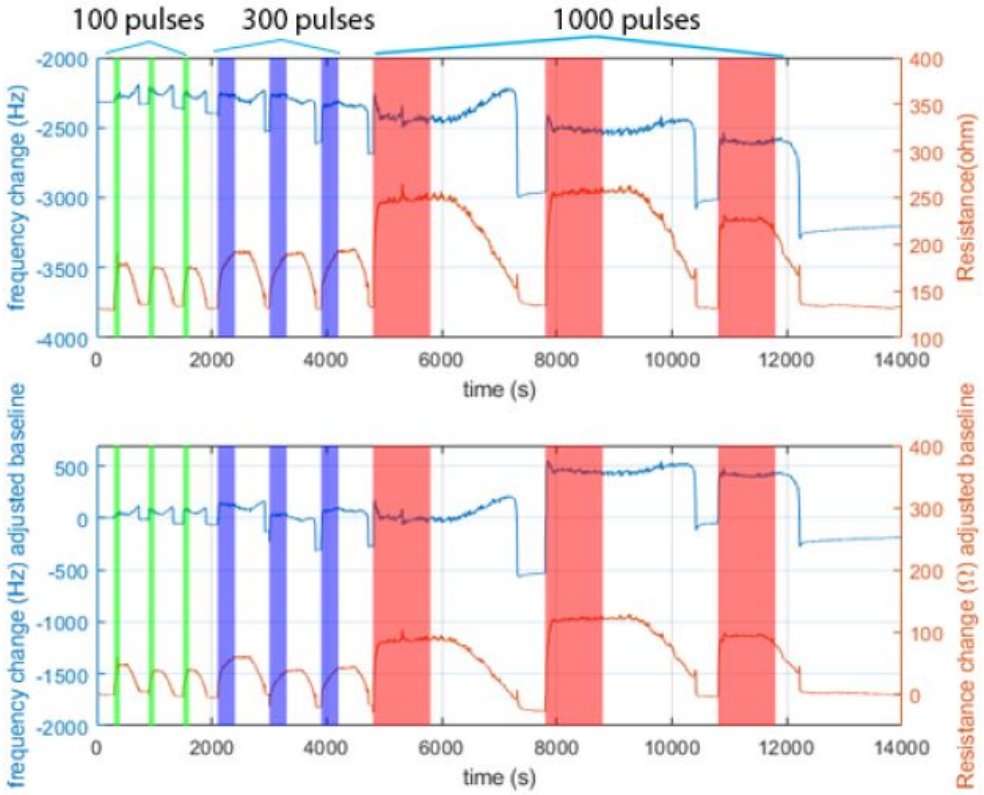

Figure 4.24: Raw frequency change and resistance value of QCM data on the deposition of water over PEG2000 film. Top figure shows the raw data; the bottom figure shows the data after adjusting the baseline before each deposition.

4.6 Summary

In this chapter including all the experimental data of deposition over bare QCM and film coated QCM. The deposition volume of the dispenser was confirmed to be 3nL /pulse for water, 5 nL/pulse for PEG dissolved in chloroform and 6 nL/pulse for glycerol dissolve in acetone.

Film coating with a dipcoator was optimized by the pull-up speed. The glycerol solutions of 0.01 g/cm^3 and 0.001 g/cm^3 were used. The slower pull-up speed produced the thicker film at the same solution concentration. The pull-up speed of 30 um/s showed the best film consistency. Film thickness can be adjusted by the coating solution concentration.

The rigid film material as PEG20M produces a well predicted response agreeable with Sauerbrey's equation when deposited over bare QCM. While glycerol shows both frequency and resistance change, Kanazawa's equation predicts only bulk liquid makes it not applicable to glycerol deposition.

The water deposition over films were investigated. 3 film materials Glycerol, PEG20M, and PEG2000 represented different film viscosity. Glycerol solution has the highest viscosity and the water deposition can express both positive and negative frequency change depending on film thickness, but more likely to have positive frequency change and negative resistance change which can be simply explained by the water dissolve glycerol and dilute the overall film viscosities. PEG20M also had positive frequency change and negative resistance change when exposed to water, the

similar explanation in film dissolves by water. The experiment with PEG2000 had a positive frequency and also a positive resistance. This response cannot be interpreted directly by a combination of Sauerbrey's equation and Kanazawa's equation. Our proposed Mason equivalent circuit has a positive frequency region and is expected to be able to interpret these results.

Chapter 5

Characterization of QCM behavior

5.1 Introduction

In chapter 2 we thoroughly explore the condition for the Mason equivalent circuit. The model for viscous film is the more generalized for representing both rigid and viscous film. While the two-layer model extended the single viscous film concept and deposition may be treated as the top film layer.

5.2 Simulation of QCM frequency and resistance change using Mason equivalent circuit

5.2.1 Viscous film condition

To simulate the viscous film model, the parameters of the deposited films are viscosity(μ_L), density(ρ_L) and film thickness (h). Typically, viscosity and density are the product term, making it difficult to separate these two parameters. While film thickness is within function tangent in equation 2.42 and reaches saturation as the film grows. Our simulation simplifies viscosity-density terms by selecting constant value for density, then only varying viscosity and film height.

Figure 5.1 shows the simulation of frequency change using equation 2.42 which derived from Mason equivalent circuit. The simulation uses parameters of water as is shown in table 5.1 The dashed line indicates Sauerbrey equation calculated from water mass if it uniformly spreads over QCM electrodes. Horizontal fine dashed line indicate frequency change using Kanazawa's equation, this line should represent bulk water loading, this is viable since as the film thickness grows frequency change approaches this line. However there is a difference around 200 Hz, between Kanazawa's equation and the simulation of viscous film condition. Nonetheless, the equation adequately predicts both thin film and bulk loading and the film thickness increases.

Figure 5.2 shows similar plot with glycerol. The simulation uses parameters of glycerol as is shown in table 5.1. Please be noted that the viscosity of glycerol used in the simulation is much lower than the viscosity in the literature. Calculated frequency change from Kanazawa's equation is extremely large (>20 kHz) for the viscosity of 1261 cP. The viscosity value of 5 cP was used to represent high viscosity film when compared to water. The plot also including dashed line represent Sauer-

brey's equation and fine dashed line represent bulk liquid frequency change from Kanazawa's equation.

Both graphs have a reversing point. As film thickness increases, the frequency continues to decrease until at some point (170 nm in case of water) frequency becomes increasing and reaches a constant value. However, the simulation of glycerol (figure 5.2) the frequency turning point turning was at around 350 nm while water was at 170 nm. This behavior predicts the positive frequency occur when the deposited film thickness is increased. From mathematical point of view, by expanding tangent function using Taylor series, we can suspect the higher order terms cause the positive frequency change, the exponential of complex number may result in the change of sign to positive frequency change. From the physical of viewpoint, at small film thickness deposited film behave similar to rigid film. The film thickness increase causes acoustic wavelength (λ) to increase as well, thus the frequency decrease. As the film thickness increase some energy is dissipate in the film layer while most of the energy still contain within QCM substrate and film layer. However, at some film thickness (approximately 170 nm in figure 5.1) may reach a critical thickness that the reflected wave interfere with traveling wave and increase it frequency resonant. This frequency increase stop when the film thickness is high enough for the travelling to be completely decayed.

Table 5.1: simulation parameters

Parameters	**Viscosity(cP)**	**Density(g/ml)**	**Notes**
Glycerol	5	1.261	Viscosity of 5 cP was our assumption. The viscosity from literature [ref] is 1261 cP.
Water	0.89.	1.0	

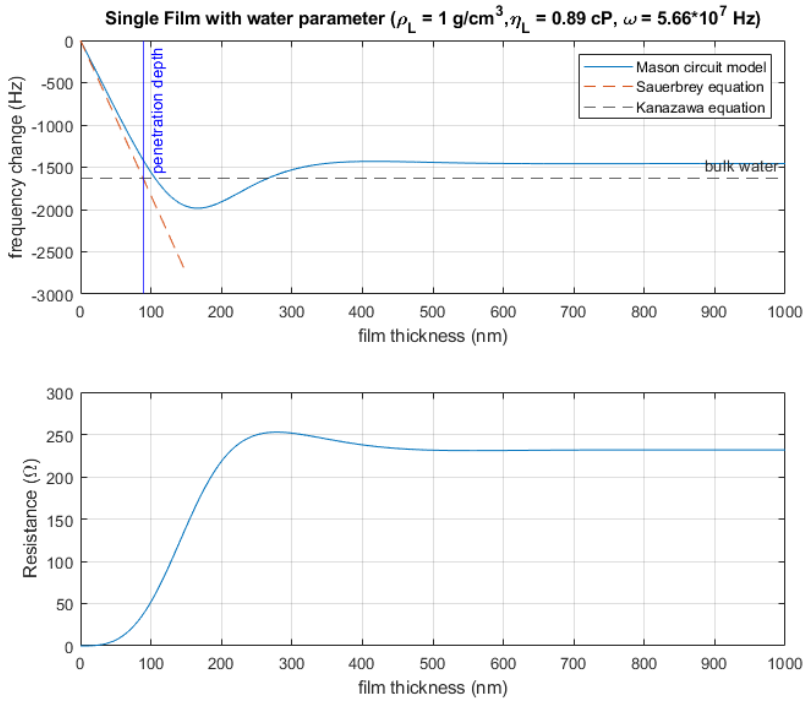

Figure 5.1: QCM response simulation using Mason equivalent circuit, using parameters of water.

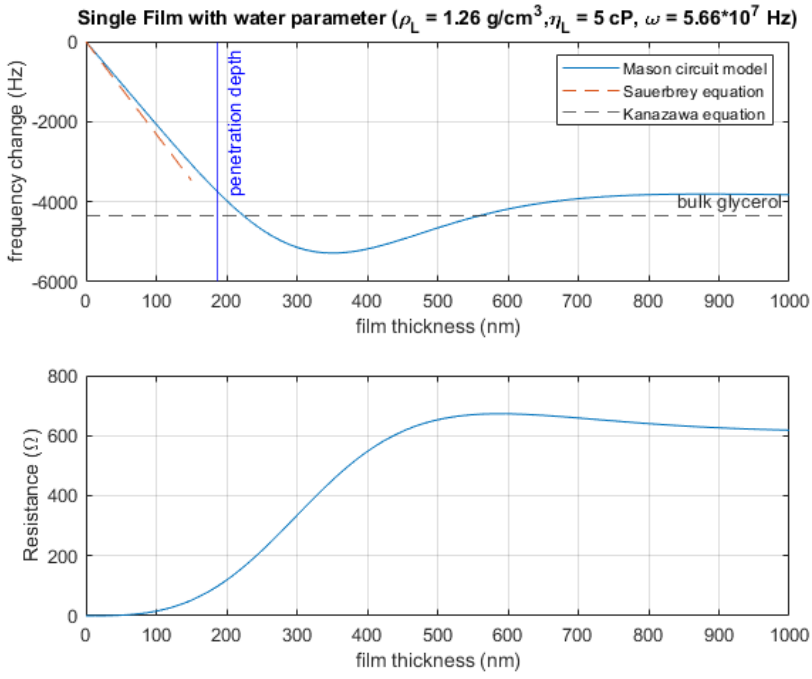

Figure 5.2: QCM response simulation using Mason equivalent circuit, using parameters of glycerol.

5.2.2 Two-layer film condition

We also proposed the two-layer viscous film model in section 2.4.4. This time we model the base layer film using glycerol parameters and the top layer film using water, similar to our experiment of depositing water over glycerol film.

Figure 5.3 was mentions again from 2.15a and 2.15b shows the simulation using the same film parameter as the previous section (5.1). Both figures express the same data but the representation is different.

Figure 5.3a shows the plot of both frequency and resistance change with top layer film thickness as a parameter of base layer. The blue dashed line representing Sauerbrey's equation and a fine dashed line representing Kanazawa's equation for bulk water loading and bulk glycerol loading.

When, base layer thickness is 0, this can be treated as no glycerol layer. As the top layer film thickness increases, the frequency change approaches the frequency change of bulk water from Kanazawa's equation. This proves the validity of the 2 layer model when the condition is approached by the single layer model. Interesting behaviour from this plot occurs when the base layer (glycerol) film thickness increases. Base layer film thickness influences the initial frequency change, as the base layer film thickness increases, we may observe the positive frequency change as the top film thickness increases. For example base layer thickness of 375 nm, frequency change start at -5200 Hz then increase to -4300 Hz as top layer film thickness increases. Another speculation is that as the base film thickness increases, the final frequency change as the top layer grows is approached by the frequency change of bulk glycerol. This is possible as the film in contact with QCM thickness increases the shear wave travel most in this layer and has the most influence on QCM frequency change. The resistance plot shows that base layer film thickness indicates over resistance value as the base layer grows the resistance increases significantly compared to slightly changing when the top layer film thickness increases.

Figure 5.3b shows the plot of both frequency and resistance change with base layer film thickness as a parameter of top layer. For all cases of top layer film thicknesses, as the base layer film thickness increases the frequency change approaches bulk glycerol from Kanazawa's equation, similar to figure 5.3a. Top layer film thickness shifts the valley (frequency reversing point) to the left as the film thickness and the sharpness of this curve also get duller. For the resistance change the resistance approaches 600 Ω as the base layer film thickness increases. This indicates that the top film layer becomes less influenced as the base layer becomes dominant. This conclusion is consistent with the figure 5.3a.

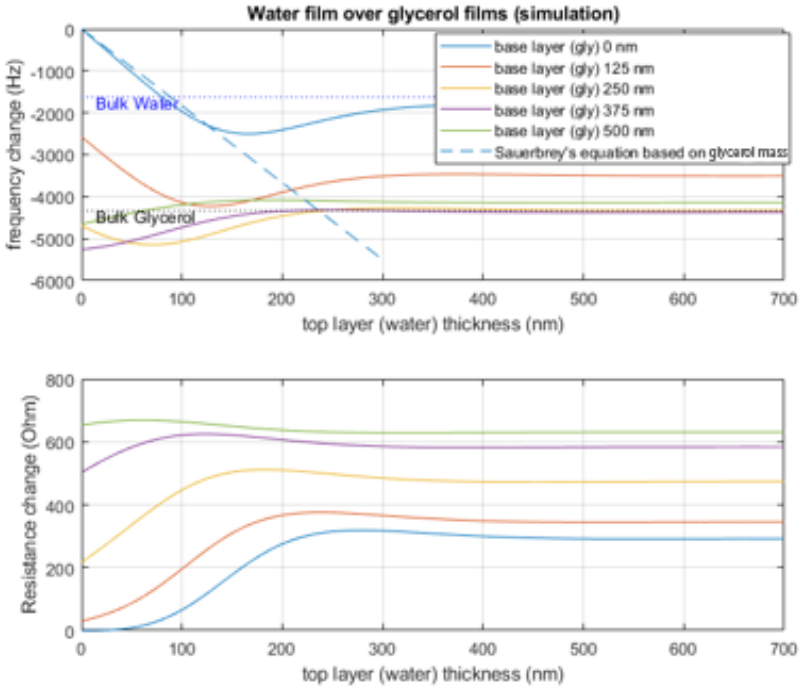

(a)

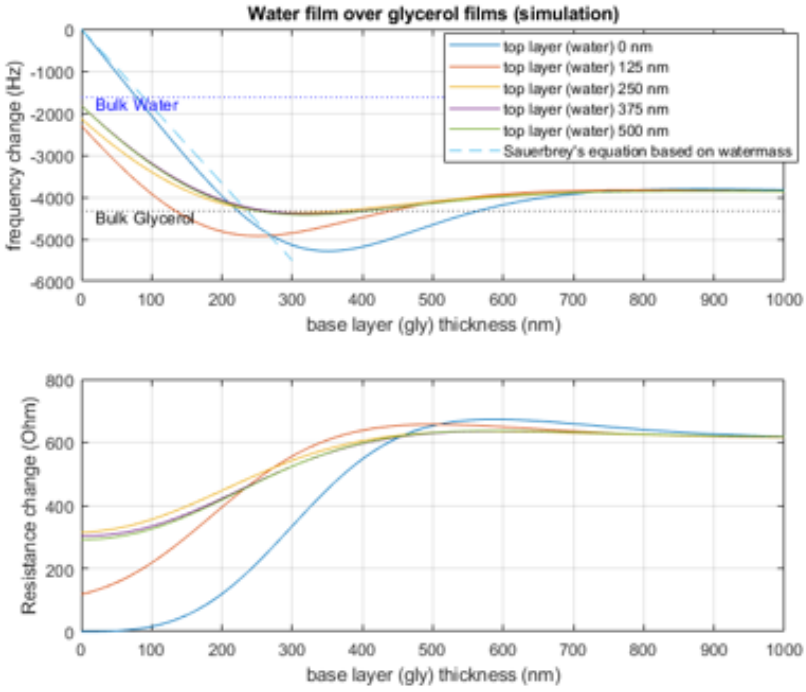

(b)

Figure 5.3: Simulation of frequency and resistance change using two-layer viscous film condition: (a)based layer film thickness as parameter, (b) top layer film thickness as parameter

5.3 Glycerol film thickness and viscosity estimation

One approach of applying our developed Mason equivalent circuit is to estimate the film parameters from experimental data. However, as the number of parameters increasing the optimized parameter result may not have been meaningful. We should make some preliminary assumptions to reduce some parameters and also be mindful of the results. In this section we tried to estimate film thickness and viscosity from several dip coating data. The film thickness is unknown but expected to be relatively similar form the same dip coating pull-up speed. Four groups of QCMs with different pull-up speeds were dip into glycerol solution, concentration 0.01 g/ml. The pull-up speed, frequency change and resistance change of the QCM is shown in the table 5.2.

Table 5.2: simulation parameters

QCM group	**QCM No.**	**Dip coater pull-up speed (um/s)**	**Δ R (Ω)**	**Δ f (Hz)**
A	1	10	575	-4900
A	2	10	463	-4284
B	3	50	126	-3238
B	4	50	139	-3131
C	5	30	122	-1551
C	6	30	127	-1429
D	7	80	26	-717

As discussed previously the unknown parameters from viscous film are film thickness and viscosity, film density is kept constant by the assumption that many viscous film has density comparable to water. One assumption is that viscosity should be a constant value among various film thickness. This means that for measured data, the estimation was made to a single value of viscosity but various film thickness in accordance with each experiment. Table 5.3 shows the optimized result using equation 2.42. The estimated viscosity from the experimental data is 3 cP, which is much smaller than its reference value. Since QCM resonant frequency is very high, compared to almost static frequency of the measurement from a traditional viscometer. Also the film thickness estimation is from minimization the error between measured impedance and the impedance calculated from estimated parameters. The estimation of film thickness works quite well at small film thickness, as the film thickness increases the rate of frequency change and reaches saturation. If the frequency change data approach saturation, the estimated film thickness fluctuates around high film thickness and does not provide a good estimation.

Next experiment is the estimation of film viscosity and film height from depositing glycerol solution over bare QCM. The glycerol solution concentration was 0.01

Table 5.3: film viscosity and film thickness estimation by curve fitting

QCM	**viscosity (cP)**	**film thickness(nm)**
1		411.93
2		500.69
3		157.47
4	3.05	153.09
5		74.46
6		69.10
7		33.85

g/ml. The depositions were conducted is shown in table 5.4. The frequency change and resistance plot is as shown in figure 5.4. This experiment is progressively deposited until QCM reaches almost saturation. The estimation of film thickness and viscosity is expressed in figure 5.5. The estimated viscosity is 12.83 cP as is shown in plot legion. The number above the red circle is the order of data used in calculation. The blue line is the simulation using the estimated viscosity (12.83 cP). The impedance used in calculation average from 100 s data before the each depositions. After calculation each datapoint(red circle) was assigned to its designated film height. From the plot we expected the number above data to gradually increase from left to right, meaning the film thickness continuously grows as the deposition continues. However, the data point did not assign orderly with the deposition sequence. And also the deviation of resistance is larger than the frequency change. Nonetheless, the estimation was somewhat predicts the trend of deposition data. However, the positive frequency change cannot be observed here.

Table 5.4: time and number of pulses

time (s)	0	600	1200	1800	2400	3000	3600	4200	4800	5700
deposition pulses	0	10	10	10	30	30	30	100	100	100
datapoint label number		1	2	3	4	5	6	7	8	9
time (s)	6300	7200	8100	9000	9900	10800	11700	14100	17000	
deposition pulses	300	300	300	300	300	300	1000	1000	1000	
datapoint label number	10	11	12	13	14	15	16	17	18	

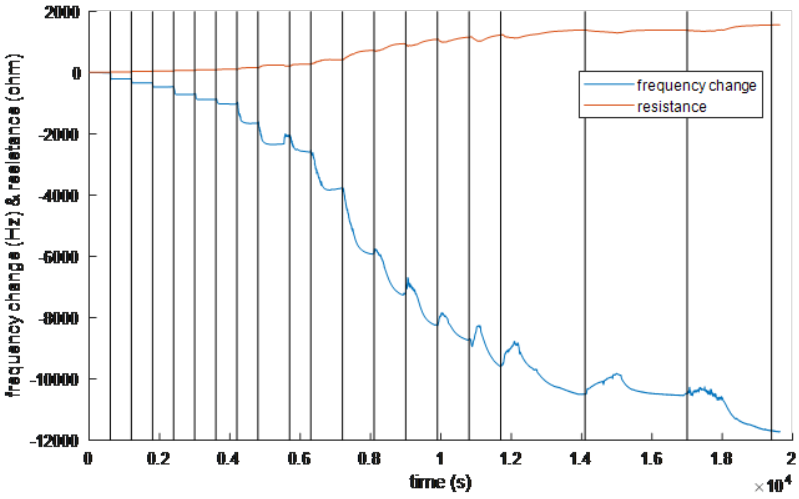

Figure 5.4: frequency change and resistance plot of deposition of glycerol over bare QCM, solvent concentration of 0.01 g/ml.

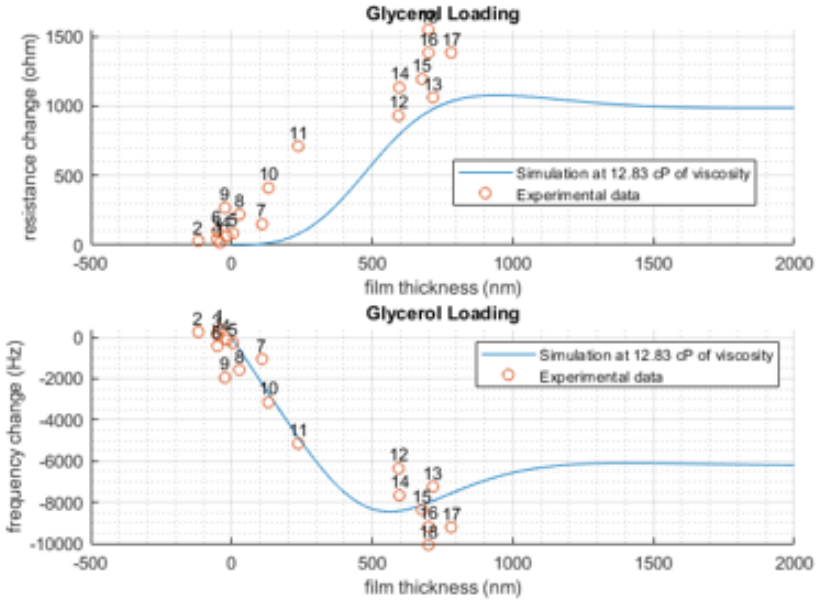

Figure 5.5: Estimation of deposited film an film viscosity

5.4 Qualitative interpretation of QCM responses with water exposure

As discussed in the previous section, to directly estimate film thickness from optimization technique does not give any insight or intuition of the interaction of depositing water and underlying coated film. Figure 5.6 shows the simplified one-dimensional model of the film change when exposing it to water. The water sorption causes the overall film thickness to increase and the film viscosity to decrease. This assumption is expected to be able to adequately explain the experimental data so that the Mason circuit model can work.

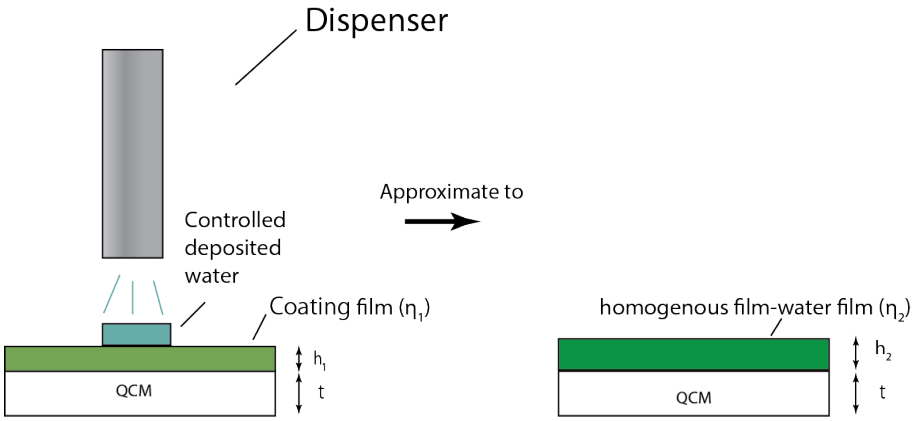

Figure 5.6: Simplified model of the expected film change when exposed to water.

Figure 5.7 is a surface 3D plot of a Mason circuit model with viscous film boundary condition. There were 3 variables related to the properties of the coating film: film thickness h, film viscosity η_L , and film density ρ_L . Assuming the film density is relatively constant at 1 g/cm^3. Figure 5.7a shows the frequency shift as a function of film thickness and film viscosity from equation 2.42. The same color indicates the same frequency change. We can observe that for any given viscosity value, as the film height increases the frequency increases first then at certain film thickness the frequency begins to increase then approaches saturation. Figure 5.7b shows a similar phenomenon for the resistance value, as film height increases, the resistance also reaches saturation.

These plots can be flattened into contour plots for better visualization. Figure 5.7a and 5.7b are flatten to figure 5.8a and 5.8b,respectively. As discussed previously. First, we observed the frequency decreases, then at a certain range of film thickness, the frequency increases and reaches a constant value. This positive frequency shift due to film thickness change in Figure 5.8a may explain why, in some cases, the sorption takes place and the positive frequency shift occurs experimentally. This can lead us to some explanation about why a positive frequency change occurs simultaneously with a positive resistance change.

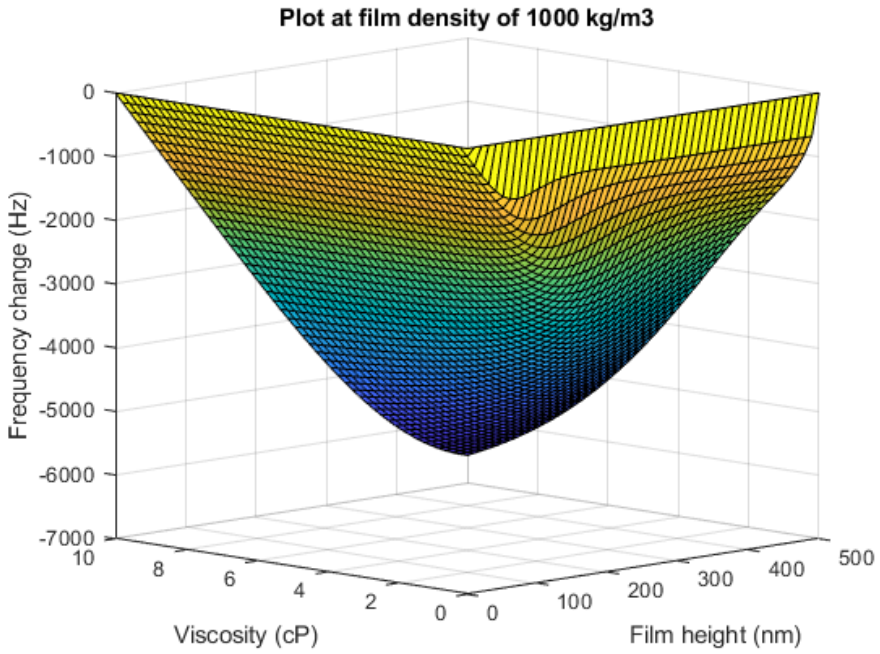

(a)

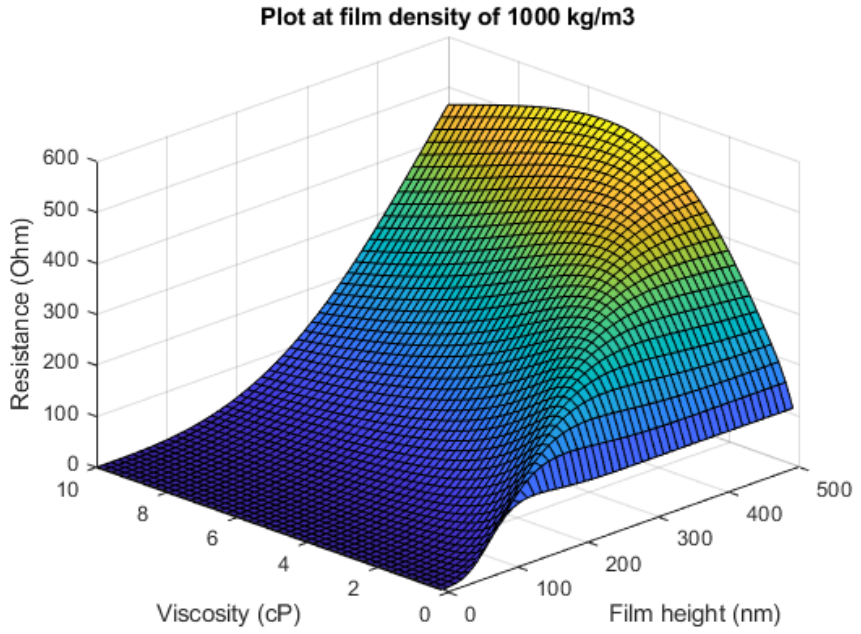

(b)

Figure 5.7: 3D plot of the frequency shift and resistance at a film density of 1000 kg m^{-3}: (a) 3D plot of the calculated frequency shift. (b) 3D plot of the calculated resistance shift.

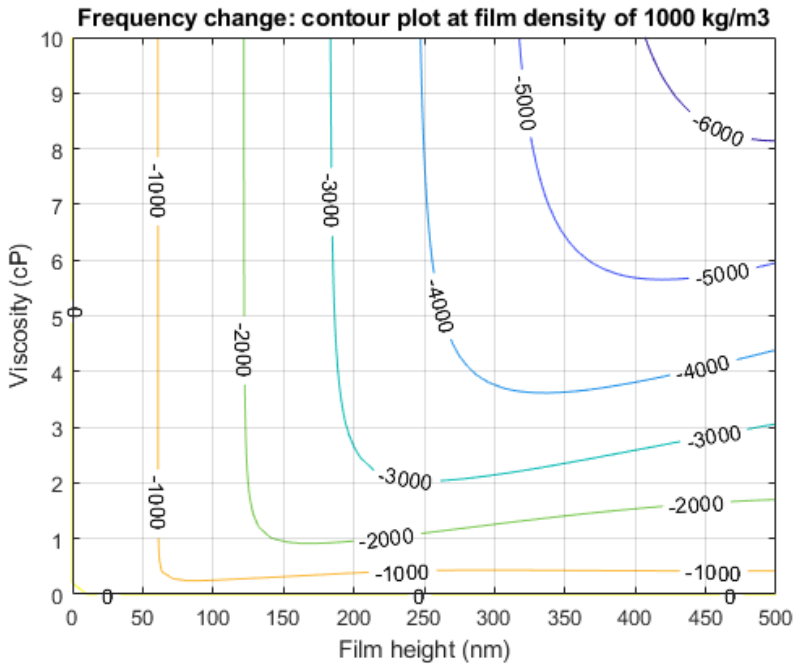

(a)

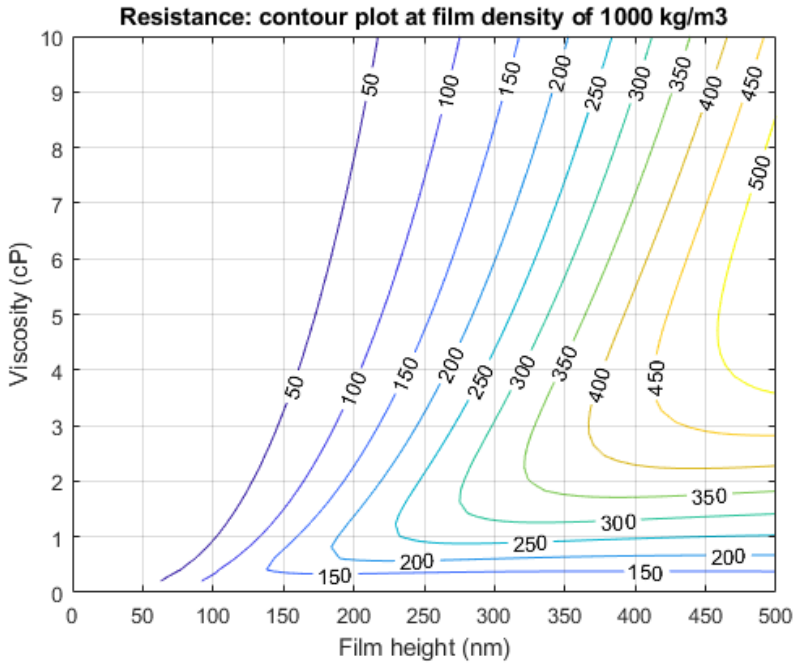

(b)

Figure 5.8: Contour plot of the frequency shift and resistance at a film density of 1000 kg m^{-3}: (a) Contour plot of the frequency change. (b) Contour plot of the resistance.

5.4.1 Glycerol film

Experiments were conducted to investigate the response of the QCMs coated with glycerol film. The microdispenser was used to simulate odor exposure; however, we simplified it to use only water deposition. Three different coating films were applied to the QCMs using the dip-coater. Table 5.5 shows the QCM frequency and resistance change before and after coating. Glycerol had the highest frequency and resistance change, indicating that glycerol is highly viscous.

Table 5.5: Film coating conditions.

Film materials	f_{pre} **(Hz)**	f_{post} **(Hz)**	Δf **(Hz)**	R_{pre} **(Hz)**	R_{post} **(Hz)**	ΔR **(Hz)**
Glycerol	9004436	8991551	-12886	19	740	721
PEG20M	9001721	8999474	-2246	15.92	18.28	2.36
PEG2000	9001739	8999439	-2300	10.98	172.22	161.2

Figure 5.9 shows the raw QCM data on the water sorption with the glycerol coating. Figure 5.9a shows the frequency plot, and Figure 5.9b shows the plot with the adjusted baseline before each exposure. The orange line shows the resistance change. Exposure was in the order of 1 pulse, 3 pulses, 10 pulses, 30 pulses, and 100 pulses. The depositions were repeated three times for each number of pulses. The deposition amount had not saturated the glycerol film yet. Since glycerol is highly viscous, the film height at saturation was very large, as is shown in Figure 5.7a and 5.8a. The dispenser was operated at 1 Hz, yielding 1 pulse per second. There was a positive frequency change during the depositions, but a continuing response after the depositions did not occur. There was a steady-state frequency after each deposition. However, the frequency drift normally occurred independent of water exposure. This was due to the coated film having a large viscosity change even with the small temperature change, and viscous films are more sensitive to this effect. Another cause might be the shape of the film gradually changing due to vapor exposure.

The experimental result of water sorption with glycerol coating can also be roughly explained by the contour plot of the Mason equivalent circuit. The challenge was that the experiment with glycerol had a significant frequency drift independent of the coated film's condition. The blue arrow line in Figure 5.10 shows the direction of the frequency drift,which in this case tended toward the negative frequency shift. This frequency drift effect did not depend on the coated film and can occur in both positive or negative frequency change. We tried to focus only on explaining the results after the sorption (orange arrows). The orange arrow shows the peak frequency and resistance change after each deposition. To avoid clutter in the plot, we selected only the first deposition out of the three repeated depositions. Our assumption that viscosity decreases as film thickness increases can roughly explain the data. The interesting point is that as the negative frequency change became larger, the resistance became almost constant. This can be explained in the case of 100 pulses. The change might occur along the resistance contour line, but the frequency change still occurs in effect. This may explain why sometimes a frequency change occurs without a resistance change.

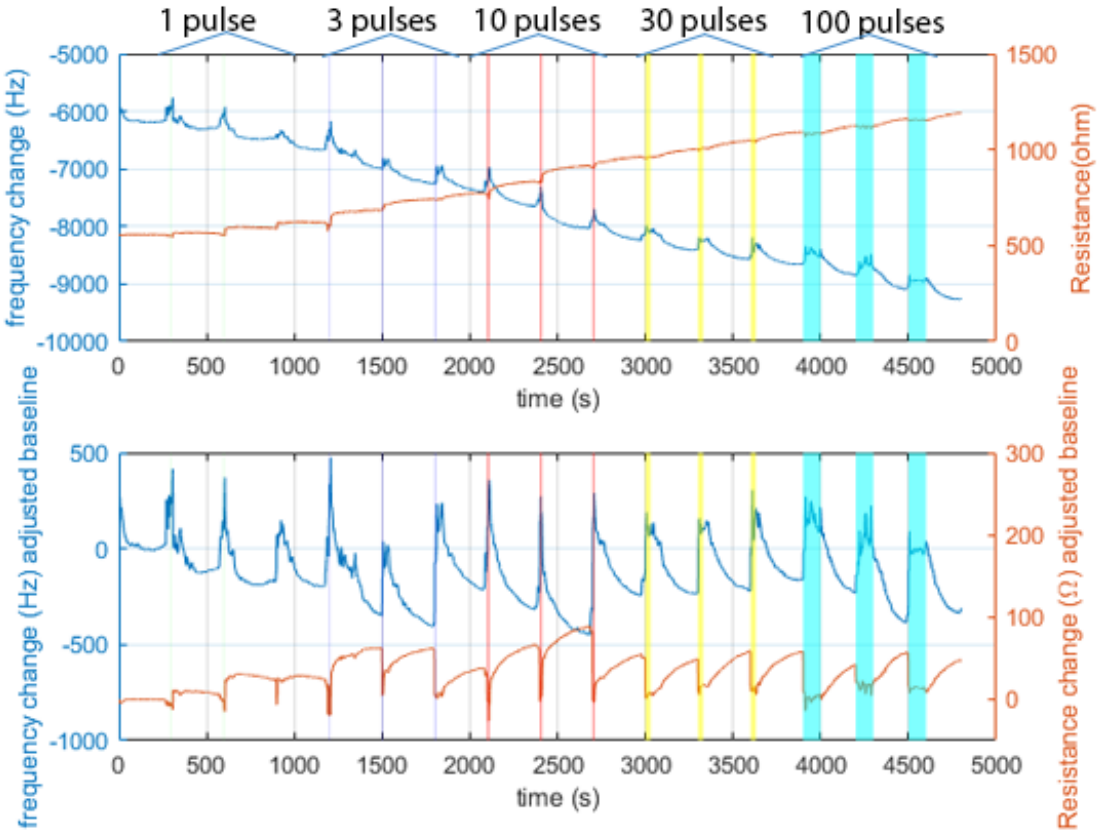

Figure 5.9: QCM data on the deposition of water over glycerol films: (**a**) Frequency change and resistance value. (**b**) Frequency change and resistance value after adjusting the baseline before every deposition.

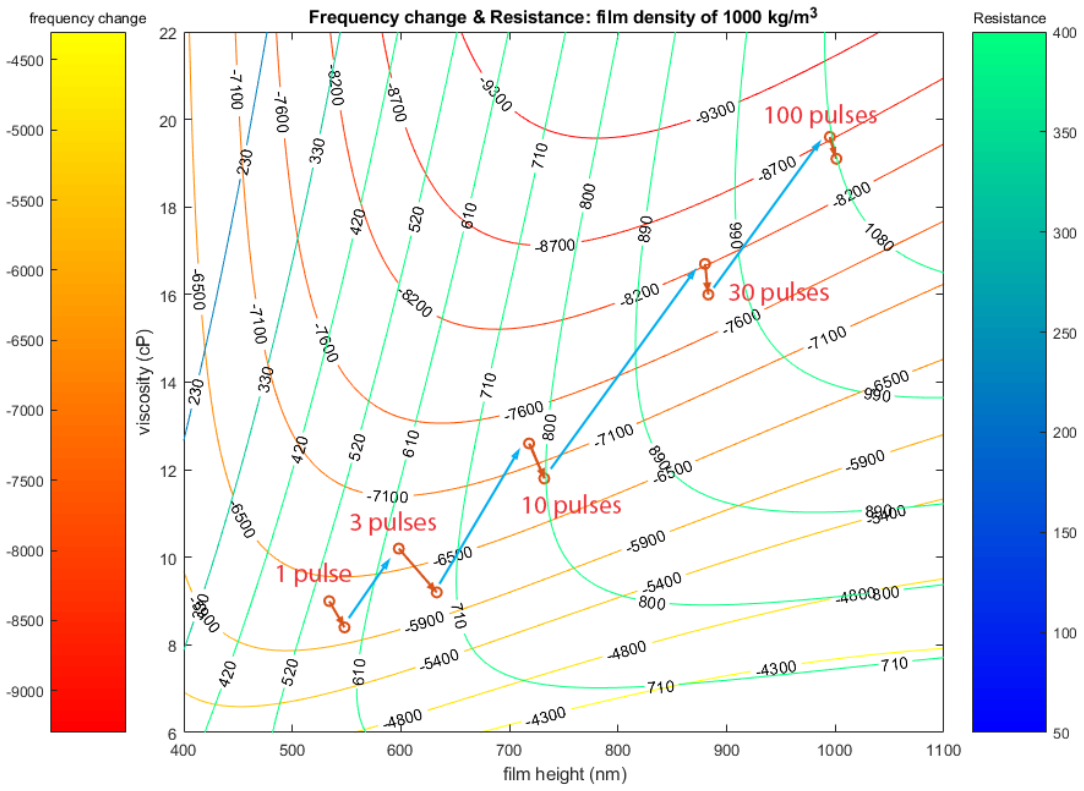

Figure 5.10: Combined contour plot of both resistance and frequency when glycerol film is exposed to water. The orange arrow represents the frequency and resistance change of the coated QCM when exposed to water; the blue arrow indicates the direction of the frequency drift.

5.4.2 PEGs film

The experiment was further conducted with Polyethylene Glycol (PEG) film. PEG2000 and PEG20M were chosen as lossy and lossless films, respectively. A lossy material is viscous, and the acoustic energy is consumed at the film; while a lossless material is rigid, and the acoustic energy is seldom consumed there. Figure 5.11 shows the raw QCM data on the deposition of water over PEG films. The exposure was done in the order of 100 pulses, 300 pulses, and 1000 pulses, respectively. The depositions were repeated three times for each number of pulses, similar to Figure 5.9. Both PEG films had an apparent response after every exposure. PEG20M (Figure 5.11a) had a negative frequency shift and a positive resistance change. This negative frequency and positive resistance shift response can be interpreted as viscous loading. However, PEG2000 (Figure 5.11b) had a positive frequency and also a positive resistance. This response cannot be interpreted directly by a combination of Sauerbrey's equation and Kanazawa's equation. Our proposed Mason equivalent circuit had a surface plot with both a positive and negative frequency and resistance change. This makes our model able to describe various types of responses, including this case.

Figure 5.12 shows the combined contour plot of both the frequency shift and resistance. By assuming that the water deposition increases the overall film thickness and decreases the film viscosity by dilution, the direction of change should be from top-left to bottom-right. The frequency shift and resistance data at 100 pulses are drawn for the PEG20M film and the PEG2000 film. PEG20M had a frequency decrease from -2100 to -2400 Hz and had a resistance increase from 7 to 65 Ohm, while PEG2000 had a frequency increase from -2300 to -2200 Hz and had a resistance increase from 130 to 190 ohm. Both films' behavior can be explained by the 3D plot of the Mason circuit. The Mason equivalent circuit can explain the positive frequency change that occurs together with the positive resistance change. This phenomenon cannot be explained using the conventional Kanazawa's equation.

The data near the bottom right have a tendency toward positive change due to the contour lines of the frequency change being relatively parallel to the film height, making the positive frequency occur when the viscosity decreases. On the contrary, data near the top left have an inverse effect: the frequency shift increases when the film thickness increases. For the resistance change, for almost every case, the resistance increased when there was additional loading. This can be explained by the contour plot. The resistance contour lines always lie diagonally when the viscosity is over 1 cP (viscosity of water = 0.89 cP), which is always the case for almost every coating film. Interestingly, for the thin film (<50 nm), the film behaved as a mass loading only, regardless of the viscosity. We can estimate the film thickness quite accurately by using only the frequency change if the film thickness is thin enough.

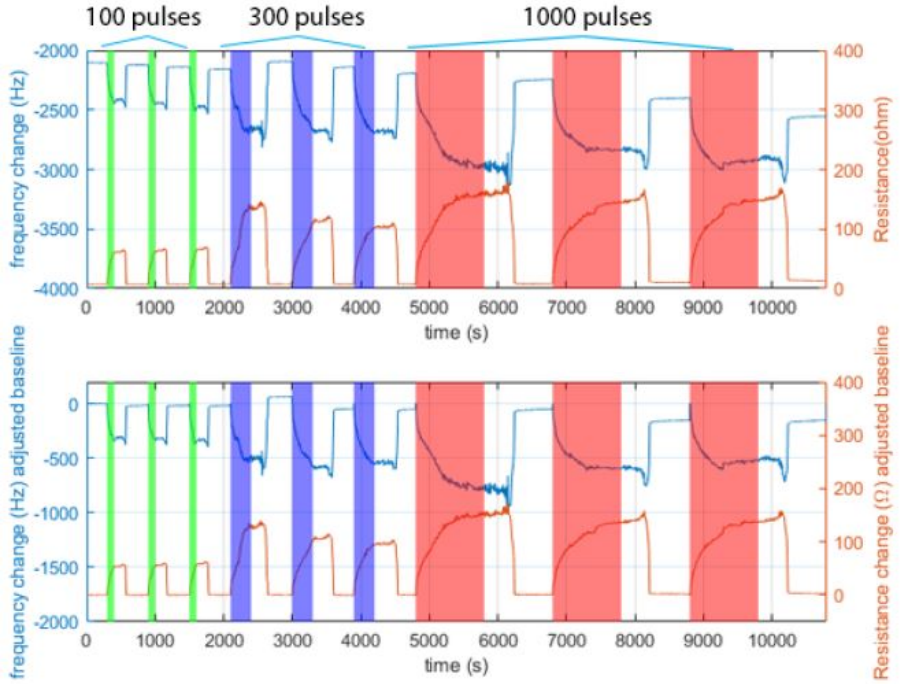

(a)

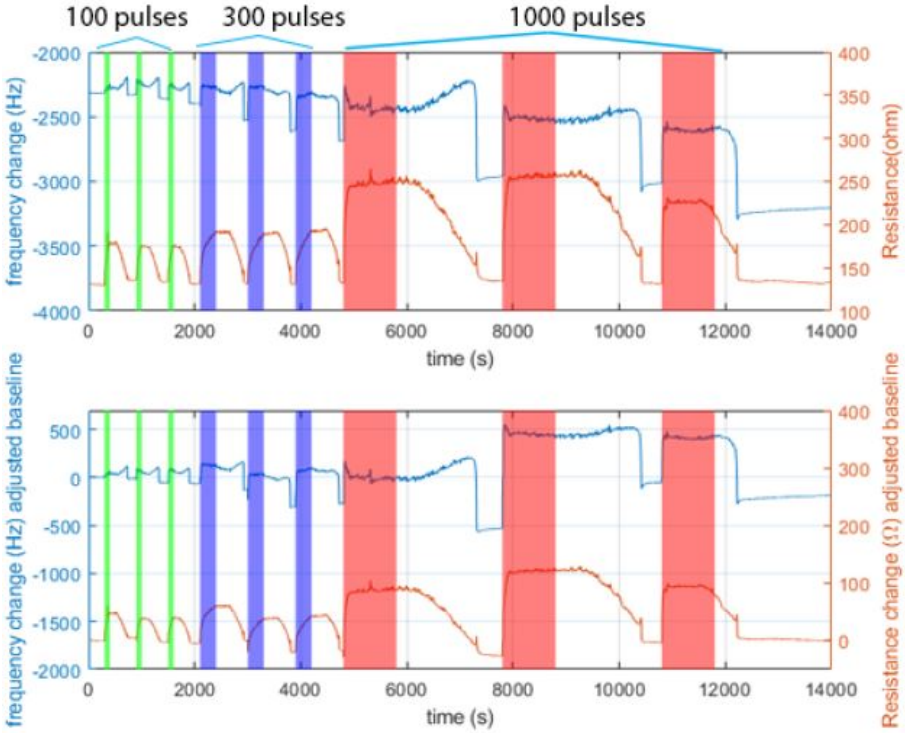

(b)

Figure 5.11: QCM data on the deposition of water over PEG film. Both top figures show the raw data; the bottom figures show the data after adjusting the baseline before each deposition: (**a**) Frequency change and resistance value of PEG20M. (**b**) Frequency change and resistance value of PEG2000.

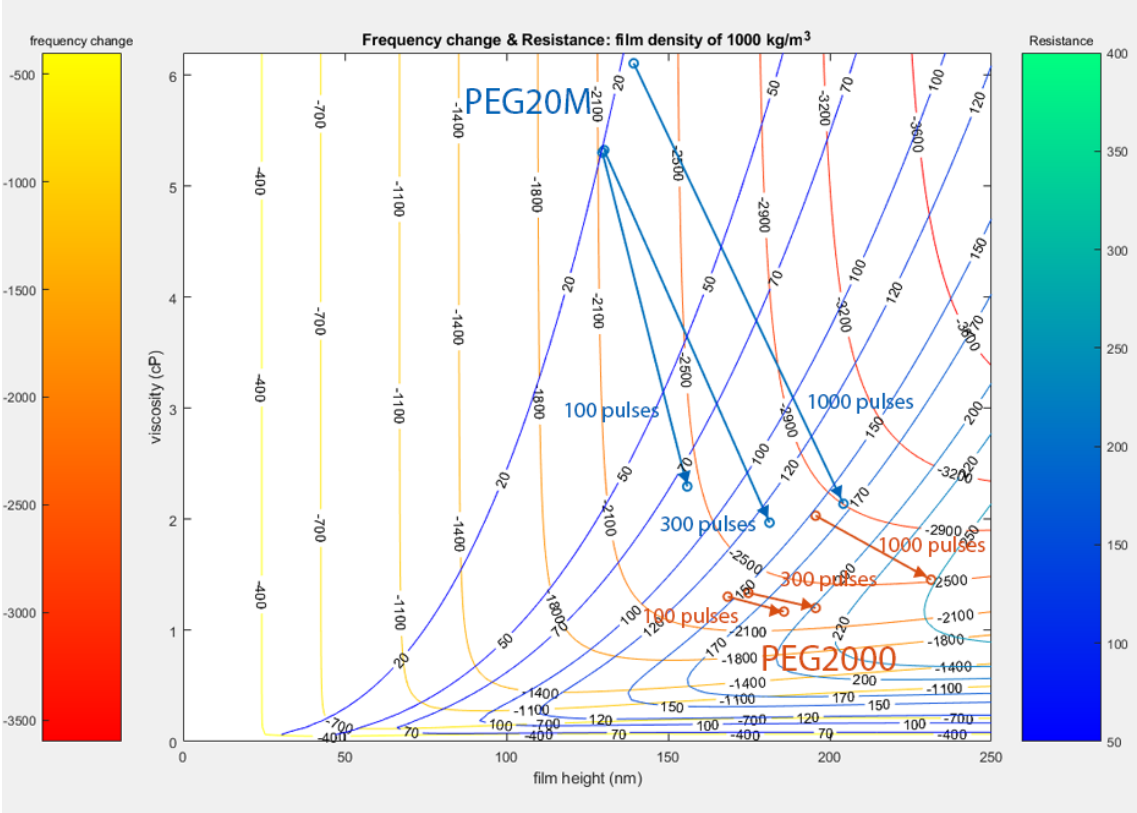

Figure 5.12: contour plot of both resistance and frequency. The arrow line represents the frequency and resistance change of the coated QCM when exposed to 100, 300, and 1000 pulses of water; blue arrow: PEG20M, orange arrow: PEG2000.

5.5 Summary

We further explore the Mason equivalent circuit and find its feasibility in predicting a positive frequency change when a certain viscous film is exposed to vapor to simulate an odorant. The Mason model expresses the impedance of the loading material, which can be converted into a frequency and resistance change for more universal representations.

With a viscous film, the measurement of the frequency alone is not sufficient to detect the material's property changes. The property change due to the viscoelasticity affects both the real and imaginary parts of the impedance; to measure both parts, the measurement of both the frequency change and resistance change is necessary. The Mason equivalent circuit provides an analytical equation and is valid for a wide range of viscosities.

Even with a simple assumption of film thickness increase and viscosity decrease when sorption takes place on the viscous film, our equation can roughly explain the scenarios of both a lossy film (PEG2000) and a low loss film (PEG20M). For the glycerol film, if we consider the peak signal change after the depositions, the result can also be explained. Since the derived model is basically equivalent to a transmission line model, it can also be extended to a multi-layer model or even treat the water deposition as an additional layer. Although this study focuses only on the explanation of the positive frequency shift, the sensitivity of a QCM coated with a viscous film will be investigated in the future.

Chapter 6

Conclusion

The study of QCM behavior with viscous film was motivated by curiosity due to unusual behavior. QCM response typically explained by mass loading or bulk liquid loading. In both cases frequency always decreases as the loading increases. However, many studies about QCM sensors found that frequency increases after sorption on many occasions. Some explanations and specific models to explain QCM positive frequency change were developed; most of them require specific adsorb molecular shapes to justify their explanation. We want to develop a model based on the Mason equivalent circuit, this way we can obtain a universal model with only the different boundary conditions for each specific condition. Also we want to be able to reproduce positive frequency change responses to an interpret its result with our models. The highly robust measured system based on VNWA was fabricated. The measurement setup consisting of viscous film coated QCM and microdispenser were developed with the goal to simulated sensor sorption with a controlled precision. The feasibility of applying this model to various cases of frequency change is to be expected.

Chapter 2
The fundamental principle of QCM was explained here including the piezoelectric effect, The physical structure of QCM, and the crystal cut. Next, the explanation of QCM response using conventional equations such as Sauerbrey's equation which explains mass loading effect and Kanazawa's equation which explains bulk liquid loading were described. Our proposed Mason equivalent circuit was expanded to various conditions including viscous film condition. Also the interpretation of electrical impedance as electrical admittance, the calculation of resonant frequency and resistance.

Chapter 3
The measurement system which ensures that our measurement retains its performance when coated with viscous film was developed for a highly viscous measurement. The development was based on small-sized VNWA. The conductance curve fitting technique which utilizes all data from VNWA frequency sweep was developed. Further noise reduction was obtained by applying Savitzky-golay filter. The noise performance and detection limit of the developed was evaluated using high concentration of aqueous glycerol solution. The data acquisition parameters of VNWA were optimized. Savitzky-golay parameters were also optimized based on small step-

wise glycerol solution concentrations, The independent t-test was used to select the minimum value parameters that distinguish the frequency change.

Chapter 4

The measurement setup consisted of a micro dispenser and QCM holder. The purpose of microdispenser is to imitate analyte molecules deposited on QCM. The experiment was conducted on microdispenser to determine deposition volume. The QCM holder was designed to fixate the dispenser tip location related to QCM electrodes. Dipcoating method was used to coat film materials, the pull-up speed of dipcoater determine film thickness and condition. Bare QCM experiment was conducted with various substances. PEG20M represents rigid film, the experimental result agrees well with Sauerbrey's equation. Water and glycerol solution was also tested until frequency change saturated. Lastly, the QCMs coated with PEG20M, PEG2000 and Glycerol were deposited with water. The result shows positive frequency occured with PEG2000 film when deposited with water.

Chapter 5

The developed viscous model from chapter 2 was simulated by varying the parameter of film thickness. The viscosity and density values were used from reference. The simulation of glycerol and water frequency agreed with with Kanazawa's equation at large film thickness. Also the two-layer simulation was also investigated using a parameter of glycerol as based layer and water as top layer. Then, the application of the developed model to estimated film thickness and viscosity from experimental results was also feasible. To gain some insight using our developed mason equivalent circuit, the contour plot of frequency and resistance change together can predict some direction of response from experimental data.

The simulation result from our single viscus film model predicts that there is a region of film thickness that the increase of film thickness causes a positive frequency shift. However, from our experimental results with the controlled depositions over bare QCM, this positive frequency behavior did not appear. This may due to the deposition is not uniformly covering the QCM surface and some unknown factors need further investigation.

A further experiment of water deposition over the viscous film was conducted to replicate the actual sensor response. We found that only PEG2000 exhibited positive frequency change. We can interpret this behavior qualitatively using an assumption that overall film thickness increases and viscosity decreases. From our model, the film parameters are film thickness and film viscosity that contribute to QCM response. The model is only one dimension and did not include many more parameters such as the depositing locations, geometry of the depositing film, and also the property of stiffness. Also, the assumption of water deposition is oversimplified to a homogeneous film and may deviate from an actual uniform deposition.

Despite some drawbacks, our developed Mason equivalent circuit model gave a simplified explanation of the positive frequency change during sorption. The benefit of using Mason's equivalent circuit comes from its analytical results. This gave us an explanation of its phenomenon when the film parameters change. This expands our understanding of the relationship between film thickness and frequency change. Our equation can be applied throughout every film thickness and converge to the values from conventional equations on both thin film and bulk liquid conditions. This

model also suggests that at some region the sensitivity of frequency or resistance change are higher. This may help us to optimize the film thickness for the highest sensor sensitivity for sensor application.

Many researchers have studied QCM behavior for more than 60 years. However, there is still somethings not to be explained well. This study contribute to acoustic wave device mainly for sensor field.

Chapter 7

Future works

7.1 Model improvement with different deposition locations

The deposition location can helps us expanding the 1 dimension model to 2 dimension model. The deposition at a location away from the center of electrode has different influence to QCM response. To be able to measure both responses, we can develop a better model related to sorption location.

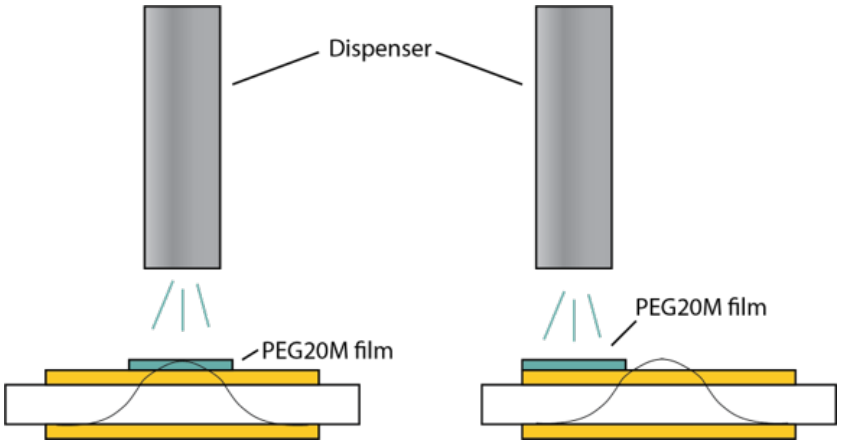

Figure 7.1: By moving the dispenser tip to various location on the electrode helps us gain more information of how QCM response.

7.2 Optimize condition to improve sensor sensitivity

From figure 7.2, the contour plot of frequency change shows that in some portion such as the area in the red circle, the contour line is more dense compare to other area, this may indicate that if we can coat the film conditions to remain this region the highest sensitivity can be achieved. Similarly, figure 7.3 shows the resistance change the region in red circle seems to be more dense compare to other area (ignore the area where viscosity less than 1 cP). This is just a preliminary speculation,

the mathematical approach for the most optimized condition need to be further conducted.

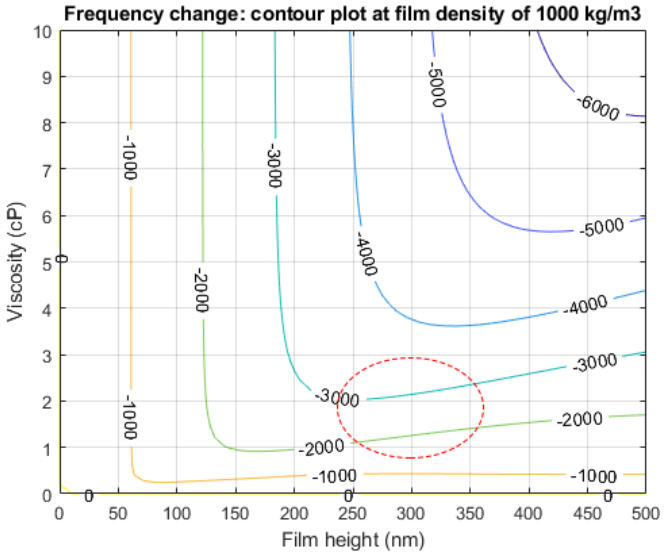

Figure 7.2: By moving the dispenser tip to various location on the electrode helps us gain more information of how QCM response.

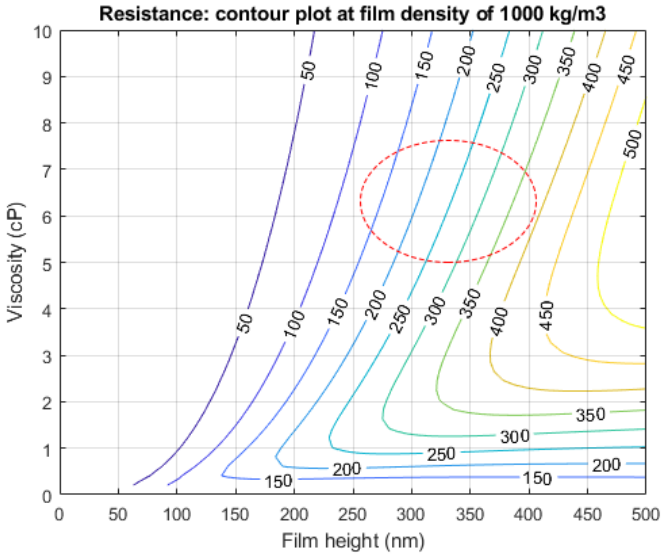

Figure 7.3: By moving the dispenser tip to various location on the electrode helps us gain more information of how QCM response.

Appendix A: QCM holder Design and Diagram

Drawing of 3D printed QCM holder

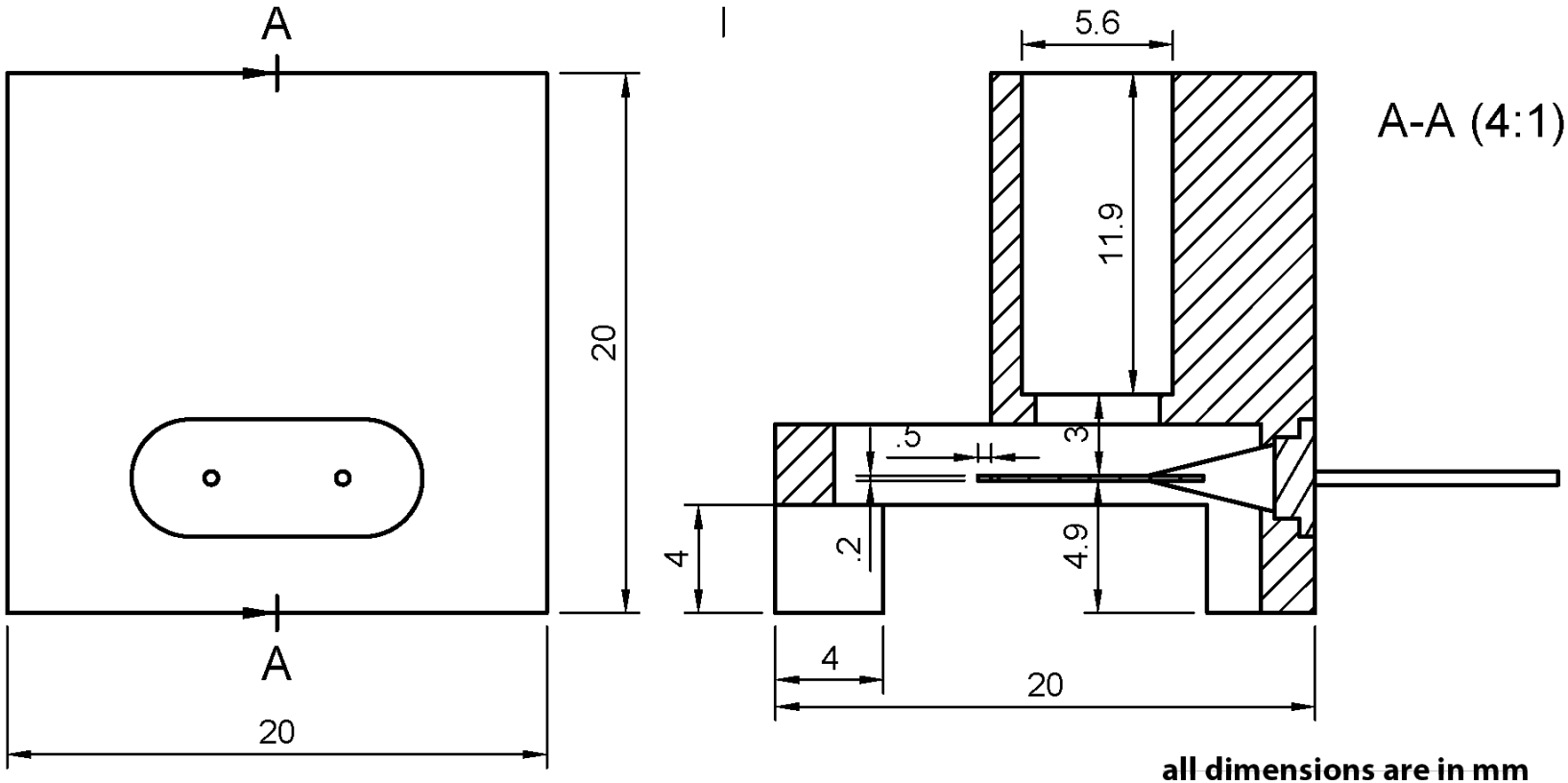

all dimensions are in mm

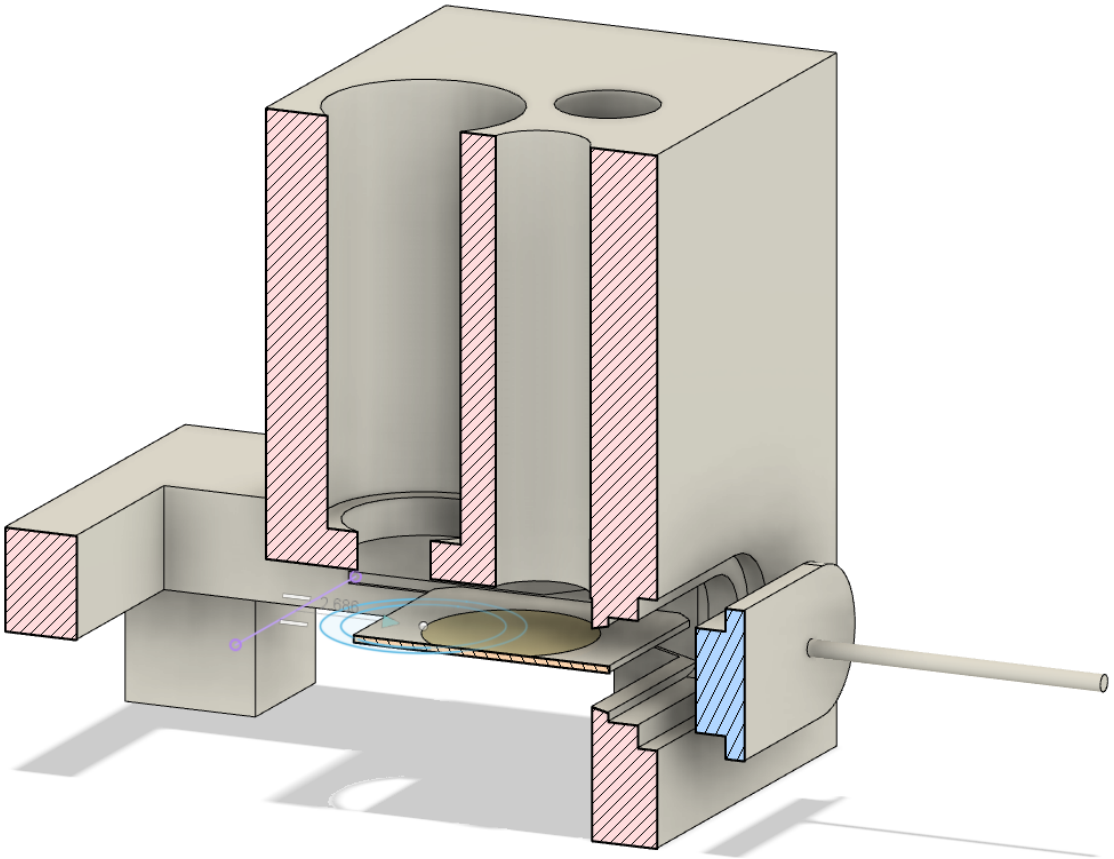

Appendix B: MATLAB Codes

Matlab software for QCM measurement

Screen capture of QCM measurement software

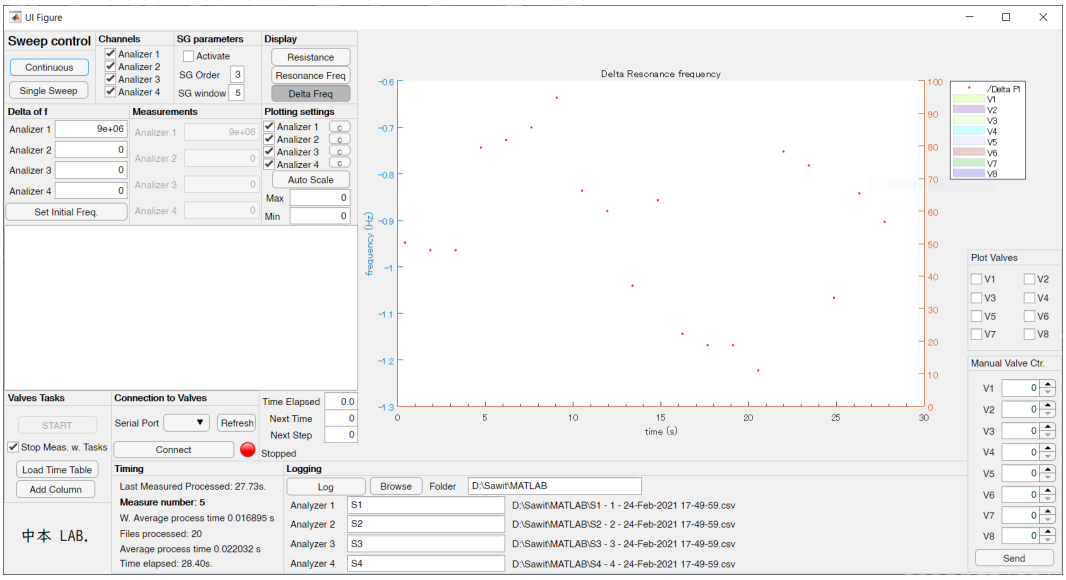

Source code of QCM measurement software

This source code was developed on Matlab App Designer which is different from typical Matlab M file.

Source code below was listed without highlight code due to it is not supported by latex code listing package.

```
classdef FourCHApp_ContSweepVal_v26_exported < matlab.apps.AppBase

% Properties that correspond to app components
properties (Access = public)
    UIFigure                    matlab.ui.Figure
    UIAxes                      matlab.ui.control.UIAxes
    SweepcontrolPanel           matlab.ui.container.Panel
    ContinuousButton            matlab.ui.control.StateButton
    SingleSweepButton           matlab.ui.control.Button
    LoggingPanel                matlab.ui.container.Panel
    FolderEditFieldLabel        matlab.ui.control.Label
    FolderEditField             matlab.ui.control.EditField
    Analyzer1EditFieldLabel     matlab.ui.control.Label
    Analyzer1EditField          matlab.ui.control.EditField
    Analyzer2EditFieldLabel     matlab.ui.control.Label
    Analyzer2EditField          matlab.ui.control.EditField
    Analyzer3EditFieldLabel     matlab.ui.control.Label
    Analyzer3EditField          matlab.ui.control.EditField
    Analyzer4EditFieldLabel     matlab.ui.control.Label
    Analyzer4EditField          matlab.ui.control.EditField
    LLogFilename1               matlab.ui.control.Label
    LLogFilename2               matlab.ui.control.Label
```

```
LLogFilename3               matlab.ui.control.Label
LLogFilename4               matlab.ui.control.Label
LogButton                   matlab.ui.control.StateButton
BrowseButton                matlab.ui.control.Button
DisplayButtonGroup          matlab.ui.container.ButtonGroup
ResistanceButton            matlab.ui.control.ToggleButton
ResonanceFreqButton         matlab.ui.control.ToggleButton
DeltaFreqButton             matlab.ui.control.ToggleButton
ChannelsPanel               matlab.ui.container.Panel
CB_Analz_1                  matlab.ui.control.CheckBox
CB_Analz_2                  matlab.ui.control.CheckBox
CB_Analz_4                  matlab.ui.control.CheckBox
CB_Analz_3                  matlab.ui.control.CheckBox
PlottingsettingsPanel       matlab.ui.container.Panel
CB_plot_Analizer1           matlab.ui.control.CheckBox
CB_AutoScale1               matlab.ui.control.Button
CB_plot_Analizer2           matlab.ui.control.CheckBox
CB_AutoScale2               matlab.ui.control.Button
CB_AutoScale3               matlab.ui.control.Button
CB_plot_Analizer3           matlab.ui.control.CheckBox
CB_AutoScale4               matlab.ui.control.Button
CB_plot_Analizer4           matlab.ui.control.CheckBox
CB_AutoScale                matlab.ui.control.Button
MaxEditFieldLabel           matlab.ui.control.Label
EPlotMaxY                   matlab.ui.control.NumericEditField
MinEditFieldLabel           matlab.ui.control.Label
EPlotMinY                   matlab.ui.control.NumericEditField
SGparametersPanel           matlab.ui.container.Panel
SGOrderEditFieldLabel       matlab.ui.control.Label
ESGOrder                    matlab.ui.control.NumericEditField
SGwindowEditFieldLabel      matlab.ui.control.Label
ESGWindow                   matlab.ui.control.NumericEditField
CBActivateSG                matlab.ui.control.CheckBox
MeasurementsPanel           matlab.ui.container.Panel
Analizer1EditFieldLabel     matlab.ui.control.Label
EBDipAnaliz_1               matlab.ui.control.NumericEditField
Analizer2Label              matlab.ui.control.Label
EBDipAnaliz_2               matlab.ui.control.NumericEditField
Analizer3Label              matlab.ui.control.Label
EBDipAnaliz_3               matlab.ui.control.NumericEditField
Analizer4Label              matlab.ui.control.Label
EBDipAnaliz_4               matlab.ui.control.NumericEditField
DeltaoffPanel               matlab.ui.container.Panel
Analizer1EditFieldLabel_2   matlab.ui.control.Label
EBIniAnaliz_1               matlab.ui.control.NumericEditField
Analizer2Label_2            matlab.ui.control.Label
EBIniAnaliz_2               matlab.ui.control.NumericEditField
Analizer3Label_2            matlab.ui.control.Label
EBIniAnaliz_3               matlab.ui.control.NumericEditField
Analizer4Label_2            matlab.ui.control.Label
EBIniAnaliz_4               matlab.ui.control.NumericEditField
SetInitialFreq              matlab.ui.control.Button
TimingPanel                 matlab.ui.container.Panel
LoopLabel                   matlab.ui.control.Label
LAverageTimeProcess         matlab.ui.control.Label
LMaxTimeProcess             matlab.ui.control.Label
LTotalTime                  matlab.ui.control.Label
LMeasureNumber              matlab.ui.control.Label
LTotalTimeElapsed           matlab.ui.control.Label
UITableTimesValves          matlab.ui.control.Table
ConnectiontoValvesPanel     matlab.ui.container.Panel
ConnectButton               matlab.ui.control.Button
SerialPortDropDownLabel     matlab.ui.control.Label
SerialPortDropDown          matlab.ui.control.DropDown
Lamp                        matlab.ui.control.Lamp
RefreshButton               matlab.ui.control.Button
ValvesTasksPanel            matlab.ui.container.Panel
LoadTimeTableButton         matlab.ui.control.Button
BStartStopTimeTable         matlab.ui.control.StateButton
AddColumnButton             matlab.ui.control.Button
CBFinishMeasWTask           matlab.ui.control.CheckBox
NextStepLabel               matlab.ui.control.Label
ENextStep                   matlab.ui.control.NumericEditField
NextTimeEditFieldLabel      matlab.ui.control.Label
ENextTime                   matlab.ui.control.NumericEditField
TimeElapsedEditFieldLabel   matlab.ui.control.Label
TimeElapsedEditField        matlab.ui.control.NumericEditField
LABLabel                    matlab.ui.control.Label
ManualValveCtrPanel         matlab.ui.container.Panel
V1SpinnerLabel              matlab.ui.control.Label
VSpinner_1                  matlab.ui.control.Spinner
V2Label                     matlab.ui.control.Label
VSpinner_2                  matlab.ui.control.Spinner
V3Label                     matlab.ui.control.Label
VSpinner_3                  matlab.ui.control.Spinner
V4Label                     matlab.ui.control.Label
VSpinner_4                  matlab.ui.control.Spinner
V5Label                     matlab.ui.control.Label
VSpinner_5                  matlab.ui.control.Spinner
V6Label                     matlab.ui.control.Label
VSpinner_6                  matlab.ui.control.Spinner
V7Label                     matlab.ui.control.Label
VSpinner_7                  matlab.ui.control.Spinner
V8Label                     matlab.ui.control.Label
VSpinner_8                  matlab.ui.control.Spinner
SendButton                  matlab.ui.control.Button
PlotValvesPanel             matlab.ui.container.Panel
CB_ValvPlot                 matlab.ui.control.CheckBox
CB_ValvPlot_2               matlab.ui.control.CheckBox
```

```
    CB_ValvPlot_3              matlab.ui.control.CheckBox
    CB_ValvPlot_4              matlab.ui.control.CheckBox
    CB_ValvPlot_5              matlab.ui.control.CheckBox
    CB_ValvPlot_6              matlab.ui.control.CheckBox
    CB_ValvPlot_7              matlab.ui.control.CheckBox
    CB_ValvPlot_8              matlab.ui.control.CheckBox
    StoppedLabel               matlab.ui.control.Label
end


   properties (Access = private)
    N                       % Files processed
    %MaxTimeProcess = 0;     % Max time that takes to process a file
    WeightedAverageTimeProcess = [];
    AverageTimeProcess = 0; % Average teime that takes to process a file
    Loop = 0;               % gloval loop of measurements (all n. analyzers)
    StartTime;               % Start time of the current measurements
    DateFormat;
    RuningAverage;

    % Hardware
    Analz_Channels = [1 2 3 4];         % Channels we will measure (number will measure, 0 will not measure)
    SweepSize = 1000;

    % Initial values for aproximating RLC
    RLC = {[400 11.400000000000 27.52015748915769 0],...
        [400 11.400000000000 27.52015748915769 0],...
        [400 11.400000000000 27.52015748915769 0],...
        [400 11.400000000000 27.52015748915769 0]};

    % SGolay parameters
    framelen        % Sgolay window
    order           % Sgolay order

    % Data storage and calculus
    DataArray = { [] , [] ,[] , [] };
    InitResonanceF  = {0 0 0 0};        % For calculating delta F
    ResonanceOfBaseLine = {0 0 0 0};    % For storing resonance baseline


    % Valves
    SerialPort          % Serial port to comunicate with valves
    StartTimeT          % Starting Time of the TimeTable task
    StatusValves = [0 0 0 0 0 0 0 0];    % Current pwd sent to the valves, always true
    NextIndexTimeT      % Next step on the time table
    NextTimeT           % How many seconds to the next step of the time table (valid only when calculated recently)
    TimeTTimer          % timer for the table task of the valves
    HistoryValves = []; % since manual valves, tasktimetable valves and sweep analysis are not sincronous,
                        % we record here the history of valves while logging
                        % same format as timetable
end

methods (Access = private)




    % Loads the timetable from a excel file
    function LoadTimeTable(app,FileName,FilePath)
        [Steps,theader] = xlsread(fullfile(FilePath,FileName));
        app.UITableTimesValves.Data=array2table(Steps');
        app.UITableTimesValves.ColumnWidth = 'auto';
        if size(theader,1) == 2
            theader = theader(2,1:end);
            theader{1} = 'Time (s)';
            app.UITableTimesValves.RowName = theader;
        else
            app.UITableTimesValves.RowName = {'Time (s)','V1','V2','V3','V4','V5','V6','V7','V8'};
        end
        tcolumns{1} = 'Start';
        for i=1:(size(Steps,1)-1)
            tcolumns{i+1} = ['Step ' num2str(i)];
        end
        app.UITableTimesValves.ColumnName = tcolumns;
        app.UITableTimesValves.ColumnEditable = boolean(ones(1,i+1));
    end




    % function that calculate the time intervals
    function CalculateNextTime(app)
        % calculate next time and its column index on the time table
        Tiempos = table2array(app.UITableTimesValves.Data(1,:));
        CurrentSeconds = etime(clock,app.StartTimeT);
        Tiempos = Tiempos > CurrentSeconds;
        if sum(Tiempos) ~=0
            Nextindextimet = find(Tiempos==1, 1, 'first');
            % set edition enable
            c = length(app.UITableTimesValves.ColumnName);
            c = boolean([zeros(1,Nextindextimet-1) ones(1,c-Nextindextimet+1)]);
            app.UITableTimesValves.ColumnEditable = c;
            % calculate the time needed for next task
            nexttime = table2array(app.UITableTimesValves.Data(1,Nextindextimet));
            Nexttime = nexttime-etime(clock,app.StartTimeT);
            % setup timer for next step
            if ~isempty(app.TimeTTimer)
                stop(app.TimeTTimer);
                delete(app.TimeTTimer);
```

```
        end

                        app.TimeTTimer = timer('ExecutionMode','SingleShot','StartDelay',Nexttime,'TimerFcn',{@SendValveDataTimeT,app,Nextindextimet});
        start(app.TimeTTimer);
        % update the controls
        app.ENextTime.Value = nexttime;
        app.ENextStep.Value = Nextindextimet-1;
        app.TimeElapsedEditField.Value = etime(clock,app.StartTimeT);
        duration = app.UITableTimesValves.Data{1,end};
        d = datenum(app.StartTimeT) + datenum([0 0 0 0 0 duration]);
        app.StoppedLabel.Text = ['End: ' datestr(d,'HH:MM:SS')];
    else
        % Time valves schedule finished
        % stop timmer
        stop(app.TimeTTimer);
        % i dont know how to interrogate the existance of a deleted timer,
        % neither with isempty or by properties will work
        % so i dont delete here.
        % delete(app.TimeTTimer);
        % interfaz update
        app.BStartStopTimeTable.Value = 0;
        BStartStopTimeTableValueChanged(app,[]);
        app.ENextTime.Value = 0;
        app.ENextStep.Value = 0;
        app.TimeElapsedEditField.Value = 0;
        app.UITableTimesValves.ColumnEditable = true;
        app.StoppedLabel.Text = 'Stopped';
        % if check bos finish measurements is selected, Stop measurements
        if app.CBFinishMeasWTask.Value
            % Stop Measurements
            app.ContinuousButton.Value = 0;
            ContinuousButtonValueChanged(app,[]);
        end
    end

    function SendValveDataTimeT(obj, event, app, index)
        % Get data to send to serial
        Data2Send = table2array(app.UITableTimesValves.Data(2:end,index))';

        % Send the data of the valves
        SendCommandValves(app,Data2Send);

        % setup next timer event
        CalculateNextTime(app);
    end

end




% Send the data of the valves
function SendCommandValves(app,Data2Send)
        % send twice, because sometimes it doesnt not success

        % make command
        t = 'pwm\n';
        for i=1:8
            t = [t num2str(Data2Send(i)) ' '];
        end
        t = [t '0\n'];

        % send command
        %fclose('all');
        %delete(instrfind);
        app.SerialPort = serial(app.SerialPortDropDown.Value,'BaudRate',115200);
        fopen(app.SerialPort);
        fprintf(app.SerialPort,t);
        fclose(app.SerialPort);
        delete(instrfind);


        % update data
        app.StatusValves = Data2Send;
        if app.LogButton.Value
            app.HistoryValves(end+1,:) = [datenum(clock) app.StatusValves];
        end

        %update display
        for i = 1:8
            switch i
                case 1
                    app.VSpinner_1.Value = Data2Send(1);
                case 2
                    app.VSpinner_2.Value = Data2Send(2);
                case 3
                    app.VSpinner_3.Value = Data2Send(3);
                case 4
                    app.VSpinner_4.Value = Data2Send(4);
                case 5
                    app.VSpinner_5.Value = Data2Send(5);
                case 6
                    app.VSpinner_6.Value = Data2Send(6);
                case 7
                    app.VSpinner_7.Value = Data2Send(7);
                case 8
                    app.VSpinner_8.Value = Data2Send(8);
            end
        end
```

```
end



% Function to draw a graph
% Just draw the plot with the data passed to it
function Dibuja_Graficas(app,datatoplot,color,linewidth)
    yyaxis(app.UIAxes,'left');
    hold(app.UIAxes,'on');
    for iplot = 1:length(datatoplot)
        plot(app.UIAxes,datatoplot{iplot}(:,1),datatoplot{iplot}(:,2),color{iplot},'linewidth',linewidth);
    end
    hold(app.UIAxes,'off');
end



% Function that compose autonames for log files
% Also write those autonames to the interface controls
function LogFileName = AutoName(app)
    % clean displayed filename
    app.LLogFilename1.Text = 'No File';
    app.LLogFilename2.Text = 'No File';
    app.LLogFilename3.Text = 'No File';
    app.LLogFilename4.Text = 'No File';

    % path for the filenames
    pathname = app.FolderEditField.Value;

    % For each analizer we are measuring
    for number = app.Analz_Channels(app.Analz_Channels~=0)
        % Add tag to the file
        switch number
            case 1
                BaseFileName = [app.Analyzer1EditField.Value ' - 1 - '];
            case 2
                BaseFileName = [app.Analyzer2EditField.Value ' - 2 - '];
            case 3
                BaseFileName = [app.Analyzer3EditField.Value ' - 3 - '];
            case 4
                BaseFileName = [app.Analyzer4EditField.Value ' - 4 - '];
        end

        % add time steamp
        tiempo = datestr(clock);
        tiempo =strrep(tiempo,':','-');
        BaseFileName = [BaseFileName tiempo '.csv'];
        LogFileName = fullfile(pathname,BaseFileName);

        % update filenames
        switch number
            case 1
                app.LLogFilename1.Text = LogFileName;
            case 2
                app.LLogFilename2.Text = LogFileName;
            case 3
                app.LLogFilename3.Text = LogFileName;
            case 4
                app.LLogFilename4.Text = LogFileName;
        end

    end
end



% Function that tracks the files in the log folders.
%   number ==1 2 3 4 gives the new files in that log directory
%       Gets a list of files that are in a directory
%       then compare that file list with the old file list in that same directory
%       outputs the difference files
%       updates the stored file list
%   number == 0 compile a new list
%       Updates all stored file lists for all folders
%   number == -1 returns a list of all files used in the current measurement
%       Used to complie a big data file with all the raw data plus the online measurement
function new_files = CheckNewFiles(app,number)
    persistent ListofFiles;
    persistent ProcessedFiles;

    switch number
        case -1
            new_files{1} = ProcessedFiles{1};
            new_files{2} = ProcessedFiles{2};
            new_files{3} = ProcessedFiles{3};
            new_files{4} = ProcessedFiles{4};
        case 0
            dir_content1 = dir('log1'); % list the file from log folder
            dir_content2 = dir('log2');
            dir_content3 = dir('log3');
            dir_content4 = dir('log4');

            filenames1 = {dir_content1.name}; % get file name from struct
            filenames2 = {dir_content2.name};
            filenames3 = {dir_content3.name}; % get file name from struct
            filenames4 = {dir_content4.name};
```

```
                ListofFiles{1} = filenames1; % current list of file name
                ListofFiles{2} = filenames2;
                ListofFiles{3} = filenames3;
                ListofFiles{4} = filenames4;

                ProcessedFiles={{},{},{},{}};
            case 1
                dir_content1 = dir('log1');
                filenames1 = {dir_content1.name}; % get file name from struct
                new_files = setdiff(filenames1,ListofFiles{1});
                ListofFiles{1} = filenames1;
                ProcessedFiles{1} = [ProcessedFiles{1}{:} new_files];
            case 2
                dir_content2 = dir('log2');
                filenames2 = {dir_content2.name}; % get file name from struct
                new_files = setdiff(filenames2,ListofFiles{2});
                ListofFiles{2} = filenames2;
                ProcessedFiles{2} = [ProcessedFiles{2}{:} new_files];
            case 3
                dir_content3 = dir('log3');
                filenames3 = {dir_content3.name}; % get file name from struct
                new_files = setdiff(filenames3,ListofFiles{3});
                ListofFiles{3} = filenames3;
                ProcessedFiles{3} = [ProcessedFiles{3}{:} new_files];
            case 4
                dir_content4 = dir('log4');
                filenames4 = {dir_content4.name}; % get file name from struct
                new_files = setdiff(filenames4,ListofFiles{4});
                ListofFiles{4} = filenames4;
                ProcessedFiles{4} = [ProcessedFiles{4}{:} new_files];
        end
    end



    % function to compile all data at the end in a big data file
    function CompileData(app)
        CData = {};
        % for each analizer we are measuring
        for ianalizer = app.Analz_Channels(app.Analz_Channels~=0)
            % Even if the analyzer are being measured maybe there is no data recorded
            FilesToRecord = CheckNewFiles(app,-1);
            if ~isempty(FilesToRecord{ianalizer})
                % common data
                CData{ianalizer}.Analizer = ianalizer;
                CData{ianalizer}.StartTime = app.StartTime;
                CData{ianalizer}.TaskTable = app.UITableTimesValves.Data;
                CData{ianalizer}.SweepDataIndexName = {'Measurement','SweepStep','Column-Measure'};
                CData{ianalizer}.SweepData3ColumnName = {'Frecuency (MHz)','Real Y (real)','Real Y (img)'};
                switch ianalizer
                    case 1
                        CData{ianalizer}.Sensor = app.Analyzer1EditField.Value;
                    case 2
                        CData{ianalizer}.Sensor = app.Analyzer2EditField.Value;
                    case 3
                        CData{ianalizer}.Sensor = app.Analyzer3EditField.Value;
                    case 4
                        CData{ianalizer}.Sensor = app.Analyzer4EditField.Value;
                end


                % Load raw data
                % **** not used, use the one below

% %                   % Load from temporal data file, no tested
% %                   %fid = fopen(['templog' num2str(ianalizer) '.dat'],'r');
% %                   %for ifile = 1:length(FilesToRecord{ianalizer})
% %                   %   a = fread(fid,[1000 3],'float32');
% %                   %   CData{ianalizer}.SweepData(ifile,1,:) = a(:,1)';
% %                   %   CData{ianalizer}.SweepData(ifile,2,:) = a(:,2)';
% %                   %   CData{ianalizer}.SweepData(ifile,3,:) = a(:,3)';
% %                   %   CData{ianalizer}.Date(ifile,:) = FilesToRecord{ianalizer}{ifile}(9:31);
% %                   %end
% %                   %fclose(fid);


                % load from temp file to recover the data faster
                fid = fopen(['templog' num2str(ianalizer) '.dat'],'r');
                ifile = 1;
                DateTemp = fread(fid,[3,1],'float64');
                DatosTemp = fread(fid,[app.SweepSize,3],'float64');
                while not(feof(fid))
                    CData{ianalizer}.SweepData(ifile,1,:) = DatosTemp(:,1);
                    CData{ianalizer}.SweepData(ifile,2,:) = DatosTemp(:,2);
                    CData{ianalizer}.SweepData(ifile,3,:) = DatosTemp(:,3);
                    CData{ianalizer}.Date(ifile,:) = datestr(DateTemp(1));
                    ifile = ifile + 1;
                    DateTemp = fread(fid,[3,1],'float64');
                    DatosTemp = fread(fid,[app.SweepSize,3],'float64');
                end
                fclose(fid);


                % load from analyzer files, slow!
                %fullfilename = fullfile(['log' num2str(ianalizer)],FilesToRecord{ianalizer});
                %for ifile = 1:length(FilesToRecord{ianalizer})
                %    fid = fopen(fullfilename{ifile});
```

```
            %    A = textscan(fid,'%f %f %f','HeaderLines',2);
            %    %a = fread(fid,[1000 3],'float32');
            %    fclose(fid);
            %    CData{ianalizer}.SweepData(ifile,1,:) = A{1};
            %    CData{ianalizer}.SweepData(ifile,2,:) = A{2};
            %    CData{ianalizer}.SweepData(ifile,3,:) = A{3};
            %    CData{ianalizer}.Date(ifile,:) = FilesToRecord{ianalizer}{ifile}(9:30);
            %end

            % The calculated data
            % Maybe the data were logged but they were not analyzed, we record those because it could be a mistake
            % but we dont have calculated data
            if ~isempty(app.DataArray{ianalizer})
                CData{ianalizer}.Time = app.DataArray{ianalizer}(:,1);
                CData{ianalizer}.Valves = app.DataArray{ianalizer}(:,8:15);
                CData{ianalizer}.RLC = app.DataArray{ianalizer}(:,2:4);
                CData{ianalizer}.Fs = app.DataArray{ianalizer}(:,5);
            end

        end
    end
    if ~isempty(CData)
        save(['Experiment - ' strrep(datestr(clock),':','-')], 'CData');
    end
end



% Function to change the scale to try to see only one plot
function AutoChangeScalePlot(app,NumAnalizer)

    % select left plot
    yyaxis(app.UIAxes,'left');

    % select what data are we centering on
    if app.ResistanceButton.Value == 1
        columna = 2;
    elseif   app.ResonanceFreqButton.Value == 1
        columna = 5;
    elseif app.DeltaFreqButton.Value == 1
        %% error, no done
        columna = 7;
    end

    % try to guess the best values for plottign the data
    mediana = median(app.DataArray{NumAnalizer}(:,columna));
    desv = std(app.DataArray{NumAnalizer}(:,columna));

    % setting graph and controls to those values
    if desv ~=0
        app.UIAxes.YLimMode = 'manual';
        app.UIAxes.YLim = real([max(0,mediana-desv),mediana+desv]);
        app.EPlotMaxY.Value = real(mediana+desv);
        app.EPlotMinY.Value = max(0,real(mediana-desv));
    else
        app.UIAxes.YLimMode = 'auto';
    end
end



% Main function that process a data variable from the Analizers to add its values to the data
function ProcessFile(app,new_files,number)

    % Get the new file and read it
    fullfilenames = fullfile(['log' num2str(number)],new_files);


    % if we have several files no processed we process all them
    for ifile = 1:length(fullfilenames)

        % To track how much time takes the function
        tic;
        app.N = app.N + 1;

        [fid,errmsg] = fopen(fullfilenames{ifile});
        if errmsg<0
            break
        end
        A = textscan(fid,'%f %f %f','HeaderLines',2);
        fclose(fid);




        % Code to calculate LRC equivalent
        try
            freq_Array = A{1}*1E6;
            z0 = 50;
            s11_Array = complex(A{2},A{3});
            y_Array = s2y(s11_Array,z0);
            y_Array = squeeze(y_Array);

            % Initial condition for curve fit
            % Idea: what about using the last measured values as initial conditions?
            % R = 400 ohm, L= 11.4 mH, C = 27.52 fF, conductance diff = 0}
            % a = [400 11.400000000000 27.52015748915769 0];
```

```
    % Curve fitting and find minimum point
    % MaxFunEvals = Maximum number of function evaluations
    % MaxIter = Maximum number of iterations allowed
    % TolX = Termination tolerance on x, a positive scalar. The default value is 1e-4
    % TolFun = Termination tolerance on the function value, a positive scalar. The default is 1e-4
    % Display = 'final' displays just the final output
    options = optimset('MaxFunEvals',150000,'MaxIter',15000,'TolX',1e-12,'TolFun',1e-12,'Display','off');

    % fixed start point to optimize
    % a = [400 11.400000000000 27.52015748915769 0];
    %[x0,fval,exitflag]=fminsearch(@(v) fitcon2(app,v,freq_Array,real(y_Array)),a,options);
    % former end point as start point to optimize
    [x0,fval,exitflag]=fminsearch(@(v) fitcon2(app,v,freq_Array,real(y_Array)),app.RLC{number}(1:4),options);
    app.RLC{number} = [x0 0 0 0 0];
catch
    % Error in the calculus
    % we take the measurement as the last valid one
    x0 = app.RLC{number}(1:4);
end

% format of the x
%ÿstr = sprintf('R1 = %f ohm, L1 = %f mH, C1 = %f fF',x0(1),x0(2),x0(3));

%Calculate resonance frequency
ResonanceFreq = (1/(2*pi*sqrt(x0(2)*x0(3))))*1e9;

% simple method
%[maxy,index] = max(y_Array);
%ResonanceFreq = freq_Array(index);

%-----------------------------------------------
%   Tag time for measurement
%-----------------------------------------------
% Data format changes with language setting of windows
%if new_files{ifile}(13) == '_' % it is 'yyyy_mm_dd_HH_MM_SS'
%    MeasureTime = datevec(new_files{ifile}(9:31),'yyyy_mm_dd_HH_MM_SS_FFF');
%else   % probably is usa style 'mm_dd_yyyy_HH_MM_SS_FFF' But could be also 'dd_mm_yyyy_HH_MM_SS_FFF'
%    %MeasureTime = datevec(new_files{ifile}(9:31),'mm_dd_yyyy_HH_MM_SS_FFF');
%    MeasureTime = datevec([datestr(clock,'mm_dd_yyyy_') new_files{ifile}(20:31)], 'mm_dd_yyyy_HH_MM_SS_FFF'); %
%    %MeasureTime = datevec(new_files{ifile}(9:31),'mm_dd_yyyy_HH_MM_SS_FFF'); % no cross days, at 00:00 we would have problems
%end


if app.DateFormat == 'M'
    MeasureTime = datevec(new_files{ifile}(9:31),'mm_dd_yyyy_HH_MM_SS_FFF');
elseif app.DateFormat =='d'
    MeasureTime = datevec(new_files{ifile}(9:31),'dd_mm_yyyy_HH_MM_SS_FFF');
else
    MeasureTime = datevec(new_files{ifile}(9:31),'yyyy_mm_dd_HH_MM_SS_FFF');
end

% Save to matlab variable to recover the data faster
% first a number that is the date, then the auctual sweep data
%   fid = fopen(['templog' num2str(number) '.dat'],'a');
%   fwrite(fid,[datenum(MeasureTime);0;0;A{1};A{2};A{3}],'float64');
%   fclose(fid);
%  app.SweepSize = length(A{1});


TaggingTime = etime(MeasureTime,app.StartTime);
%-----------------------------------------------

% the data from the valves is not measured, only controlled
% The status of the valves is not the state of the valves when the file is processed
% but the time at the measuring time, so we have to get the valve status from the valve recorded status
indice = find(app.HistoryValves(:,1)>datenum(MeasureTime),1);
if isempty(indice)
    TimedStatusValves = app.StatusValves;
elseif indice==1
    TimedStatusValves = app.StatusValves;
else
    TimedStatusValves = app.HistoryValves(indice-1,2:9);
end


% if we have enough data to perform sg filter we add them the filtered R and F in the 6 and 7 column
% if not we add 0 0 in those columns
if (size(app.DataArray{number},1) > app.framelen ) && app.CBActivateSG.Value

    app.DataArray{number} = [app.DataArray{number};[TaggingTime x0(1:end-1) ResonanceFreq 0 0 TimedStatusValves(:)']];

    SgolayResonanceFreq = sgolayfilt(app.DataArray{number}(:,5),app.order,app.framelen); %Use data from col 5 which is Frequency
    app.DataArray{number}(:,7) = SgolayResonanceFreq; %place smooth freq data to col 7

    SgolayResonanceRes =  sgolayfilt(app.DataArray{number}(:,2),app.order,app.framelen); %Use data from col 2 which is Resistance
    app.DataArray{number}(:,6) = SgolayResonanceRes; %place smooth freq data to col 6

    % we store in the frequency the resonance from the filtered one
    app.InitResonanceF{number} = real(SgolayResonanceFreq(end));
else
    % 1 = [Time R L C ResonanceFreq ] = 5 col
    app.DataArray{number} = [app.DataArray{number};[TaggingTime x0(1:end-1) ResonanceFreq 0 0 TimedStatusValves(:)']];
    % we store in the frequency the resonance from the filtered one
    app.InitResonanceF{number} = real(ResonanceFreq);
end

%[m,~] = size(app.DataArray{number});
%app.InitIndex = m;
```

```
        % display instant frequencies
        switch number
            case 1
                app.EBDipAnaliz_1.Value = real(app.InitResonanceF{number});
            case 2
                app.EBDipAnaliz_2.Value = real(app.InitResonanceF{number});
            case 3
                app.EBDipAnaliz_3.Value = real(app.InitResonanceF{number});
            case 4
                app.EBDipAnaliz_4.Value = real(app.InitResonanceF{number});
        end

        % Write log file format
        if (app.LogButton.Value == 1) && (~isempty(app.DataArray{number}(end,:)))
            switch number
                case 1
                    FileName = app.LLogFilename1.Text;
                case 2
                    FileName = app.LLogFilename2.Text;
                case 3
                    FileName = app.LLogFilename3.Text;
                case 4
                    FileName = app.LLogFilename4.Text;
            end
            %[Time R L C ResonanceFreq GolayR GolarResFre] total 7 col
            % The golay filter is fully calculated on every measurement
            % but only the last value is added in each measurement.
            fid = fopen(FileName, 'a');
            fprintf(fid, '%.3f,%6.3f,%6.5f,%6.5f,%10.2f,%6.3f,%10.2f,', app.DataArray{number}(end,1:7));
            fprintf(fid,'%g,%g,%g,%g,%g,%g,%g,%g\n',app.DataArray{number}(end,8:15));

            fclose(fid);
        end

        % Stop traking time
        TimeProcess = toc;
        %---------------------------------------------
        %   Time show in textboxes
        %---------------------------------------------
        app.LoopLabel.Text = ['Files processed: ' int2str(app.N)];
        app.LMeasureNumber.Text = ['Measure number: ' num2str(app.N/sum(app.Analz_Channels==1:4))];
        app.AverageTimeProcess = app.AverageTimeProcess*(app.N-1)/app.N + TimeProcess/app.N;
        app.WeightedAverageTimeProcess = mean([app.AverageTimeProcess TimeProcess]);
        %%app.MaxTimeProcess = max(app.MaxTimeProcess,TimeProcess);
        app.LAverageTimeProcess.Text = sprintf('Average process time %s s', num2str(app.AverageTimeProcess));
        if app.AverageTimeProcess>0.4
            app.LAverageTimeProcess.FontColor = 'r';
        else
            app.LAverageTimeProcess.FontColor = 'k';
        end
        app.LMaxTimeProcess.Text = sprintf('W. Average process time %s s', num2str(app.WeightedAverageTimeProcess));
        if app.WeightedAverageTimeProcess>0.4
            app.LMaxTimeProcess.FontColor = 'r';
        else
            app.LMaxTimeProcess.FontColor = 'k';
        end
        app.LTotalTime.Text = ['Last Measured Processed: ' num2str(TaggingTime) 's.'];
        %---------------------------------------------
    end
end

function app.RuningAverage(app,time)
    if isempty(time)
        app.WeigthedAverage = [];
    else
        if isempty(app.WeigthedAverage)
            app.WeigthedAverage = time;
        else
            app.WeigthedAverage = 0.7 * app.WeigthedAverage + time * 0.3;
        end
    end



end



% Function that run while measuring, monitoring new files, draw if new data comes
function RunContinueButton(app)
    %last_loop_time =0;
    continuar = 1;
    while continuar
        drawnow;
        if app.ContinuousButton.Value == 1

            % Update times in interfaz
            if app.BStartStopTimeTable.Value
                app.TimeElapsedEditField.Value = etime(clock,app.StartTimeT);
            end
            app.LTotalTimeElapsed.Text = ['Time elapsed: ' num2str(etime(clock,app.StartTime),'%.2f') 's.'];

            % unless new data comes, we do not draw
            dibuja = 0;

            % check new files
            new_files1 = CheckNewFiles(app,1);
            new_files2 = CheckNewFiles(app,2);
```

```
            new_files3 = CheckNewFiles(app,3);
            new_files4 = CheckNewFiles(app,4);

            % if new files exists, process and flag to draw
            if ~isempty(new_files1) && ismember(1,app.Analz_Channels)
                ProcessFile(app,new_files1,1);
                dibuja = 1;
            end

            if ~isempty(new_files2) && ismember(2,app.Analz_Channels)
                ProcessFile(app,new_files2,2);
                dibuja = 1;
            end

            if ~isempty(new_files3) && ismember(3,app.Analz_Channels)
                ProcessFile(app,new_files3,3);
                dibuja = 1;
            end

            if ~isempty(new_files4) && ismember(4,app.Analz_Channels)
                ProcessFile(app,new_files4,4);
                dibuja = 1;
            end

            if dibuja
                UpdateGraph(app);
            end
        else % app.ContinuousButton.Value == 1
            continuar = 0;
        end % if app.ContinuousButton.Value == 1
    end % while
end % function



% function that plot the data
function UpdateGraph(app)
    % we build the data to plot first
    colors = 'rbmk';
    indice_points = [ismember(1,app.Analz_Channels) ismember(2,app.Analz_Channels)...
        ismember(3,app.Analz_Channels) ismember(4,app.Analz_Channels)].*...
        ~[isempty(app.DataArray{1}) isempty(app.DataArray{2})...
        isempty(app.DataArray{3}) isempty(app.DataArray{4})].*...
        [app.CB_plot_Analizer1.Value app.CB_plot_Analizer2.Value...
        app.CB_plot_Analizer3.Value app.CB_plot_Analizer4.Value];
    indice_SG = [ismember(1,app.Analz_Channels) ismember(2,app.Analz_Channels)...
        ismember(3,app.Analz_Channels) ismember(4,app.Analz_Channels)].*...
        [size(app.DataArray{1},1) > app.framelen size(app.DataArray{2},1) > app.framelen...
        size(app.DataArray{3},1) > app.framelen size(app.DataArray{4},1) > app.framelen].*...
        [app.CB_plot_Analizer1.Value app.CB_plot_Analizer2.Value...
        app.CB_plot_Analizer3.Value app.CB_plot_Analizer4.Value];
    indice_SG = indice_SG*app.CBActivateSG.Value;
    datatoplot_po ={};
    datatoplot_sg ={};
    color_po ={};
    color_sg ={};
    leyenda = {};
    i=1;
    % Make data points
    for idatatoplot = [1 2 3 4]
        if indice_points(idatatoplot)
            if app.ResistanceButton.Value == 1
                datatoplot_po{i} = [app.DataArray{idatatoplot}(:,1),app.DataArray{idatatoplot}(:,2)];
                leyenda{end+1} = ['Measured R' num2str(idatatoplot)];
            elseif app.ResonanceFreqButton.Value == 1
                datatoplot_po{i} = [app.DataArray{idatatoplot}(:,1),app.DataArray{idatatoplot}(:,5)];
                leyenda{end+1} = ['Calculated F' num2str(idatatoplot)];
            elseif app.DeltaFreqButton.Value == 1
                % not done yet!!!
                % app.EBIniAnaliz_4.Text = num2str(app.InitResonanceF(4));
                % app.ResonanceOfBaseLine
                leyenda{end+1} = ['/Delta F' num2str(idatatoplot)];
                datatoplot_po{i} = [app.DataArray{idatatoplot}(:,1),...
                    app.DataArray{idatatoplot}(:,5)-app.ResonanceOfBaseLine{idatatoplot}];
            end

            color_po{i}=[colors(idatatoplot) '.'];
            i = i+1;
        end
    end

    % make lines for savit golay filters
    i=1;
    for idatatoplot = [1 2 3 4]
        if indice_SG(idatatoplot)
            if app.ResistanceButton.Value == 1
                datatoplot_sg{i} = [app.DataArray{idatatoplot}(:,1),app.DataArray{idatatoplot}(:,6)];
                leyenda{end+1} = ['Fitted R' num2str(idatatoplot)];
            elseif app.ResonanceFreqButton.Value == 1
                datatoplot_sg{i} = [app.DataArray{idatatoplot}(:,1),app.DataArray{idatatoplot}(:,7)];
                leyenda{end+1} = ['Fitted F' num2str(idatatoplot)];
            elseif app.DeltaFreqButton.Value == 1
                datatoplot_sg{i} = [app.DataArray{idatatoplot}(:,1),...
                    app.DataArray{idatatoplot}(:,7)-app.ResonanceOfBaseLine{idatatoplot}];
                leyenda{end+1} = ['Fitted F' num2str(idatatoplot)];
            end
            color_sg{i}=[colors(idatatoplot) '-'];
            i=i+1;
```

```
            end
        end
        leyenda = {leyenda{:},'V1','V2','V3','V4','V5','V6','V7','V8'};
        %leyenda = {leyenda,{'V1','V2','V3','V4','V5','V6','V7','V8'}};
        yyaxis(app.UIAxes,'left');
        app.UIAxes.cla;
        Dibuja_Graficas(app,datatoplot_po,color_po,5);
        Dibuja_Graficas(app,datatoplot_sg,color_sg,1);


        % Valves, they go to the other axes, trasnparence high
        yyaxis(app.UIAxes,'right');
        v = app.HistoryValves;
        v(:,1) = etime(datevec(v(:,1)),app.StartTime);
        v(end+1,:) = [etime(clock,app.StartTime) app.StatusValves];
        vi=v;
        vi(:,1) = v(:,1)+0.001*ones(size(v,1),1);
        vis = sortrows([v;vi],1);
        Colores = colorcube;
        app.UIAxes.cla;
        hold(app.UIAxes,'on');
        for i=1:8
            h(i)=area(app.UIAxes,vis(2:end,1),vis(1:end-1,i+1));
            ylim(app.UIAxes,[0 100]);
            set(h(i),'FaceAlpha',0.2,'EdgeAlpha',0.1,'FaceColor',Colores(i*7-1,:));
        end
        hold(app.UIAxes,'off');

                    legend(app.UIAxes,leyenda,'Location','NorthEastOutside');
    end




    % Read serial ports and send back to dropdown box
    function SetupSerial(app)
        delete(instrfindall);
        info = instrhwinfo('serial');
        serial_num = size(info.SerialPorts,1);
        for i = 1 : serial_num
            dropdown_m(i) = info.SerialPorts(i,1);
        end
        if serial_num
            app.SerialPortDropDown.Items = dropdown_m;
        end
    end

end % methods


methods (Access = public)

    function results = concal2(app,v,fre)
        x = v(1);
        y = v(2)/1000;
        z = v(3)*1e-15;
        results = x./(x.^2+(2*pi*fre*y-1./2/pi./fre/z).^2);
    end

    function results = fitcon2(app,v,Fre,Conductance)
        x = v(1);%ohm
        y = v(2)/1000;%mH
        z = v(3)*1e-15;%fF

        f = x./(x.^2+(2*pi*Fre*y-1./2/pi./Fre/z).^2)-Conductance;
        results=f'*f;

    end

end


% Callbacks that handle component events
methods (Access = private)

    % Code that executes after component creation
    function startupFcn(app)
        app.N = 0;
        app.StartTime = clock;
        app.framelen = 5;
        app.ESGWindow.Value = app.framelen;
        app.order = 3;
        app.ESGOrder.Value = app.order;
        app.FolderEditField.Value = pwd;

        % Set the channels to measure
        CB_Analz_xValueChanged(app);

        % Setup Serial port connection
        SetupSerial(app);


        % load timetable if exists
        if exist('.\Default.xlsx','file')
            LoadTimeTable(app,'Default.xlsx','.');
        end

        % Window position
        p = get(app.UIFigure,'Position');
```

```
            p(1) = 10;
            p(2) = 50;
            set(app.UIFigure,'Position',p);

        end

        % Button pushed function: BrowseButton
        function BrowseButtonPushed(app, event)
            pathname = uigetdir;
            app.FolderEditField.Value  = pathname;
        end

        % Value changed function: ContinuousButton
        function ContinuousButtonValueChanged(app, event)
              if app.ContinuousButton.Value == 1

                % clean up data
                app.DataArray = { [] , [] , [] , [] }; % data
                app.N = 0;
                app.WeightedAverageTimeProcess = [];
                app.AverageTimeProcess = 0;

                app.RLC = {[400 11.400000000000 27.52015748915769 0],...
                    [400 11.400000000000 27.52015748915769 0],...
                    [400 11.400000000000 27.52015748915769 0],...
                    [400 11.400000000000 27.52015748915769 0]};

                yyaxis(app.UIAxes,'left');
                cla(app.UIAxes);
                yyaxis(app.UIAxes,'right');
                cla(app.UIAxes);

                % We cant change channels during measurement
                app.CB_Analz_1.Enable = 'off';
                app.CB_Analz_2.Enable = 'off';
                app.CB_Analz_3.Enable = 'off';
                app.CB_Analz_4.Enable = 'off';
                app.SingleSweepButton.Enable = 'off';

                % Get the files
                CheckNewFiles(app,0);

                % time of the start of experiment
                app.StartTime = clock;

                % Build array of valves
                app.HistoryValves = [datenum(app.StartTime) app.StatusValves];

                % start logging
                app.LogButton.Value = 1;
                LogButtonValueChanged(app,[]);

                % Clean temporal files
%                 delete('templog1.dat');
%                 delete('templog2.dat');
%                 delete('templog3.dat');
%                 delete('templog4.dat');

                % java call to get date format
                dateInstance = java.text.DateFormat.getDateInstance();
                app.DateFormat = char(dateInstance.toPattern());app.DateFormat=app.DateFormat(1);


                %Call loop function
                RunContinueButton(app);




              else
                % stop logging
                app.LogButton.Value = 0;
                LogButtonValueChanged(app,[]);

%                 % compile file with raw measurements and analyzed data
%                 app.ContinuousButton.Enable = 0;
%                 CompileData(app);
%                 app.ContinuousButton.Enable = 1;
%
%                 % Clean temporal files
%                 delete('templog1.dat');
%                 delete('templog2.dat');
%                 delete('templog3.dat');
%                 delete('templog4.dat');


                % buttons
                app.CB_Analz_1.Enable = 'on';
                app.CB_Analz_2.Enable = 'on';
                app.CB_Analz_3.Enable = 'on';
                app.CB_Analz_4.Enable = 'on';
                app.SingleSweepButton.Enable = 'on';


            end


        end
```

```
% Selection changed function: DisplayButtonGroup
function DisplayButtonGroupSelectionChanged(app, event)
    yyaxis(app.UIAxes,'left');
    %selectedButton = app.DisplayButtonGroup.SelectedObject;
    if app.ResistanceButton.Value == 1
        app.UIAxes.YLabel.String = 'resistance (Ohm)';
        app.UIAxes.Title.String = 'Series Resistance';
        app.SetInitialFreq.Visible = 'off';
        app.SetInitialFreq.Enable = 'off';
    elseif   app.ResonanceFreqButton.Value == 1
        app.UIAxes.YLabel.String = 'frequency (Hz)';
        app.UIAxes.Title.String = 'Resonance frequency';
        app.SetInitialFreq.Visible = 'off';
        app.SetInitialFreq.Enable = 'off';
    elseif app.DeltaFreqButton.Value == 1
        app.UIAxes.YLabel.String = 'frequency (Hz)';
        app.UIAxes.Title.String = 'Delta Resonance frequency';
        app.SetInitialFreq.Visible = 'on';
        app.SetInitialFreq.Enable = 'on';
        for number = app.Analz_Channels(app.Analz_Channels~=0)
            switch number
                case 1
                    app.EBIniAnaliz_1.Value = app.InitResonanceF{1};
                case 2
                    app.EBIniAnaliz_2.Value = app.InitResonanceF{2};
                case 3
                    app.EBIniAnaliz_3.Value = app.InitResonanceF{3};
                case 4
                    app.EBIniAnaliz_4.Value = app.InitResonanceF{4};
            end
        end
        app.ResonanceOfBaseLine = app.InitResonanceF;
    end
end

% Value changed function: LogButton
function LogButtonValueChanged(app, event)
       value = app.LogButton.Value;
    if value == 1

        % Build filenames
        AutoName(app);
        FileNames = {app.LLogFilename1.Text,app.LLogFilename2.Text...
            app.LLogFilename3.Text,app.LLogFilename4.Text};
        number = 1;

        % Build header of the file, then
        % dump all measured data since the start to the file
        % *** What happens when FileName{1} is not a valid filename?
        for FileName = FileNames
            fid = fopen(FileName{1}, 'a');
            fprintf(fid, '%s\n', ['Start Time: ' datestr(app.StartTime)]);
            fprintf(fid, '%s%g%s%g\n', 'Golay filter window length, ', app.framelen, ', Golay filter order, ', app.order);
            fprintf(fid, '%s ', 'Time,R1,L1,C1,ResFreq,R1_Golay,ResFreq_Golay,');
            if isempty(app.UITableTimesValves.RowName)
                fprintf(fid, 'V1,V2,V,V4,V5,V6,V7,V8\n');
            else
                fprintf(fid, '%s,%s,%s,%s,%s,%s,%s,%s\n', app.UITableTimesValves.RowName{2:end});
            end
            %[Time R L C ResonanceFreq GolayR GolarResFre] total 7 col
            if ~isempty(app.DataArray{number})
                %fprintf(fid, '%.3f,%6.3f,%6.5f,%6.5f,%10.2f,%6.3f,%10.2f\n', app.DataArray{number}(:,:)');
                fprintf(fid, '%.3f,%6.3f,%6.5f,%6.5f,%10.2f,%6.3f,%10.2f,%g,%g,%g,%g,%g,%g,%g,%g\n', app.DataArray{number}(:,1:15)');
            end
            fclose(fid);
            number = number + 1;
        end

        % interfaz updates
        app.LogButton.Text = 'Logging...';

        % lock options during log in
        app.FolderEditField.Enable = 0;
        app.Analyzer1EditField.Enable = 0;
        app.Analyzer2EditField.Enable = 0;
        app.Analyzer3EditField.Enable = 0;
        app.Analyzer4EditField.Enable = 0;
        app.BrowseButton.Enable = 0;
    else
        app.LogButton.Text = 'Log';
        app.FolderEditField.Enable = 1;
        app.Analyzer1EditField.Enable = 1;
        app.Analyzer2EditField.Enable = 1;
        app.Analyzer3EditField.Enable = 1;
        app.Analyzer4EditField.Enable = 1;
        app.BrowseButton.Enable = 1;
    end
end

% Button pushed function: SingleSweepButton
function SingleSweepButtonPushed(app, event)
    % clean up data
    app.DataArray = { [] , [] , [] , [] }; % data

    % We cant change channels during measurement
    app.CB_Analz_1.Enable = 'off';
    app.CB_Analz_2.Enable = 'off';
    app.CB_Analz_3.Enable = 'off';
    app.CB_Analz_4.Enable = 'off';
```

```
    app.ContinuousButton.Enable = 'off';

    % Get the files
    CheckNewFiles(app,0);

    % time of the start of experiment
    app.StartTime = clock;

    % start logging
    app.LogButton.Value = 1;
    LogButtonValueChanged(app,[]);

    % control to take a measurement of each network analizer
    AMeasured = [0 0 0 0];

    % while there is less channels measured than the number of channels to measure, we keep measuring
    while sum(AMeasured) < sum(app.Analz_Channels~=0)

        % check new files
        new_files1 = CheckNewFiles(app,1);
        new_files2 = CheckNewFiles(app,2);
        new_files3 = CheckNewFiles(app,3);
        new_files4 = CheckNewFiles(app,4);

        % if new files exists, process and flag as read
        if ~isempty(new_files1) && ismember(1,app.Analz_Channels)
            ProcessFile(app,new_files1,1);
            AMeasured(1) = 1;
        end

        if ~isempty(new_files2) && ismember(2,app.Analz_Channels)
            ProcessFile(app,new_files2,2);
            AMeasured(2) = 1;
        end

        if ~isempty(new_files3) && ismember(3,app.Analz_Channels)
            ProcessFile(app,new_files3,3);
            AMeasured(3) = 1;
        end

        if ~isempty(new_files4) && ismember(4,app.Analz_Channels)
            ProcessFile(app,new_files4,4);
            AMeasured(4) = 1;
        end
    end
    % we have measured all channels at least once, we plot
    UpdataGraph(app);

    % finish

    % stop logging
    app.LogButton.Value = 0;
    LogButtonValueChanged(app,[]);

    % restore functionality to software
    app.ContinuousButton.Enable = 'on';
    app.CB_Analz_1.Enable = 'on';
    app.CB_Analz_2.Enable = 'on';
    app.CB_Analz_3.Enable = 'on';
    app.CB_Analz_4.Enable = 'on';
end

% Button pushed function: SetInitialFreq
function SetInitialFreqButtonPushed(app, event)
    for number = app.Analz_Channels(app.Analz_Channels~=0)
        switch number
            case 1
                app.EBIniAnaliz_1.Value = app.InitResonanceF{1};
            case 2
                app.EBIniAnaliz_2.Value = app.InitResonanceF{2};
            case 3
                app.EBIniAnaliz_3.Value = app.InitResonanceF{3};
            case 4
                app.EBIniAnaliz_4.Value = app.InitResonanceF{4};
        end
    end
    app.ResonanceOfBaseLine = app.InitResonanceF;
end

% Callback function
function BrowseButton_2Pushed(app, event)
    [filename, pathname] = uiputfile('*.csv', 'Save a .csv log file');
    app.Analyzer1EditField.Value  = fullfile(pathname,filename);
end

% Value changed function: CB_Analz_1, CB_Analz_2,
% CB_Analz_3, CB_Analz_4
function CB_Analz_xValueChanged(app, event)
    % when changing the analyzer option it will measure and record only those
    % encode the checkboxes into the variable app.AC;
    % Compose list of channels, 0 is not measuring, number is measuring that channel
    % [1 2 0 3] will measure 1 2 and 4 network analizers
    % Also update the interface
    % ... probably overcomplicated way of doing things
    v1 = app.CB_Analz_1.Value;
    v2 = app.CB_Analz_2.Value;
    v3 = app.CB_Analz_3.Value;
    v4 = app.CB_Analz_4.Value;
```

```
            app.Analz_Channels = [1 2 3 4].*[v1 v2 v3 v4];

            app.CB_plot_Analizer1.Enable = v1;
            app.CB_plot_Analizer1.Value = v1;
            app.CB_AutoScale1.Enable = v1;

            app.CB_plot_Analizer2.Enable = v2;
            app.CB_plot_Analizer2.Value = v2;
            app.CB_AutoScale2.Enable = v2;

            app.CB_plot_Analizer3.Enable = v3;
            app.CB_plot_Analizer3.Value = v3;
            app.CB_AutoScale3.Enable = v3;

            app.CB_plot_Analizer4.Enable = v4;
            app.CB_plot_Analizer4.Value = v4;
            app.CB_AutoScale4.Enable = v4;
        end

        % Button pushed function: CB_AutoScale1
        function CB_AutoScale1Pushed(app, event)
            AutoChangeScalePlot(app,1);
        end

        % Button pushed function: CB_AutoScale2
        function CB_AutoScale2Pushed(app, event)
            AutoChangeScalePlot(app,2);
        end

        % Button pushed function: CB_AutoScale
        function CB_AutoScaleButtonPushed(app, event)
            app.UIAxes.YLimMode = 'auto';
        end

        % Button pushed function: CB_AutoScale3
        function CB_AutoScale3ButtonPushed(app, event)
            AutoChangeScalePlot(app,3);
        end

        % Button pushed function: CB_AutoScale4
        function CB_AutoScale4ButtonPushed(app, event)
            AutoChangeScalePlot(app,4);
        end

        % Value changed function: EPlotMaxY
        function EPlotMaxYValueChanged(app, event)
            valueMax = app.EPlotMaxY.Value;
            valueMin = app.EPlotMinY.Value;
            app.UIAxes.YLimMode = 'manual';
            if valueMin<valueMax
                app.UIAxes.YLim = [valueMin,valueMax];
            end
        end

        % Value changed function: ESGOrder
        function ESGOrderValueChanged(app, event)
            value = app.ESGOrder.Value;
            if value >= app.ESGWindow.Value
                value = app.ESGWindow.Value-1;
            end
            app.order = value;
            app.ESGOrder.Value = value;
        end

        % Value changed function: ESGWindow
        function ESGWindowValueChanged(app, event)
            value = app.ESGWindow.Value;
            if value < app.ESGOrder.Value
                value = app.ESGOrder.Value+1;
            end
            if ~mod(value,2)
                value = value+1;
            end
            app.framelen = value;
            app.ESGWindow.Value = value;
        end

        % Value changed function: CBActivateSG
        function CBActivateSGValueChanged(app, event)
            value = app.CBActivateSG.Value;
            if value
                app.MeasurementsPanel.Title = 'Measurements (SG)';
                app.DeltaoffPanel.Title = 'Increment of f (SG)';
            else
                app.MeasurementsPanel.Title = 'Measurements';
                app.DeltaoffPanel.Title = 'Increment of f';
            end
        end

        % Button pushed function: ConnectButton
        function ConnectButtonPushed(app, event)
            % clear the serial port
%             delete(instrfind);
%             fclose('all');

            % open the serial port
            try
                app.SerialPort = serial(app.SerialPortDropDown.Value,'BaudRate',115200);
                fopen(app.SerialPort);
```

```
            % Interfaz: allow valve controls
            if ~isempty(app.UITableTimesValves.Data)
                app.BStartStopTimeTable.Enable = 1;
            else
                app.BStartStopTimeTable.Enable = 0;
            end
            fclose(app.SerialPort);
            app.Lamp.Color = 'g';
            app.BrowseButton.Enable = 'on';
        catch
            % Interfaz: dont allor valve controls
            app.BStartStopTimeTable.Enable = 0;
            app.Lamp.Color = 'r';
            app.BrowseButton.Enable = 'off';
        end

%             delete(instrfind);
%             fclose('all');

    end

    % Button pushed function: RefreshButton
    function RefreshButtonPushed(app, event)
        SetupSerial(app);
    end

    % Button pushed function: LoadTimeTableButton
    function LoadTimeTableButtonPushed(app, event)
        %get timetable
        [FileName,FilePath] = uigetfile('*.xlsx','Select the TimeTable File');
        % recover focus of app
        app.UIFigure.Visible = 'off';
        app.UIFigure.Visible = 'on';
        LoadTimeTable(app,FileName,FilePath);
    end

    % Value changed function: BStartStopTimeTable
    function BStartStopTimeTableValueChanged(app, event)
        value = app.BStartStopTimeTable.Value;
        switch value
            case 1
                % interfaz update
                app.BStartStopTimeTable.Text = 'Running...';
                app.ConnectButton.Enable = 0;
                app.RefreshButton.Enable = 0;

                % Get data to send to serial
                Data2Send = table2array(app.UITableTimesValves.Data(2:end,1))';

                % Send the data of the valves
                SendCommandValves(app,Data2Send);

                % start timer of measurements
                % Get the start time of the table
                app.StartTimeT = clock;

                % calculate next time and its column index on the time table
                CalculateNextTime(app);

                % Setup timer for next step
                %app.TimeTTimer = timer('ExecutionMode','SingleShot','StartDelay',app.NextTimeT,'TimerFcn',{@SendValveDataTimeT,app});
                %start(app.TimeTTimer);


            case 0
                % Stop timer
                stop(app.TimeTTimer);

                % close serial port
                %delete(instrfind);
                %fclose('all');

                % interfaz update
                app.BStartStopTimeTable.Text = 'Start';
                app.ConnectButton.Enable = 1;
                app.RefreshButton.Enable = 1;
        end



    end

    % Cell edit callback: UITableTimesValves
    function UITableTimesValvesCellEdit(app, event)
        if ~isempty(app.TimeTTimer)
            switch app.TimeTTimer.Running
                case 'on'
                    CalculateNextTime(app);
                otherwise
                    app.BStartStopTimeTable.Enable = 1;
            end
        else
            app.BStartStopTimeTable.Enable = 0;
        end
    end

    % Button pushed function: AddColumnButton
    function AddColumnButtonPushed(app, event)
```

```
        numbername = num2str(size(app.UITableTimesValves.Data,2));
        column = table(zeros(9,1),'VariableNames',{['Var' num2str(numbername+1)]});
        app.UITableTimesValves.Data = [app.UITableTimesValves.Data column];
        app.UITableTimesValves.ColumnName{end+1} = ['Step ' num2str(numbername)];
        app.UITableTimesValves.ColumnEditable(end+1) = true;
    end

    % Callback function
    function SaveTimeTableButtonPushed(app, event)
        % Save data from ui to excel file
        % maybe use another sheet to store configuration data
        % and later use that sheet to restore configuration data
        %
        %  TO BE DONE
        %
        %

    end

    % Button pushed function: SendButton
    function SendButtonPushed(app, event)
        for i = 1:8
            switch i
                case 1
                    Data2Send(1) = app.VSpinner_1.Value;
                case 2
                    Data2Send(2) = app.VSpinner_2.Value;
                case 3
                    Data2Send(3) = app.VSpinner_3.Value;
                case 4
                    Data2Send(4) = app.VSpinner_4.Value;
                case 5
                    Data2Send(5) = app.VSpinner_5.Value;
                case 6
                    Data2Send(6) = app.VSpinner_6.Value;
                case 7
                    Data2Send(7) = app.VSpinner_7.Value;
                case 8
                    Data2Send(8) = app.VSpinner_8.Value;
            end
        end
        SendCommandValves(app,Data2Send);
    end
end

% Component initialization
methods (Access = private)

    % Create UIFigure and components
    function createComponents(app)

        % Create UIFigure and hide until all components are created
        app.UIFigure = uifigure('Visible', 'off');
        app.UIFigure.Position = [100 100 1341 690];
        app.UIFigure.Name = 'UI Figure';

        % Create UIAxes
        app.UIAxes = uiaxes(app.UIFigure);
        title(app.UIAxes, 'Resonance frequency')
        xlabel(app.UIAxes, 'time (s)')
        ylabel(app.UIAxes, 'frequency (Hz)')
        app.UIAxes.PlotBoxAspectRatio = [1.62028985507246 1 1];
        app.UIAxes.GridAlpha = 0.15;
        app.UIAxes.MinorGridAlpha = 0.25;
        app.UIAxes.XMinorTick = 'on';
        app.UIAxes.Position = [454 151 865 539];

        % Create SweepcontrolPanel
        app.SweepcontrolPanel = uipanel(app.UIFigure);
        app.SweepcontrolPanel.Title = 'Sweep control';
        app.SweepcontrolPanel.FontWeight = 'bold';
        app.SweepcontrolPanel.FontSize = 16;
        app.SweepcontrolPanel.Position = [2 597 116 93];

        % Create ContinuousButton
        app.ContinuousButton = uibutton(app.SweepcontrolPanel, 'state');
        app.ContinuousButton.ValueChangedFcn = createCallbackFcn(app, @ContinuousButtonValueChanged, true);
        app.ContinuousButton.Text = 'Continuous';
        app.ContinuousButton.Position = [7 36 100 22];

        % Create SingleSweepButton
        app.SingleSweepButton = uibutton(app.SweepcontrolPanel, 'push');
        app.SingleSweepButton.ButtonPushedFcn = createCallbackFcn(app, @SingleSweepButtonPushed, true);
        app.SingleSweepButton.Position = [6 7 100 22];
        app.SingleSweepButton.Text = 'Single Sweep';

        % Create LoggingPanel
        app.LoggingPanel = uipanel(app.UIFigure);
        app.LoggingPanel.Title = 'Logging';
        app.LoggingPanel.FontWeight = 'bold';
        app.LoggingPanel.Position = [355 3 868 143];

        % Create FolderEditFieldLabel
        app.FolderEditFieldLabel = uilabel(app.LoggingPanel);
        app.FolderEditFieldLabel.HorizontalAlignment = 'right';
        app.FolderEditFieldLabel.VerticalAlignment = 'top';
        app.FolderEditFieldLabel.Position = [179 97 40 22];
        app.FolderEditFieldLabel.Text = 'Folder';
```

```
% Create FolderEditField
app.FolderEditField = uieditfield(app.LoggingPanel, 'text');
app.FolderEditField.Position = [234 100 220 22];

% Create Analyzer1EditFieldLabel
app.Analyzer1EditFieldLabel = uilabel(app.LoggingPanel);
app.Analyzer1EditFieldLabel.HorizontalAlignment = 'right';
app.Analyzer1EditFieldLabel.VerticalAlignment = 'top';
app.Analyzer1EditFieldLabel.Position = [4 73 62 22];
app.Analyzer1EditFieldLabel.Text = 'Analyzer 1';

% Create Analyzer1EditField
app.Analyzer1EditField = uieditfield(app.LoggingPanel, 'text');
app.Analyzer1EditField.Position = [81 76 200 22];
app.Analyzer1EditField.Value = 'S1';

% Create Analyzer2EditFieldLabel
app.Analyzer2EditFieldLabel = uilabel(app.LoggingPanel);
app.Analyzer2EditFieldLabel.HorizontalAlignment = 'right';
app.Analyzer2EditFieldLabel.VerticalAlignment = 'top';
app.Analyzer2EditFieldLabel.Position = [4 49 62 22];
app.Analyzer2EditFieldLabel.Text = 'Analyzer 2';

% Create Analyzer2EditField
app.Analyzer2EditField = uieditfield(app.LoggingPanel, 'text');
app.Analyzer2EditField.Position = [81 52 200 22];
app.Analyzer2EditField.Value = 'S2';

% Create Analyzer3EditFieldLabel
app.Analyzer3EditFieldLabel = uilabel(app.LoggingPanel);
app.Analyzer3EditFieldLabel.HorizontalAlignment = 'right';
app.Analyzer3EditFieldLabel.VerticalAlignment = 'top';
app.Analyzer3EditFieldLabel.Position = [4 24 62 22];
app.Analyzer3EditFieldLabel.Text = 'Analyzer 3';

% Create Analyzer3EditField
app.Analyzer3EditField = uieditfield(app.LoggingPanel, 'text');
app.Analyzer3EditField.Position = [81 27 200 22];
app.Analyzer3EditField.Value = 'S3';

% Create Analyzer4EditFieldLabel
app.Analyzer4EditFieldLabel = uilabel(app.LoggingPanel);
app.Analyzer4EditFieldLabel.HorizontalAlignment = 'right';
app.Analyzer4EditFieldLabel.VerticalAlignment = 'top';
app.Analyzer4EditFieldLabel.Position = [4 -1 62 22];
app.Analyzer4EditFieldLabel.Text = 'Analyzer 4';

% Create Analyzer4EditField
app.Analyzer4EditField = uieditfield(app.LoggingPanel, 'text');
app.Analyzer4EditField.Position = [81 2 200 22];
app.Analyzer4EditField.Value = 'S4';

% Create LLogFilename1
app.LLogFilename1 = uilabel(app.LoggingPanel);
app.LLogFilename1.Position = [290 76 564 22];
app.LLogFilename1.Text = 'No file';

% Create LLogFilename2
app.LLogFilename2 = uilabel(app.LoggingPanel);
app.LLogFilename2.Position = [290 52 564 22];
app.LLogFilename2.Text = 'No file';

% Create LLogFilename3
app.LLogFilename3 = uilabel(app.LoggingPanel);
app.LLogFilename3.Position = [290 27 563 22];
app.LLogFilename3.Text = 'No file';

% Create LLogFilename4
app.LLogFilename4 = uilabel(app.LoggingPanel);
app.LLogFilename4.Position = [290 2 563 22];
app.LLogFilename4.Text = 'No file';

% Create LogButton
app.LogButton = uibutton(app.LoggingPanel, 'state');
app.LogButton.ValueChangedFcn = createCallbackFcn(app, @LogButtonValueChanged, true);
app.LogButton.Text = 'Log';
app.LogButton.Position = [4 99 100 22];

% Create BrowseButton
app.BrowseButton = uibutton(app.LoggingPanel, 'push');
app.BrowseButton.ButtonPushedFcn = createCallbackFcn(app, @BrowseButtonPushed, true);
app.BrowseButton.Position = [110 100 66 22];
app.BrowseButton.Text = 'Browse';

% Create DisplayButtonGroup
app.DisplayButtonGroup = uibuttongroup(app.UIFigure);
app.DisplayButtonGroup.SelectionChangedFcn = createCallbackFcn(app, @DisplayButtonGroupSelectionChanged, true);
app.DisplayButtonGroup.Title = 'Display';
app.DisplayButtonGroup.FontWeight = 'bold';
app.DisplayButtonGroup.Position = [327 597 123 93];

% Create ResistanceButton
app.ResistanceButton = uitogglebutton(app.DisplayButtonGroup);
app.ResistanceButton.Text = 'Resistance';
app.ResistanceButton.Position = [13 49 100 22];

% Create ResonanceFreqButton
app.ResonanceFreqButton = uitogglebutton(app.DisplayButtonGroup);
app.ResonanceFreqButton.Text = 'Resonance Freq';
```

```
app.ResonanceFreqButton.Position = [13 26 100 22];
app.ResonanceFreqButton.Value = true;

% Create DeltaFreqButton
app.DeltaFreqButton = uitogglebutton(app.DisplayButtonGroup);
app.DeltaFreqButton.Text = 'Delta Freq';
app.DeltaFreqButton.Position = [13 3 100 22];

% Create ChannelsPanel
app.ChannelsPanel = uipanel(app.UIFigure);
app.ChannelsPanel.Title = 'Channels';
app.ChannelsPanel.FontWeight = 'bold';
app.ChannelsPanel.Position = [117 597 100 93];

% Create CB_Analz_1
app.CB_Analz_1 = uicheckbox(app.ChannelsPanel);
app.CB_Analz_1.ValueChangedFcn = createCallbackFcn(app, @CB_Analz_xValueChanged, true);
app.CB_Analz_1.Text = 'Analizer 1';
app.CB_Analz_1.Position = [12 53 75 22];
app.CB_Analz_1.Value = true;

% Create CB_Analz_2
app.CB_Analz_2 = uicheckbox(app.ChannelsPanel);
app.CB_Analz_2.ValueChangedFcn = createCallbackFcn(app, @CB_Analz_xValueChanged, true);
app.CB_Analz_2.Text = 'Analizer 2';
app.CB_Analz_2.Position = [12 37 75 22];
app.CB_Analz_2.Value = true;

% Create CB_Analz_4
app.CB_Analz_4 = uicheckbox(app.ChannelsPanel);
app.CB_Analz_4.ValueChangedFcn = createCallbackFcn(app, @CB_Analz_xValueChanged, true);
app.CB_Analz_4.Text = 'Analizer 4';
app.CB_Analz_4.Position = [12 5 75 22];
app.CB_Analz_4.Value = true;

% Create CB_Analz_3
app.CB_Analz_3 = uicheckbox(app.ChannelsPanel);
app.CB_Analz_3.ValueChangedFcn = createCallbackFcn(app, @CB_Analz_xValueChanged, true);
app.CB_Analz_3.Text = 'Analizer 3';
app.CB_Analz_3.Position = [12 21 75 22];
app.CB_Analz_3.Value = true;

% Create PlottingsettingsPanel
app.PlottingsettingsPanel = uipanel(app.UIFigure);
app.PlottingsettingsPanel.Title = 'Plotting settings';
app.PlottingsettingsPanel.FontWeight = 'bold';
app.PlottingsettingsPanel.Position = [327 443 123 155];

% Create CB_plot_Analizer1
app.CB_plot_Analizer1 = uicheckbox(app.PlottingsettingsPanel);
app.CB_plot_Analizer1.Text = 'Analizer 1';
app.CB_plot_Analizer1.Position = [3 115 75 22];

% Create CB_AutoScale1
app.CB_AutoScale1 = uibutton(app.PlottingsettingsPanel, 'push');
app.CB_AutoScale1.ButtonPushedFcn = createCallbackFcn(app, @CB_AutoScale1Pushed, true);
app.CB_AutoScale1.FontSize = 8;
app.CB_AutoScale1.Position = [86 119 27 14];
app.CB_AutoScale1.Text = 'C';

% Create CB_plot_Analizer2
app.CB_plot_Analizer2 = uicheckbox(app.PlottingsettingsPanel);
app.CB_plot_Analizer2.Text = 'Analizer 2';
app.CB_plot_Analizer2.Position = [3 99 75 22];

% Create CB_AutoScale2
app.CB_AutoScale2 = uibutton(app.PlottingsettingsPanel, 'push');
app.CB_AutoScale2.ButtonPushedFcn = createCallbackFcn(app, @CB_AutoScale2Pushed, true);
app.CB_AutoScale2.FontSize = 8;
app.CB_AutoScale2.Position = [86 104 27 14];
app.CB_AutoScale2.Text = 'C';

% Create CB_AutoScale3
app.CB_AutoScale3 = uibutton(app.PlottingsettingsPanel, 'push');
app.CB_AutoScale3.ButtonPushedFcn = createCallbackFcn(app, @CB_AutoScale3ButtonPushed, true);
app.CB_AutoScale3.FontSize = 8;
app.CB_AutoScale3.Position = [86 89 27 14];
app.CB_AutoScale3.Text = 'C';

% Create CB_plot_Analizer3
app.CB_plot_Analizer3 = uicheckbox(app.PlottingsettingsPanel);
app.CB_plot_Analizer3.Text = 'Analizer 3';
app.CB_plot_Analizer3.Position = [3 83 75 22];

% Create CB_AutoScale4
app.CB_AutoScale4 = uibutton(app.PlottingsettingsPanel, 'push');
app.CB_AutoScale4.ButtonPushedFcn = createCallbackFcn(app, @CB_AutoScale4ButtonPushed, true);
app.CB_AutoScale4.FontSize = 8;
app.CB_AutoScale4.Position = [86 74 27 14];
app.CB_AutoScale4.Text = 'C';

% Create CB_plot_Analizer4
app.CB_plot_Analizer4 = uicheckbox(app.PlottingsettingsPanel);
app.CB_plot_Analizer4.Text = 'Analizer 4';
app.CB_plot_Analizer4.Position = [3 67 75 22];

% Create CB_AutoScale
app.CB_AutoScale = uibutton(app.PlottingsettingsPanel, 'push');
app.CB_AutoScale.ButtonPushedFcn = createCallbackFcn(app, @CB_AutoScaleButtonPushed, true);
```

```
app.CB_AutoScale.Position = [14 48 98 22];
app.CB_AutoScale.Text = 'Auto Scale';

% Create MaxEditFieldLabel
app.MaxEditFieldLabel = uilabel(app.PlottingsettingsPanel);
app.MaxEditFieldLabel.HorizontalAlignment = 'right';
app.MaxEditFieldLabel.Position = [4 25 25 22];
app.MaxEditFieldLabel.Text = 'Max';

% Create EPlotMaxY
app.EPlotMaxY = uieditfield(app.PlottingsettingsPanel, 'numeric');
app.EPlotMaxY.Limits = [0 Inf];
app.EPlotMaxY.ValueChangedFcn = createCallbackFcn(app, @EPlotMaxYValueChanged, true);
app.EPlotMaxY.Position = [36 25 77 22];

% Create MinEditFieldLabel
app.MinEditFieldLabel = uilabel(app.PlottingsettingsPanel);
app.MinEditFieldLabel.HorizontalAlignment = 'right';
app.MinEditFieldLabel.Position = [4 2 20 22];
app.MinEditFieldLabel.Text = 'Min';

% Create EPlotMinY
app.EPlotMinY = uieditfield(app.PlottingsettingsPanel, 'numeric');
app.EPlotMinY.Limits = [0 Inf];
app.EPlotMinY.Position = [36 2 77 22];

% Create SGparametersPanel
app.SGparametersPanel = uipanel(app.UIFigure);
app.SGparametersPanel.Title = 'SG parameters';
app.SGparametersPanel.FontWeight = 'bold';
app.SGparametersPanel.Position = [216 597 112 93];

% Create SGOrderEditFieldLabel
app.SGOrderEditFieldLabel = uilabel(app.SGparametersPanel);
app.SGOrderEditFieldLabel.HorizontalAlignment = 'right';
app.SGOrderEditFieldLabel.Position = [2 27 57 22];
app.SGOrderEditFieldLabel.Text = 'SG Order';

% Create ESGOrder
app.ESGOrder = uieditfield(app.SGparametersPanel, 'numeric');
app.ESGOrder.ValueChangedFcn = createCallbackFcn(app, @ESGOrderValueChanged, true);
app.ESGOrder.Position = [72 27 18 22];

% Create SGwindowEditFieldLabel
app.SGwindowEditFieldLabel = uilabel(app.SGparametersPanel);
app.SGwindowEditFieldLabel.HorizontalAlignment = 'right';
app.SGwindowEditFieldLabel.Position = [1 4 66 22];
app.SGwindowEditFieldLabel.Text = 'SG window';

% Create ESGWindow
app.ESGWindow = uieditfield(app.SGparametersPanel, 'numeric');
app.ESGWindow.ValueChangedFcn = createCallbackFcn(app, @ESGWindowValueChanged, true);
app.ESGWindow.Position = [70 4 20 22];

% Create CBActivateSG
app.CBActivateSG = uicheckbox(app.SGparametersPanel);
app.CBActivateSG.ValueChangedFcn = createCallbackFcn(app, @CBActivateSGValueChanged, true);
app.CBActivateSG.Text = 'Activate';
app.CBActivateSG.Position = [12 50 65 22];

% Create MeasurementsPanel
app.MeasurementsPanel = uipanel(app.UIFigure);
app.MeasurementsPanel.Title = 'Measurements';
app.MeasurementsPanel.FontWeight = 'bold';
app.MeasurementsPanel.Position = [160 443 168 155];

% Create Analizer1EditFieldLabel
app.Analizer1EditFieldLabel = uilabel(app.MeasurementsPanel);
app.Analizer1EditFieldLabel.HorizontalAlignment = 'right';
app.Analizer1EditFieldLabel.Enable = 'off';
app.Analizer1EditFieldLabel.Position = [2 108 59 22];
app.Analizer1EditFieldLabel.Text = 'Analizer 1';

% Create EBDipAnaliz_1
app.EBDipAnaliz_1 = uieditfield(app.MeasurementsPanel, 'numeric');
app.EBDipAnaliz_1.Enable = 'off';
app.EBDipAnaliz_1.Position = [70 108 95 22];

% Create Analizer2Label
app.Analizer2Label = uilabel(app.MeasurementsPanel);
app.Analizer2Label.HorizontalAlignment = 'right';
app.Analizer2Label.Enable = 'off';
app.Analizer2Label.Position = [2 75 59 22];
app.Analizer2Label.Text = 'Analizer 2';

% Create EBDipAnaliz_2
app.EBDipAnaliz_2 = uieditfield(app.MeasurementsPanel, 'numeric');
app.EBDipAnaliz_2.Enable = 'off';
app.EBDipAnaliz_2.Position = [70 75 95 22];

% Create Analizer3Label
app.Analizer3Label = uilabel(app.MeasurementsPanel);
app.Analizer3Label.HorizontalAlignment = 'right';
app.Analizer3Label.Enable = 'off';
app.Analizer3Label.Position = [2 42 59 22];
app.Analizer3Label.Text = 'Analizer 3';

% Create EBDipAnaliz_3
app.EBDipAnaliz_3 = uieditfield(app.MeasurementsPanel, 'numeric');
```

```
app.EBDipAnaliz_3.Enable = 'off';
app.EBDipAnaliz_3.Position = [70 42 95 22];

% Create Analizer4Label
app.Analizer4Label = uilabel(app.MeasurementsPanel);
app.Analizer4Label.HorizontalAlignment = 'right';
app.Analizer4Label.Enable = 'off';
app.Analizer4Label.Position = [2 9 59 22];
app.Analizer4Label.Text = 'Analizer 4';

% Create EBDipAnaliz_4
app.EBDipAnaliz_4 = uieditfield(app.MeasurementsPanel, 'numeric');
app.EBDipAnaliz_4.Enable = 'off';
app.EBDipAnaliz_4.Position = [70 9 95 22];

% Create DeltaoffPanel
app.DeltaoffPanel = uipanel(app.UIFigure);
app.DeltaoffPanel.Title = 'Delta of f';
app.DeltaoffPanel.FontWeight = 'bold';
app.DeltaoffPanel.Position = [2 443 159 155];

% Create Analizer1EditFieldLabel_2
app.Analizer1EditFieldLabel_2 = uilabel(app.DeltaoffPanel);
app.Analizer1EditFieldLabel_2.HorizontalAlignment = 'right';
app.Analizer1EditFieldLabel_2.Position = [1 112 59 22];
app.Analizer1EditFieldLabel_2.Text = 'Analizer 1';

% Create EBIniAnaliz_1
app.EBIniAnaliz_1 = uieditfield(app.DeltaoffPanel, 'numeric');
app.EBIniAnaliz_1.Position = [64 112 92 22];

% Create Analizer2Label_2
app.Analizer2Label_2 = uilabel(app.DeltaoffPanel);
app.Analizer2Label_2.HorizontalAlignment = 'right';
app.Analizer2Label_2.Position = [1 86 59 22];
app.Analizer2Label_2.Text = 'Analizer 2';

% Create EBIniAnaliz_2
app.EBIniAnaliz_2 = uieditfield(app.DeltaoffPanel, 'numeric');
app.EBIniAnaliz_2.Position = [64 86 92 22];

% Create Analizer3Label_2
app.Analizer3Label_2 = uilabel(app.DeltaoffPanel);
app.Analizer3Label_2.HorizontalAlignment = 'right';
app.Analizer3Label_2.Position = [1 60 59 22];
app.Analizer3Label_2.Text = 'Analizer 3';

% Create EBIniAnaliz_3
app.EBIniAnaliz_3 = uieditfield(app.DeltaoffPanel, 'numeric');
app.EBIniAnaliz_3.Position = [64 60 92 22];

% Create Analizer4Label_2
app.Analizer4Label_2 = uilabel(app.DeltaoffPanel);
app.Analizer4Label_2.HorizontalAlignment = 'right';
app.Analizer4Label_2.Position = [1 34 59 22];
app.Analizer4Label_2.Text = 'Analizer 4';

% Create EBIniAnaliz_4
app.EBIniAnaliz_4 = uieditfield(app.DeltaoffPanel, 'numeric');
app.EBIniAnaliz_4.Position = [64 34 92 22];

% Create SetInitialFreq
app.SetInitialFreq = uibutton(app.DeltaoffPanel, 'push');
app.SetInitialFreq.ButtonPushedFcn = createCallbackFcn(app, @SetInitialFreqButtonPushed, true);
app.SetInitialFreq.Enable = 'off';
app.SetInitialFreq.Visible = 'off';
app.SetInitialFreq.Position = [1 7 155 22];
app.SetInitialFreq.Text = 'Set Initial Freq.';

% Create TimingPanel
app.TimingPanel = uipanel(app.UIFigure);
app.TimingPanel.Title = 'Timing';
app.TimingPanel.FontWeight = 'bold';
app.TimingPanel.Position = [137 3 219 143];

% Create LoopLabel
app.LoopLabel = uilabel(app.TimingPanel);
app.LoopLabel.VerticalAlignment = 'top';
app.LoopLabel.Position = [11 44 203 15];
app.LoopLabel.Text = 'Loop: ';

% Create LAverageTimeProcess
app.LAverageTimeProcess = uilabel(app.TimingPanel);
app.LAverageTimeProcess.VerticalAlignment = 'top';
app.LAverageTimeProcess.Position = [11 25 203 15];
app.LAverageTimeProcess.Text = '';

% Create LMaxTimeProcess
app.LMaxTimeProcess = uilabel(app.TimingPanel);
app.LMaxTimeProcess.VerticalAlignment = 'top';
app.LMaxTimeProcess.Position = [11 64 203 15];
app.LMaxTimeProcess.Text = '';

% Create LTotalTime
app.LTotalTime = uilabel(app.TimingPanel);
app.LTotalTime.VerticalAlignment = 'top';
app.LTotalTime.Position = [11 97 203 22];
app.LTotalTime.Text = '';
```

```
% Create LMeasureNumber
app.LMeasureNumber = uilabel(app.TimingPanel);
app.LMeasureNumber.VerticalAlignment = 'top';
app.LMeasureNumber.FontWeight = 'bold';
app.LMeasureNumber.Position = [11 84 203 15];
app.LMeasureNumber.Text = '';

% Create LTotalTimeElapsed
app.LTotalTimeElapsed = uilabel(app.TimingPanel);
app.LTotalTimeElapsed.VerticalAlignment = 'top';
app.LTotalTimeElapsed.Position = [11 6 203 15];
app.LTotalTimeElapsed.Text = '';

% Create UITableTimesValves
app.UITableTimesValves = uitable(app.UIFigure);
app.UITableTimesValves.ColumnName = '';
app.UITableTimesValves.RowName = {};
app.UITableTimesValves.CellEditCallback = createCallbackFcn(app, @UITableTimesValvesCellEdit, true);
app.UITableTimesValves.Position = [2 235 448 209];

% Create ConnectiontoValvesPanel
app.ConnectiontoValvesPanel = uipanel(app.UIFigure);
app.ConnectiontoValvesPanel.Title = 'Connection to Valves';
app.ConnectiontoValvesPanel.FontWeight = 'bold';
app.ConnectiontoValvesPanel.Position = [137 145 188 90];

% Create ConnectButton
app.ConnectButton = uibutton(app.ConnectiontoValvesPanel, 'push');
app.ConnectButton.ButtonPushedFcn = createCallbackFcn(app, @ConnectButtonPushed, true);
app.ConnectButton.Position = [3 4 153 22];
app.ConnectButton.Text = 'Connect';

% Create SerialPortDropDownLabel
app.SerialPortDropDownLabel = uilabel(app.ConnectiontoValvesPanel);
app.SerialPortDropDownLabel.HorizontalAlignment = 'right';
app.SerialPortDropDownLabel.VerticalAlignment = 'top';
app.SerialPortDropDownLabel.Position = [-1 42 62 15];
app.SerialPortDropDownLabel.Text = 'Serial Port';

% Create SerialPortDropDown
app.SerialPortDropDown = uidropdown(app.ConnectiontoValvesPanel);
app.SerialPortDropDown.Items = {};
app.SerialPortDropDown.Position = [66 38 59 22];
app.SerialPortDropDown.Value = {};

% Create Lamp
app.Lamp = uilamp(app.ConnectiontoValvesPanel);
app.Lamp.Position = [163 5 20 20];
app.Lamp.Color = [1 0 0];

% Create RefreshButton
app.RefreshButton = uibutton(app.ConnectiontoValvesPanel, 'push');
app.RefreshButton.ButtonPushedFcn = createCallbackFcn(app, @RefreshButtonPushed, true);
app.RefreshButton.Position = [134 38 49 22];
app.RefreshButton.Text = 'Refresh';

% Create ValvesTasksPanel
app.ValvesTasksPanel = uipanel(app.UIFigure);
app.ValvesTasksPanel.Title = 'Valves Tasks';
app.ValvesTasksPanel.FontWeight = 'bold';
app.ValvesTasksPanel.Position = [2 92 136 143];

% Create LoadTimeTableButton
app.LoadTimeTableButton = uibutton(app.ValvesTasksPanel, 'push');
app.LoadTimeTableButton.ButtonPushedFcn = createCallbackFcn(app, @LoadTimeTableButtonPushed, true);
app.LoadTimeTableButton.Position = [15 32 104 22];
app.LoadTimeTableButton.Text = 'Load Time Table';

% Create BStartStopTimeTable
app.BStartStopTimeTable = uibutton(app.ValvesTasksPanel, 'state');
app.BStartStopTimeTable.ValueChangedFcn = createCallbackFcn(app, @BStartStopTimeTableValueChanged, true);
app.BStartStopTimeTable.Enable = 'off';
app.BStartStopTimeTable.Text = 'START';
app.BStartStopTimeTable.Position = [17 88 100 22];

% Create AddColumnButton
app.AddColumnButton = uibutton(app.ValvesTasksPanel, 'push');
app.AddColumnButton.ButtonPushedFcn = createCallbackFcn(app, @AddColumnButtonPushed, true);
app.AddColumnButton.Position = [15 7 100 22];
app.AddColumnButton.Text = 'Add Column';

% Create CBFinishMeasWTask
app.CBFinishMeasWTask = uicheckbox(app.ValvesTasksPanel);
app.CBFinishMeasWTask.Text = 'Stop Meas. w. Tasks';
app.CBFinishMeasWTask.Position = [4 60 131 22];
app.CBFinishMeasWTask.Value = true;

% Create NextStepLabel
app.NextStepLabel = uilabel(app.UIFigure);
app.NextStepLabel.HorizontalAlignment = 'right';
app.NextStepLabel.Position = [334 168 58 22];
app.NextStepLabel.Text = 'Next Step';

% Create ENextStep
app.ENextStep = uieditfield(app.UIFigure, 'numeric');
app.ENextStep.Position = [407 168 43 22];

% Create NextTimeEditFieldLabel
app.NextTimeEditFieldLabel = uilabel(app.UIFigure);
```

```
app.NextTimeEditFieldLabel.HorizontalAlignment = 'right';
app.NextTimeEditFieldLabel.Position = [332 189 60 22];
app.NextTimeEditFieldLabel.Text = 'Next Time';

% Create ENextTime
app.ENextTime = uieditfield(app.UIFigure, 'numeric');
app.ENextTime.Position = [407 189 43 22];

% Create TimeElapsedEditFieldLabel
app.TimeElapsedEditFieldLabel = uilabel(app.UIFigure);
app.TimeElapsedEditFieldLabel.HorizontalAlignment = 'right';
app.TimeElapsedEditFieldLabel.Position = [324 210 78 22];
app.TimeElapsedEditFieldLabel.Text = 'Time Elapsed';

% Create TimeElapsedEditField
app.TimeElapsedEditField = uieditfield(app.UIFigure, 'numeric');
app.TimeElapsedEditField.ValueDisplayFormat = '%.1f';
app.TimeElapsedEditField.Position = [407 210 43 22];

% Create LABLabel
app.LABLabel = uilabel(app.UIFigure);
app.LABLabel.FontName = 'UD Digi Kyokasho N-R';
app.LABLabel.FontSize = 20;
app.LABLabel.Position = [22 18 95 62];
app.LABLabel.Text = 'ÿÿ LAB.';

% Create ManualValveCtrPanel
app.ManualValveCtrPanel = uipanel(app.UIFigure);
app.ManualValveCtrPanel.Title = 'Manual Valve Ctr.';
app.ManualValveCtrPanel.Position = [1222 4 119 275];

% Create V1SpinnerLabel
app.V1SpinnerLabel = uilabel(app.ManualValveCtrPanel);
app.V1SpinnerLabel.HorizontalAlignment = 'right';
app.V1SpinnerLabel.Position = [9 223 25 22];
app.V1SpinnerLabel.Text = 'V1';

% Create VSpinner_1
app.VSpinner_1 = uispinner(app.ManualValveCtrPanel);
app.VSpinner_1.Step = 100;
app.VSpinner_1.Limits = [0 100];
app.VSpinner_1.RoundFractionalValues = 'on';
app.VSpinner_1.ValueDisplayFormat = '%.0f';
app.VSpinner_1.Position = [43 223 71 22];

% Create V2Label
app.V2Label = uilabel(app.ManualValveCtrPanel);
app.V2Label.HorizontalAlignment = 'right';
app.V2Label.Position = [9 196 25 22];
app.V2Label.Text = 'V2';

% Create VSpinner_2
app.VSpinner_2 = uispinner(app.ManualValveCtrPanel);
app.VSpinner_2.Step = 100;
app.VSpinner_2.Limits = [0 100];
app.VSpinner_2.RoundFractionalValues = 'on';
app.VSpinner_2.ValueDisplayFormat = '%.0f';
app.VSpinner_2.Position = [43 196 71 22];

% Create V3Label
app.V3Label = uilabel(app.ManualValveCtrPanel);
app.V3Label.HorizontalAlignment = 'right';
app.V3Label.Position = [9 169 25 22];
app.V3Label.Text = 'V3';

% Create VSpinner_3
app.VSpinner_3 = uispinner(app.ManualValveCtrPanel);
app.VSpinner_3.Step = 100;
app.VSpinner_3.Limits = [0 100];
app.VSpinner_3.RoundFractionalValues = 'on';
app.VSpinner_3.ValueDisplayFormat = '%.0f';
app.VSpinner_3.Position = [43 169 71 22];

% Create V4Label
app.V4Label = uilabel(app.ManualValveCtrPanel);
app.V4Label.HorizontalAlignment = 'right';
app.V4Label.Position = [9 142 25 22];
app.V4Label.Text = 'V4';

% Create VSpinner_4
app.VSpinner_4 = uispinner(app.ManualValveCtrPanel);
app.VSpinner_4.Step = 100;
app.VSpinner_4.Limits = [0 100];
app.VSpinner_4.RoundFractionalValues = 'on';
app.VSpinner_4.ValueDisplayFormat = '%.0f';
app.VSpinner_4.Position = [43 142 71 22];

% Create V5Label
app.V5Label = uilabel(app.ManualValveCtrPanel);
app.V5Label.HorizontalAlignment = 'right';
app.V5Label.Position = [9 115 25 22];
app.V5Label.Text = 'V5';

% Create VSpinner_5
app.VSpinner_5 = uispinner(app.ManualValveCtrPanel);
app.VSpinner_5.Step = 100;
app.VSpinner_5.Limits = [0 100];
app.VSpinner_5.RoundFractionalValues = 'on';
app.VSpinner_5.ValueDisplayFormat = '%.0f';
```

```
app.VSpinner_5.Position = [43 115 71 22];

% Create V6Label
app.V6Label = uilabel(app.ManualValveCtrPanel);
app.V6Label.HorizontalAlignment = 'right';
app.V6Label.Position = [9 88 25 22];
app.V6Label.Text = 'V6';

% Create VSpinner_6
app.VSpinner_6 = uispinner(app.ManualValveCtrPanel);
app.VSpinner_6.Step = 100;
app.VSpinner_6.Limits = [0 100];
app.VSpinner_6.RoundFractionalValues = 'on';
app.VSpinner_6.ValueDisplayFormat = '%.0f';
app.VSpinner_6.Position = [43 88 71 22];

% Create V7Label
app.V7Label = uilabel(app.ManualValveCtrPanel);
app.V7Label.HorizontalAlignment = 'right';
app.V7Label.Position = [9 62 25 22];
app.V7Label.Text = 'V7';

% Create VSpinner_7
app.VSpinner_7 = uispinner(app.ManualValveCtrPanel);
app.VSpinner_7.Step = 100;
app.VSpinner_7.Limits = [0 100];
app.VSpinner_7.RoundFractionalValues = 'on';
app.VSpinner_7.ValueDisplayFormat = '%.0f';
app.VSpinner_7.Position = [43 62 71 22];

% Create V8Label
app.V8Label = uilabel(app.ManualValveCtrPanel);
app.V8Label.HorizontalAlignment = 'right';
app.V8Label.Position = [9 36 25 22];
app.V8Label.Text = 'V8';

% Create VSpinner_8
app.VSpinner_8 = uispinner(app.ManualValveCtrPanel);
app.VSpinner_8.Step = 100;
app.VSpinner_8.Limits = [0 100];
app.VSpinner_8.RoundFractionalValues = 'on';
app.VSpinner_8.ValueDisplayFormat = '%.0f';
app.VSpinner_8.Position = [43 36 71 22];

% Create SendButton
app.SendButton = uibutton(app.ManualValveCtrPanel, 'push');
app.SendButton.ButtonPushedFcn = createCallbackFcn(app, @SendButtonPushed, true);
app.SendButton.Position = [9 8 100 22];
app.SendButton.Text = 'Send';

% Create PlotValvesPanel
app.PlotValvesPanel = uipanel(app.UIFigure);
app.PlotValvesPanel.Title = 'Plot Valves';
app.PlotValvesPanel.Position = [1222 285 119 128];

% Create CB_ValvPlot
app.CB_ValvPlot = uicheckbox(app.PlotValvesPanel);
app.CB_ValvPlot.Text = 'V1';
app.CB_ValvPlot.Position = [4 80 37 22];

% Create CB_ValvPlot_2
app.CB_ValvPlot_2 = uicheckbox(app.PlotValvesPanel);
app.CB_ValvPlot_2.Text = 'V3';
app.CB_ValvPlot_2.Position = [4 56 37 22];

% Create CB_ValvPlot_3
app.CB_ValvPlot_3 = uicheckbox(app.PlotValvesPanel);
app.CB_ValvPlot_3.Text = 'V5';
app.CB_ValvPlot_3.Position = [4 33 37 22];

% Create CB_ValvPlot_4
app.CB_ValvPlot_4 = uicheckbox(app.PlotValvesPanel);
app.CB_ValvPlot_4.Text = 'V7';
app.CB_ValvPlot_4.Position = [4 10 37 22];

% Create CB_ValvPlot_5
app.CB_ValvPlot_5 = uicheckbox(app.PlotValvesPanel);
app.CB_ValvPlot_5.Text = 'V6';
app.CB_ValvPlot_5.Position = [71 33 37 22];

% Create CB_ValvPlot_6
app.CB_ValvPlot_6 = uicheckbox(app.PlotValvesPanel);
app.CB_ValvPlot_6.Text = 'V8';
app.CB_ValvPlot_6.Position = [71 10 37 22];

% Create CB_ValvPlot_7
app.CB_ValvPlot_7 = uicheckbox(app.PlotValvesPanel);
app.CB_ValvPlot_7.Text = 'V4';
app.CB_ValvPlot_7.Position = [71 56 37 22];

% Create CB_ValvPlot_8
app.CB_ValvPlot_8 = uicheckbox(app.PlotValvesPanel);
app.CB_ValvPlot_8.Text = 'V2';
app.CB_ValvPlot_8.Position = [71 80 37 22];

% Create StoppedLabel
app.StoppedLabel = uilabel(app.UIFigure);
app.StoppedLabel.Position = [327 145 123 22];
app.StoppedLabel.Text = 'Stopped';
```

```
            % Show the figure after all components are created
            app.UIFigure.Visible = 'on';
        end
    end

    % App creation and deletion
    methods (Access = public)

        % Construct app
        function app = FourCHApp_ContSweepVal_v26_exported

            % Create UIFigure and components
            createComponents(app)

            % Register the app with App Designer
            registerApp(app, app.UIFigure)

            % Execute the startup function
            runStartupFcn(app, @startupFcn)

            if nargout == 0
                clear app
            end
        end

        % Code that executes before app deletion
        function delete(app)

            % Delete UIFigure when app is deleted
            delete(app.UIFigure)
        end
    end
end
```

Mason equivalent circuit simulation

Single layer viscous film

```
% Simulate single layer plot
% Usage:    To simulate the plot frequency change and resistance change using Mason equivalent circuit
    with
%           by varying film thickness while using a constant value of viscosity and density
%
% Output:   Plot 1: consist of 2 subplot first plot is the frequency change and the
%           second is resistance change as a parameter of viscosity change.
%           Sauerbrey equation was also plotted.
%
%           Plot 2: this plot also have frequency change of sauerbrey
%           equation and kanazawa equation. This second plot you can use
%           between water or glycerol, uncomment the section before the
%           plot. Also the title of the plot is hardcoded, please
%           modify accordingly.
%
% Parameters:
%           density1: density of glycerol (1261 kg/ml)
%           density2: density of water (1000 kg/ml)
%             viscos: array of viscosity change for plot 1

% Author: Sawit Na songkhla
%   Date: 1 March 2021
clear all;
close all;

%------QCM parameters-----------
% 9 MHz sim
L0 = 0.012654492; % Henry
C0 = 2.47E-14; % Farad

% %8.3MHz sim
% L0 = 0.012590629; % Henry
% C0 = 2.92036E-14; % Farad


f0 = 1/(2*pi*sqrt(L0*C0));
w0 = 2*pi*f0;
%---------------------------------

%----------quartz constant----------
e35 = -0.095;
%try something
%e35 = -0.09;
t = 181e-6; % quartz thickness
SA = pi*(2.5e-3)^2;  % m2 electrode area: diameter of 5 mm
SA_cm2 = pi*(0.25)^2; % cm2
rhoQ = 2.648; %g/vm3
muQ = 2.947e11; %g cm-1 s-2
%-----------------------------------


%----------Copper constant-----------
%  wave_velocity = 2200; % m/s
```

```
%  density = 8900; %kg / m3
%  density_g_cm3 = 8.9 %g / cm3
%-------------------------------------

%----------Glycerol Constant----------
 density1 = 1261; %kg / m3
 density_gly_g_cm3 = 1.261; %g / cm3
 viscosity1 = 1.412; %Pa.s

 %Speculated Viscosity
 viscosity1 = 5e-3;

 %viscosity1 = 8.9e-4; %Pa.s
 gly_wav_velo = sqrt(1i*w0*viscosity1/density1);
%-------------------------------------

%---------Water Constant----------
 density2 = 1000; %kg / m3
 density_water_g_cm3 = 1; %g / cm3
 viscosity2 = 8.89e-4; %Pa.s
%viscosity2=viscosity1;
 water_wav_velo = sqrt(1i*w0*viscosity2/density2);
%-------------------------------------

df_100pulse = sauerbrey_basic(f0,0.3e-3,SA_cm2,rhoQ,muQ)

BulkWater = kanazawa(f0,density_water_g_cm3,viscosity2*10,rhoQ,muQ);
BulkGlycerol = kanazawa(f0,density_gly_g_cm3,viscosity1*10,rhoQ,muQ);

h1 = linspace(0,1000e-9,1000);
h2 = linspace(0,500e-9,5) ;
h_water_sauerbrey = linspace(0,150e-9,500);
%h2 = 0 ; %Not assign the water layer
QCM_Z3e = [];

% -------------- DAta processing ------------------------
%--------- For the first figure----------
%For plot 1, x axis is base layer
%for parameter of viscosity top film thickness change
% for n = 1:length(h2)
%     QCM_Z3e = [QCM_Z3e  ; impedance2layer(gly_wav_velo,water_wav_velo,density1,h1,h2(n),w0,e35,t,SA)];
% end




%for parameter of viscosity change
viscos = linspace(1e-3,10e-3,4); % 1 cp to 10 cp
wav_velo = sqrt(1i*w0*viscos/density2);

for n = 1:length(wav_velo)
    QCM_Z3e = [QCM_Z3e  ; impedanceCal(wav_velo(n),density2,h1,w0,e35,t,SA)];
end



QCM_delta_f = delta_f_Cal(QCM_Z3e,w0,f0,L0,C0);
%water
df_sauerbrey=sauerbrey(f0,h_water_sauerbrey,density_water_g_cm3,rhoQ,muQ);
%Glycerol
%df_sauerbrey=sauerbrey(f0,h_water_sauerbrey,density_gly_g_cm3,rhoQ,muQ);

%----------------------------------------
%--------- For the second figure----------
%CHoose
%this is glycerol
% QCM_Z3e_single = impedanceCal(gly_wav_velo,density1,h1,w0,e35,t,SA);
% QCM_delta_f_single = delta_f_Cal(QCM_Z3e_single,w0,f0,L0,C0);

%this is water
QCM_Z3e_single = impedanceCal( water_wav_velo,density2,h1,w0,e35,t,SA);
QCM_delta_f_single = delta_f_Cal(QCM_Z3e_single,w0,f0,L0,C0);
%----------------------------------------

%------------------ Not use Now---------------
%----------------------------------------
%--------- For the third figure----------
QCM_Z3e_mass_in_liquid = impedanceMassInLiquid(gly_wav_velo,density1,density2,viscosity2,h1,w0,e35,t,SA);
QCM_delta_f_mass_liquid = delta_f_Cal(QCM_Z3e_mass_in_liquid,w0,f0,L0,C0);

        %----*****************Not in use Now**************************---------
        %This is water
        %QCM_Z3e_l = impedanceCal(water_wav_velo,density2,h1,w0,e35,t,SA);
        %QCM_delta_f_l = delta_f_Cal(QCM_Z3e_l,w0,f0,L0,C0);
        %QCM_Z3e_l = impedanceLiq(viscosity2,density2,w0,e35,t,SA);
        %--------- Make shift water film plot ---------
        %water
         %depth = penetration_depth_Cal(viscosity2,density2,w0);
         %glycerol
         depth = penetration_depth_Cal(viscosity1,density1,w0);
        % disp(depth);
        % figure;
        % plot(h1*1e9,QCM_delta_f_l);
        % title("single film with water param");
        % hold on;
        % grid on;
        % hline(BulkWater);
%----------------------------------------
```

```
%----------------------
% First figure
%-----------------------
figure;
subplot(2,1,1);

%Plot frequency change vs. film thickness
plot(h1*1e9,QCM_delta_f);
hold on;

% This is the additional plot sauerbrey and kanazawa
plot(h_water_sauerbrey*1e9,df_sauerbrey,'--');
% hline(BulkWater,"b:","Bulk Water");
% hline(BulkGlycerol,"k:",'Bulk Glycerol');

formatspec = '\\eta_L = %d cP';
viscos_mod = viscos.*1e3;

%initialize matrix
str=string(zeros(1,length(viscos)));

for n=1:length(wav_velo)
    k = sprintf(formatspec ,viscos_mod(n));
    str(n) = k;
end

str(end+1) = "Sauerbrey's equation";
legend(str);
title("Single Film varying viscosity (\rho_L = 1 g/cm^3, \omega = 5.66*10^7 Hz)");

xlabel('film thickness (nm)');
ylabel('frequency change (Hz)');
grid on;
hold on;
%legend(str,'Sauerbrey based on water mass');
legend(str);
subplot(2,1,2);
%Plot resistance change vs. film thickness
plot(h1*1e9,real(QCM_Z3e));
xlabel('film thickness (nm))');
ylabel('Resistance change (Ohm)');
grid on;
%------------------------
%   Second plot
%------------------------
figure;
subplot(2,1,1);

%Plot resistance change vs. film thickness
plot(h1*1e9,QCM_delta_f_single);
title("Single Film with water parameter (\rho_L = 1 g/cm^3,\eta_L = 0.89 cP, \omega = 5.66*10^7 Hz)");

%title("Single Film with water parameter (\rho_L = 1.26 g/cm^3,\eta_L = 5 cP, \omega = 5.66*10^7 Hz)");

xlabel('film thickness (nm)');
ylabel('frequency change (Hz)');
grid on;
hold on;

plot(h_water_sauerbrey*1e9,df_sauerbrey,'--');
yline(BulkWater,'--','bulk water');
%yline(BulkGlycerol,'--','bulk glycerol');
xline(depth*1e9,'-b','penetration depth');
legend('Mason circuit model','Sauerbrey equation','Kanazawa equation');

subplot(2,1,2);
%plot resistance
plot(h1*1e9,real(QCM_Z3e_single));
grid on;
xlabel('film thickness (nm)');
ylabel('Resistance (\Omega)');
%------------------------
%   Third plot
%------------------------

% figure;
%
% %Plot resistance change vs. film thickness
% plot(h1*1e9,QCM_delta_f_mass_liquid);
% title("ViscousFilmInLiquidEquation");
% %legend('frequency');
% xlabel('film thickness (nm)');
% ylabel('frequency change (Hz)');
% hold on;
% grid on;
% hline(BulkWater);
% plot(h_water_sauerbrey*1e9,df_sauerbrey,'--');
% %--------- For the fourth figure----------
% %Resue param
% QCM_Z3e =[];
% QCM_delta_f =[];
% %For plot 4, x axis is top layer
% %h1 is base layer
% h1_2 = linspace(0,500e-9,5);
% %h2 is top layer
% h2_2 = linspace(0,700e-9,1000) ;
% for n = 1:length(h1_2)
```

```
%     QCM_Z3e = [QCM_Z3e  ; impedance2layer(gly_wav_velo,water_wav_velo,density1,h1_2(n),h2_2,w0,e35,t,SA)
     ];
% end
% QCM_delta_f = delta_f_Cal(QCM_Z3e,w0,f0,L0,C0);
% %---------------------------------
%
% %---------------------
% % Forth figure This is base layer varying
% %------------------------
% figure;
% subplot(2,1,1);
% %Plot resistance change vs. film thickness
% plot(h2_2*1e9,QCM_delta_f);
% hold on;
%
% hline(BulkWater,"b:",'Bulk Water');
% hline(BulkGlycerol,"k:",'Bulk Glycerol');
% formatspec = 'base layer (gly) %d nm';
% h_mod = h1_2.*1e9;
%
% %initialize matrix
% str=string(zeros(1,length(h1_2)));
%
% for n=1:length(h1_2)
%     k = sprintf(formatspec ,h_mod(n));
%     str(n) = k;
% end
% %str(length(h1_2)) = "Sauerbrey's equation";
%
% title("Water film over glycerol films (simulation)");
% xlabel('top layer (water) thickness (nm)');
% ylabel('frequency change (Hz)');
% grid on;
% hold on;
% plot(h_water_sauerbrey*1e9,df_sauerbrey,'--');
% str(end+1) = "Sauerbrey's equation based on watermass";
% legend(str);
%
% subplot(2,1,2);
% plot(h2_2*1e9,real(QCM_Z3e));
% xlabel('top layer (water) thickness (nm)');
% ylabel('Resistance change (Ohm)');
% grid on;
%----------------------
% Fifth figure
%------------------------
% figure;
% plot(h_water_sauerbrey*1e9,df_sauerbrey);
% grid on;




function Z3e = impedance2layer(velocity_1,velocity_2,density,h1,h2,w0,e35,t,SA)
    Vsum  = velocity_1+velocity_2;
    Vdiff = velocity_1-velocity_2;
    U1 = (1-exp(2*1i*w0*((h2/velocity_2)+(h1/velocity_1))));
    U2 = (exp(2*1i*w0*(h2/velocity_2))-exp(2*1i*w0*(h1/velocity_1)));

    U3 = (1+exp(2*1i*w0*((h2/velocity_2)+(h1/velocity_1))));
    U4 = (exp(2*1i*w0*(h2/velocity_2))+exp(2*1i*w0*(h1/velocity_1)));

    Z3 = -density*velocity_1*((Vsum.*U1+Vdiff.*U2)./(Vsum.*U3+Vdiff.*U4));


    Z3e = ((t^2)*Z3)/(4*(e35^2)*SA);
end


function Z3e = impedanceCal(wave_velocity,density,h,w0,e35,t,SA)
    Z3 = 1i*density*wave_velocity*tan(w0.*h./wave_velocity);
    Z3e = ((t^2)*Z3)/(4*(e35^2)*SA);
end

function Z3e = impedanceLiq(viscosity,density,w0,e35,t,SA)
    Z3 = sqrt(1i*w0*viscosity*density);
    Z3e = ((t^2)*Z3)/(4*(e35^2)*SA);
end


function Z3e = impedanceMassInLiquid(wave_velocity,densityF,densityL,viscosity,h,w0,e35,t,SA)

    x = w0*h/wave_velocity;
    k=sqrt(1i*w0*viscosity*densityL);
    ZA1= densityF*wave_velocity;
    Z3 = ZA1*(((1i*ZA1.*sin(x))+k.*cos(x))./(ZA1.*cos(x)+1i*k.*sin(x)));

    %Z3 = (1i*w0*densityF.*h)+sqrt(1i*w0*viscosity*densityL);

    Z3e = ((t^2)*Z3)/(4*(e35^2)*SA);
end

function df = delta_f_Cal(Z,w0,f0,L0,C0)
    L_change = imag(Z)/w0;
    df = (1./(2*pi*sqrt((L0+L_change)*C0)))-f0;
end

function depth = penetration_depth_Cal(viscosity,density,w0)
```

```
    depth = (1/2)*(sqrt(density*w0/(2*viscosity)))^-1;
end

function df = kanazawa(f0,rho_l,eta_l,rho_q,mu_q)
    df = -(f0^(3/2))*(eta_l*rho_l/(pi*rho_q*mu_q))^(1/2);
end

function df = sauerbrey(f0,h,rho_l,rho_q,mu_q)
    h_cm = h.*100;
    df = -(2*(f0^2)*rho_l.*h_cm)./(sqrt(rho_q*mu_q));
end

function df = sauerbrey_basic(f0,m,area,rho_q,mu_q)
    df = -(2*(f0^2)*m)./area*(sqrt(rho_q*mu_q));
end
```

Contour plot of Mason equivalent circuit

```
% Simulate one layer surface and contour plot
% Usage:    To simulate surface plot and contour plot using Mason equivalent
%           This program produces 7 plots
%
% Output:   Plot 1: frequency change surface plot as a parameter of
%           viscosity amd film height, consist of 4 subplots with different
%           film density .
%
%           Plot 2: similar to plot 1 but plot the resistance values (4 subplots)
%
%           Plot 3: Surface plot of frequency change (film density
%           at 1000 kg/m3)
%
%           Plot 4: Contour plot of frequency change (film density
%           at 1000 kg/m3)
%
%           Plot 5: Surface plot of resistance (film density
%           at 1000 kg/m3)
%
%           Plot 6: Plot 5: Contour plot of resistance (film density
%           at 1000 kg/m3)
%
%           Plot 7: Combined contour plot of both frequency change and
%           resistance. This plot also included a makeshift datapoint marking
%           and line drawing, Please consider modifying the code or remove it.
%
% Parameters:
%           viscosity_array: viscosity values plotting range
%           h1_array: film height plotting range
%           density_array : for plot 1 and 2, 4 values of density the third value is used for plot 3 to 7

% Author: Sawit Na songkhla
%   date: 1 March 2021

close all;
clear all;
%-- 3d view angle
caz = 154;
cel = 25;
%------QCM parameters-----------
% 9 MHz sim
L0 = 0.012654492; % Henry
C0 = 2.47E-14; % Farad

% %8.3MHz sim
% L0 = 0.012590629; % Henry
% C0 = 2.92036E-14; % Farad


f0 = 1/(2*pi*sqrt(L0*C0));
w0 = 2*pi*f0;
%---------------------------------

%----------quartz constant----------
e35 = -0.095;
t = 181e-6; % quartz thickness
SA = pi*(2.5e-3)^2;  % m2 electrode area: diameter of 5 mm

SA_cm2 = pi*(0.25)^2; % cm2
rhoQ = 2.648; %g/vm3
muQ = 2.947e11; %g cm-1 s-2
%-----------------------------------


 % ------------- Plot parameters ---------------
 %Uncomment the set that you want

 %Optimized for results
%  viscosity_array = linspace(0,0.006,100); % viscosity 0 to 6 cP
%  h1_array = linspace(0,250e-9,100);
%  density_array = [250 500 1000 1250];
%

 %Optimized for Glycerol
 viscosity_array = linspace(0.006,0.022,100); % viscosity 10cp to 100 cP
 h1_array = linspace(400e-9,1100e-9,100); %1000 um film thickness
 density_array = [250 500 1000 1250];

 %optimized for visibility
```

```
%  viscosity_array = linspace(0,0.01,50); % viscosity 0 to 3 cP
%  h1_array = linspace(0,500e-9,50);
%  density_array = [250 500 1000 1250];

 clevels=10;

 %viscosity1 = 8.9e-4; %Pa.s
%  rho_eta = density1.*viscosity1;
%  gly_wav_velo = sqrt(1i*w0*viscosity1/density1);
%-------------------------------------

% %---------Water Constant----------
%  density2 = 1000; %kg / m3
%  density_water_g_cm3 = 1; %g / cm3
%  viscosity2 = 9.97e-4; %Pa.s
% %viscosity2=viscosity1;
%
%  water_wav_velo = sqrt(1i*w0*viscosity2/density2);
% %-------------------------------------

% df_100pulse = sauerbrey_basic(f0,0.3e-3,SA_cm2,rhoQ,muQ)
%
% BulkWater = kanazawa(f0,density_water_g_cm3,viscosity2*10,rhoQ,muQ);
% BulkGlycerol = kanazawa(f0,density_gly_g_cm3,viscosity1*10,rhoQ,muQ);




% -------------- DAta processing ------------------------
%--------- For the first figure----------

[height,visco] = meshgrid(h1_array,viscosity_array);

%Initialize null cell
QCM_Z3e = cell(length(density_array),1);
QCM_delta_f = cell(length(density_array),1);
QCM_R = cell(length(density_array),1);


%Delta f calculation
for n=1:length(density_array)
    QCM_Z3e(n) = {impedanceCal(visco,density_array(n),h1_array,w0,e35,t,SA)};

    K = cell2mat(QCM_Z3e(n));
    QCM_delta_f(n) = {delta_f_Cal(K,w0,f0,L0,C0)};
    QCM_R(n)={real(K)};
end

%-------------------------------------------

%abs_QCM_delta_f = -1.*QCM_delta_f;
%ix = find(imregionalmax(abs_QCM_delta_f ));
figure;
X = height.*1e9;  % height nm
Y = visco.*1000; %viscosity cP

titletext = 'Plot at film density of %d kg/m3';

for n=1:length(density_array)
Z = cell2mat(QCM_delta_f(n));
%---------------------
% frequency change figure 1
%-----------------------
subplot(2,2,n);
%mesh(X,Y,Z);
%------If using surface plot
mesh(X,Y,Z);

%shading interp
%-----------
view(caz,cel);
xlabel('film height (nm)');
ylabel('viscosity (cP)');
zlabel('(frequency change) (Hz)');

k = sprintf(titletext ,density_array(n));
title(k);
end

figure;
for n=1:length(density_array)
Z = cell2mat(QCM_R(n));
%---------------------
% Resistance figure 2
%-----------------------
subplot(2,2,n);
%mesh(X,Y,Z);
%------If using surface plot
mesh(X,Y,Z);

%shading interp
%-----------
view(caz,cel);
xlabel('film height (nm)');
ylabel('viscosity (cP)');
zlabel('(frequency change) (Hz)');

k = sprintf(titletext ,density_array(n));
title(k);
```

```
end

%This is a plot for density of water 1000 kg/m3
k = sprintf(titletext ,density_array(3));

%----------------------------------------
%This is for surf and contour of frequency, figure 3
%----------------------------------------
% Use the data number 3 which is density of 1000 kg/ml
Z = cell2mat(QCM_delta_f(3));
figure; %Figure 3
surf(X,Y,Z);
xlabel('Film height (nm)');
ylabel('Viscosity (cP)');
zlabel('Frequency change (Hz)');
title(k);
view(-45,10)

figure; %Figure 4
[c,h] = contour(X,Y,Z);
clabel(c,h);
xlabel('Film height (nm)');
ylabel('Viscosity (cP)');
zlabel('Frequency change (Hz)');
title('Frequency change: contour plot at film density of 1000 kg/m3');
%plot3(x(ix),y(ix),z(ix),'r*','MarkerSize',24)
grid on;
%----------------------------------------
%This is for surf and contour of resistance
%----------------------------------------
Z2 = cell2mat(QCM_R(3));
figure;
surf(X,Y,Z2);
xlabel('Film height (nm)');
ylabel('Viscosity (cP)');
zlabel('Resistance (Ohm)');
title(k);
view(-45,30)

figure;
[c,h] = contour(X,Y,Z2);
clabel(c,h);
xlabel('Film height (nm)');
ylabel('Viscosity (cP)');
zlabel('Resistance (Ohm)');
title('Resistance: contour plot at film density of 1000 kg/m3');
%plot3(x(ix),y(ix),z(ix),'r*','MarkerSize',24)

grid on;

%----------------------------------------
%Combination contour of frequency change and resistance
%----------------------------------------
% Plot 7
figure;
ax1 = axes;
ax2 = axes;
[c,h1] = contour(ax1,X,Y,Z,clevels);
caxis([-5000 -500])
clabel(c,h1);
h1.LevelList=round(h1.LevelList,-2);
hold on;

% %PEG20M line plot
% line([130 155],[5.4 2.25],'Marker','o','Color',[0, 0.4470, 0.7410],'LineWidth',1.5);

% %Peg2000 line plot
% line([164 185],[1.3 1.1],'Marker','o','Color',[0.8500, 0.3250, 0.0980],'LineWidth',1.5);


%Glycerol line plot
%1 deposition
line([534 548],[9 8.4],'Marker','o','Color',[0.8500, 0.3250, 0.0980],'LineWidth',1.5);
%3 depositon
line([598 633],[10.2 9.2],'Marker','o','Color',[0.8500, 0.3250, 0.0980],'LineWidth',1.5);
%10 depositon
line([718 732],[12.6 11.8],'Marker','o','Color',[0.8500, 0.3250, 0.0980],'LineWidth',1.5);
%30 depositon
line([880 883],[16.7 16],'Marker','o','Color',[0.8500, 0.3250, 0.0980],'LineWidth',1.5);
%100 depositon
line([995 1001],[19.6 19.1],'Marker','o','Color',[0.8500, 0.3250, 0.0980],'LineWidth',1.5);


[c,h2] = contour(ax2,X,Y,Z2,clevels);
caxis([50 400])
clabel(c,h2);
h2.LevelList=round(h2.LevelList,-1)
grid on;
linkaxes([ax1,ax2])

%%Hide the top axes
ax2.Visible = 'off';
ax2.XTick = [];
ax2.YTick = [];


colormap(ax1,'autumn')
colormap(ax2,'winter')
```

```
set([ax1,ax2],'Position',[.17 .11 .685 .815]);
cb1 = colorbar(ax1,'Position',[.05 .11 .0675 .815]);
cb2 = colorbar(ax2,'Position',[.88 .11 .0675 .815]);

cb1.Title.String = 'frequency change';
cb2.Title.String = 'Resistance';

ax1.Title.String = 'Frequency change & Resistance: film density of 1000 kg/m3';

ax1.XLabel.String = 'film height (nm)';
ax1.YLabel.String = 'viscosity (cP)';




function Z3e = impedance2layer(velocity_1,velocity_2,density,h1,h2,w0,e35,t,SA)
    Vsum  = velocity_1+velocity_2;
    Vdiff = velocity_1-velocity_2;
    U1 = (1-exp(2*1i*w0*((h2/velocity_2)+(h1/velocity_1))));
    U2 = (exp(2*1i*w0*(h2/velocity_2))-exp(2*1i*w0*(h1/velocity_1)));

    U3 = (1+exp(2*1i*w0*((h2/velocity_2)+(h1/velocity_1))));
    U4 = (exp(2*1i*w0*(h2/velocity_2))+exp(2*1i*w0*(h1/velocity_1)));

    Z3 = -density*velocity_1*((Vsum.*U1+Vdiff.*U2)./(Vsum.*U3+Vdiff.*U4));


    Z3e = ((t^2)*Z3)/(4*(e35^2)*SA);
end


function Z3e = impedanceCal(viscosity,density,h,w0,e35,t,SA)
    wave_velocity=sqrt(1i*w0.*viscosity./density);
    Z3 = 1i.*density.*wave_velocity.*tan(w0.*h./wave_velocity);
    Z3e = ((t^2).*Z3)./(4*(e35^2)*SA);
end

function df = delta_f_Cal(Z,w0,f0,L0,C0)
    L_change = imag(Z)/w0;
    df = (1./(2*pi*sqrt((L0+L_change)*C0)))-f0;
end

function depth = penetration_depth_Cal(viscosity,density,w0)
    depth = (1/2)*(sqrt(density*w0/(2*viscosity)))^-1;
end

function df = kanazawa(f0,rho_l,eta_l,rho_q,mu_q)
    df = -(f0^(3/2))*(eta_l*rho_l/(pi*rho_q*mu_q))^(1/2);
end

function df = sauerbrey(f0,h,rho_l,rho_q,mu_q)
    h_cm = h.*100;
    df = -(2*(f0^2)*rho_l.*h_cm)./(sqrt(rho_q*mu_q));
end

function df = sauerbrey_basic(f0,m,area,rho_q,mu_q)
    df = -(2*(f0^2)*m)./area*(sqrt(rho_q*mu_q));
end
```

Bibliography

[1] Günter Sauerbrey. "Verwendung von Schwingquarzen zur Wägung dünner Schichten und zur Mikrowägung". In: *Zeitschrift für Physik* 155.2 (1959). ISSN: 00443328. DOI: 10.1007/BF01337937.

[2] K. Keiji Kanazawa and Joseph G. Gordon. "The oscillation frequency of a quartz resonator in contact with liquid". In: *Analytica Chimica Acta* 175.C (1985). ISSN: 00032670. DOI: 10.1016/S0003-2670(00)82721-X.

[3] Michael Thompson, Catherine L. Arthur, and Gurbaksh K. Dhaliwal. "Liquid-Phase Piezoelectric and Acoustic Transmission Studies of Interfacial Immunochemistry". In: *Analytical Chemistry* 58.6 (1986). ISSN: 15206882. DOI: 10.1021/ac00297a051.

[4] Oliver Hayden et al. "Artificial antibodies for bioanalyte detection - Sensing viruses and proteins". In: *Advanced Functional Materials* 16.10 (2006). ISSN: 1616301X. DOI: 10.1002/adfm.200500626.

[5] Usman Latif et al. "Sauerbrey and anti-Sauerbrey behavioral studies in QCM sensors-Detection of bioanalytes". In: *Sensors and Actuators, B: Chemical* 176 (2013). ISSN: 09254005. DOI: 10.1016/j.snb.2012.09.064.

[6] Fahrettin Yakuphanoglu. "Semiconducting and quartz microbalance (QCM) humidity sensor properties of TiO 2 by sol gel calcination method". In: *Solid State Sciences* 14.6 (2012). ISSN: 12932558. DOI: 10.1016/j.solidstatesciences.2012.03.016.

[7] Lord Rayleigh. "On waves propagated along the plane surface of an elastic solid". In: *Proceedings of the London Mathematical Society* s1-17.1 (1885). ISSN: 1460244X. DOI: 10.1112/plms/s1-17.1.4.

[8] Franz L. Dickert et al. "SAW devices-sensitivity enhancement in going from 80 MHz to 1 GHz". In: *Sensors and Actuators, B: Chemical* 46.2-3 (1998). ISSN: 09254005. DOI: 10.1016/S0925-4005(98)00097-5.

[9] Jun Phil Jung et al. "Fabrication and characterization of high frequency SAW device with IDT/ZnO/AlN/Si configuration: Role of AlN buffer". In: *Thin Solid Films*. Vol. 447-448. 2004. DOI: 10.1016/j.tsf.2003.07.022.

[10] Adnan Mujahid and Franz L. Dickert. *Surface acousticwave (SAW) for chemical sensing applications of recognition layers*. 2017. DOI: 10.3390/s17122716.

[11] Henry Wohltjen and Raymond Dessy. "Surface Acoustic Wave Probe for Chemical Analysis. I. Introduction and Instrument Description". In: *Analytical Chemistry* 51.9 (1979). ISSN: 15206882. DOI: 10.1021/ac50045a024.

[12] Jay W. Grate et al. "Smart Sensor System for Trace Organophosphorus and Organosulfur Vapor Detection Employing a Temperature-Controlled Array of Surface Acoustic Wave Sensors, Automated Sample Preconcentration, and Pattern Recognition". In: *Analytical Chemistry* 65.14 (1993). ISSN: 15206882. DOI: 10.1021/ac00062a011.

[13] Hung Bin Lin and Jeng Shong Shih. "Fullerene C60-cryptand coated surface acoustic wave quartz crystal sensor for organic vapors". In: *Sensors and Actuators, B: Chemical* 92.3 (2003). ISSN: 09254005. DOI: 10.1016/S0925-4005(03)00159-X.

[14] María Jesús Fernández et al. "Discrimination of volatile compounds through an electronic nose based on ZnO SAW sensors". In: *Sensors and Actuators, B: Chemical* 127.1 (2007). ISSN: 09254005. DOI: 10.1016/j.snb.2007.07.054.

[15] T. T. Sunil, Subhasis Chaudhuri, and Vibha Mishra. "Optimal selection of SAW sensors for E-Nose applications". In: *Sensors and Actuators, B: Chemical* 219 (2015). ISSN: 09254005. DOI: 10.1016/j.snb.2015.04.107.

[16] Prabha Verma and R. D.S. Yadava. "Polymer selection for SAW sensor array based electronic noses by fuzzy c-means clustering of partition coefficients: Model studies on detection of freshness and spoilage of milk and fish". In: *Sensors and Actuators, B: Chemical* 209 (2015). ISSN: 09254005. DOI: 10.1016/j.snb.2014.11.149.

[17] Horace Lamb. "On the vibrations of an elastic sphere". In: *Proceedings of the London Mathematical Society* s1-13.1 (1881). ISSN: 1460244X. DOI: 10.1112/plms/s1-13.1.189.

[18] Stuart W. Wenzel and Richard M. White. "A Multisensor Employing an Ultrasonic Lamb-Wave Oscillator". In: *IEEE Transactions on Electron Devices* 35.6 (1988). ISSN: 15579646. DOI: 10.1109/16.2525.

[19] Jay W. Grate, Stuart W. Wenzel, and Richard M. White. "Flexural Plate Wave Devices for Chemical Analysis". In: *Analytical Chemistry* 63.15 (1991). ISSN: 15206882. DOI: 10.1021/ac00015a011.

[20] Andreas Hierlemann and Henry Baltes. *CMOS-based chemical microsensors*. 2003. DOI: 10.1039/b208563c.

[21] Qing Yun Cai et al. "Vapor recognition with an integrated array of polymer-coated flexural plate wave sensors". In: *Sensors and Actuators, B: Chemical* 62.2 (2000). ISSN: 09254005. DOI: 10.1016/S0925-4005(99)00381-0.

[22] Jane Pepper et al. "Detection of proteins and intact microorganisms using microfabricated flexural plate silicon resonator arrays". In: *Sensors and Actuators, B: Chemical* 96.3 (2003). ISSN: 09254005. DOI: 10.1016/S0925-4005(03)00641-5.

[23] Je Wei Lan et al. "Highly sensitive FPW-based microsystem for rapid detection of tetrahydrocannabinol in human urine". In: *Sensors (Switzerland)* 17.12 (2017). ISSN: 14248220. DOI: 10.3390/s17122760.

[24] Christian Walk et al. "A Piezoelectric Flexural Plate Wave (FPW) Bio-MEMS Sensor with Improved Molecular Mass Detection for Point-of-Care Diagnostics". In: *Current Directions in Biomedical Engineering* 5.1 (2019). ISSN: 23645504. DOI: 10.1515/cdbme-2019-0067.

[25] K. M. Lakin and J. S. Wang. "Acoustic bulk wave composite resonators". In: *Applied Physics Letters* 38.3 (1981). ISSN: 00036951. DOI: 10.1063/1.92298.

[26] J. Bjurström et al. "Design and fabrication of temperature compensated liquid FBAR sensors". In: *Proceedings - IEEE Ultrasonics Symposium*. Vol. 1. 2006. DOI: 10.1109/ULTSYM.2006.240.

[27] Jan Weber et al. "Shear mode FBARs as highly sensitive liquid biosensors". In: *Sensors and Actuators, A: Physical* 128.1 (2006). ISSN: 09244247. DOI: 10.1016/j.sna.2006.01.005.

[28] K. Tukkiniemi et al. "Fully integrated FBAR sensor matrix for mass detection". In: *Procedia Chemistry*. Vol. 1. 1. 2009. DOI: 10.1016/j.proche.2009.07.262.

[29] R. Gabl et al. "Novel Integrated FBAR Sensors: A Universal Technology Platform for Bio- and Gas-Detection". In: *Proceedings of IEEE Sensors*. Vol. 2. 2. 2003. DOI: 10.1109/icsens.2003.1279132.

[30] Jizhou Hu et al. "Miniaturized polymer coated film bulk acoustic wave resonator sensor array for quantitative gas chromatographic analysis". In: *Sensors and Actuators, B: Chemical* 274 (2018). ISSN: 09254005. DOI: 10.1016/j.snb.2018.07.162.

[31] Jihang Liu et al. "Analyzing the effect of the Front-end circuit for the FBAR sensor". In: *Measurement: Journal of the International Measurement Confederation* 151 (2020). ISSN: 02632241. DOI: 10.1016/j.measurement.2019.107237.

[32] T. Mirea et al. "Impact of FBAR design on its sensitivity as in-liquid gravimetric sensor". In: *Sensors and Actuators, A: Physical* 289 (2019). ISSN: 09244247. DOI: 10.1016/j.sna.2019.02.012.

[33] William H. King. "Piezoelectric Sorption Detector". In: *Analytical Chemistry* 36.9 (1964). ISSN: 15206882. DOI: 10.1021/ac60215a012.

[34] D. James et al. "Classification of fresh edible oils using a coated piezoelectric sensor array-based electronic nose with soft computing approach for pattern recognition". In: *Transactions of the Institute of Measurement & Control* 26.1 (2004). ISSN: 01423312. DOI: 10.1191/0142331204tm0102oa.

[35] Shunzo Suematsu et al. "Conducting polymer films of cross-linked structure and their QCM analysis". In: *Electrochimica Acta* 45.22 (2000). ISSN: 00134686. DOI: 10.1016/S0013-4686(00)00466-7.

[36] Masato Tominaga et al. "Electrochemical, AFM and QCM studies on ferritin immobilized onto a self-assembled monolayer-modified gold electrode". In: *Journal of Electroanalytical Chemistry* 566.2 (2004). ISSN: 15726657. DOI: 10.1016/j.jelechem.2003.11.056.

[37] Li Jiang Wang et al. "Sensing Escherichia coli O157:H7 via frequency shift through a self-assembled monolayer based QCM immunosensor". In: *Journal of Zhejiang University: Science B* 9.2 (2008). ISSN: 16731581. DOI: 10.1631/jzus.B0710307.

[38] Michael Jenik et al. "Pollen-imprinted polyurethanes for QCM allergen sensors". In: *Analytical and Bioanalytical Chemistry* 394.2 (2009). ISSN: 16182642. DOI: 10.1007/s00216-009-2718-8.

[39] Kazuya Matsumoto et al. "QCM sensing of bisphenol A using molecularly imprinted hydrogel/conducting polymer matrix". In: *Polymer Journal* 48.4 (2016). ISSN: 13490540. DOI: 10.1038/pj.2016.23.

[40] Zdeněk Farka, David Kovář, and Petr Skládal. "Rapid detection of microorganisms based on active and passive modes of QCM". In: *Sensors (Switzerland)* 15.1 (2015). ISSN: 14248220. DOI: 10.3390/s150100079.

[41] T. Nakamoto, A. Fukuda, and T. Moriizumi. "Perfume and flavour identification by odour-sensing system using quartz-resonator sensor array and neural-network pattern recognition". In: *Sensors and Actuators: B. Chemical* 10.2 (1993). ISSN: 09254005. DOI: 10.1016/0925-4005(93)80030-F.

[42] Hamdi Melih Saraoglu et al. "Electronic nose system based on quartz crystal microbalance sensor for blood glucose and hba1c levels from exhaled breath odor". In: *IEEE Sensors Journal* 13.11 (2013). ISSN: 1530437X. DOI: 10.1109/JSEN.2013.2265233.

[43] Sunil K. Jha and Kenshi Hayashi. "Polyacrylic acid polymer and aldehydes template molecule based MIPs coated QCM sensors for detection of pattern aldehydes in body odor". In: *Sensors and Actuators, B: Chemical* 206 (2015). ISSN: 09254005. DOI: 10.1016/j.snb.2014.09.102.

[44] I. Y. Huang et al. "Development of a flexural plate-wave (FPW) immunoglobulin-E (IgE) allergy bio-sensing microsystem". In: *Sensors and Actuators, B: Chemical* 162.1 (2012). ISSN: 09254005. DOI: 10.1016/j.snb.2011.12.065.

[45] Rosamaria Capuano et al. "An investigation about the origin of the lung cancer signalling VOCs in breath". In: *Proceedings of IEEE Sensors*. Vol. 2014-Decem. December. 2014. DOI: 10.1109/ICSENS.2014.6985267.

[46] Qiang Li, Yu Gu, and Jing Jia. "Classification of multiple chinese liquors by means of a QCM-based e-nose and MDS-SVM classifier". In: *Sensors (Switzerland)* 17.2 (2017). ISSN: 14248220. DOI: 10.3390/s17020272.

[47] Pintu Adhikari et al. "Investigation of Polymer-Plasticizer Blends as SH-SAW Sensor Coatings for Detection of Benzene in Water with High Sensitivity and Long-Term Stability". In: *ACS Sensors* 2.1 (2017). ISSN: 23793694. DOI: 10.1021/acssensors.6b00659.

[48] Feng Gao et al. "Dual transduction on a single sensor for gas identification". In: *Sensors and Actuators, B: Chemical* 278 (2019). ISSN: 09254005. DOI: 10.1016/j.snb.2018.09.029.

[49] Wen Wang et al. "Development of a Pd/Cu nanowires coated SAW hydrogen gas sensor with fast response and recovery". In: *Sensors and Actuators, B: Chemical* 287 (2019). ISSN: 09254005. DOI: 10.1016/j.snb.2019.02.047.

[50] Manuel Aleixandre and Takamichi Nakamoto. "Study of room temperature ionic liquids as gas sensing materials in quartz crystal microbalances". In: *Sensors (Switzerland)* 20.14 (2020). ISSN: 14248220. DOI: 10.3390/s20144026.

[51] Hiroshi Muramatsu, Eiichi Tamiya, and Isao Karube. "Computation of Equivalent Circuit Parameters of Quartz Crystals in Contact with Liquids and Study of Liquid Properties". In: *Analytical Chemistry* 60.19 (1988). ISSN: 15206882. DOI: 10.1021/ac00170a032.

[52] L. Rodriguez-Pardo, A. M. Cao-Paz, and J. Fariña. "Design and characterization of an active bridge oscillator as a QCM sensor for the measurement of liquid properties and mass films in damping media". In: *Sensors and Actuators, A: Physical* 276 (2018). ISSN: 09244247. DOI: 10.1016/j.sna.2018.04.012.

[53] Takamichi Nakamoto and Takayoshi Inuma. "Odor preconcentrator using SAW device and QCM in liquid phase for odor measurement". In: *IEEE International Conference on Multisensor Fusion and Integration for Intelligent Systems*. Vol. 2015-Octob. 2015. DOI: 10.1109/MFI.2015.7295808.

[54] Xiao Fan and Binyang Du. "Selective detection of trace p-xylene by polymer-coated QCM sensors". In: *Sensors and Actuators, B: Chemical* 166-167 (2012). ISSN: 09254005. DOI: 10.1016/j.snb.2012.03.060.

[55] Liping Du et al. "Piezoelectric olfactory receptor biosensor prepared by aptamer-assisted immobilization". In: *Sensors and Actuators, B: Chemical* 187 (2013). ISSN: 09254005. DOI: 10.1016/j.snb.2013.02.009.

[56] Olga S. Papadopoulou et al. "Sensory and microbiological quality assessment of beef fillets using a portable electronic nose in tandem with support vector machine analysis". In: *Food Research International* 50.1 (2013). ISSN: 09639969. DOI: 10.1016/j.foodres.2012.10.020.

[57] Stijn Saevels et al. "Electronic nose as a non-destructive tool to evaluate the optimal harvest date of apples". In: *Postharvest Biology and Technology* 30.1 (2003). ISSN: 09255214. DOI: 10.1016/S0925-5214(03)00059-0.

[58] Takamichi Nakamoto and Takeharu Kobayashi. "Development of Circuit for Measuring Both Q Variation and Resonant Frequency Shift of Quartz Crystal Microbalance". In: *IEEE Transactions on Ultrasonics, Ferroelectrics and Frequency Control* 41.6 (1994). ISSN: 08853010. DOI: 10.1109/58.330261.

[59] Michael Rodahl, Fredrik Höök, and Bengt Kasemo. "QCM operation in liquids: An explanation of measured variations in frequency and Q factor with liquid conductivity". In: *Analytical Chemistry* 68.13 (1996). ISSN: 00032700. DOI: 10.1021/ac951203m.

[60] Michael Rodahl and Bengt Kasemo. "Frequency and dissipation-factor responses to localized liquid deposits on a QCM electrode". In: *Sensors and Actuators, B: Chemical* 37.1-2 (1996). ISSN: 09254005. DOI: 10.1016/S0925-4005(97)80077-9.

[61] Agata Pomorska et al. "Positive frequency shifts observed upon adsorbing micron-sized solid objects to a quartz crystal microbalance from the liquid phase". In: *Analytical Chemistry* 82.6 (2010). ISSN: 00032700. DOI: 10.1021/ac902012e.

[62] Marco Ferrari and Vittorio Ferrari. "An oscillator circuit for dual-harmonic tracking of frequency and resistance in quartz resonator sensors". In: *Measurement Science and Technology* 20.12 (2009). ISSN: 09570233. DOI: 10.1088/0957-0233/20/12/124005.

[63] T. Addabbo et al. "A DDS-based multi-harmonic frequency meter for QCM sensor applications". In: *Procedia Engineering*. Vol. 87. 2014. DOI: 10.1016/j.proeng.2014.11.664.

[64] T. Nakamoto, K. Nakamura, and T. Moriizumi. "Study of oscillator-circuit behavior for QCM gas sensor". In: *Proceedings of the IEEE Ultrasonics Symposium*. Vol. 1. 1996. DOI: 10.1109/ultsym.1996.583990.

[65] Guili Liu et al. "Impedance measurement of quartz crystal based on network analysis method". In: *Fourth International Seminar on Modern Cutting and Measurement Engineering*. Vol. 7997. 2010. DOI: 10.1117/12.888541.

[66] Vu Anh Minh et al. "Enhanced NH 3 gas sensing properties of a QCM sensor by increasing the length of vertically orientated ZnO nanorods". In: *Applied Surface Science* 265 (2013). ISSN: 01694332. DOI: 10.1016/j.apsusc.2012.11.028.

[67] Yuchen Yang et al. "Stability enhanced, repeatability improved Parylene-C passivated on QCM sensor for aPTT measurement". In: *Biosensors and Bioelectronics* 98 (2017). ISSN: 18734235. DOI: 10.1016/j.bios.2017.06.021.

[68] Ahmad Anwar Zainuddin et al. "Verification of quartz crystal microbalance array using vector network analyzer and openQCM". In: *Indonesian Journal of Electrical Engineering and Computer Science* 10.1 (2018). ISSN: 25024760. DOI: 10.11591/ijeecs.v10.i1.pp84-93.

[69] Arnab Guha et al. "Simple and ultrafast resonance frequency and dissipation shift measurements using a fixed frequency drive". In: *Sensors and Actuators, B: Chemical* 281 (2019). ISSN: 09254005. DOI: 10.1016/j.snb.2018.11.052.

[70] M. V. Voinova, M. Jonson, and B. Kasemo. "'Missing mass' effect in biosensor's QCM applications". In: *Biosensors and Bioelectronics* 17.10 (2002). ISSN: 09565663. DOI: 10.1016/S0956-5663(02)00050-7.

[71] Antonio Arnau et al. "A different point of view on the sensitivity of quartz crystal microbalance sensors". In: *Measurement Science and Technology* 20.12 (2009). ISSN: 09570233. DOI: 10.1088/0957-0233/20/12/124004.

[72] Z. Parlak, C. Biet, and S. Zauscher. "Decoupling mass adsorption from fluid viscosity and density in quartz crystal microbalance measurements using normalized conductance modeling". In: *Measurement Science and Technology* 24.8 (2013). ISSN: 13616501. DOI: 10.1088/0957-0233/24/8/085301.

[73] Feng Tan et al. "Separate density and viscosity measurements of unknown liquid using quartz crystal microbalance". In: *AIP Advances* 6.9 (2016). ISSN: 21583226. DOI: 10.1063/1.4963298.

[74] Ariela Tarnapolsky and Viatcheslav Freger. "Modeling QCM-D Response to Deposition and Attachment of Microparticles and Living Cells". In: *Analytical Chemistry* 90.23 (2018). ISSN: 15206882. DOI: 10.1021/acs.analchem.8b03411.

[75] Fedor N. Dultsev and Eugeny A. Kolosovsky. "QCM model as a system of two elastically bound weights". In: *Sensors and Actuators, B: Chemical* 242 (2017). ISSN: 09254005. DOI: 10.1016/j.snb.2016.09.158.

[76] Takamichi Nakamoto and Toyosaka Moriizumi. "A theory of a quartz crystal microbalance based upon a mason equivalent circuit". In: *Japanese Journal of Applied Physics* 29.5 R (1990). ISSN: 13474065. DOI: 10.1143/JJAP.29.963.

[77] "PROPERTIES OF ORDINARY WATER-SUBSTANCE". In: *News Edition, American Chemical Society* 18.5 (1940), p. 215. DOI: 10.1021/cen-v018n005.p215. eprint: https://pubs.acs.org/doi/pdf/10.1021/cen-v018n005.p215. URL: https://pubs.acs.org/doi/abs/10.1021/cen-v018n005.p215.

[78] Shingo Kato and Takamichi Nakamoto. "Control System of Micro Droplet using Microdispenser Based on Solenoid Valve and its Application for Highly Efficient SAW Atomizer". In: *IEEJ Transactions on Sensors and Micromachines* 138.6 (2018), pp. 220–225. DOI: 10.1541/ieejsmas.138.220.

[79] Walter A. Aue, Corazon R. Hastings, and Shubhender Kapila. "On the unexpected behavior of a common gas chromatographic phase". In: *Journal of Chromatography A* 77.2 (1973), pp. 299–307. ISSN: 0021-9673. DOI: https://doi.org/10.1016/S0021-9673(00)92196-4. URL: http://www.sciencedirect.com/science/article/pii/S0021967300921964.